Design, Synthesis and Evaluation of Organic and Metal Based Antimicrobial Agents

Niamh Anne Dolan, B.Sc.

NUI MAYNOOTH

Ollscoil na hÉireann Má Nuad

A thesis submitted to the National University of Ireland Maynooth in accordance with the requirements for the Degree of Doctor of Philosophy in the Faculty of Science

November 2013

Department of Chemistry

NUI Maynooth

Supervisors: Dr. John C. Stephens and Dr. John McGinley

Head of Dept.: Dr. John C. Stephens

Declaration of Authorship

I hereby certify that the work presented within this thesis, except where acknowledged and cited, is my own work and has not been previously submitted for a Degree to this University or elsewhere.

<div align="right">

Niamh Anne Dolan

_____

</div>

National University of Ireland, Maynooth   November 2013

<u>Acknowledgements</u>

I would also like to thank all of postgrads and postdocs in the Chemistry Department, for your help and for the many laughs. A special thank you to the girls from the biosensors lab, Keeley, Saidhbhe and Andy. Thank you for the many cups of tea, the many laughs and advice and for always lending an ear. Thank you also to the staff and lecturers of the NUIM chemistry department for your help and advice it was always very much appreciated.

To Carol, Alanna and Trish. Thank you so much for your friendship over these last few years, for the many laughs, for listening, for your advice and continuous encouragement and support. I would've been lost without you. Thank you so much girls.

It has been a pleasure to work with you all, and I wish you all the greatest success and happiness in your future work.

To my parents, thank you for everything. I could not have come this far without you, your advice, your support, your endless encouragement and love. Thank you so much. To my sisters, Tina and Denise, for your endless support and encouragement, your advice, for your friendship and your love, thank you so much. I am very lucky to have been blessed with you as my family.

To Joe, thank you for your love and understanding over these last few years. For the many trips and activities for helping me to de-stress. For your encouragement, advice and support, you made it all that little bit easier, thank you.

To my parents

Kathleen and Brian, with love.

Abstract

The European Centre for Disease Prevention and Control (ECDC) have estimated that on any given day 1 in 18 hospitalised patients have a healthcare-associated infection (HAI) and that a large percentage of these infections are caused by resistant strains of bacteria. With the global spread of antibiotic-resistance and the emergence of bacteria resistant to 'last-resort antibiotics', along with the lack of new classes of antibiotics being discovered, there is an urgent need for antibacterial research.

Herein, three compound families were designed and synthesised in an effort to ascertain a compound with improved antibacterial activity. Each of the compounds synthesised were evaluated for their bacteriostatic activity against the Gram-negative bacteria *Escherichia coli* and *Pseudomonas aeruginosa* and the Gram positive bacterium *Staphylococcus aureus*. A selection of the compounds were also evaluated for their *in vivo* toxicity using the larvae of the greater wax moth, *Galleria mellonella*.

Firstly, a structure-activity relationship (SAR) study of a thiourea-based, bifuctional organocatalyst, which was found to exhibit bacteriostatic activity (MIC_{90} of 4.69-6.25 μg/mL against *E. coli*) comparable to that of vancomycin hydrochloride, was used to assess the structural components responsible for its activity. A number of structural features important for the overall activity of this compound were identified. Additionally, the hit compound and a selection of the SAR study compounds were also found to be non-toxic to the larvae of *Galleria mellonalla*.

Secondly, modifications were made to the C-3 position of the well-known antibacterial quinolone structure. Two functionalities were chosen to replace the quinolone C-3 carboxylic acid, (1) the well-known carboxylic acid bioisostere, the (1*H*)-tetrazole, and (2) a hydroxamic acid. Both the (1*H*)-tetrazole and hydroxamic acid derivatives were found to exhibit bacteriostatic activity similar to that of their carboxylic acid analogues.

Finally, the synthesis of a family of dioganotin(IV) dicarboxylates, including acetates, picolinates and nicotinates, as well as diorgantin(IV) dichlorides and their

complexes with the ligands 1,10-phenanthroline (phen), 1,10-phenanthroline-5,6-dione (dione) and dipyrido[3,2-a:2',3'-c]phenazine (dppz) were also carried out. Of the compounds synthesised, the dibutyltin(IV) derivatives exhibited the broadest range of activity in comparison to the dimethyltin(IV) or diphenyltin(IV) derivatives. The addition of the picolinate or nicotinate group did not promote activity against any of the bacteria. Furthermore, only in the case of $[Ph_2SnCl_2(dione)]$ was there improved activity compared to the organic ligand itself.

Abbreviations

Å	Angstrom
α	Alpha
ADP	Adenosine diphosphate
A/E	Attaching and effacing
AcOH	Acetic acid
AI	Autoinducer
amu	Atomic mass unit
ATCC	American Type Culture Collection
ATP	Adenosine triphosphate
β	Beta
bs	Broad singlet
BuLi	Butyllithium
^{o}C	Degrees Celsius
ca.	Circa
CDC	Centers for Disease Control and Prevention
CF	Cystic fibrosis
CHN	Carbon Hydrogen Nitrogen microanalysis
Clf	Clumping factor
cm^{-1}	Wavenumber
Cna	Collagen-binding protein
CNF	Cytotoxic necrotising factor

^{13}C NMR	Carbon-13 Nuclear Magnetic Resonance
COMU	(1-Cyano-2-ethoxy-2-oxoethylidenaminooxy)dimethylamino-morpholino-carbenium hexafluorophosphate
COSY	Correlation spectroscopy
CRE	Carbapenem-resistant Enterobacteriaceae
δ	Delta
d	Doublet
DCM	Dichloromethane
dd	Doublet of doublets
DIAD	Diispropyl azidodicarboxylate
DIEA	*N,N*-diisopropylethylamine
Dione	1,10-Phenanthroline-5,6-dione
DMF	*N,N*-Dimethylformamide
DMSO	Dimethyl sulfoxide
DNA	Deoxyribonucleic acid
Dppz	Dipyrido[3,2-a:2',3'-c]phenazine
DPPA	Diphenylphosphoryl azide
EARS-Net	European Antimicrobial Resistance Surveillance Network
ECDC	European Centre for Disease Prevention and Control
ECDC-PPS	European Centre for Disease Prevention and Control Point Prevalence Surveillance
eEf	Eukaryotic elongation factor
EHEC	Enterohaemorhagic *Escherichia coli*

EPA	Environmental Protection Agency
EPEC	Enteropathogenic *Escherichia coli*
ESBL	Extended-β-lactamase (ESBL) producing *Escherichia coli*
EtCO$_2$Cl	Ethyl chloroformate
Et$_3$N	Triethylamine
Et$_3$N.HCl	Triethylammonium chloride
Et$_2$O	Diethyl ether
EtOAc	Ethyl acetate
EtOH	Ethanol
^{19}F NMR	Fluorine-19 Nuclear Magnetic Resonance
FBDD	Fragment-based drug design
Fnbp	Fibrinogen-binding proteins
γ	Gamma
g	Gram(s)
GI	Gastrointestinal
GSK	GlaxoSmithKline
h	Hour(s)
HAI	Hospital-associated infection
HCl	Hydrochloric acid
^{1}H NMR	Proton Nuclear Magnetic Resonance
H$_2$O	Water
HOBt	Hydroxybenzotriazole

HOMO	Highest occupied molecular orbital
HSQC	Heteronuclear Single Quantum Correlation
HTS	High-throughput screening
HUS	Haemolytic Uraemic Syndrome
Hz	Hertz
I	Nuclear spin
ID	Inhibitory dose
Ig	Immunoglobulin
IMO	International maritime organisation
IR	Infra-red
J	Coupling constant
KBr	Potassium bromide
K_2CO_3	Potassium carbonate
Kg	Kilogram
KOH	Potassium hydroxide
L	Litre
$LiAlH_4$	Lithium aluminium hydride
LDA	Lithium diisoproplyamide
LTA	Lipoteichoic acid
LPS	Lipopolysaccharide
LUMO	Lowest unoccupied molecular orbital
M^+	Parent molecular ion

μg	Microgram
μM	Micromolar
MDR	Multi-drug resistant
Me	Methyl
MeCN	Acetonitrile
MeOH	Methanol
Me_4Si	Tetramethylsilane
mg	Milligram
MHz	Megahertz
MIC	Minimum Inhibitory Concentration
min	Minute(s)
mL	Millilitre
mmol	Millimoles
m.p.	Melting point
MS	Mass spectrometry
MRSA	Methicillin-Resistant *Staphylococcus aureus*
MSCRAMM	Microbial surface components recognising adhesive matrix molecules
MSSA	Methicillin-Susceptible *Staphylococcus aureus*
M.W.	Molecular weight
$NaBH_4$	Sodium borohydride
NaCl	Sodium chloride
NAD	Nicotinamide Adenine Dinucleotide

NaH	Sodium hydride
n-Bu	n-Butyl
n-BuNH$_2$	n-Butylamine
NCIMB	National Collection of Industrial, Food and Marine Bacteria
NH$_4$OH	Ammonium hydroxide
NH$_2$OH.HCl	Hydroxylamine hydrochloride
NMM	*N*-Methylmorpholine
NOE	Nuclear Overhauser Effect
NMR	Nuclear Magnetic Resonance
o-	Ortho
OD	Optical density
π	Pi
PBP	Penicillin-binding-protein
Ph	Phenyl
Phen	1,10-Phenanthroline
ppm	Parts per million
PVC	Polyvinyl chloride
PVL	Panton-Valentine leukocidin
q	Quartet
QS	Quorum-sensing
rt	Room temperature
s	Singlet

SAR	Structure-activity relationship
SBDD	Structure based drug discovery
Scc	Staphylococcal cassestte chromosome
SE	Staphylococcal enterotoxins
SEM	Scanning electron micrograph
STEC	Shiga toxin *Escherichia coli*
Stx	Shiga toxin
t	Triplet
TA	Teichoic acid
TBTA	Tributyltin azide
TBTU	*O*-(Benzotriazol-1-yl)-*N,N,N′,N′*-tetramethyluronium-tetrafluoroborate
TLC	Thin layer chromatography
T3SS	Type III secretion system
TSS	Toxic shock syndrome
UTI	Urinary tract infections
VHTS	Virtual high-throughput screening
VRSA	Vancomycin-resistant *Staphyloccous aureus*
VTEC	Verotoxin *Escherichia coli*
[α]	Specific rotation (expressed without units, the units are (deg/mL)/(g/dm))
Δν	The difference between the infrared asymmetric and symmetric stretching frequencies

ν_{as} Infrared asymmetric stretching frequency

ν_{sym} Infrared symmetric stretching frequency

Table of Contents

Chapter I: *Introduction*

Chapter II: *A structure-activity relationship study of thiourea-based antibacterial agents*

Chapter III: *A study of quinolone antibacterial agents*

Chapter IV: *A study of organotin(IV) antibacterial agents*

XX

Chapter I

Introduction

1.1 Introduction

Almost one century ago, an outstanding, novel antibiotic was discovered in a London laboratory. Named after the mould from which it was derived, penicillin was active against a host of microbes including Gram-positive bacteria and those responsible for syphilis.[1] It demonstrated bacteriostatic, bactericidal, and bacteriolytic activity but most importantly it was non-toxic to animals.[1] In 1945, its discoverer, Sir Alexander Fleming gave his Nobel lecture entitled 'Penicillin', but it came with a warning:[1]

> *'There is the danger that the ignorant man may easily underdose himself and by exposing his microbes to non-lethal quantities of the drug make them resistant.'*

Two years after the introduction of penicillin the first penicillin-resistant *Staphylococcus aureus* (*S. aureus*) strain was reported.[2] In the 1960s methicillin was introduced and was closely followed by the emergence of the infamous methicillin-resistant *S. aureus* (MRSA).[3] Today, bacterial resistance to antibiotics is a serious public health problem.

The European Centre for Disease Prevention and Control (ECDC) have estimated that on any given day 1 in 18 hospitalised patients have a healthcare-associated infection (HAI).[4] The four most frequently isolated microorganisms from HAIs are *Escherichia coli* (*E. coli*), *S. aureus*, *Enterococcus spp.* and *Pseudomonas aeruginosa* (*P. aeruginosa*).[5] Overall, of the HAIs caused by *S. aureus*, 41% of these are caused by MRSA with 10% of *Enterococci spp.* infections caused by vancomycin-resistant *Enterococci spp.*, 23% of *E. coli* HAIs caused by cephalosporin-resistant strains and 32% of *P. aeruginosa* HAIs caused by carbapenem-resistant strains.[5] According to the ECDC, infections resulting from Gram-negative, multidrug-resistant (MDR) bacteria are on the rise and in Ireland alone the percentage of MDR *E. coli* has increased from 5.6% in 2006 to 13.5% in 2012.[6] In the United States (U.S.) at least 2,000,000 people become infected each year with bacteria that are resistant to one or more of the antibiotics used for treatment of the infection.[7] Of the 2 million infections, approximately 23,000 people die as a direct result of infection by the resistant-bacteria.[7] However, the increase in

existing antibiotic-resistant bacterial infections and emergence of new resistant strains are only half of the problem.

Antibiotics are short-term use drugs, thus the return on investment is not as good as the return from long-term use drugs, such as antidiabetics. Therefore, pharmaceutical companies are not that interested in antibacterial research. Of the classes of antibiotics used today almost all of them belong to classes discovered before the 1980s with the exception of the lipopeptides.[8] Most of the advances that have been made since the 1980s have been by modifications/improvements made to existing antibiotic classes, for example, the fluoroquinolones are more active than nalidixic acid.[8a]

With the global spread of antibiotic-resistance and the emergence of bacteria resistant to 'last-resort antibiotics', along with the lack of new classes of antibiotics being discovered, there is an urgent need for antibacterial research.[7,9]

1.1.1 Drug discovery

There are three main drug discovery methods; 1. whole-cell screening, 2. genomic-based discovery and 3. structure-based drug discovery (SBDD).[8b] Whole-cell screening is the original method by which many of the currently used antibiotics were discovered.[8b] It is a non-target-based, high-throughput screening (HTS) method in which a number of compounds are screened *in vitro* for activity.[10] The mode of action can be investigated after activity has been established.

Structure-based discovery is a newer, *in silico* drug discovery method that includes virtual HTS (VHTS) and fragment-based drug discovery (FBDD).[8b,11] This method involves the design of compounds based on the structure of the desired target.[11] The target structures are determined using X-ray crystallography and uploaded on to a computer.[11] Molecular modelling software is then used to design novel compounds that have good affinity for the target binding sites.[11] Once designed, the compounds can be synthesised and tested *in vitro* with their targets.[11] SBDD has a lot of potential, however, although it may produce compounds that have a good binding affinity for a given target, the compound may not exhibit antibacterial activity.[12] This has already been observed in SBDD studies for antibacterial agents and may be due

to a compounds lack of ability to transverse the cell membrane thus preventing it from reaching its target.[12]

Genomic-based discovery is a method that involves the sequencing of pathogen genomes and the identification of genes that are conserved amongst a given group of pathogens, which encode targets that lack mammalian cell homologues.[8a] A HTS of existing compound libraries is then ran to identify molecules that may bind to, and inhibit these targets.[8a] This method sounds very promising and was embraced by a number of pharmaceutical companies but unfortunately gave very disappointing results.[8a,10] GlaxoSmithKline (GSK) spent a number of years (1995-2001) exploring the genomics-derived, target-based approach. Over 350 genes were evaluated, out of which 67 HTS were carried out using 260,000-530,000 compounds.[10] Of the 67 HTS, 16 hits were found and only 5 of these resulted in lead compounds. According to Payne *et al*.[10], lead compounds from only one of the targets are still being pursued. However, none of the lead compounds from the genomics-based discovery approach have made it to the market.[8a,10] As a result, GSK changed their strategy. GSK went back to known antibacterials and investigating ways to improve them for example, pleuromutilins, and at the same time shifted back towards an 'old-fashioned' whole-cell screening approach through which they have found a novel class of compounds.[10,13]

For our research into potential antibacterial compounds we decided to take a similar, whole-cell screening approach, as was used by GSK. Our research included an investigation into new antibacterial compounds through a structure-activity relationship (SAR) study of a well-known compound, an attempt to optimise an existing antibacterial compound and the synthesis and optimisation of both known and new metal-based compounds that may exhibit antibacterial activity. Herein, three families of compounds have been synthesised and evaluated against three bacterial species that are frequently isolated in HAIs and are known for developing resistance to antibiotics.

1.1.2 The bacteria

For this study, two Gram-negative bacteria, *Escherichia coli* (*E. coli*) and *Pseudomonas aeruginosa* (*P. aeruginosa*), and one Gram-positive bacterium, *Staphylococcus aureus* (*S. aureus*), were chosen. The details for the bacterial strains are shown in Table 1.1, section 1.2.2. Compounds were tested for their bacteriostatic activity (ability to inhibit bacterial growth) using the susceptibility assay described in section 1.2.5. The details of the procedure are given in section 1.2.5.

1.1.3 Bacteria cell structure
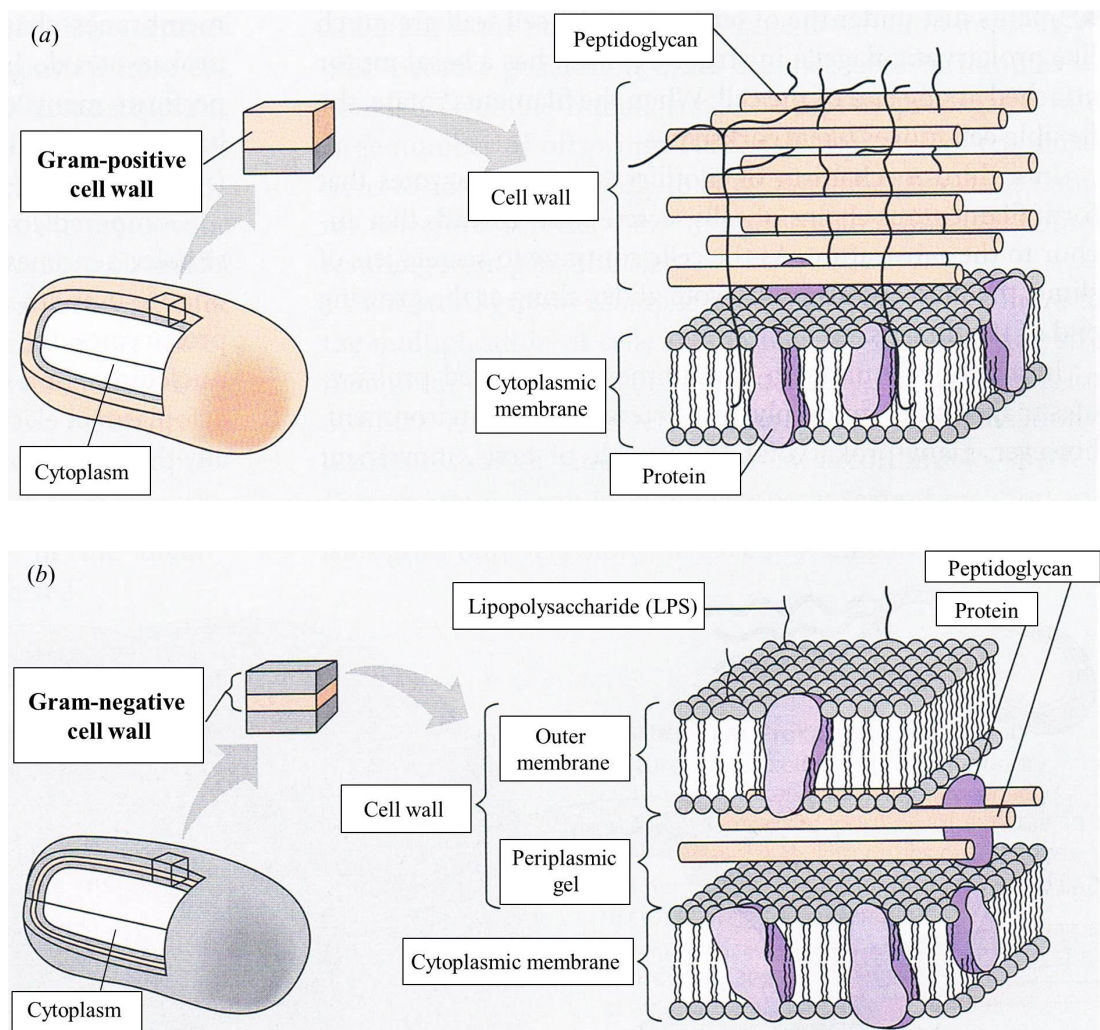
Figure 1.1: Bacteria cell structures for (*a*) Gram-positive bacteria, and (*b*) Gram-negative bacteria.[14]

Bacteria are prokaryotes and can be identified by their shape. The three most common shapes are spheres (cocci), rods (bacilli) and helices (spirilla and spirochetes).[14] Bacterial cells are (1-5 µm in diameter) made up of a cytoplasm centre, containing the nucleoid, surrounded by a cytoplasmic membrane (Figure 1.1). The cytoplasmic membrane is surrounded and supported by a cell wall.[14] Bacteria can be assigned to two main groups based on differences in their cell walls, that is, Gram-positive and Gram-negative bacteria.

As shown in Figure 1.1, the cell wall of a Gram-positive bacterium is larger than that of the Gram-negative bacterium and is made up of mainly peptidoglycan. The Gram-negative cell wall is made up of an outer membrane containing lipopolysaccharide (LPS) and a peptidoglycan layer. Cell membranes are made up of glycerolphospholipid bilayers (Figure 1.2).[14-15]
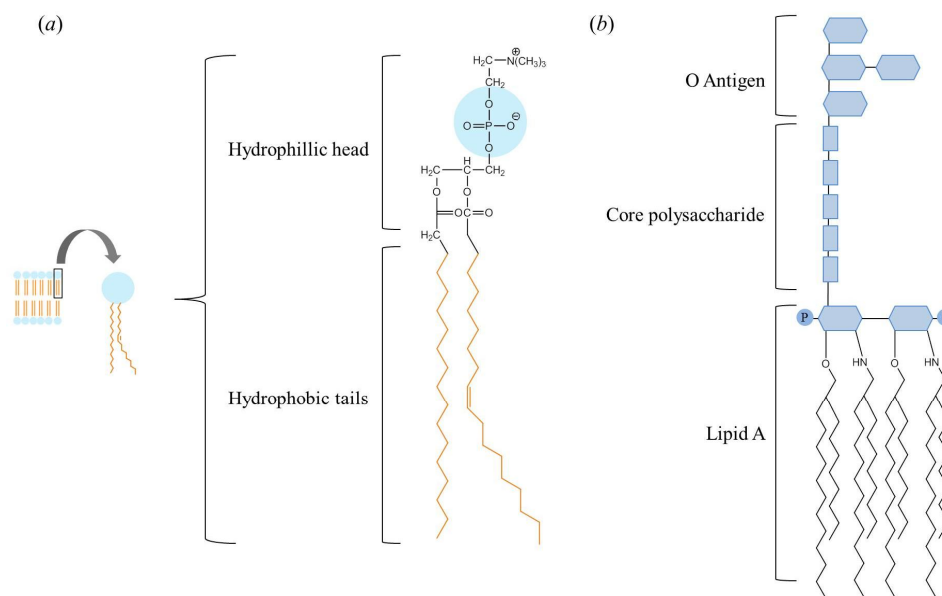
Figure 1.2: Representative structures of (*a*) a phospholipid (phosphatidylcholine) and (*b*) LPS.[14,16] LPS consists of three domains; 1. lipid A, made up of a disaccharide diphosphate and fatty acid chains, 2. the core polysaccharide and 3. the O Antigen.

The presence of unsaturated fatty acid residues prevent the tight packing of hydrocarbon chains resulting in lipid bilayers that are fluid in nature.[15] LPS contain

saturated fatty acid residues, which allow for the tight packing of hydrocarbon chains and thus decreases the fluidity of the membrane (Figure 1.2).[15] Furthermore, in comparison to the phospholipid that has only two fatty acid residues, LPS also has additional covalently linked fatty acid chains.[17] The reduced fluidity of the Gram-negative bacteria outer membrane prevents rapid penetration of lipophilic molecules which in turn makes Gram-negative bacteria difficult to treat in comparison to Gram-positive bacteria.[17-18]

1.1.4 *Staphylococcus aureus*

Saphylococcus aureus (*S. aureus*) is a spherical Gram-positive bacterium (Figure 1.3), distinguished from other staphylococcal species by its gold pigmentation.[19] A commensal, found primarily in the anterior nares, *S. aureus* colonizes approximately 20% of the human population.[20] The cell wall of *S. aureus* is 50% peptidoglycan (by weight) and also contains teichoic (TAs) and lipoteichoic acids (LTAs).[21] *S. aureus* has a variety of surface and secreted components that enable it to compromise immune responses and evade host defences.
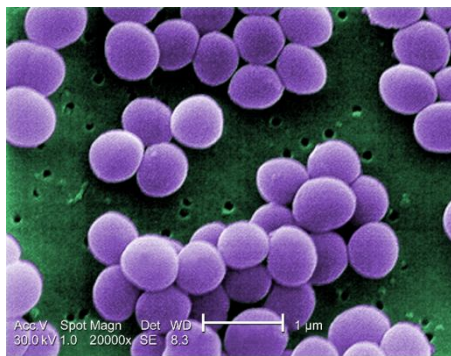
Figure 1.3: Scanning electron micrograph (SEM) of *S. aureus* (magnification 20,000x), a spherical Gram-positive bacterium.[22]

Infections of *S. aureus* occurs when a breach in the host's physical defences, the skin or mucosal barriers, allows access to adjoining tissues or the bloodstream.[19] The risk of infection is increased in patients after surgery, and by the presence of foreign materials, such as long-term indwelling catheters which have led to cases of nosocomial endocarditis.[19-20] Initial attachment of *S. aureus* to surfaces is mediated by several cell-associated proteins, the microbial surface components recognising

adhesive matrix molecules (MSCRAMMs).[20b,21] The fibrinogen-binding proteins (Fnbp), FnbpA and FnbpB, the collagen-binding protein (Cna) and the fibrinogen-binding proteins clumping factor (Clf), ClfA and ClfB, are the most well-known MSCRAMMs.[20b,21] Once attached, *S. aureus* has an army of toxins it can unleash on its host facilitating the progression of infection.

The majority of *S. aureus* strains can secrete four haemolysins, α-, β-, γ- and δ-haemolysin.[23] These cytolytic toxins work by damaging the membranes of host cells.[20a,23] Of the four toxins, α-haemolysin has been studied the most and is known for its ability to lyse erythrocytes.[23] It works by integrating into the target cell membrane where it forms cylindrical heptamers, resulting in a pore (1-2 nm) in the membrane. This pore allows for the rapid efflux and influx of ions and other small molecules leading to osmotic swelling of the cell causing the cell to rupture.[23] γ-Haemolysin and the Panton-Valentine (PV) leukocidin are bi-component leukotoxins. These toxins are made of two, non-associated secreted proteins, S and F, which can combine in six different forms, each of which can lyse leukocytes.[23]

S. aureus can also produce eight staphylococcal enterotoxins (SEA, SEB, SEC, SED, SEE, SEG, SEH, SEI) and toxic shock syndrome toxin-1 (TSST-1).[20a,23] The SE's are known to be the causative agent of staphylococcal food poisoning (SFP), a condition that usually resolves itself after 24-48 hours.[23] However, TSST-1 causes toxic shock syndrome (TSS), an acute and potentially fatal condition.[20b]

Not only can *S. aureus* compromise its host but it also has a number of virulence factors that facilitate its evasion of the host's immune response. *S. aureus* has an outer layer, known as a capsule, made up of polysaccharides. The capsule prevents binding of opsonins which in turn reduces the uptake of *S. aureus* cells by phagocytes.[19-20] Protein A, a cell surface protein, can bind the opsonin IgG. However, it binds IgG in such a way that it is presented to the neutrophil in the incorrect orientation thus preventing the binding of the neutrophil and its ability to engulf the cell.[20a] If *S. aureus* is engulfed by a phagocyte it has the ability to survive within the phagosome.[20a] For example, modifications of TAs can reduce the affinity of cationic antimicrobial defensin peptides that are secreted into the phagosome.[20]

The expression of a variety of the *S. aureus* virulence factors are controlled by its quorum-sensing (QS) system.[24] Quorum-sensing is a process by which bacterial cells communicate through the production and detection of signalling molecules known as autoinducers (AIs).[25] Gram-positive bacteria have two QS systems, the accessory gene regulator (*agr*) QS system and the *luxS* QS system.[24] The *agr* system has been shown to be essential in the virulence of *S. aureus* infection.[24] It is believed that the *agr* system also influences the formation of biofilms by *S. aureus*.[24]

Biofilms are sessile microbial communities of cells, enclosed in a self-produced exopolymer matrix (Figure 1.4).[26] Bacterial biofilms can prevent or delay the entry of antimicrobial agents, deactivate antimicrobial agents and produce persister cells.[26-27] Persister cells are cells that do not grow or die in the presence of antimicrobial agents thus enabling the survival of bacteria populations.[27]
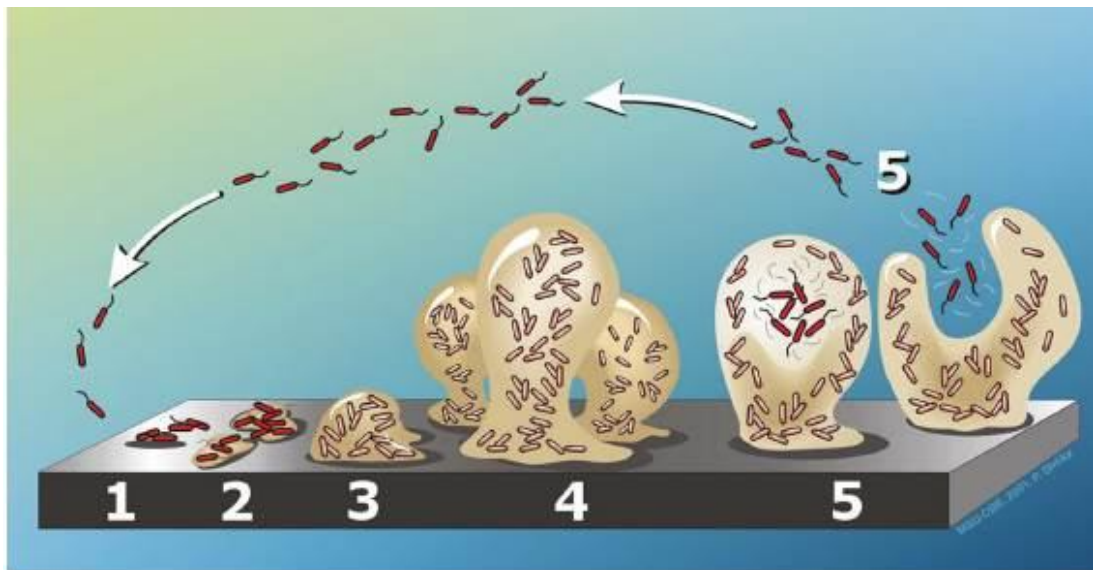
Figure 1.4: Biofilm stages of development; 1. Reversible adherence, 2. Irreversible adherence, 3. Maturation, 4. Microcolony development, 5. Dispersion of cells from the biofilm.[28]

S. aureus has also been successful at developing resistance to antibiotics. Penicillin was first introduced in the 1940s, however, two years later the first penicillin-resistant *S. aureus* strain was reported.[2] Methicillin was introduced in 1960 and in the following year Methicillin-Resistant *S. aureus* (MRSA) strains were isolated.[3]

Methicillin-resistance of *S. aureus* stems from a genetic element known as the staphylococcal cassestte chromosome *mec* (SCC*mec*).[29] In Methicillin-susceptible *S. aureus* (MSSA) strains, the cell walls contain penicillin-binding-proteins (PBPs). β-Lactam antibiotics bind to the PBPs resulting in the disruption of the synthesis of the peptidoglycan layer and preventing cell survival.[2] SCC*mec* carries the *mec* gene complex which encodes PBP2a.[29] PBP2a has a low affinity for β-lactam antibiotics.[30] The presence of PBP2a prevents β-lactam antibiotics from binding to the cell wall and disrupting the synthesis of peptidoglycan thus allowing MRSA to survive.[2]

Although we have seen a decrease in the rate of MRSA infection across Europe, *S. aureus* is still the second most frequently isolated microorganism in HAIs.[5,31] Furthermore, in 1996, a MRSA strain resistant to vancomycin was isolated in Japan.[32] Vancomycin, often referred to as a drug of 'last resort', has been the drug of choice to treat MRSA infections.[7] In addition to Japan, a number of vancomycin-resistant *S. aureus* (VRSA) strains have since been reported around the world.[7,32] *S. aureus* is an ever evolving pathogen with an ability to evade both host and external defences. A bacterium that is always one step ahead.

1.1.5 *Pseudomonas aeruginosa*

Pseudomonas aeruginosa (*P. aeruginosa*) is a Gram-negative bacillus, commonly found throughout the environment in water, vegetation and soil (Figure 1.5).[33] When given the opportunity, *P. aeruginosa* can cause serious infections in humans. *P. aeruginosa* infections usually occur in patients that have an underlying disease or injury with three of the most common sites of *P. aeruginosa* infection being in burn wounds, the cornea and the lung.[33b,34] Infections can range from acute infections such as endocarditis and septicemia to chronic lung infections in people with cystic fibrosis (CF).[35] Approximately 80% of CF patients may be colonised with *P. aeruginosa*.[33a]
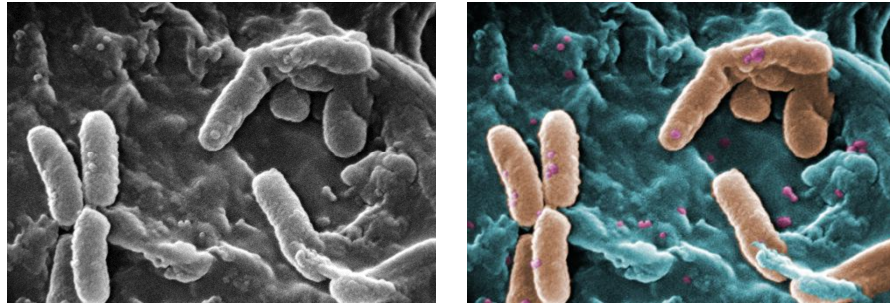
Figure 1.5: SEM and colourised version of SEM of *P. aeruginosa*, a rod-shaped Gram-negative bacterium.[22]

Being a Gram-negative bacterium, *P. aeruginosa* has the advantage of an additional outer membrane assisting in its resistance to antibiotics. With the reduced fluidity of the Gram-negative outer membrane, however, the bacterium needs an alternative method by which it takes up nutrients and disposes of waste products. This is carried out by pores or channels known as porins.[17] *P. aeruginosa* lacks the 'classical' high permeability porins that are found in most Gram-negative bacteria.[15] The porin protein, OprF, the homolog of the *E. coli* porin protein, OmpA, only produces channels when it is folded into a rare conformation.[18] Furthermore, in comparison to OmpA of *E. coli*, the diffusion of molecules through the *P. aeruginosa* OprF channel is two orders of magnitude slower.[36] The presence of an outer membrane and inefficient porins makes *P. aeruginosa* intrinsically very resistant to antibiotics.

In addition to the permeability barriers, *P. aeruginosa* also has an arsenal of membrane-bound and secreted virulence factors. *P. aeruginosa* possess straight, filamentous appendages on the cell surface known as pili, specifically type IV pili.[37] They are retractable structures responsible for adhesion to the host cell surface but also give the bacterium a unique form of movement known as twitching motility.[37-38] Type IV pili consist of a hollow, cylindrical structure made up of pilin proteins with the region responsible for adhesion presented at the top of the pilus.[37] Studies have shown that *P. aeruginosa* pili are responsible for approximately 90% of the adherence to human lung cells and that they can discriminate between healthy and damaged canine tracheal cells.[37]

Another important adhesin associated with *P. aeruginosa* is alginate. Alginate is a linear co-polymer exopolysaccharide that forms a capsule-like structure around the *P. aeruginosa* bacterium.[18] As mentioned earlier, *P. aeruginosa* are a particular problem for CF patients. One of the reasons for this being that it undergoes a phenotypic change from non-mucoid to mucoid (alginate-producing) *P. aeruginosa* in the lungs of chronically infected CF patients.[39] The mucoid, capsule-like structure can act as a barrier against phagocytes and opsonisation, it may also be capable of acting as an immunomodulator and may be involved in the formation of biofilms, all of which contribute to the pathogenesis of *P. aeruginosa*.[39]

Once adherence has been established there are a number of secreted proteins that play a part in the progression of *P. aeruginosa* infection. The most toxic substance secreted by *P. aeruginosa* is exotoxin A.[35] Exotoxin A binds to a receptor known as CD91 on the host cell surface. Once bound, it is internalized into the cell where it is broken down into N-terminal and C-terminal fragments.[35] The C-terminal fragment makes its way to the endoplasmic reticulum and on to the cytosol where it catalyzes the ADP ribosylation of the eukaryotic elongation factor-2 (eEF-2).[35] The ADP ribosylation of eEF-2 results in the inhibition of protein synthesis and ultimately cell death.[35,40] Other virulence factors secreted by *P. aeruginosa* include; elastases LasA and LasB, type III secretion system (T3SS) effector proteins ExoS, ExoT, and ExoU, and phenazines such as pyocyanin.[33b,40] Pyocyanin gives the green-blue colour to pus associated with *P. aeruginosa* infections.[33b,41] *P. aeruginosa* are also well-known for their ability to form biofilms. Chronic *P. aeruginosa* infections of the lungs of CF patients are associated with biofilm formation.[40,42]

As with *S. aureus*, a number of the *P. aeruginosa* virulence factors are controlled by its QS system including; alginate, exotoxin A, elastase, pyocyanin and biofilm formation.[43] *P. aeruginosa* has two QS systems, the *lasI* system that encodes for the AI known as PAI-1 and the *rhlR*/*rhlI* system the AI of which is PAI-2.[43]

The European Centre for Disease Prevention and Control Point Prevalence Surveillence (ECDC-PPS) report 2011-2012 listed *P. aeruginosa* as the fourth most frequently isolated organism in HAIs.[5] *P. aeruginosa* infections are difficult to

eradicate due to its intrinsic resistance, however, as observed with *S. aureus*, *P. aeruginosa* strains resistant to antibiotics have also been isolated. Resistance due to the loss of porins has been observed in *P. aeruginosa* isolates, for example, the loss of OprD resulted in resistance to imipenem.[15]

P. aeruginosa is particularly known for its multidrug resistance. Multidrug resistance is a mechanism of resistance that involves drug efflux by membrane transporters.[44] It has been demonstrated that the expression of efflux systems in *P. aeruginosa* is greatest when the bacteria is under stress, for example, growth in a nutrient poor medium.[45] In the case of *P. aeruginosa*, active efflux pumps contribute significantly to its multidrug resistance.[46] These pumps are composed of three subunits, the pump protein, an outer membrane channel and an accessory protein (Figure 1.6).[18] The mexA-OprM efflux system is the most well known in *P. aeruginosa* and is responsible for the efflux of fluoroquinolones, β-lactams, tetracyclines and erythromycin.[36,47] The U.S. Department of Health and Human services Centers for Disease Control and Prevention (CDC) have classified *P. aeruginosa* infections as a serious threat with 13% of severe HAIs being caused by multidrug resistant (Mdr) *P. aeruginosa*.[7]
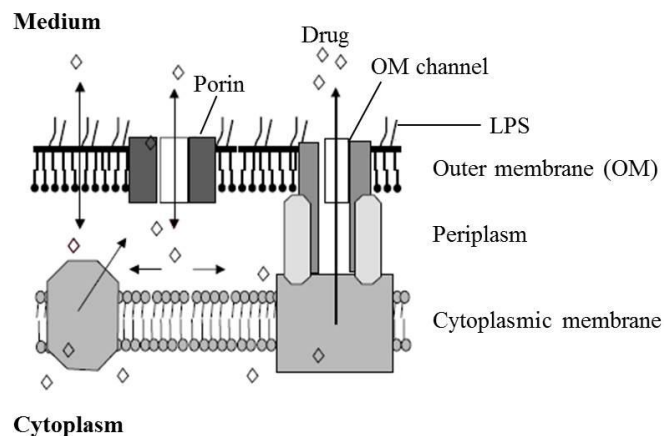
Figure 1.6: Schematic of a Gram-negative bacterial efflux pump. Drugs can transverse the outer membrane through the LPS/lipid bilayer or through porin channels. From the cytoplasm they are brought into the periplasm where they are expelled from the cell by the efflux pump.[48]

1.1.6 *Escherichia coli*

A Gram-negative, rod shaped bacterium, *Escherichia coli* (*E. coli*), is found in the gastrointestinal (GI) tract of healthy humans and other animals (Figure 1.7).[49] However, some *E. coli* strains are pathogenic. The two most common infections associated with *E. coli* are urinary tract infections (UTIs) and diarrhoeal infections.[50] UTIs are caused by *E. coli* that spread from the gut to the sterile urinary tract.[50] The clinical syndromes of UTIs are dependent on the location of infection, that is, cystitis is a lower UTI and pyelonephritis is an upper UTI.[50] Pyelonephritis can be associated with septicaemia.[50] There are a number of *E. coli* pathotypes associated with diarrhoeal infections, two well-known pathotypes being enteropathogenic *E. coli* (EPEC) and enterohaemorhagic *E. coli* (EHEC).[49,51] The main difference between these two pathotypes is that, EHEC produces Shiga toxins (Stx) whereas EPEC do not produce a detectable toxin.[50] EHEC is also commonly referred to as VTEC (verotoxin *E. coli*) or STEC (Shiga toxin *E. coli*).[51a]
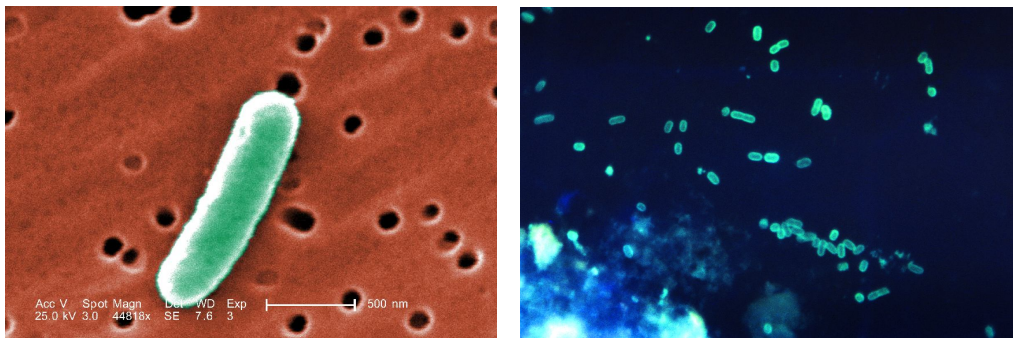
Figure 1.7: SEM of a single Gram-negative *E. coli* bacterium (left) and a fluorescent antibody-stained photomicrograph (right) of *E. coli* found in a faecal smear.[22]

EPEC is associated with diarrhoea in young children in developing countries with transmission linked to close human contact, for example, in nurseries.[50,51b] EHEC is transmitted through food, water and animal contact (in particular ruminants) and as the name suggests causes bloody diarrhoea.[49,51b] Approximately 10% of EHEC cases go on to develop Haemolytic Uraemic Syndrome (HUS), a clinical syndrome that leads to renal failure.[49] Children under the age of five and the elderly are most at risk.[49,52] Over 90% of HUS cases are believed to be caused by EHEC.[49]

The pathogenesis of *E. coli* can be attributed to a number of virulence factors. As with other Gram-negative bacteria, *E. coli* has an outer membrane containing LPS and porins.[18] A combination of LPS and small size porin channels gives *E. coli* greater protection against antibiotics in comparison to Gram-positive bacteria.[17-18] *E. coli* can also form capsules made up of linear polymers of repeating carbohydrate subunits known as K antigens.[50] Encapsulated *E. coli* are usually more virulent than unencapsulated *E. coli.* with the quantity of K antigen being proportional to the degree of virulence.[53] The capsule is believed to protect the bacteria from phagocytosis.[53]

E. coli also produces a number of toxins including haemolysins and cytotoxic necrotising factor 1 (CNF1).[50] *E. coli* have three haemolysins, α-, β-, and γ-haemolysin, all of which can lyse red blood cells.[51b] CNF1 has been shown to cause the necrosis of rabbit skin and also has the ability to induce the reorganisation of the host actin cytoskeleton.[50,54] Pathogenic EHEC also produces two types of Shiga toxins, SLT-I and SLT-II.[50,52] Ninety-seven per cent of EHEC strains produce SLT-II with or without SLT-I.[50] These Shiga toxins are internalised by host cells in which they inhibit protein synthesis resulting in cell death.[52] The production of Shiga toxins is required for the development of renal complications with SLT-II shown to be responsible for HUS in mice.[50]

A particularly important step in initiating infection is the initial adherence to the host cell surface. A characteristic feature of EHEC and EPEC infection is the formation of 'attaching and effacing' (A/E) lesions (Figure 1.8).[55] The formation of A/E lesions can be divided into three stages, initial adherence, signal transduction through secreted proteins, and intimate attachment.[56]
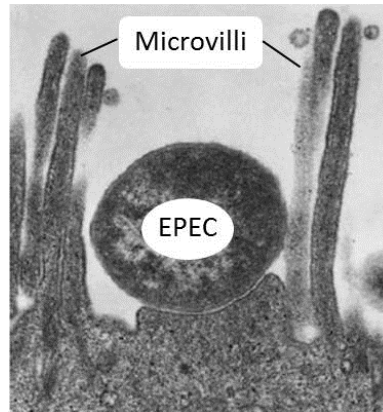
Figure 1.8: A/E lesion formed by EPEC.[57]

For initial adherence *E. coli* use filamentous cell surface appendages known as fimbriae. Specifically, EPEC uses type IV pili known as bundle forming pili (BFP).[56] Little is known of the EHEC adhesins.[51b] Once fimbriae adhere to the host cell surface, EPEC and EHEC have a T3SS that can translocate effector proteins into the host cell.[55] The Tir protein is an effector protein that is translocated to the host cell where it can act as a receptor for intimin, a bacterial outer membrane protein.[55-56] Intimin binds to Tir to give an irreversible intimate cell attachment that results in downstream signalling events leading to the reorganisation of actin filaments of the host cell cytoskeleton.[55] This reorganisation results in the formation of actin pedestals directly beneath the bacterial attachment sites (Figure 1.9).[55] The exact role of pedestals in the pathogenesis of EHEC and EPEC is not fully understood but it has been suggested that actin assemblies may be involved in the expansion and proliferation of *E. coli* infection.[58] Pedestals may also help resist bacterial detachment during diarrhoea.[58]
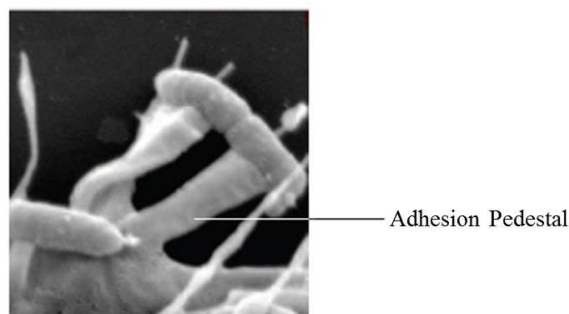
Figure 1.9: EPEC adhesion pedestal formed on a eukaryotic cell.[59]

Unlike most Gram-negative bacteria, *E. coli* does not produce the AHL autoinducers.[28] However, it does produce AI-2, an autoinducer which is believed to be involved in interspecies communication, as it is produced by both Gram-negative and Gram-positive bacteria.[25,60] AI-2 is regulated by the *luxS* QS system.[60] Regulation of the T3SS of EHEC and EPEC by the QS system has been observed.[61] It has been suggested that the low infection dose of EHEC (as low as two or three *E. coli*) may be due to the ability of non-pathogenic *E. coli* to produce AI-2 in turn activating the T3SS of EHEC.[49,61] Furthermore, studies have shown that the flagella (a cell surface appendage involved in cell locomotion[14]) and motility of *E. coli* are regulated by its QS system, as well as *E. coli* biofilm formation.[28,60,62] The ability to form biofilms, as with other bacteria, may help in the resistance of *E. coli* to antibiotics.[28,63]

According to the ECDC-PPS report 2011-2012 *E. coli* is the most frequently isolated organism in HAIs.[5] As seen with *P. aeruginosa*, the multidrug resistance of *E. coli* has been associated with the over expression of efflux pumps.[45] The AcrAB-TolC efflux system is the predominant efflux pump in *E. coli* and has the ability to efflux fluoroquinolones, β-lactams, novobiocin, and rifampicin as well as some dyes and organic solvents.[45,48]

E. coli can also produce β-lactamases and in the last few years extended-β-lactamase (ESBL)-producing *E. coli* have emerged as an important cause of UTIs.[64] ESBL-producing *E. coli* that exhibit cross-resistance to gentamicin and ciprofloxacin have also been reported.[64] The 2013 first quarter EARS-Net report has shown that from 2004 to 2012 the number of extended spectrum β-lactamase-producing (ESBL) *E. coli* infections has been continuously increasing (1.1% in 2004 to 9.5% to the end of quarter one in 2013).[6b] Furthermore, carbapenemems are considered the drug of last resort for the treatment of these multiresistant *E. coli*, however, carbapenem-resistant *E. coli* are also on the rise.[65] The CDC have classified carbapenem-resistant Enterobacteriaceae (CRE) infections as an immediate public health threat.[7] Of the estimated 9000 CRE infections in the U.S. per year, 1,400 of these are carbapenem-resistant *E. coli* infections.[7]

1.1.7 The immune system

In mammals, there are two systems involved in the protection from and response to infection by an invading pathogen. These systems are known as the innate and specific adaptive immune response.[66] The innate immune response is the first line of defence and also plays a role in the initiation of the adaptive immune response, a system responsible for long-lasting protective immunity.[66]

Insects and mammals have been shown to share many similarities in their innate immune systems.[67] For example, the cuticle of insects provides a physical barrier preventing the entry of pathogens, a feature similar to the skin of mammals.[66-67] When a pathogen enters the human body, cells known as macrophages and neutrophils can bind to the microbe and engulf them by a process known as phagocytosis.[66] The resulting, microbe-containing phagosome can fuse with lysosomes which release substances such as lysozyme that digest the microbe.[66] In insects, within the haemolymph (analogous to the blood of mammals), haemocytes or blood cells are responsible for the phagocytosis of foreign bodies.[67a] Lysozyme has also been found in insect haemocytes along with a number of antimicrobial peptides similar to those found in mammals, such as defensins and transferrin.[67a,b] These similarities, along with many others, between the innate immune system of insects and mammals have led to the use of insects as *in vivo* models for investigating the virulence of many human pathogens including Gram-negative bacteria, Gram-positive bacteria and fungi.[68]

1.1.8 *Galleria mellonella* and insects as *in vivo* models

The greater wax moth, *Galleria mellonella* (*G. mellonella*), is of the order Lepidoptera and the family Pyralidade.[67a] *G. mellonella* live in beehives in which the larvae feed on the honeycomb and undergo metamorphosis to become a grey moth (Figure 1.10).[67a,69] As shown in Figure 1.11 the *G. mellonella* larvae are a dull white colour and approximately 3 cm in length.

Figure 1.10: Adult wax moth *Galleria mellonella* (printed with permission).[69]

9 cm
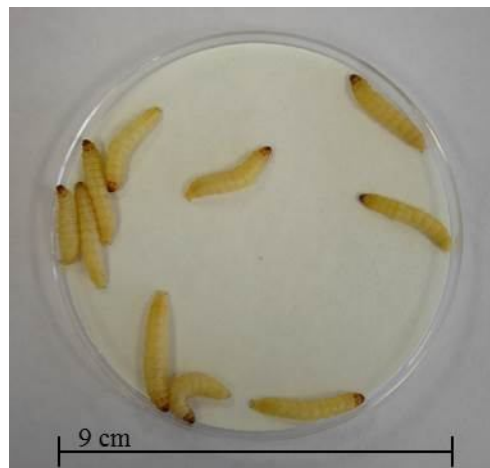
Figure 1.11: *G. mellonella* larvae.

G. mellonella larvae have been used as an *in vivo* model in a number of studies to investigate the virulence of human pathogens. For example, Peleg *et al*.[68e] have demonstrated that *G. mellonella* can be used to investigate both the virulence and the relationship between the pathogensis of *S. aureus* and drug resistance. Studies by Cotter *et al*.[68c] have shown that the wax moth larvae could be used to differentiate between non-pathogenic and pathogenic strains of *C. albicans*. Furthermore, Brennan *et al*.[68d] have demonstrated that there is a high degree of similiarity between the *G. mellonella* and the mouse innate immune response to infection by *C. albicans*. Similar studies investigating the virulence of the Gram-negative bacterium *P. aeruginosa* have shown that there is a positive correlation between the virulence of

P. aeruginosa in both *G. mellonella* and in mice and that insects are a suitable model for identifying and characterising virulence genes.[68b]

An important phase in drug discovery is the assessment of the toxicity of new drug candidates. Before a new drug candidate can reach the clinic it needs to be tested to ensure it is safe and effective.[11] Toxicity testing is usually carried out using animal models such as mice, rabbits, dogs and monkeys.[11] However, the use of mammalian models is expensive, labour intensive, time consuming and requires full ethical consideration. Insects such as *G. mellonella* are lower in cost, do not require a large amount of space for storage and experimental work and can give results within 24 to 48 hours. These advantages combined with the similarity to the mammalian innate immune system render insects a useful preliminary model for the *in vivo* testing of new drug candidates.

Drosphilia melanogaster (fruit fly) has been used to evaluate the therapeutic effect of known antifungals, alone and in combination, against *Aspergillus fumigatus*.[68g] The silkworm, *Bombyx mori*, have also been used to evaluate the effect of current clinical antibiotics against bacterial and fungal infections.[68a] The results obtained were consistent with those reported in mice models.[68a] Furthermore, silkworms have also been employed in investigations of the toxicity and metabolism of known compounds.[68f] These studies gave results consistent with those observed in mammals demonstrating that insects are a good model for studying the *in vivo* therapeutic effect of antibiotics.[68f]

G. mellonella have also been used to evaluate both the therapeutic effect of current and novel antimicrobial agents and the *in vivo* tolerance of novel antimicrobial agents.[70] Desbois *et al*.[70a] have shown that the treatment of *G. mellonella* infected with *S. aureus* using vancomycin, daptomycin or penicillin improved survival of larvae in a dose dependant manner. However, treatment of MRSA infected *G. mellonella* with penicillin did not improve the survival of the wax moth larvae. The doses administered to the infected *G. mellonella* that were most effective, were similar to those recommended for use in humans.[70a] An investigation into the toxicity of copper(II) and silver(I) complexes by McCann *et al*.[71] have demonstrated

that the level of toxicity exhibited by the test compounds in *G. mellonella* was similar to that observed in Swiss mice.

Although the use of mammals as *in vivo* models for testing new drug candidates is necessary, *G. mellonella* can be used as a good preliminary *in vivo* toxicity model. On average, only 500 compounds out of 10,000 compounds synthesised will reach animal testing with only 10 reaching phase one clinical trials.[11] The use of insects allows for the early optimisation of compounds that exhibit therapeutic potential which in turn reduces the number of mammals used. Insect experiments may also be able to supply information relating to suitable dosages and drug metabolism.[68f,70a]

1.1.9 *In vivo* toxicity using *G. mellonella*

G. mellonella are very easy to work with. In general, experiments are carried out in triplicate using ten healthy *G. mellonella* per experiment, within three weeks of receiving the larvae. As shown in Figure 1.12, test compounds can be administered into the haemocoel (body cavity) *via* injection into the last left pro-leg. By applying gentle pressure to the sides of the leg, the base of the pro-leg opens and will re-seal once the syringe needle has been removed, without leaving a scar (Figure 1.12). This needs to be carried out with care as rough handling of the larvae can affect survival and lead to expression of stress proteins.[72] To ensure proper handling of the larvae an injected control can be used whereby the larvae are injected with the appropriate syringe needle but no substance is administered.
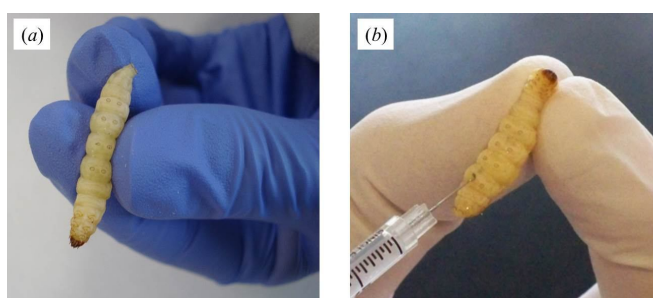
Figure 1.12: Compound administration to *G. mellonella* larvae, (*a*) apply pressure to the sides of the larva to open the base of the pro-leg and (*b*) inject into the haemoceol through the last left pro-leg (reproduced from *Fungal Biol. Rev.* 24 (**2010**) with permission).

A detailed account of the toxicity assay procedure is given in section 1.2.8. The toxicity of a given compound is determined by calculating the percentage of *G. mellonella* larvae that survive over a period of 72 hours. The larvae are monitored every 24 hours and death is assessed based on a lack of movement in response to stimulation together with discolouration of the cuticle (Figure 1.13). Melanisation (discolouration of the cuticle) and development of the larvae (Figure 1.14) can also be monitored to determine if the larvae are responding to the test compound and if it is effecting larval development.

Figure 1.13: A dead *G. mellonella* larva.

Figure 1.14: *G. mellonella* pupal stage of development.

1.2 Biological studies

1.2.1 Materials and methods

Nutrient Broth was obtained from Scharlau Microbiology.

Nutrient Agar was obtained from Oxoid Ltd.

OD_{600nm} values were determined using a spectrophotometer (Biophotometer, Eppendorf).

Optical density was read using a microplate reader (Bio-Tek. Synergy HT Spectrophotometer).

A TOMY SX-500 E autoclave ($121^{o}C$ and 18 lb/sp.in) was used for the sterilization of all growth media and materials required for aseptic techniques.

1.2.2 Bacterial strains

The bacterial strains used in this study are shown in Table 1.1.

Table 1.1: Bacterial strains used in this study

Bacterial strain	Origin	Reference
Staphylococcus aureus	Urinary tract infection, St. James' Hospital, Dublin	Clinical Isolate
Escherichia coli	Gastro-intestinal tract infection, St. James' Hospital, Dublin	Clinical isolate
Pseudomonas aeruginosa 10145	American Type Culture Collection (ATCC) Marassas, VA, USA	ATCC

1.2.3 Media for culturing bacteria

Nutrient Broth

Nutrient Broth was prepared according to the manufacturer's instructions by dissolving 13 g/L in distilled water and autoclaved prior to use.

Nutrient Agar

Nutrient agar was prepared according to the manufacturer's instructions by dissolving 28 g/L in distilled water and autoclaved. The warm agar was poured into sterile 9 cm petri dishes and allowed to set. The nutrient agar petri dishes were stored at 4 $^{\circ}$C.

1.2.4 Bacterial culture conditions

For long term storage, all parent bacterial stocks were stored at -70 $^{\circ}$C in a sterile mixture of 50% (v/v) glycerol and 50% nutrient broth media (v/v). For short term storage, bacterial strains were grown on nutrient agar plates at 37 $^{\circ}$C for 24 hours and stored at 4 $^{\circ}$C. Working stocks of the bacteria were routinely sub-cultured onto fresh agar plates every 4-6 weeks.

1.2.5 Susceptibiltiy assay

The bacterial strains used in this study are shown in Table 1.1, section 1.2.2.

All workspaces were washed down with 70% (v/v) ethanol prior to use. Bacterial strains were taken from nutrient agar plates and cultures were grown in nutrient broth overnight in an orbital shaker at 37 °C and 200 rpm in a fully aerated conical flask. The cells were diluted to give an $OD_{600} = 0.1$.

Fresh solutions (200 μg/mL) of the complexes were prepared with distilled water and less than 1% DMSO immediately prior to testing. Complexes with low solubility were tested as fine suspensions.

Nutrient broth (100 μl) was added to each well of a 96-well flat-bottomed microtitre plate. An additional 100 μl was added to columns 1 and 2 of the plate. Serial dilutions (1:1) of the test complex were made from columns 12-4 giving a test

concentration range of 100–0.39 μg/mL. For example, 100 μL of the compound solution was added to column 12, and mixed thoroughly using the pipette, followed by the transfer of 100 μL of the final solution in column 12 to column 11. This process is repeated down to column 4 from which the final 100 μL is disposed of (see Figure 1.15).The appropriate bacteria cell suspension to be tested against (100 μL) was added to columns 12-3. Column 3 served as the negative control.
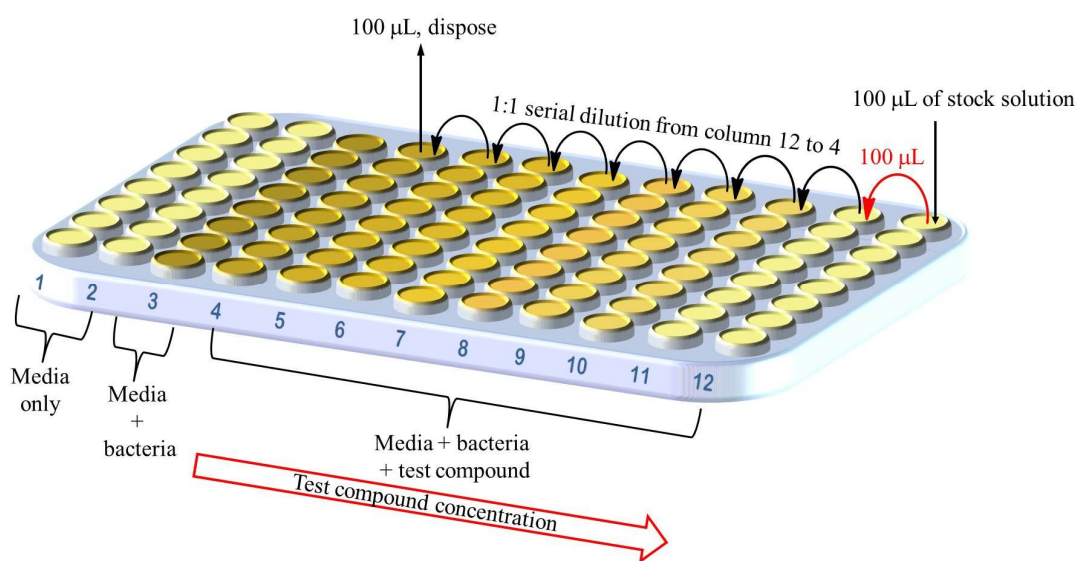
Figure 1.15: Bacteria susceptibility assay

The plate was incubated for 24 hours at 37 °C. The optical density was read at λ_{max} 540 nm and growth was then quantified as a percentage of control. All assays were run in triplicate. The results were analysed using Excel©.

The MIC_{50} (Minimum Inhibitory Concentration), MIC_{80} and MIC_{90} were taken to signify the concentration of compound that would inhibit the growth of the microorganism in question by 50%, 80% and 90%, respectively.

1.2.6 *In vivo* toxicity

In vivo toxicity was investigated using larvae of the Greater Wax Moth, *Galleria mellonella* (Figure 1.16).

Figure 1.16: *G. mellonella* larvae.

1.2.7 *Galleria mellonella* (*G. mellonella*)

G. mellonella in the sixth developmental stage were obtained from The Mealworm Company (Sheffield, England) and stored in wood shavings in the dark at 15 ^{o}C.

1.2.8 *G. mellonella* toxicity assay

The experiments were carried out using ten healthy *G. mellonella* (between 0.20-0.30 g in weight) placed in sterile, 9 cm petri dishes containing a sheet of Whatman filter paper and wood shavings.

Test compound solutions were made fresh on the day of testing prior to administration. Each compound was dissolved in DMSO and added to sterile, distilled water to give stock solutions consisting of less than 1% (v/v) DMSO. The compounds were tested across the concentration range of 1-100 μg/mL. Using a 300 μL Thermo Myjector syringe (29G), sterile test solutions (20 μL) were administered to the larvae by injection. Injections were made into the last, left pro-leg, of the *G. mellonella* larvae, directly into the haemocoel.

After injection, the larvae were incubated at 30 ^{o}C for a total of seven days. Larvae were monitored for survival and melanisation, at 24 hour intervals. Death was assessed based on the lack of movement in response to stimulation together with discolouration of the cuticle. Three controls were employed for the assay:

(1) untreated larvae maintained under the same conditions as the treated larvae,

(2) larvae pierced with an inoculation needle into the last, left pro-leg, but no solution injected, and

(3) larvae treated with 20 μL of sterile water/DMSO solution, in concentrations analogous to those of the test compounds.

The results are presented as the mean percentage survival of *G. mellonella* larvae, as a function of the test compounds administered dosage. All experiments were run in triplicate. Analysis of the results was carried out using Graph Pad Prism$^{©}$.

1.3 Instrumentation

Nuclear magnetic resonance spectra (^{1}H, ^{13}C and ^{19}F NMR) were recorded on a Bruker Avance 300 MHz NMR spectrometer with resolution of 0.18 Hz at a probe temperature of 25 ^{o}C, except where stated otherwise. Spectra were recorded in DMSO-d_6, CDCl$_3$ or CD$_3$OD with Me$_4$Si used as the internal standard.

Infrared (IR) spectra were recorded as KBr disks or liquid films between NaCl plates using a Perkin Elmer System 2000 FT-IR spectrometer in the region of 4000-370 cm^{-1}.

Melting points were determined using a Stewart Scientific SMP 1 melting point machine.

Microanalysis was carried out using a Flash EA 1112 Series Elemental Analyser. The sample is burned in oxygen and a helium carrier gas at 900 ^{o}C in a combustion tube.

Mass spectrometry (MS) data were obtained with a LC/TOF-MS (Agilent Corp, model 6210 Time-Of-Flight LC/MS). The LC was a model 1200 Series (Agilent Corp) and the column was an Agilent Eclipse XBD-C18. Where required, samples were also obtained *via* direct injection.

Optical rotations were measured with a Bellinghem and Stanley ADP410 polarimeter in a 0.5 dm^{-1} polarimeter tube.

Reagents were purchased from Sigma-Aldrich, Alfa Aesar, Acros Organics, Fluorochem and TCI Europe and used without further purification.

Chapter II

A structure-activity relationship study of

thiourea-based antibacterial agents

2.1 Introduction

Asymmetric synthesis, by means of organocatalysis, is another active area of research within the Stephens group.[73] Taking advantage of the organocatalysts available within the group, a number of these were screened for their antibacterial activity in the search for a lead compound. Antibacterial screening was carried out in the Institute of Technology Tallaght (ITT) against *S. aureus* and *E. coli*, the results of which have been previously reported by Gavin.[74] The majority of the organocatalysts exhibited bacteriostatic activity against the Gram-positive *S. aureus* with only two of the compounds exhibiting activity against the Gram-negative *E. coli*. The two compounds found to be the most active of the series of screened organocatalysts are shown in Figure 2.1 with their minimum inhibitory concentrations (MIC) given in Table 2.1.

(*a*)

(*b*)
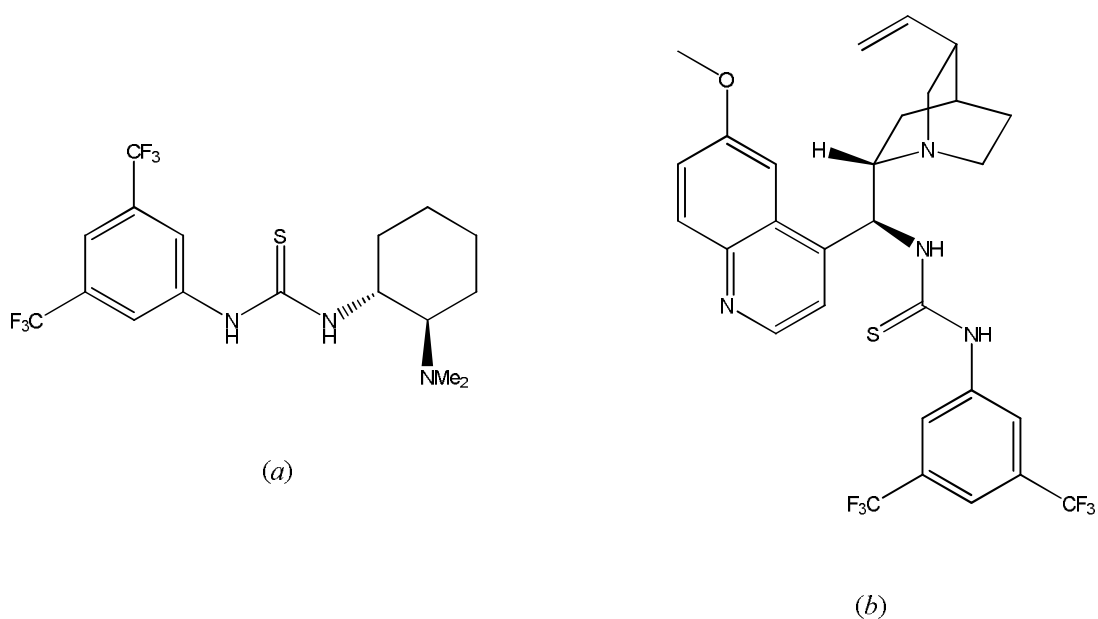
Figure 2.1: Bifunctional thiourea catalysts that exhibited greatest activity in antimicrobial screening.[74]

Table 2.1: MIC_{90}[a] values for organocatalysts (*a*) and (*b*).[74]

Organocatalyst	*S. aureus*[b]	*E. coli*[c]
	MIC_{90} (μM)	MIC_{90} (μM)
Takemotos catalyst (*a*)	23.8 +/- 0.1	119.9 +/- 13.8
Quinine derived catalyst (*b*)	< 6.25	166.7 +/- 13.7

[a] The minimum inhibitory concentration required to inhibit 90% of bacterial growth, [b] *S. aureus* NCIMB 12702, [c] *E. coli* NCIMB 9485.

The organocatalysts shown in Figure 2.1 are bifunctional, hydrogen-bonding (H-bonding) catalysts. Organocatalyst (*a*), known as Takemotos catalyst, was the first chiral thiourea H-bonding catalyst designed for a Michael reaction (Scheme 2.1).[75]

(*S*)-diethyl 2-(2-nitro-1-phenylethyl)malonate
93 % ee
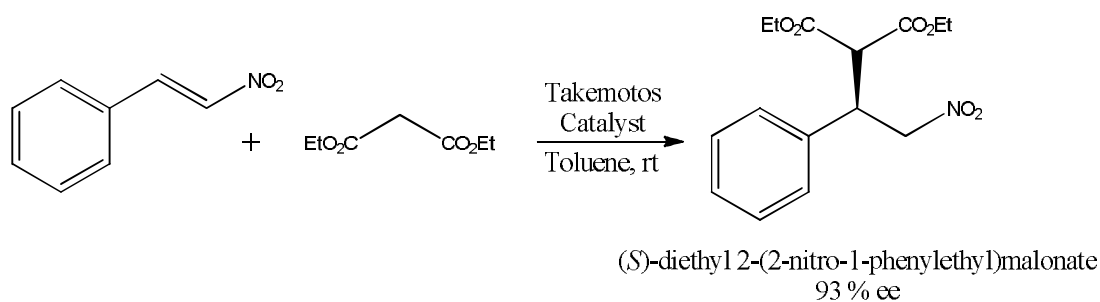
Scheme 2.1: Michael reaction of diethyl malonate to *trans*-β-nitrostyrene using Takemotos catalyst.[75b]

Investigations into the catalytic reaction mechanism have been carried out and it is believed to occur by deprotonation of a malonate acidic proton by the tertiary amine of the organocatalyst.[76] H-bonding of the nitrostyrene *via* the catalyst thiourea moiety results in the formation of a ternary complex as depicted in Figure 2.2. The presence of the chiral scaffold restricts the approach of attack by the malonate nucleophile to the electrophilic nitrostyrene giving rise to the high enantioselectivity of the reaction.[76] The thiourea-stabilised nitronate can then remove the proton from the protonated amino group of the catalyst resulting in formation of the product and regeneration of the catalyst.[76]
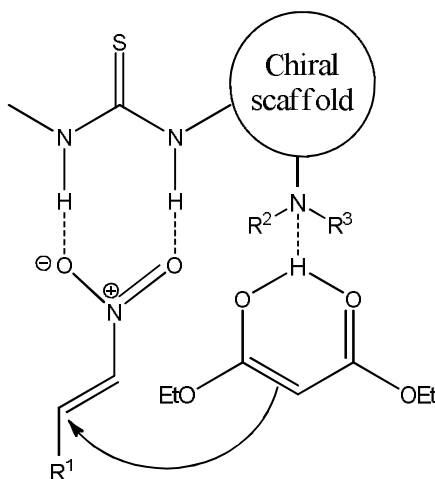
Figure 2.2: Bifunctional activation by thiourea catalyst.[76]

The quinine derived organocatalyst (*b*) (Figure 2.1) was later designed by Connon[77] and Soós[78] (independently) and has been used for a number of reactions such as the Mannich reaction.[79] Investigations into the Michael addition of β-diketones to β-nitrostyrene using organocatalyst (*b*) have also been carried out.[73a] It is believed that organocatalyst (*b*) works by a similar mechanism as that described above (Figure 2.2).[80]

As seen in Table 2.1, Takemotos catalyst exhibited slightly better activity against *E. coli* in comparision to organocatalyst (*b*). However, the anti-*staphylococcal* activity demonstrated by organocatalyst (*b*) was superior to that of Takemotos catalyst. For this reason, it was decided that the quinine derived organocatalyst (*b*) would act as our hit compound, and so, would be studied further in an attempt to understand its structure-activity relationship and to improve its activity and drug-like properties.

With organocatalyst (*b*) as our hit compound we decided to carry out a structure-activity relationship (SAR) study. Synthesising a series of compounds based on our hit compound would allow us to identify which functional groups are essential for activity. We could then build on this information by designing and optimising subsequent compounds with the intent of generating a final compound possessing optimum antibacterial activity. On comparing the structures of the two catalysts, (*a*) and (*b*), it can be seen that these compounds share a structural component, the 3,5-

bis(trifluoromethyl))phenyl thiourea connected to a tertiary amine by a two-carbon chain (Figure 2.3).

(*a*)

(*b*)
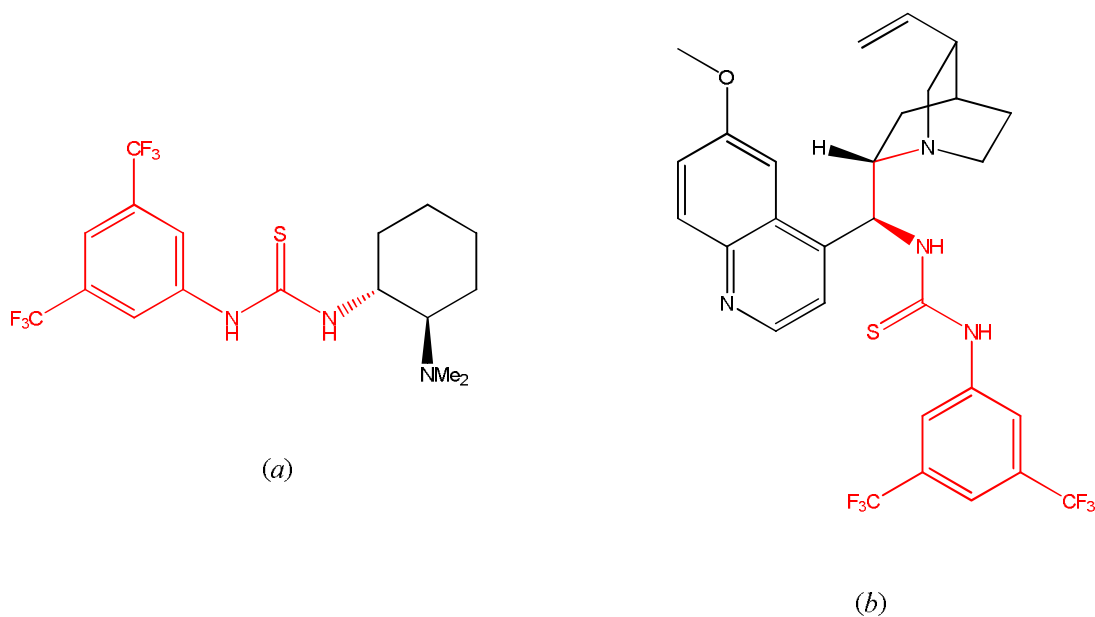
Figure 2.3: Organocatalyst (*a*) and (*b*) share a similar structural component.

Thiourea-based compounds are well-known for their antithyroid activity and have been in use for over 70 years in the treatment of hyperthyroidism.[81] Moreover, a vast array of biological activities including antitubercular, insectididal, rodenticidal, antiviral, antifungal and antibacterial activities have been associated with thiourea derivatives.[82] A recent study on thiourea-based compounds incorporating a hippuric acid moiety, as shown in Figure 2.4, was carried out by Abbas *et al*.[83] The majority of these compounds exhibited broad spectrum antimicrobial activity with a number of them demonstrating activity comparable to, and in some cases better than, ciprofloxacin.[83]

X = alkyl, aromatic ring
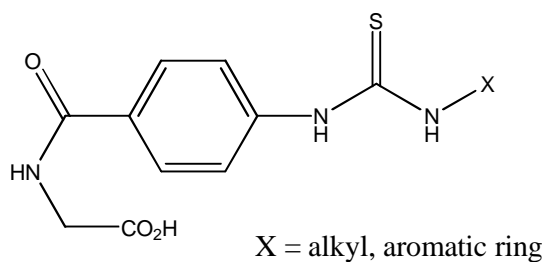
Figure 2.4: General structure of hippuric acid-based thiourea derivatives.

Based on the antibacterial activity exhibited by both Takemotos catalyst and organocatalyst (*b*) and the well-known biological activities associated with thioureas, it was thought that the 3,5-bis(trifluoromethyl))phenyl thiourea moiety could be the source of the compounds activity. Therefore, we constructed our SAR study based around this thiourea group.

2.1.1 Aim

The aim of this work was to uncover the structural components responsible for the antibacterial activity of the hit compound, organocatalyst (*b*), by means of a structure-activity relationship study. Identification of the functionalities and structural components important for its activity would allow us to design subsequent compounds that could then undergo further optimisation in the hopes of obtaining a novel compound with potent, broad spectrum antibacterial activity.

The SAR study has been divided into two parts; (1) the identification of the functionalities important for the overall activity of the hit compound and (2) an investigation into the thiourea component and the substituents which are beneficial for antibacterial activity.

The design, synthesis and biological evaluation of a series of organocatalyst (*b*) derivatives and 3,5-bis(trifluoromethyl))phenyl thiourea-based compounds was carried out and is described in the following sections.

2.2 Results and Discussion

2.2.1 Compound Design, part one
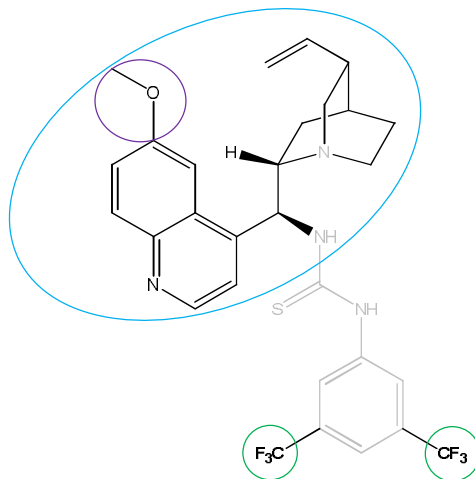
Figure 2.5: Hit compound components of possible importance; the quinine-derived amine moiety (blue), a methoxy group (purple) and two trifluoromethyl groups (green).

Our initial investigations into the SAR study of our hit compound, organocatalyst (*b*), were based on three components of the hit compound structure (Figure 2.5). Firstly, we wanted to investigate the quinine-derived amine moiety of the hit compound (blue, Figure 2.5). Quinine (Figure 2.6) is most well-known for its antimalarial properties.[84] The Peruvian Indians were the first to discover the medicinal properties of the natural source of quinine, the 'fever tree', known today as the cinchona tree.[84] However, it wasn't until the 1700's that the first European was cured of malaria using quinine and it is still in use today.[84]
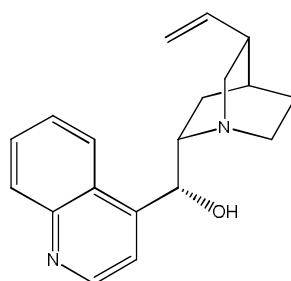
Figure 2.6: Quinine.

Studies have shown that quinine is also bactericidal to a number of Gram-positive and Gram-negative bacteria.[85] Wolf *et al*.[86] have also demonstrated that quinine sulfate has the ability to inhibit the invasion efficacy of *E. coli*. Taking these studies into account it seemed reasonable to investigate if the quinine-derived amine component of the hit compound plays a role in its overall antibacterial activity. It was thought that compound **2** (Figure 2.7) would assist in answering this question.
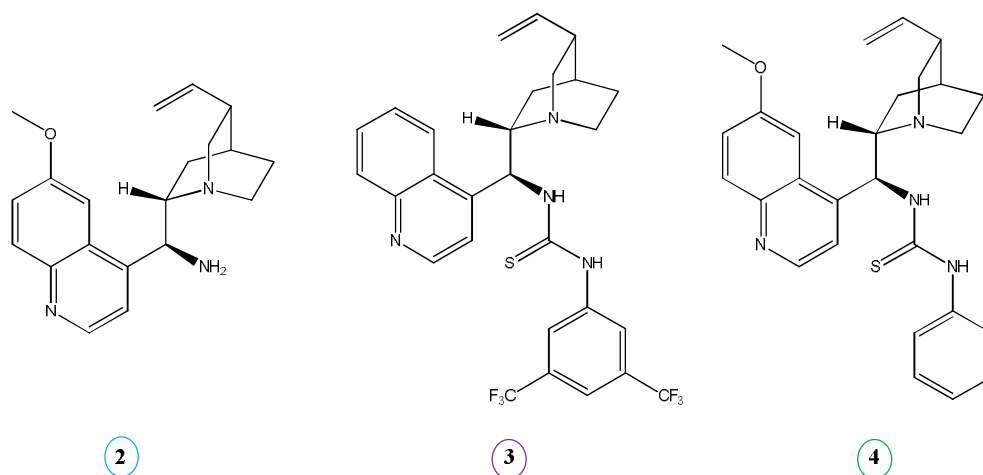
Figure 2.7: SAR study, part one, compound structures.

To further investigate the functional groups that may be important for the overall antibacterial activity of the hit compound, we decided to synthesise compounds **3** and **4** (Figure 2.7). Methoxy groups can be of importance with regard to their H-bond accepting ability and thus may be involved in the binding of the hit compound to its target site.[11] If this is the case here, then removal of this group (compound **3**, Figure 2.7) should decrease the antibacterial activity of the hit compound.

The two trifluoromethyl groups are present in both the hit compound and Takemotos catalyst suggesting that they may be important for activity. Furthermore, the addition of fluorine or –CF$_3$ groups have been shown to increase the overall potency of various drugs.[87] Therefore, to determine the importance of the –CF$_3$ groups compound **4** (Figure 2.7) was synthesised and evaluated in our initial SAR study of our hit compound.

An important factor to take into consideration when designing potential, drug-like molecules, is the ability of the compounds to be absorbed or their ability to

transverse cell membranes.[11,88] As discussed by GSK, incorporating 'drug-like' properties into a compound is important for its progression into further development.[10] A compound that may be very active may not be very effective *in vivo* if it does not bear properties such as good absorption.[11] A useful set of rules have been devised by Lipinski[88] as a guide for designing compounds with good oral absorption or permeation. The Lipinski 'rule of 5' states that good absorption is more likely when:[11,88]

(1) there are < 5 H-bond donors (expressed as the sum of –OH or –NH),

(2) the molecular weight (m.w.) is less than 500,

(3) the calculated LogP* (cLogP) is < 5, and

(4) there are < 10 H-bond acceptors (expressed as the sum of O and N)

In general, if two out of the five rules are violated poor absorption or permeability is possible. As shown in Table 2.2, we have applied the Lipinski 'rule of 5' to our compounds within our SAR study in order to gain insight into their potential ability to be absorbed. In the case described by GSK, although they had found a compound with good activity and were able to enhance its activity by further optimisation, they were unable to combine the compounds potency with necessary 'drug-like' properties.[10] It was thought that establishing which structural features may contribute to good absorption early on in the study, may assist with the optimisation of subsequent compounds in the hopes of eventually obtaining a compound with good *in vivo* activity.

---

* The partition coefficient, LogP, is a measure of the hydrophobic character of a drug.[11] It is measured experimentally by examining the drugs relative distribution in an n-octanol/water mixture i.e. *P* = concentration of drug in n-octanol/concentration of drug in aqueous layer. A high *P* value indicates hydrophobic character whereas a low *P* value indicates hydrophilic character.

Table 2.2: Lipinski rules applied to SAR study compounds.

Compound	M.W.[a]	# H-bond acceptors	# H-bond donors	cLogP[b]
Organocatalyst (*b*)	594.19	3	2	7.33 +/- 0.63
2	323.20	3	1	2.77 +/- 0.41
3	564.18	2	2	7.24 +/- 0.62
4	458.21	3	2	4.35 +/- 0.48

[a] Molecular weight (amu), [b] calculated using ACD/Labs ChemSketch 12.0.

As can be seen from Table 2.2, our hit compound violates two of the Lipinski rules, that is, it has a molecular weight greater than 500 and a cLogP greater than 5. Similarly the SAR study compound, compound **3**, also violates both the molecular weight and cLogP limits. LogP is a measure of the lipophilicity of a molecule. This is a particularly important feature with regards to the physiochemical behaviour of a molecule.[89] The higher the LogP value the more lipophilic a compound is likely to be. However, if a compound is 'too lipophilic' this may cause problems, for example, a compound may become promiscuous resulting in toxic side effects.[89] Gratifyingly, two of the SAR study compounds, **2** and **4**, do obey the 'rule of 5' suggesting that they may exhibit good absorption.

2.2.2 Synthesis of part one SAR study compounds
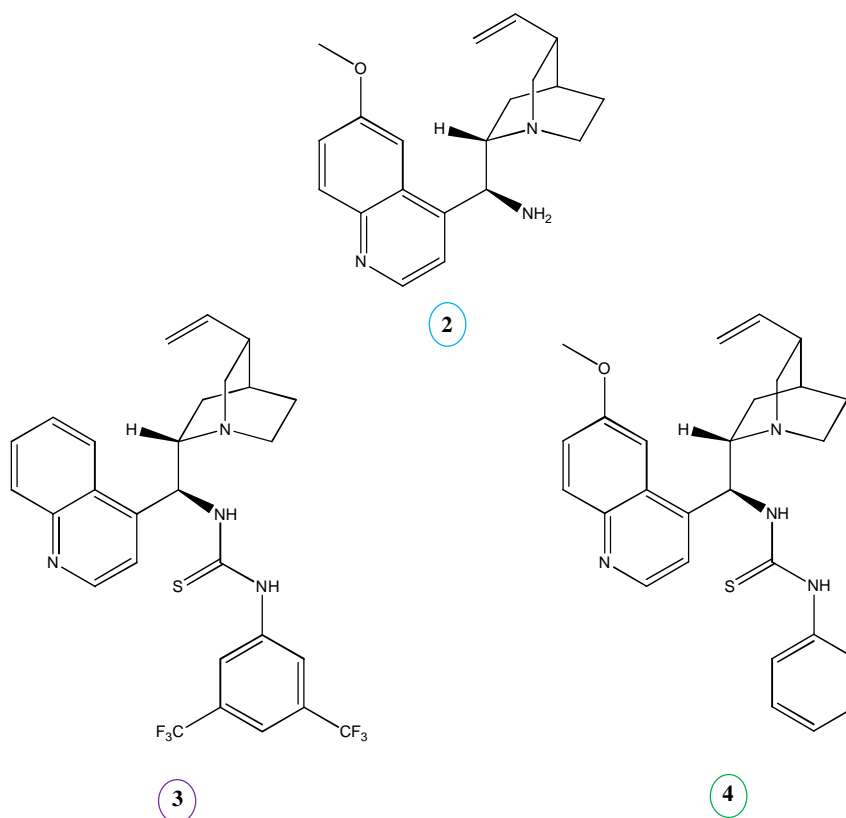
Figure 2.8: SAR study, part one, compound structures.

Quinine was obtained commercially and used without further purification in the synthesis of compound **2** (Figure 2.8). The one pot procedure used was that described by Oliva *et al.*[90], wherein quinine undergoes a Mitsunobu reaction followed by azide reduction. As shown in Scheme 2.2, reaction of diisopropyl azodicarboxylate (DIAD) and triphenylphosphine generates an anion product which deprotonates the quinine –OH group. Diphenylphosphoryl azide (DPPA) can then be used to give the azide precursor to compound **2**.
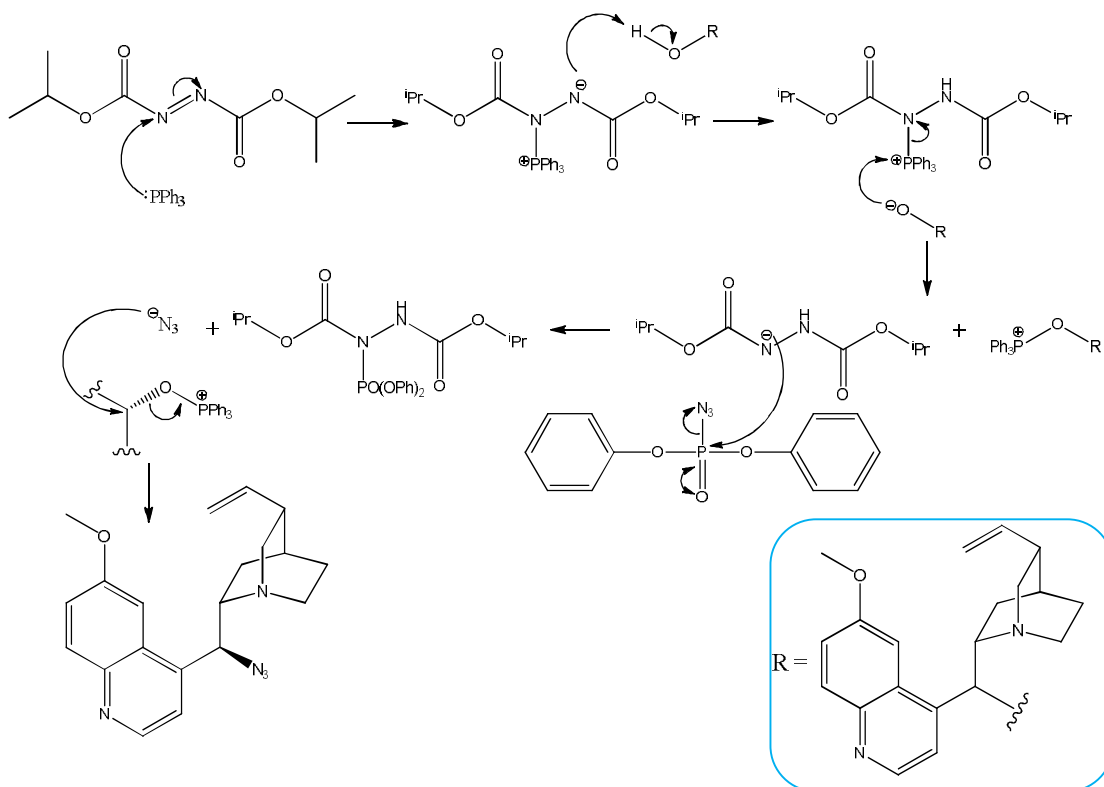
Scheme 2.2: Mitsunobu reaction.

The use of additional triphenylphosphine (Scheme 2.3) allows the azide to undergo a Staudinger reduction to give the final amine product, compound **2**.
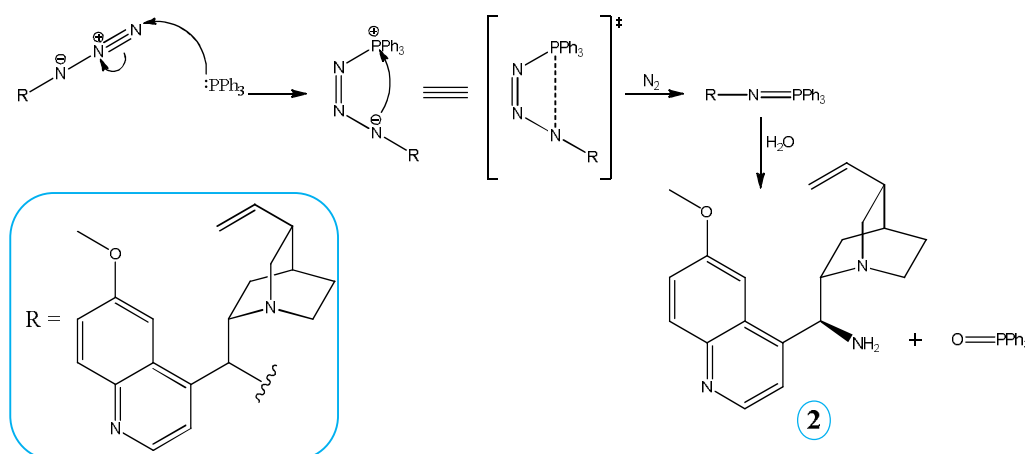
Scheme 2.3: The Staudinger reduction of the compound **2** azide precursor.

Purification of compound **2** was carried out using silica gel column chromatography. The purification of compound **2** was difficult and required an EtOAc:MeOH:NH$_4$OH

(50:50:1) mobile phase in order to facilitate elution of the primary amine. In the ^{1}H NMR spectrum (Figure 2.9) of compound **2** a large shift, approximately 1 ppm, was observed for the C9 proton (-C*H*-NH$_2$) indicating product formation. The Mitsunobu reaction involves nucleophilic attack *via* a S$_N$2 reaction, thus inversion of configuration was expected. To ensure that this was the case the optical rotation of compound **2** was measured, the result of which matches the literature and confirms the formation of the (+) enantiomer.[78] LC/TOF-MS returned a (M+H^{+}) of 324.2080 further confirming the formation of compound **2**.
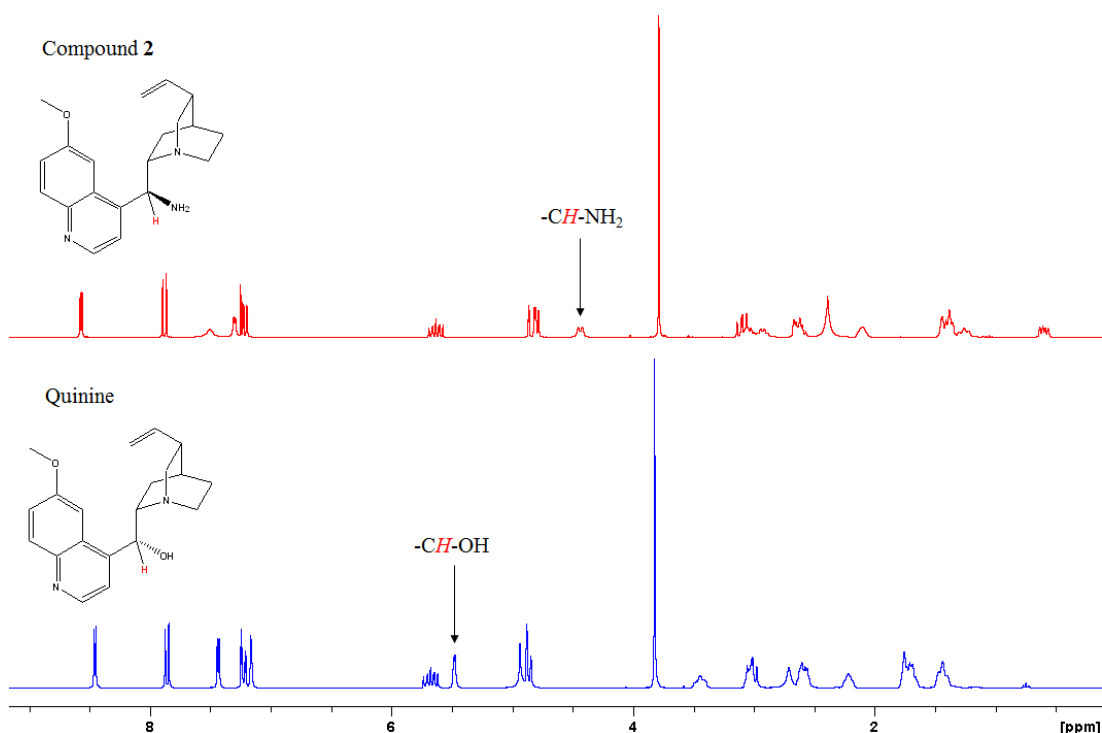
Figure 2.9: ^{1}H NMR spectra of compound **2** and quinine.

The bacterial strains (Table 1.1, section 1.2.2) used within this study are different to those used in the original screening which identified the hit compound. Therefore, in order to be able to directly compare the biological activity of the SAR study compounds to the activity of organocatalyst (*b*), this compound was also synthesised.

Organocatalyst (*b*) was synthesised as described by McCooey *et al.*[77] by the nucleophilic addition of compound **2** to 3,5-bis(trifluoromethyl)phenyl isothiocyanate (Scheme 2.4). Purification was carried out using silica gel column

chromatography followed by a cold Et$_2$O/n-hexane precipitation to give organocatalyst (*b*) in an acceptable yield of 50%.
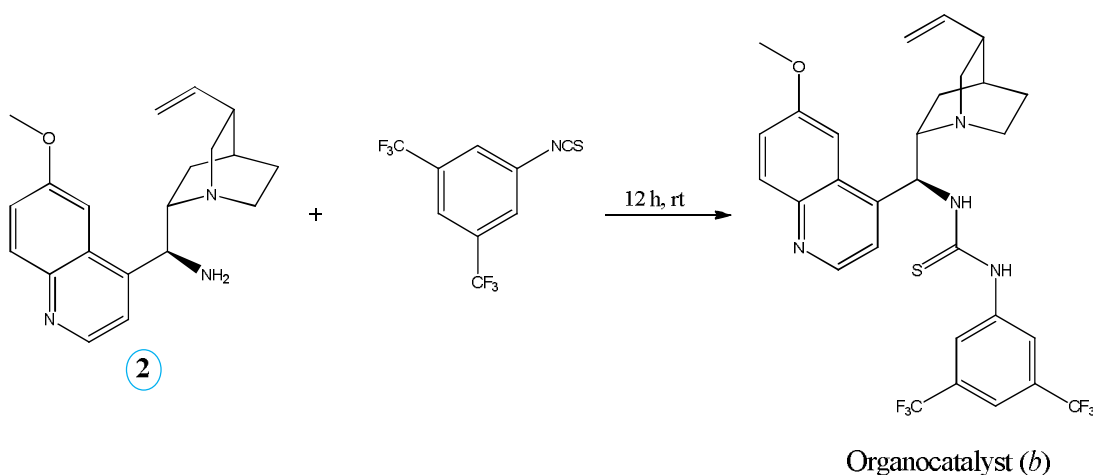
Scheme 2.4: Synthesis of hit compound, organocatalyst (*b*).

The optical rotation of organocatalyst (*b*) was measured and found to match literature data.[78] Organocatalyst (*b*) was further characterised using IR, ^{1}H and ^{13}C NMR spectroscopies. The characteristic ν(C=S) absorption band was observed at 1278 cm^{-1} in the IR spectrum. Although the NMR spectra are quite complex, a large downfield shift (4.44 ppm to 5.85 ppm) in the resonance signal for the C9 proton (-C*H*-NHC=S-), due to the electron-withdrawing effect of the 3,5-bis(trifluoromethyl)phenyl thiourea moiety, was observed in the ^{1}H NMR spectra.

The presence of fluorine on a molecule can be particularly useful in the characterisation of a compounds structure. Fluorine has I = ½ and can thus be detected using ^{19}F NMR spectroscopy. Moreover, the signals produced in ^{13}C and ^{1}H NMR spectra of a fluorinated molecule will be split due to the coupling interaction between the ^{13}C and ^{1}H atoms and neighbouring fluorine atom(s). The multiplicities of the individual signals resulting from H-F or C-F coupling will reflect the n + 1 rule. In ^{13}C NMR, the shifts for a –CF$_3$ group are found in the range of 107-285 ppm.[91] For a one-bond C-F coupling the ^1J value can be in the range of 162-280 Hz with the –CF$_3$ group ^1J usually in the range of 275-285 Hz.[91] The two-bond C-F coupling for a –CF$_3$ group (^2J) is usually in the range of 25-35 Hz and a ^3J coupling can also be observed, usually in the range of 2-3 Hz.[91]

In the ^{13}C NMR spectra of organocatalyst (*b*) a quartet with ^1J = 270.0 Hz was observed. This ^1J value falls within the C-F ^1J coupling constant range of 162-280 Hz and corresponds to the characteristic –CF$_3$ group ^1J coupling constant range. A ^2J value of 33.8 Hz was also observed representing the C atom *ipso* to the –CF$_3$ groups. Additionally, the *C*=S signal has shifted downfield from 141.0 ppm in the 3,5-bis(trifluoromethyl)phenyl isothiocyanate spectrum to 180.6 ppm indicating the formation of organocatalyst (*b*).

As shown in Scheme 2.5, the synthesis of compound **3** was carried out by the same method as described for organocatalyst (*b*) above. Cinchonidine was obtained commercially and used without further purification in the Mitsunobu reaction. Subsequent reduction of the azide resulted in compound **5** (Scheme 2.5).
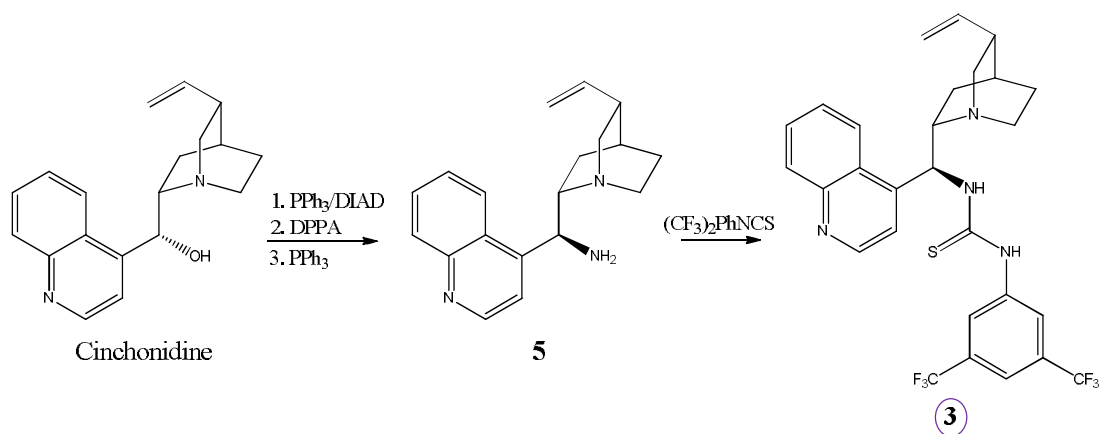
Scheme 2.5: Synthesis of compound **3** *via* compound **5**.

Similarly to compound **2**, a large upfield shift from 5.65 ppm to 4.61 ppm in the C9 proton (-C*H*-NH$_2$) of compound **5** was observed indicating the conversion of the –OH group to the primary amine. The optical rotation of compound **5** was found to be (+) 100 (*c* 0.2, DCM) confirming inversion of configuration, resulting from the Mitsunobu reaction. LC/TOF-MS further confirmed the production of compound **5** returning a (M+H$^+$) of 294.1974. As shown in Scheme 2.5, compound **5** was used in a nucleophilic addition reaction with 3,5-bis(trifluoromethyl)phenyl isothiocyanate to give compound **3**. Compound **3** was purified by silica gel column chromatography followed by cold precipitation from Et$_2$O with n-hexane.

In the ^{13}C NMR spectrum of compound **3** a quartet at 122.8 ppm with $^{1}J = 271.4$ Hz was observed for the carbon of the $-CF_3$ groups. Additionally, a $^{2}J = 34.5$ Hz for the carbon *ipso* to the $-CF_3$ group was observed along with a downfield shift in the C=S ^{13}C signal (141.0 ppm to 180.5 ppm), indicating formation of compound **3**. As observed in the ^{1}H NMR of organocatalyst (*b*), the addition of the thiourea moiety resulted in a large downfield shift from 4.61 ppm to 5.97 ppm in the C9 proton (-C*H*-NHC=S-). The IR absorption band at 1278 cm^{-1} of the ν(C=S) further confirmed the formation of compound **3**.

Compound **4** (Scheme 2.6) was also synthesised by the method used by McCooey *et al.*[77], however, phenyl isothiocyanate was used in place of the 3,5-bis(trifluoromethyl)phenyl isothiocyanate. Again, the compound was purified by silica gel column chromatography followed by precipitation from cold EtOAc with n-hexane. The white solid was obtained in a reasonable yield of 52%.
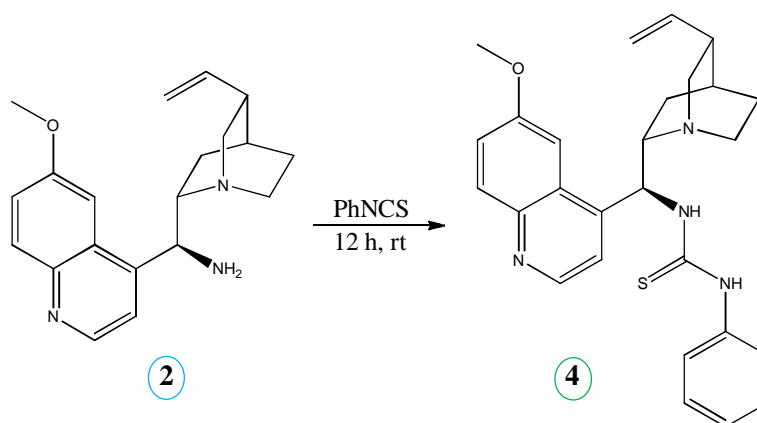
Scheme 2.6: Synthesis of compound **4**.

The loss of both $-CF_3$ groups resulted in slightly simplified ^{13}C NMR spectra with regards to the signal multiplicities, that is, only singlets were observed for the carbon signals of compound **4**. As with organocatalyst (*b*) and compound **3** the *C*=S signal has undergone a large downfield shift to 180.5 ppm indicating successful addition of the thiourea moiety. Additionally, in the IR spectrum of compound **4** a strong absorption band at 1242 cm^{-1}, characteristic of the ν(C=S) absorption, was observed. In the ^{1}H NMR spectrum the C9 proton (-C*H*-NHC=S-) has shifted downfield to 5.89 ppm further indicating the formation of compound **4**.

2.2.3 *In vitro* antibacterial activity

Organocatalyst (*b*) and each of the SAR study compounds described above (Figure 2.8, section 2.2.2) were evaluated for their *in vitro* bacteriostatic activity against *S. aureus*, *E. coli* and *P. aeruginosa*. Bacteriostatic activity was evaluated using the susceptibility assay as described in section 1.2.5. The results are expressed as the MIC_{50} and MIC_{90}, that is, the minimum inhibitory concentration that is required to inhibit 50% and 90% of bacterial growth. The results are summarised in Table 2.3 and 2.4. Two well-known antibacterial agents were chosen as the positive controls, vancomycin hydrochloride and ciprofloxacin, which have also been included in each of the MIC tables below. Any compound that did not exhibit an MIC, of the given percentage of growth inhibition, against each of the bacteria has been excluded from the tables.

In general, none of the compounds including the hit compound were active against *P. aeruginosa*. This lack of activity could be due to the intrinsic resistant mechanisms associated with *P. aeruginosa*. As mentioned previously in section 1.1.5, the uptake of molecules by *P. aeruginosa* is very slow (in comparison to *E. coli*) due to its inefficient porins.[36] Furthermore, *P. aeruginosa* is well-known for its ability to grow as a biofilm thus aiding its escape from the action of antibiotics.[40,42] *P. aeruginosa* can also form a capsule providing it with an additional physical barrier to prevent the entry of antibiotics.[18,39] One or possibly all of these mechanisms may be facilitating its resistance to the action of organocatalyst (*b*) and the SAR study compounds **2**-**5**.

Table 2.3: SAR study compounds antibacterial activity as MIC_{50} range. Values are the mean of three experiments.

Compound	E. coli		P. aeruginosa		S. aureus	
	µM	µg/mL	µM	µg/mL	µM	µg/mL
Vancomycin hydrochloride	1.58-2.10	2.35-3.13	>67.31	>100.00	1.58-2.10	2.35-3.13
Ciprofloxacin	>301.99	>100.00	1.18-1.77	0.39-0.59	>301.99	>100.00
Organocatalyst (b)	2.63-3.95	1.56-2.35	>168.30	>100.00	3.95-5.26	2.35-3.13
3	5.54-8.32	3.13-4.69	>177.25	>100.00	8.32-11.08	4.69-6.25
4	40.92-54.56	18.75-25.00	>218.24	>100.00	54.56-81.84	25.00-37.50

Table 2.4: SAR study compounds antibacterial activity as MIC_{90} range. Values are the mean of three experiments.

Compound	E. coli		P. aeruginosa		S. aureus	
	µM	µg/mL	µM	µg/mL	µM	µg/mL
Vancomycin hydrochloride	4.21-6.31	6.25-9.38	>67.31	>100.00	4.21-6.31	6.25-9.38
Ciprofloxacin	>301.99	>100.00	37.75-56.62	12.5-18.75	>301.99	>100.00
Organocatalyst (b)	7.90-10.52	4.69-6.25	>168.30	>100.00	10.52-15.78	6.25-9.38
3	8.32-11.08	4.69-6.25	>177.25	>100.00	16.62-22.16	9.38-12.50
4	81.84-109.12	37.50-50.00	>218.24	>100.00	163.68-218.24	75.00-100.00

As can be seen in Table 2.3 our hit compound organocatalyst (*b*) exhibited good activity against *E. coli*, resulting in an MIC$_{50}$ in the range of 1.56-2.35 µg/mL and 2.35-3.13 µg/mL against *S. aureus*. Gratifyingly, organocatalyst (*b*) also inhibited *E. coli* and *S. aureus* growth by 90% at MIC's comparable to that obtained for the reference antibacterial agent, vancomycin hydrochloride (Table 2.4).

In the investigation into the structure-activity relationship of organocatalyst (*b*), compound **2** (Figure 2.8, section 2.2.2) was the first to be evaluated for its bacteriostatic activity. Here, we wanted to investigate if the quinine-derived amine component of the hit compound was important for activity. The results from the susceptibility assays of compound **2** revealed that it exhibited little or no activity against *E. coli*, *P. aeruginosa* and *S. aureus*. This is an interesting result as quinine has been shown by others to exhibit bactericidal activity against all three bacteria.[85]

Compound **2** is structurally different to quinine in two ways, firstly, the replacement of the –OH group with the –NH$_2$ group and secondly, in their C9-configurations (Figure 2.10).
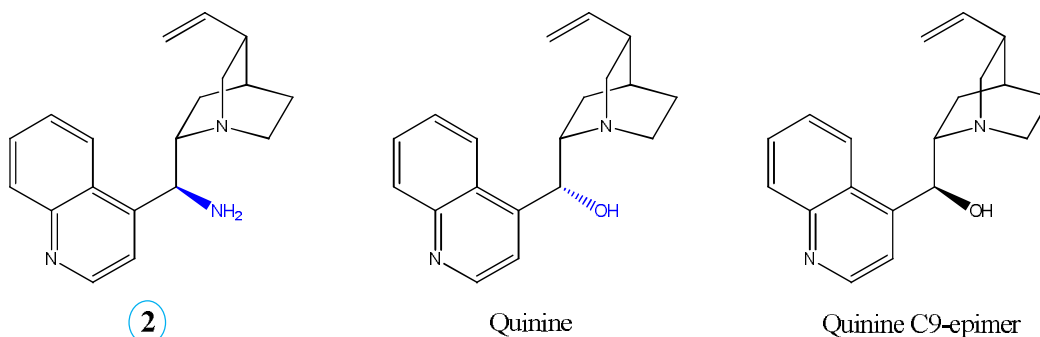
Figure 2.10: Structural differences and similarities between compound **2**, quinine and its C9-epimer.

Perhaps the –OH group of quinine is involved in binding to its target site through H-bonding interactions. A H-bonding interaction involves the orbital containing a lone pair of electrons of one molecule (H-bond acceptor) interacting with the orbitals involved in the R-H bond of a second molecule, the H-bond donor. Thus there is an important directional influence associated with H-bonding interactions, that is, the optimum orientation is where the R-X bond of the H-bond donor points directly

towards the lone pair of the H-bond acceptor. If the –OH group of quinine is involved in H-bonding interactions with its target site then replacement with the –NH_2, having two H atoms, could alter the angle at which the H-bonding interaction occurs. This in turn may reduce the strength of the interaction and therefore result in a loss of the antibacterial activity. Alternatively, it has recently been reported that the cytostatic activity of quinine is dependent on its C9 configuration.[92] Gorka *et al.*[92] evaluated the cytostatic activity of quinine and its C9-epimer against the malaria causing parasite, *Plasmodium falciparum*. The results show that the C-9 epimer of quinine (Figure 2.10) exhibited a large decrease in cytostatic activity in comparison to quinine, suggesting that the configuration may be important for activity. Taking this into consideration, it may be that compound **2** having the opposite C9-configuration to quinine results in a loss in activity. This is not unusual as differences in activity have been associated with the different enantiomers of a compound, for example ethambutol (Figure 2.11). The (*S,S*)-enantiomer of ethambutol is used in the treatment of tuberculosis whereas the (*R,R*)-enantiomer is inactive.[93]
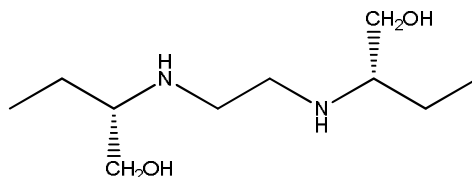
Figure 2.11: (*S,S*)-Ethambutol.

Another possible explanation for the lack of activity exhibited by **2** could be due to the presence of the three basic nitrogen groups, the quinuclidine N, the quinoline N and the primary amine. When compound **2** is in solution it may become triply charged which, in turn, may prevent it from crossing the lipid membrane of the bacteria. Consequently, compound **2** may not be able to inhibit bacterial growth.

Thus far, with regards to compound **2** and the structure of the hit compound, the quinine-derived amine component does not appear to possess antibacterial activity and therefore may not be required for the activity exhibited by organocatalyst (*b*).

Moreover, the lack of activity exhibited by compound **2** suggests that the thiourea moiety may be important for the antibacterial activity exhibited by the hit compound.

Next, the importance of the methoxy group with regards to the overall activity of organocatalyst (*b*) was investigated using compound **3** (Figure 2.8, section 2.2.2). As can be seen from Table 2.3, compound **3** exhibited activity against both *E. coli* and *S. aureus*. Although the MIC_{50} values obtained for compound **3** were slightly higher than those exhibited by the hit compound, the MIC_{90} values obtained for compound **3** were very close to that of organocatalyst (*b*) (Table 2.4). In general, the loss of the methoxy group resulted in a slight reduction in activity. However, it did not appear to have a detrimental effect on the overall activity of the compound indicating that it may not be crucial for activity.

Finally, the effect of the loss of the two –CF_3 groups was investigated using compound **4**. Compound **4** was less active than the hit compound demonstrating a 10- and 12-fold decrease in the MIC_{50} range against both *S. aureus* and *E. coli*, respectively (Table 2.3). The –CF_3 groups are sterically bulky and highly electron-withdrawing groups. Thus the loss of these groups may induce a change in the preferred molecular binding conformation of the hit compound, which in turn may reduce its binding affinity to its target site. Alternatively, the addition of fluorine is known to increase the lipophiliciy of molecules.[87] As can be seen in Table 2.2 (section 2.2.1) the cLogP of compound **4** is approximately 4.35, a value much lower than that of the hit compound (approximately 7.33). In general, the larger the LogP value the greater the lipophiliciy, therefore the loss of these groups may impair the hit compounds ability to cross the cell membranes and bind to its target site. Whatever the case may be, the –CF_3 groups appear to be very important in the overall activity of organocatalyst (*b*).

Of the active compounds here, greater activity was observed against *E. coli* in comparison to *S. aureus*. This is a little unusual as normally it is more difficult to inhibit Gram-negative bacteria in comparison to Gram-positive bacteria due to the presence of the additional bacterial outer membrane of the Gram-negative bacterial cell wall.[18] This result suggests that these compounds may be able to cross the cell

membranes of both *E. coli* and *S. aureus*, however, the target within each of the bacteria may be different thus resulting in different levels of activity. Additionally, if the compound shares a similar target amongst the two bacteria, it may be that the transport of the compound to the target site is not carried out as efficiently in *S. aureus* as it may be in *E. coli*.

The SAR study thus far has been summarised in Figure 2.12. Overall, each of the compounds tested were inactive against *P. aeruginosa*. The quinine-derived amine moiety alone does not exhibit bacteriostatic activity against *E. coli* or *S. aureus* suggesting that it may not be important in the activity of organocatalyst (*b*), however the thiourea moiety may be required for activity. Loss of the –OMe group does cause a slight reduction in the potency of the hit compound but does not appear to be essential for the overall activity. The –CF₃ groups appear to be crucial for activity with the loss of these groups resulting in higher MIC values against *E. coli* and *S. aureus* in comparison to the hit compound.
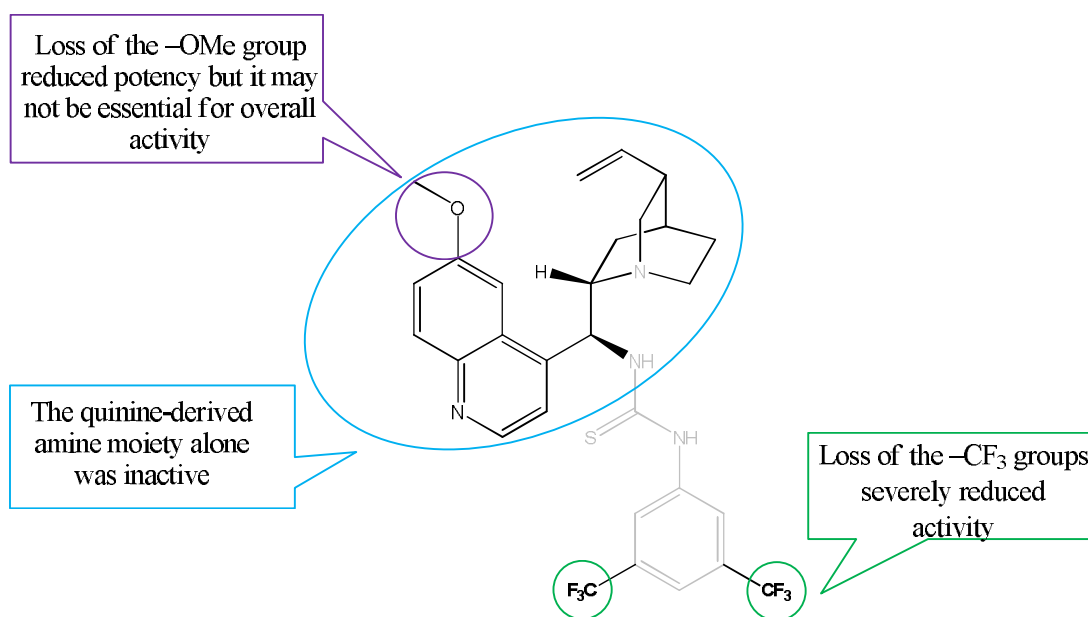
Figure 2.12: A summary of part one of the SAR study of organocatalyst (*b*).

2.2.4 Compound Design, part two

Thus far, it was clear that in order to retain bacteriostatic activity the trifluoromethyl groups are necessary whereas the loss of the methoxy group does not appear to greatly affect the overall activity of the hit compound. The quinine-derived amine component alone is inactive suggesting that it may not be required for activity. However, this also suggests that the thiourea moiety may be required for activity. Additionally, in the original screening for a hit compound, organocatalyst (*b*) and Takemotos catalyst were found to be the compounds that exhibited greatest activity. As mentioned earlier, these catalysts share similarities in their structures with both compounds bearing a 3,5-bis(trifluoromethyl)phenyl thiourea moiety attached to a tertiary amine *via* a two-carbon chain (Figure 2.3, section 2.1.1). Taking these structural similarities into account and having established the structural relationships of the –OMe, –CF$_3$ and quinine-derived amine component in part one of the SAR study, the SAR study was continued with the focus being placed on two alternative structural components of the hit compound as shown in Figure 2.13.
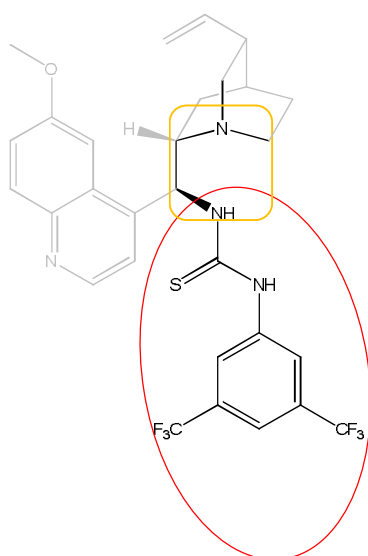
Figure 2.13: Hit compound components for investigation into its structure-activity relationship.

Firstly, we wanted to focus on the thiourea component (red, Figure 2.13). Thioureas are known for their vast array of biological properties including antibacterial activity.[82] A variety of thiourea-based compounds that have been synthesised

recently have exhibited antibacterial activity, some of which have demonstrated activity comparable to that of known antibacterial agents.[83,94]

From our initial studies we found that the presence of the $-CF_3$ groups was important for activity. Therefore, in order to combine both the thiourea functionality and the $-CF_3$ groups it was decided that a series of 3,5-bis(trifluoromethyl)phenyl thiourea-based derivatives would be synthesised in part two of the SAR study of organocatalyst (*b*) (Figure 2.14).
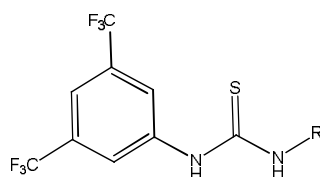
Figure 2.14: General structure of SAR study compounds.

Two simple thiourea compounds possessing the 3,5-bis(trifluoromethyl)phenyl thiourea group were designed, compound **6** and **7** (Figure 2.15). It was thought that these structurally simple molecules should help establish if the thiourea group is the source of activity.
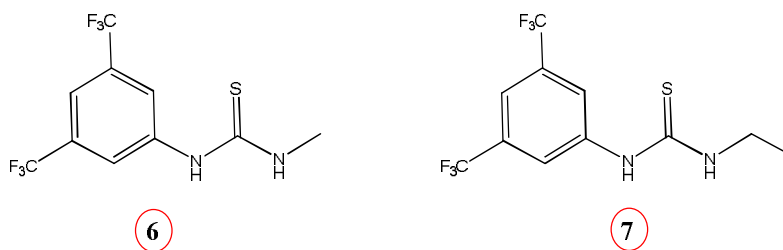
Figure 2.15: Structurally simple 1-(3,5-bis(trifluoromethyl)phenyl)-3-thiourea SAR study compounds.

Once again, the Lipinski 'rule of 5' have been applied to each of the compounds in an effort to gain insight into their potential absorption ability (Table 2.5). As shown in Table 2.5 compounds **6** and **7** obey each of the Lipinksi rules unlike the hit compound.

Table 2.5: Lipinski rules applied to SAR study compounds.

Compound	M.W.[a]	# H-bond acceptors	# H-bond donors	cLogP[b]
Organocatalyst (*b*)	594.19	3	2	7.33 +/- 0.63
6	302.03	0	2	3.87 +/- 0.49
7	316.05	0	2	4.40 +/- 0.49
8	359.09	1	2	4.03 +/- 0.54
9	387.12	1	2	5.09 +/- 0.54
10	370.09	0	2	5.93 +/- 0.50
11	364.05	0	2	5.32 +/- 0.36
12	437.14	1	2	5.63 +/- 0.59

[a] Molecular weight (amu), [b] calculated using ACD/Labs ChemSketch 12.0.

Organocatalyst (*b*) contains a quinuclidine ring linked *via* a two-carbon chain to the thiourea group. In an effort to determine the importance of having a carbon chain linking a tertiary amine to the thiourea, compounds **8** and **9** were designed (Figure 2.16). The presence of the tertiary amine provides compound **8** and **9** with an additional H-bond acceptor moiety in comparison to compounds **6** and **7**. Hydrogen bonding interactions are one of the strongest interactions involved in drug-target binding thus this feature may be important for activity.[11] Both of these compounds also obey the Lipinski rules (Table 2.5).
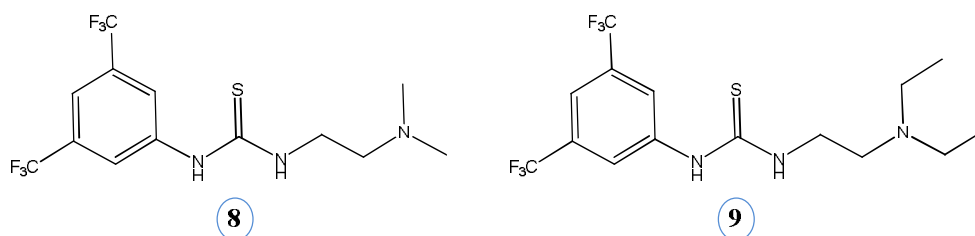
Figure 2.16: SAR study compounds bearing a tertiary amine moiety.

Next, taking the size of the quinuclidine ring into consideration, two compounds were designed in an effort to evaluate the importance of the presence of a sterically

bulky group. As shown in Figure 2.17 the two sterically bulky groups chosen were a cyclohexane ring and a phenyl ring, compound **10** and **11**, respectively. Both groups are six-membered hydrophobic carbon cycles, however, the differences in planarity and aromaticity should result in different target site binding abilities. Therefore, different levels of activity may be demonstrated by each of the compounds. As shown in Table 2.5 both compounds lack H-bond acceptors, a feature that may be disadvantageous for activity considering the hit compound contains three.
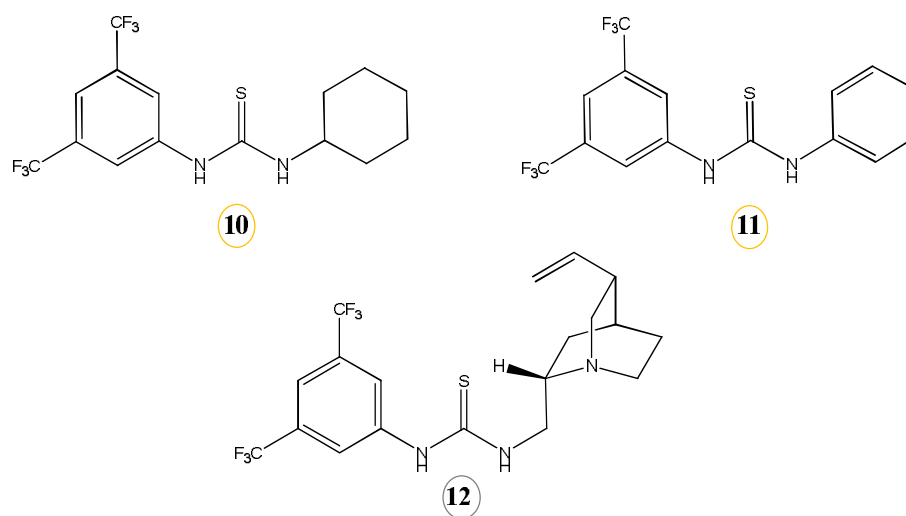
Figure 2.17: Structures of the SAR study compounds **10**, **11** and **12**.

Finally, a 3,5-bis(trifluoromethyl)phenyl thiourea attached to a quinuclidine ring *via* a two-carbon chain was designed (compound **12**, Figure 2.17). Investigating the activity of compound **12** should give insight into the structure-activity relationship of two components of the hit compound. Firstly, the importance of the sterically bulky tertiary amine containing quinuclidine ring and secondly the effect of the loss of the quinoline component. Compound **12** was also found to obey the Lipinski 'rule of 5' with regards to the molecular weight and number of H-bond donors and acceptors, however, its cLogP was found to be > 5 (Table 2.5). As it has only one violation of the Lipinski rules, compound **12** still presents as a compound with favourable absorption/permeability.

2.2.5 Synthesis of part two SAR study compounds

All of the SAR study compounds described above in section 2.2.4 were synthesised using the method described by Andrés *et al.*[95] with modifications. Each of the compounds molecular structure has been elucidated by LC/TOF-MS, ^{1}H and ^{13}C NMR and IR spectroscopies. The IR spectra of each of the compounds contained a strong absorption in the range of 1275-1281 cm^{-1} corresponding to the ν(C=S) of the thiourea moiety.

1-(3,5-Bis(trifluoromethyl)phenyl)-3-methylthiourea (compound **6**) was synthesised, as shown in Scheme 2.7, by the nucleophilic addition reaction of methylamine (2 equivalents) and 3,5-bis(trifluoromethyl)phenyl isothiocyante (1 equivalent). Purification was carried out using silica gel column chromatography to give the product as a white solid in good yield, 87%.

6: R = Me
7: R = Et
8: R = CH$_2$CH$_2$NMe$_2$
9: R = CH$_2$CH$_2$NEt$_2$
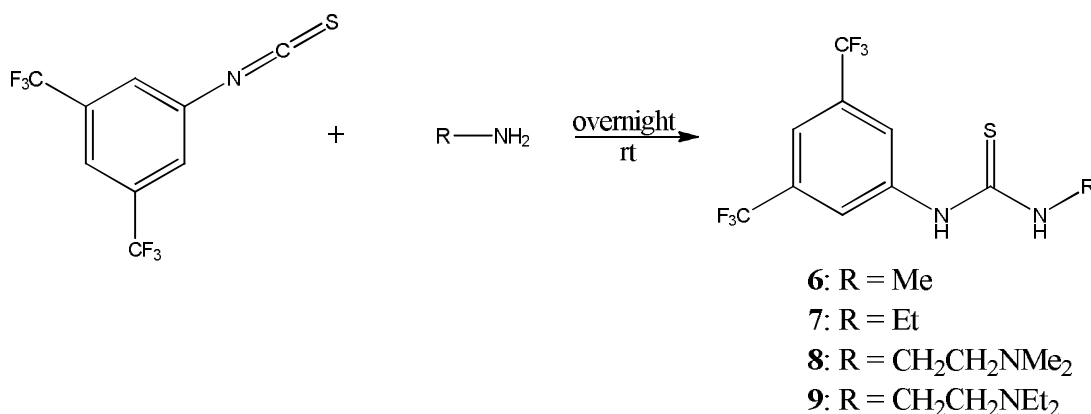
Scheme 2.7: Synthesis of SAR study compounds **6-9**.

The simplicity of the molecular structure of compound **6** gave rise to uncomplicated ^{1}H and ^{13}C NMR spectra. A singlet at 3.06 ppm with an integral of three in the ^{1}H NMR spectrum of compound **6** was observed for the three equivalent protons of the methyl group, this indicated formation of compound **6**. In the ^{13}C NMR spectrum, a characteristic quartet at 124.8 ppm with $^{1}J = 270.8$ Hz, was observed for the two –CF$_3$ groups. Additionally, a quartet at 132.8 ppm ($^{2}J = 33.0$ Hz) was observed for the aromatic carbon directly attached to the –CF$_3$ groups (-*C*-CF$_3$) with the *C*=S carbon signal at 183.7 ppm.

The synthesis of compound **7** was carried out as shown in Scheme 2.7 using a 2:1 ratio of amine:isothiocyanate. The reaction resulted in a good yield of 84%, after purification by silica gel column chromatography. A quartet at 3.60 ppm and triplet at 1.23 ppm, each with $^3J = 7.3$ Hz, corresponding to the protons of the ethyl group were observed in the ^{1}H NMR spectrum, this indicated formation of compound **7**. The quartets at 124.8 ppm and 132.7 ppm, in the ^{13}C NMR spectrum, were found to have *J* values of 270.2 and 33.0 Hz, respectively. These coupling constants correspond to values associated with one-bond and two-bond C-F coupling constants and therefore correspond to the carbons of the –CF$_3$ groups ($^1J = 270.2$ Hz) and the carbons *ipso* to the –CF$_3$ groups ($^2J = 33.0$ Hz).

Compound **8** (Scheme 2.7) was synthesised using a 1:1 ratio of amine:isothiocyanate. A white solid, in 75% yield, was generated after purification by silica gel column chromatography. LC/TOF-MS returned a (M+H$^+$) of 360.0961 indicating formation of the product. However, the ^{13}C and ^{1}H NMR spectra of compound **8**, in CDCl$_3$, were complex. Doubling and broadening of the ^{13}C signals was observed in the ^{13}C NMR spectrum whilst the proton signals of the ^{1}H NMR spectrum were broad and poorly resolved (Figure 2.18). It was thought that perhaps the complex spectra were the result of some form of chemical exchange occurring in solution, for example, restricted bond rotation or tautomerism.
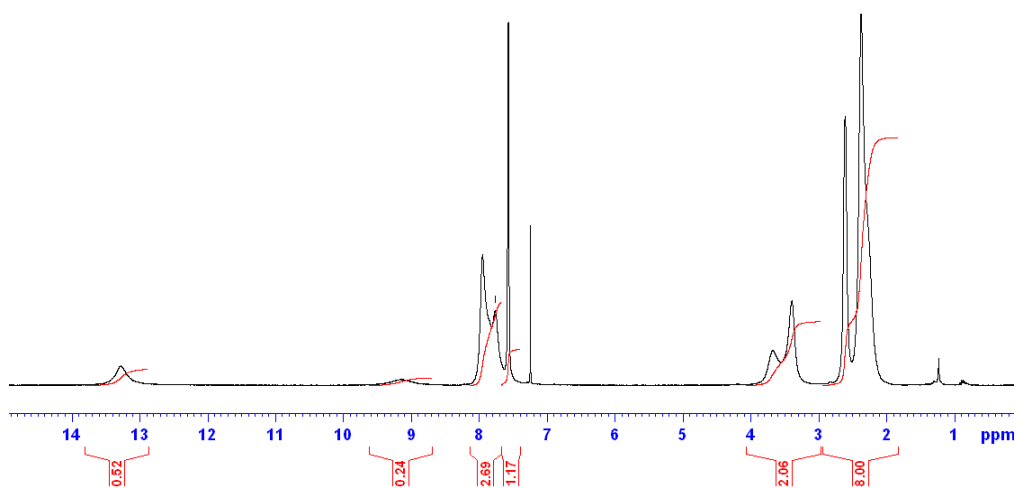
Figure 2.18: ^{1}H NMR spectrum of compound **8** in CDCl$_3$. The residual solvent ^{1}H signal was observed at 7.25 ppm.

In NMR, chemical exchange involves the movement of a nucleus from one environment to another. A commonly encountered example of chemical exchange is restricted bond rotation about the C-N bond of amides, for example, *N,N*-dimethylformamide (DMF). As shown in Figure 2.19, DMF can be represented as two resonance forms. At room temperature, the partial double bond character of the C-N bond allows each of the methyl groups to experience different environments giving rise to a resonance signal for each of the methyl groups at different chemical shifts in the NMR spectra. However, by increasing the temperature of the NMR sample, the barrier to rotation (activation energy required for rotation about the single bond) can be overcome thus resulting in an increase in rotation about the C-N bond. This increase in rotation about the C-N bond allows the methyl groups to experience the same environment resulting in an NMR spectrum wherein both of the methyl groups are represented by one single resonance signal.
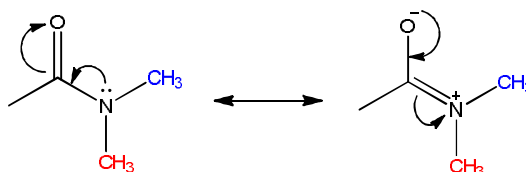
Figure 2.19: Resonance forms of DMF.

The organocatalytic property of the thiourea derivatives mentioned in section 2.1.1 is based on their ability to form H-bonds.[76] A review of the literature found that thiourea derivatives, like Takemotos catalyst, have the ability to self-associate through intra- and intermolecular H-bonding interactions.[96] In fact, this ability to self-aggregate can interfere with the catalytic ability of thiourea-based organocatalysts with high catalyst load and the use of protic solvents having been shown to result in lower enantioselectivities.[96c,97] Studies by Tárkányi *et al.*[96a,b] using low temperature NMR spectroscopy demonstrated that at low temperature both a momomeric and dimeric species resulting from H-bond interactions of the thiourea catalysts can be observed. In both the cinchona-based thiourea organocatalyst and Takemotos catalyst an intramolecular H-bond interaction occurs between the tertiary amine and one of the thiourea NH's giving rise to a monomeric species.[96a,b] Additionally, intermolecular H-bonding occurs between the thiourea NH's of one

molecule of catalyst and the thiourea sulfur atom of a second catalyst molecule resulting in the formation of a dimer.[96a] Furthermore, it is believed that the monomeric and dimeric forms are in equilibrium (chemical exchange) and that these self-aggregrates are the cause of the broadening effect of ^{1}H NMR signals at room temperature.[96b]

Taking these studies into consideration, it was believed that the thiourea derivative, compound **8**, may be undergoing self-association in $CDCl_3$ and therefore resulting in a broadening effect of the signals in the NMR spectra. In order to investigate this, the NMR experiments were carried out using CD_3OD in place of $CDCl_3$. Methanol is a polar protic solvent with the ability to accept and donate H-bonds and should therefore interfere with the H-bonding interactions and disrupt the self-association of the thiourea derivatives. The disruption of H-bonding interactions should, in turn, result in sharper resonance signals in the NMR spectra. As observed with the cinchona-based organocatalysts[96b], the ^{1}H and ^{13}C NMR spectra of compound **8** in CD_3OD exhibited one set of sharp resonance signals indicating a loss in self-association (Figure 2.20).
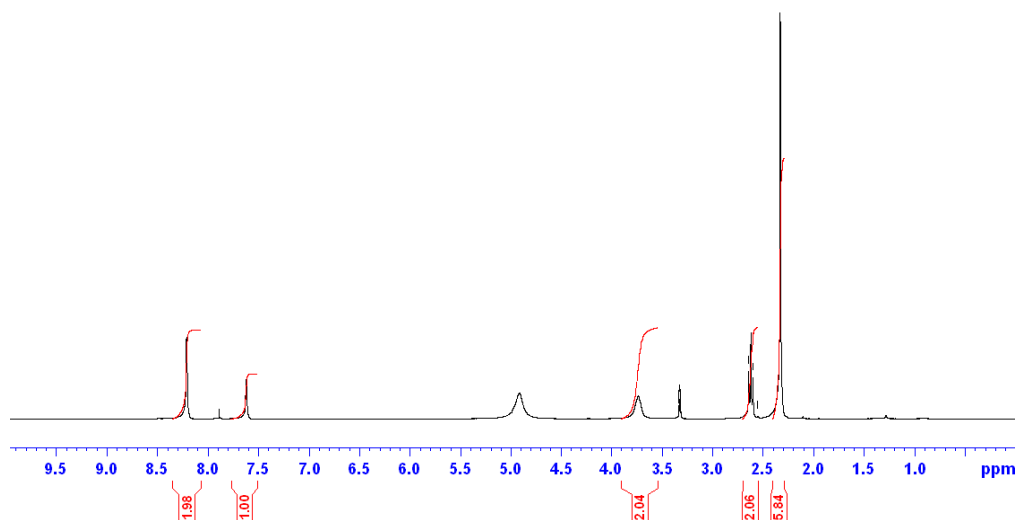
Figure 2.20: ^{1}H NMR spectrum of compound **8** in CD_3OD. The residual solvent ^{1}H signal was observed at 3.32 ppm and the ^{1}H signal for H_2O at 3.91 ppm.

To further confirm the occurrence of self-association of compound **8** a number of ^{1}H NMR experiments were ran at higher temperatures. If the monomeric and dimeric

thiourea species of the thiourea bifunctional catalysts can be observed in NMR spectra at low temperatures then by increasing the temperature the speed at which they are equilibrating should increase and give rise to sharper resonance signals in the NMR spectra. A series of experiments were carried out in CDCl$_3$ at a range of temperatures from 25 °C to 54 °C (Figure 2.21).
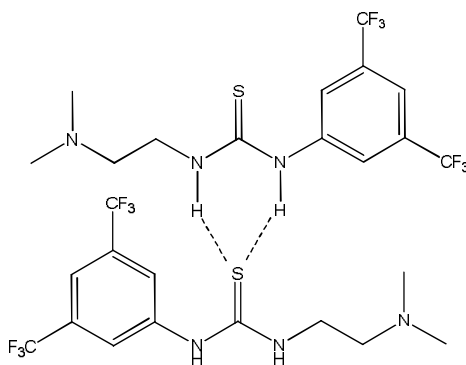
Proposed structure of the dimeric form of compound **8**.
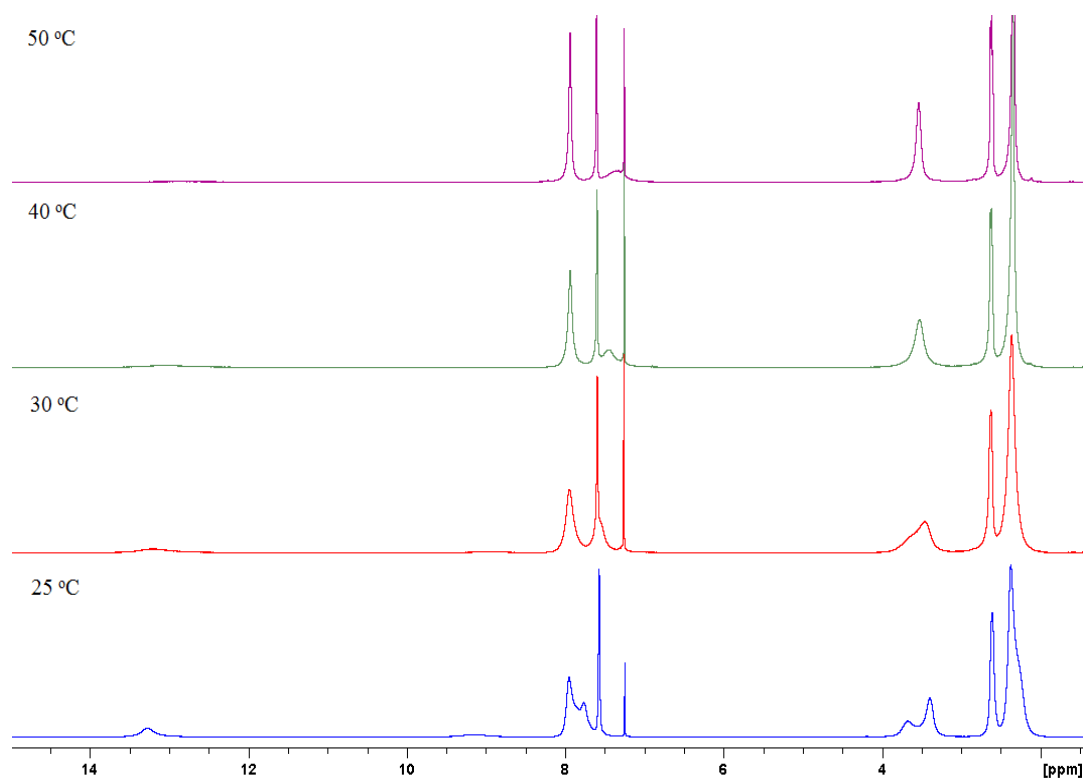
Figure 2.21: A selection of the variable temperature (VT) ^{1}H NMR spectra of compound **8** in CDCl$_3$ and a proposed structure for the dimeric form of compound **8**. Spectra recorded at (–) 25 °C, (–) 30 °C, (–) 40 °C and (–) 50 °C.

As can be seen in Figure 2.21, an increase in temperature resulted in sharper resonance signals. The ^{1}H NMR signals showed no further improvement in lineshape above 50 ^{o}C thus the ^{13}C NMR experiment (CDCl$_3$) was also carried out at this temperature. The resulting ^{13}C NMR spectrum exhibited only one set of sharper resonance signals unlike that observed at 25 ^{o}C. The results indicate that at room temperature compound **8** may exist as both a dimer and monomer as a result of H-bonding interactions and that an increase in temperature can increase the rate at which these species are interconverting. Additionally, the use of a protic solvent (CD$_3$OD) appears to interrupt the H-bonding interactions resulting in NMR spectra with a single set of sharp resonance signals.

As with compound **6** and **7**, in the ^{13}C NMR spectrum of compound **8** (CD$_3$OD) a quartet at 124.8 ppm with $^1J = 270.8$ Hz was assigned as the ^{13}C signal of the –CF$_3$ groups. The ^{13}C signal representing the carbon atoms adjacent to the –CF$_3$ groups (-*C*-CF$_3$) was found at 132.7 ppm having a characteristic two-bond C-F coupling constant of 33.0 Hz. Due to the deshielding effect of the tertiary amine moiety the ^{13}C signals for the carbon atoms of the two-carbon chain (-*C*H$_2$*C*H$_2$) were found at 58.6 and 43.0 ppm, downfield from those of the ethyl chain of compound **7**. This was also the case for the protons of the two-carbon chain in the ^{1}H NMR spectra (CD$_3$OD), indicating formation of compound **8**. The equivalent protons of the tertiary amine methyl groups were observed as a singlet at 2.33 ppm in the ^{1}H NMR spectrum.

The reaction of one equivalent of *N,N*-diethylethylenediamine and one equivalent of 3,5-bis(trifluoromethyl)phenyl isothiocyanate at room temperature generated compound **9** (Scheme 2.7). As for the thiourea derivatives described thus far, compound **9** was purified by silica gel column chromatography, which resulted in a yellow oil in a 92% yield. LC/TOF-MS returned a (M+H$^+$) of 388.1270 indicating formation of compound **9** and as seen with compound **8**, the NMR spectra obtained in CDCl$_3$ were complex with doubling of peaks and broad resonance signals being observed. Therefore, the NMR experiments were carried out in CDCl$_3$ at 50 ^{o}C and also in CD$_3$OD at room temperature (Figure 2.22). The resulting spectra exhibited only one set of sharp resonance signals indicating that in the aprotic solvent, at room

temperature, compound **9** may be equilibrating between a monomeric and dimeric form as a result of H-bonding interactions.
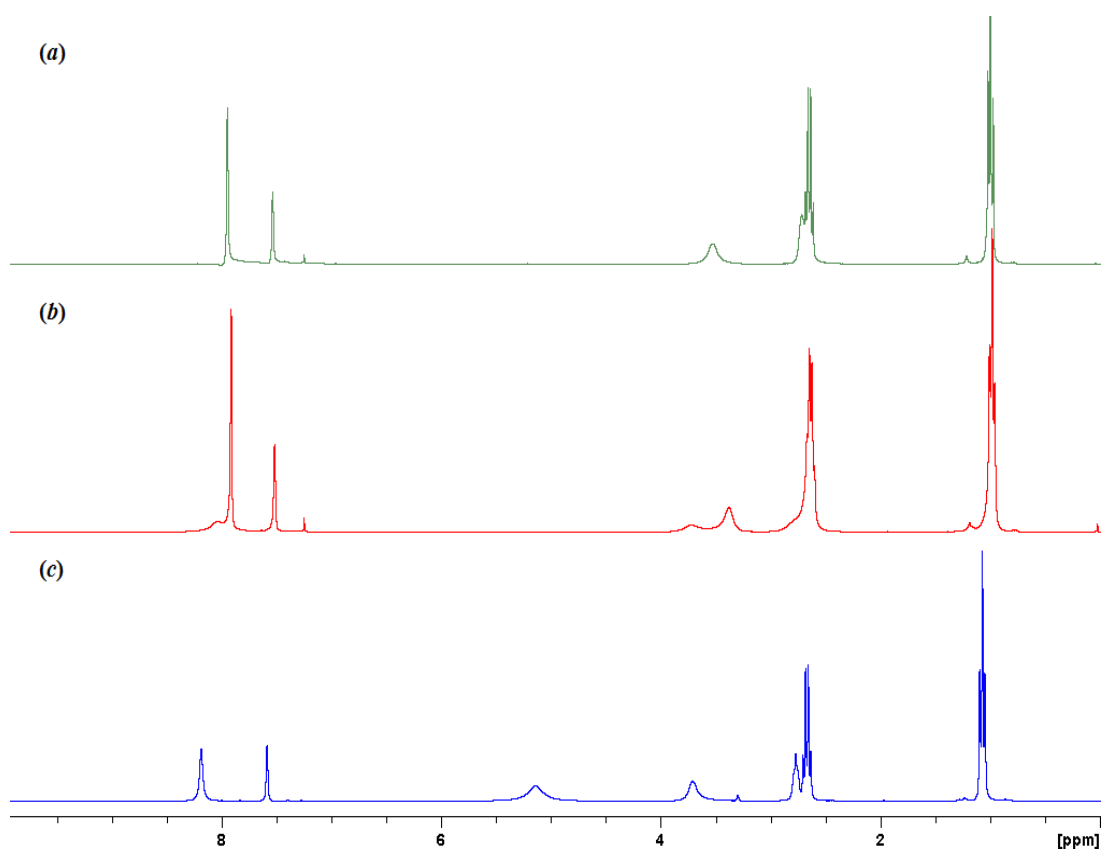
Figure 2.22: ^{1}H NMR spectra of compound **9** in (*a*) CDCl$_3$ at 50 $^{\circ}$C, (*b*) CDCl$_3$ at 25 $^{\circ}$C and (*c*) CD$_3$OD at 25 $^{\circ}$C. Solvent residual ^{1}H signals were also observed in each spectrum.

In the ^{13}C NMR spectrum the quartets at 124.7 and 132.7 ppm were found to have coupling constants characteristic of one-bond and two-bond C-F coupling (^{1}J = 270.8 and ^{2}J = 33.0 Hz, respectively,) and were therefore assigned as the carbon signals of the –CF$_3$ (124.7 ppm) and –C–CF$_3$ (132.7 ppm) moieties. As observed for compound **8**, the ^{13}C signals representing the carbons of the two-carbon chain linking the tertiary amine to the thiourea, were found downfield from those of –CH$_2$CH$_3$ group of compound **7** due to the electron-withdrawing effect of the tertiary amine N atom. The triplet and quartet found at 1.07 and 2.67 ppm in the ^{1}H NMR spectrum (CD$_3$OD), were assigned as the protons of the –CH$_2$ and –CH$_3$ of the –NEt$_2$ group each having ^{3}J = 7.1 Hz.

61

The nucleophilic addition of cyclohexylamine to 3,5-bis(trifluoromethyl)phenyl isothiocyanate generated compound **10** (Scheme 2.8). Purification by silica gel column chromatography produced compound **10** as a white solid in a 95% yield. The presence of the cyclohexyl group gives rise to a slightly more complex ^{1}H NMR spectrum in comparison to compounds **6** and **7**, with multiplets representing the cyclohexyl protons found between 1 and 2 ppm. Two broad singlets at 8.42 and 6.13 ppm, integrating for one proton each, were identified as the protons of the thiourea NH's. In the ^{13}C NMR spectrum, the quartets corresponding to the carbons of the –CF$_3$ groups and those directly attached to the –CF$_3$ groups (-*C*-CF$_3$) were observed at 122.8 and 132.9 ppm, respectively.
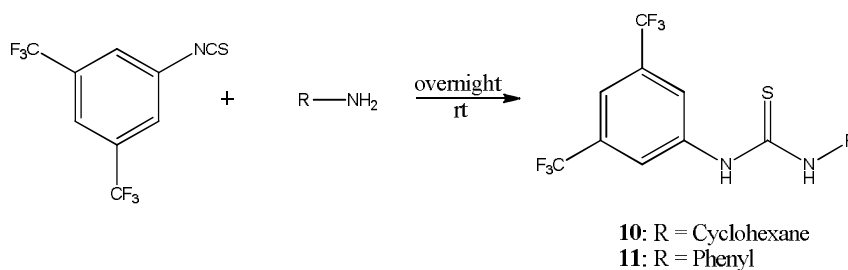
Scheme 2.8: Synthesis of SAR study compounds **10** and **11**.

The reaction of aniline with 3,5-bis(trifluormethyl)phenyl isothiocyanate produced compound **11** in good yield, 92%, after purification (Scheme 2.8). As with compound **10**, the presence of the aromatic phenyl ring resulted in a more complex ^{1}H NMR spectrum in comparison to compounds **6** and **7**, with the thiourea NH protons observed at 8.89 and 7.88 ppm as broad singlets. In the ^{13}C NMR spectrum, the carbon signal of the –CF$_3$ groups was found to have a *J* value of 270.0 Hz, which is characteristic of a one-bond C-F coupling constant. The carbon signal (a quartet) at 132.0 ppm was assigned as the carbon directly attached to the –CF$_3$ groups as it has a coupling constant of 33.0 Hz, a value which falls within the range of the [2]*J* C-F coupling constants.

Finally, compound **12** was synthesised by the reaction of quincoridine-amine (QCD-amine) with 3,5-bis(trifluoromethyl)phenyl isothiocyanate (Scheme 2.9). Compound **12** was isolated as a white solid in 93% yield after purification by silica gel column chromatography. Similar to compounds **8** and **9**, the NMR spectra of compound **12**

in CDCl$_3$ exhibited doubling and broadening of peaks. However, carrying out the NMR experiments in CDCl$_3$ at 50 ^{o}C or in CD$_3$OD at room temperature resulted in spectra containing one set of sharp resonance signals (Figure A1, Appendix A). These results suggest that compound **12** may also undergo self-association in aprotic solvents at room temperature. The presence of the quinuclidine ring results in complex ^{1}H NMR spectra having a number of multiplets representing the protons of the quinuclidine bicycle between 1.40-3.20 ppm. In the ^{13}C NMR spectrum the ^{13}C signal for the carbon of the C=S was found at 182.8 ppm with the quartets for the carbons of the –CF$_3$ groups at 124.8 ppm (^1J = 270.0 Hz) and the -C-CF$_3$ ^{13}C signal at 132.8 ppm, indicating formation of compound **12**.
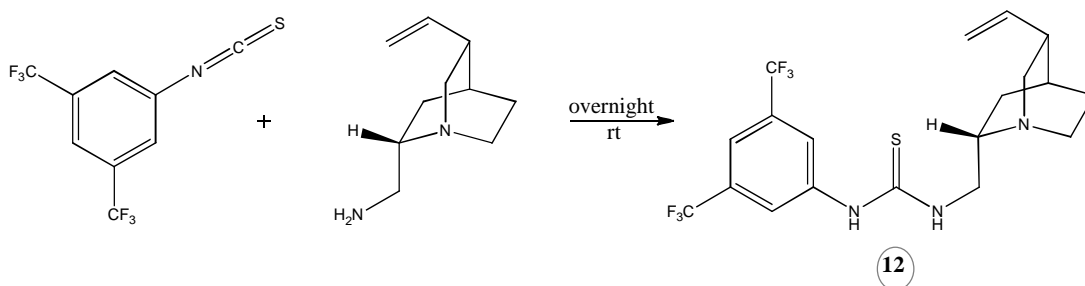
Scheme 2.9: Synthesis of compound **12**.

2.2.6 *In vitro* antibacterial activity

Each of the part two SAR study compounds (Figure 2.23) were evaluated for their bacteriostatic activity using the susceptibility assay as described in section 1.2.5. As with the part one SAR study compounds, these compounds were tested against *E. coli*, *P. aeruginosa* and *S. aureus*. Due to the structural similarities between organocatalyst (*b*) and Takemotos catalyst (Figure 2.3, section 2.1.1), and its previously reported antibacterial results[74], Takemotos catalyst was also evaluated against each of the bacteria used within this study.
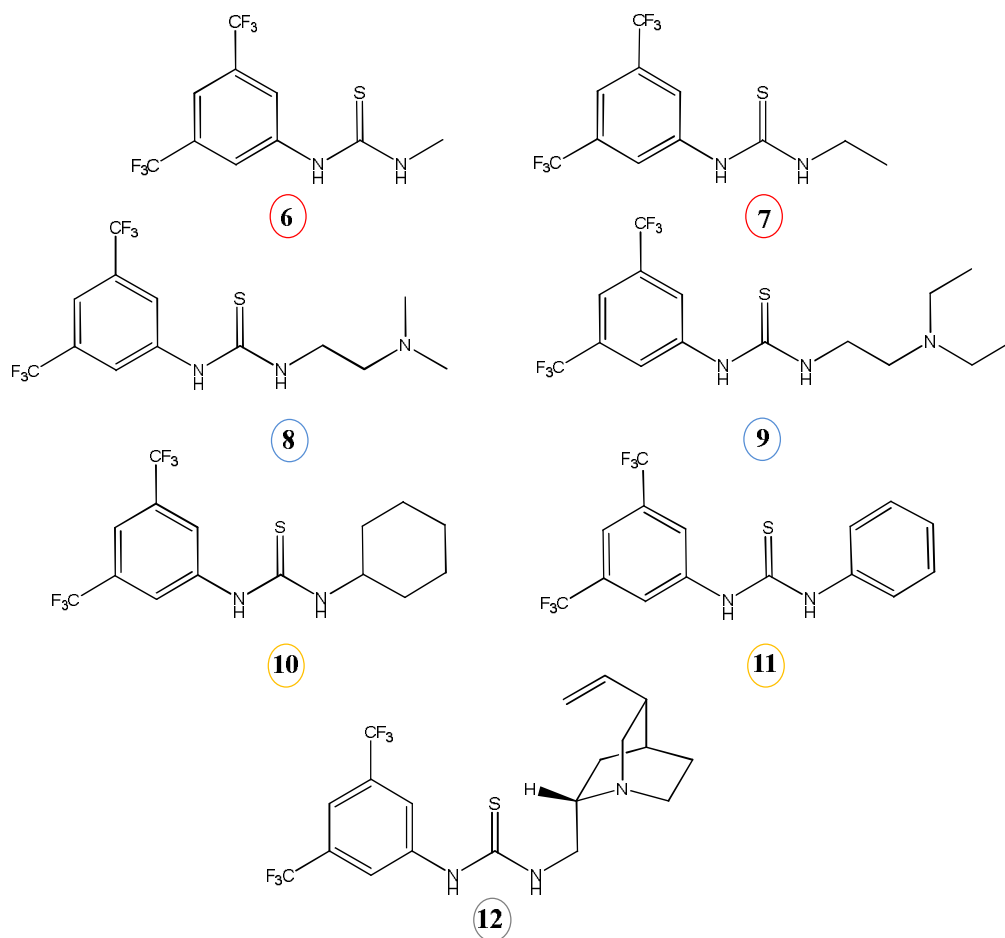
Figure 2.23: Part two SAR study compounds evaluated for their bacteriostatic activity.

The results, which have been summarised in Tables 2.6, 2.7 and 2.8, are expressed as the MIC_{50}, MIC_{80} and MIC_{90}. Again, vancomycin hydrochloride and ciprofloxacin were used as the reference drugs and their results are included in Tables 2.6, 2.7 and 2.8. Any compound that did not exhibit an MIC, of the given percentage of growth inhibition, against each of the bacteria has been excluded from the tables.

Table 2.6: SAR study compounds antibacterial activity as MIC_{50} range. Values are the mean of three experiments

Compound	*E. coli*		*P. aeruginosa*		*S. aureus*	
	μM	μg/mL	μM	μg/mL	μM	μg/mL
Vancomycin hydrochloride	1.58-2.10	2.35-3.13	>67.31	>100.00	1.58-2.10	2.35-3.13
Ciprofloxacin	>301.99	>100.00	1.18-1.77	0.39-0.59	>301.99	>100.00
Organocatalyst (*b*)	2.63-3.95	1.56-2.35	>168.30	>100.00	3.95-5.26	2.35-3.13
Takemotos catalyst	60.51-90.77	25.00-37.50	>242.05	>100.00	60.51-90.77	25.00-37.50
7	158.20-237.31	50.00-75.00	>316.41	>100.00	>316.41	>100.00
9	96.87-129.16	37.50-50.00	>258.32	>100.00	96.87-129.16	37.5-50.00
10	101.33-135.00	37.50-50.00	>270.20	>100.00	135.10-202.65	50.00-75.00
11	51.50-68.67	18.75-25.00	>274.69	>100.00	>274.69	>100.00
12	42.89-57.19	18.75-25.00	>228.76	>100.00	42.89-57.19	18.75-25.00

Table 2.7: SAR study compounds antibacterial activity as MIC_{80} range. Values are the mean of three experiments.

Compound	*E. coli*		*P. aeruginosa*		*S. aureus*	
	μM	μg/mL	μM	μg/mL	μM	μg/mL
Vancomycin hydrochloride	2.10-3.16	3.13-4.69	*>67.31*	*>100.00*	3.16-4.21	4.69-6.25
Ciprofloxacin	*>301.99*	*>100.00*	1.18-1.77	0.39-0.59	*>301.99*	*>100.00*
Organocatalyst (*b*)	5.26-7.90	3.13-4.69	*>168.30*	*>100.00*	7.90-10.52	4.69-6.25
Takemotos catalyst	90.77-121.02	37.5-50.00	*>242.05*	*>100.00*	90.77-121.02	37.50-50.00
9	129.16-193.74	50.00-75.00	*>258.32*	*>100.00*	129.16-193.74	50.00-75.00
11	103.01-137.35	37.50-50.00	*>274.69*	*>100.00*	*>274.69*	*>100.00*
12	85.79-114.38	37.50-50.00	*>228.76*	*>100.00*	85.78-114.38	37.50-50.00

Table 2.8: SAR study compounds antibacterial activity as MIC_{90} range. Values are the mean of three experiments.

Compound	E. coli		P. aeruginosa		S. aureus	
	μM	μg/mL	μM	μg/mL	μM	μg/mL
Vancomycin hydrochloride	4.21-6.31	6.25-9.38	>67.31	>100.00	4.21-6.31	6.25-9.38
Ciprofloxacin	>301.99	>100.00	37.75-56.62	12.5-18.75	>301.99	>100.00
Organocatalyst (b)	7.90-10.52	4.69-6.25	>168.30	>100.00	10.52-15.78	6.25-9.38
Takemotos catalyst	121.02-181.54	50.00-75.00	>242.05	>100.00	90.77-121.02	37.50-50.00
9	193.74-258.32	75.00-100.00	>258.32	>100.00	193.74-258.32	75.00-100.00
11	206.02-274.69	75.00-100.00	>274.69	>100.00	>274.69	>100.00
12	85.78-114.38	37.50-50.00	>228.76	>100.00	85.78-114.38	37.50-50.00

As with the SAR study compounds evaluated in part one, none of the SAR study compounds exhibited bacteriostatic activity against the Gram-negative bacterium *P. aeruginosa*. As suggested earlier, the lack of inhibition of growth may be due to the intrinsic resistance mechanisms associated with *P. aeruginosa* such as the ability to form a capsule, grow as a biofilm and its inefficient porins resulting in slow uptake of the molecules.[18,36,39-40,42]

Of the SAR study compounds evaluated in part one (Table 2.3 and 2.4, section 2.2.3), the compounds which exhibited activity did so against both *E. coli* and *S. aureus*. However, for each of the active compounds the level of activity against *E. coli* was greater than that demonstrated against *S. aureus*. Amongst the eight compounds from part two, only four of these compounds exhibited MIC_{50} values against both *E. coli* and *S. aureus* (Table 2.6). As with the active compounds in part one, each of the four compounds here demonstrated greater activity against *E. coli* in comparison to that exhibited against *S. aureus* (Table 2.6).

The first compound, from the part two SAR study, to be evaluated was the structurally simple 1-(3,5-bis(trifluoromethyl)phenyl)-3-methylthiourea (compound **6**, Figure 2.23). Compound **6** exhibited little or no activity against each of the bacteria examined suggesting that the simple 3,5-bis(trifluoromethyl)phenyl thiourea moiety alone is not the source of activity.

Next, compound **7** (Figure 2.23) was evaluated for its bacteriostatic activity. As shown in Table 2.6, compound **7** only demonstrated activity against *E. coli* resulting in a MIC_{50} of 50.00-75.00 μg/mL. Although this is a slight improvement on compound **6**, the MIC_{50} achieved by compound **7** is much greater than that observed for the hit compound (1.56-2.35 μg/mL). Furthermore, compound **7** was unable to inhibit any more than 50% of bacterial growth again suggesting that the simple nature of the thiourea structure alone is not enough to exhibit antibacterial activity.

Following on from compounds **6** and **7**, the carbon chain was extended with a terminal tertiary amine which was bound to either two methyl (compound **8**) or two ethyl groups (compound **9**). Similar to compound **6**, compound **8** demonstrated little or no bacteriostatic activity against all three bacteria. Compound **9** on the other hand

resulted in an MIC_{50} of 37.50-50.00 µg/mL against both *E. coli* and *S. aureus*. Furthermore, compound **9** had the ability to inhibit up to 90% of bacterial growth, although a higher concentration was required to do so (Table 2.8). These results indicate that although the addition of the two-carbon chain bound to a simple tertiary amine does not improve bacteriostatic activity (compound **8**), the addition of a slightly more hydrophobic and bulky tertiary amine is beneficial for activity. What's more, in comparison to compound **7**, which was inactive against *S. aureus*, the addition of the –NEt$_2$ group resulted in a compound that can inhibit up to 80% of *S. aureus* growth at a concentration range of 50.00-75.00 µg/mL (compound **9**). According to the Lipinski 'rule of 5' (Table 2.5, section 2.2.4), replacement of the tertiary amine methyl groups with the ethyl groups results in an increase in lipophilicity. If the target site of the compound is inside the bacterial cell, this increase in lipophilicity may be helping to facilitate entry into the bacterial cells and therefore aid in its ability to reach the target site.

Continuing with the investigation into the importance of the two-carbon chain linking a tertiary amine to the 3,5-bis(trifluoromethyl)thiourea moiety, compound **12** was also synthesised (Figure 2.23). As shown in Table 2.6, compound **12** was more active than compound **7** and **9** against both *E. coli* and *S. aureus*. Furthermore, compound **12** can inhibit the growth of both *E. coli* and *S. aureus* by 50% at the same concentration with an increase in concentration resulting in an increase in bacteriostatic activity (Table 2.6 and 2.7).

The cLogP of compound **12** was calculated to be approximately 5.63 (Table 2.5, section 2.2.4), which is a slight increase in cLogP compared to compound **9** (5.09 +/- 0.54). Therefore, perhaps this increase in lipophilicity improves activity. Additionally, these results suggest that the more sterically bulky quinuclidine ring is favourable for activity.

Alkyl groups and heterocycles can interact with binding regions of a target binding site through van der Waals interactions.[11] These interactions are some of the weaker types of interactions involved in target site binding, consequently the distance between the binding region and binding group is important with regards to the

strength of the interaction.[11] If the target binding site is large enough to allow the entry of a bicycle then the smaller diethylamine functionality will also, most likely, 'fit' into the binding site. However, the smaller size of the diethylamine means that the distance between it and the binding regions of the binding site would be greater than the distance between the quinuclidine ring and the binding regions (Figure 2.24). Therefore, the binding interactions between the diethylamine and the binding regions of the target site may be weaker resulting in a reduction in activity. A similar trend in activity was observed on going from compound **7** to compound **9** (Table 2.6).
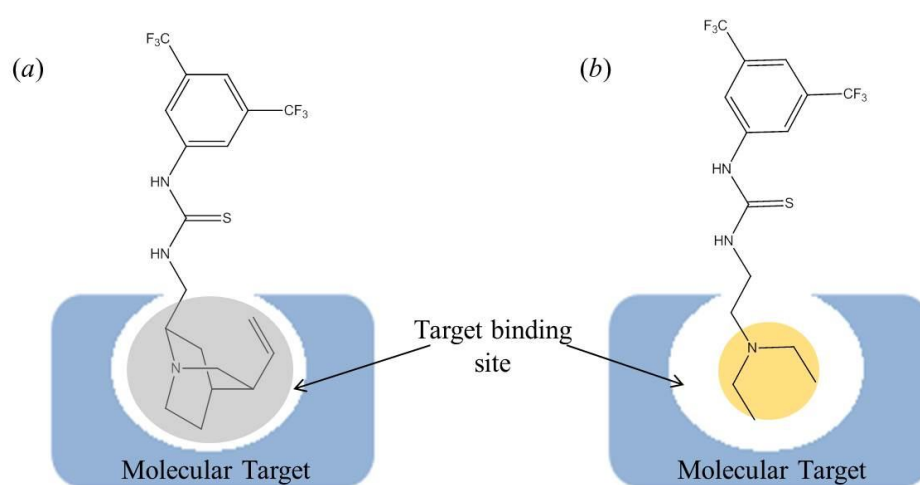
Figure 2.24: Target site binding and the effect of binding group size.

To further investigate the effect of steric bulk on the activity of the thiourea compounds, compounds **10** and **11** (Figure 2.23) were evaluated for their bacteriostatic activity. Compound **10** exhibited activity against both *E. coli* and *S. aureus* resulting in MIC_{50} ranges of 37.50-50.00 and 50.00-75.00 µg/mL, respectively. Compound **11** on the other hand only exhibited activity against *E. coli*, however, the MIC_{50} obtained was less than that of compound **10** (Table 2.6). Additionally, an increase in compound **11** concentration resulted in an increase in percentage of growth inhibition whereas compound **10** did not inhibit greater than 50% of bacterial growth (Table 2.6 and 2.7).

With regards to structure, both groups are six-membered carbon rings with the difference being that compound **11** is planar and aromatic whereas compound **10** is

non-planar and sterically bulkier. According to the cLogP values, compound **11** is only slightly less lipophilic than compound **10**. Therefore, perhaps the difference in activity against *E. coli* is due to the difference in their affinities to bind to the target site. If the two compounds share the same target then perhaps the planar aromatic cyclic ring is a better 'fit' for the target site. The presence of π-bonds means that compound **11** has a region of high electron density and perhaps this can assist in better binding interactions and therefore greater activity.

Takemotos catalyst was also evaluated for its bacteriostatic activity against the bacterial strains used within this study. The results show that Takemotos catalyst was more active than compound **10** against both *E. coli* and *S. aureus*, however, similar activity to Takemotos catalyst was exhibited by compound **11** against *E. coli* (Table 2.6). An increase in concentration resulted in an increase in bacteriostatic activity with Takemotos catalyst exhibiting lower MIC_{90} values in comparison to compound **11**. These results indicate that a sterically bulky group attached at the 3-position of the thiourea moiety is beneficial for activity. Additionally, the presence of a cyclic group bearing a tertiary amine appears to be advantageous with Takemotos catalyst and compound **12** exhibiting greatest activity amongst the eight SAR study compounds tested (Table 2.6, 2.7 and 2.8).

The lone pair of electrons present on the tertiary amine of Takemotos catalyst and compound **12** potentially allows the N atom to act as a H-bond acceptor. Hydrogen bond interactions are one of the stronger forms of target site binding interactions.[11] Therefore, the introduction of the H-bond acceptor may be increasing the binding affinity of the molecules for the target binding site leading to an increase in bacteriostatic activity. The difference in activity between Takemotos catalyst and compound **12**, compound **12** being more active (Table 2.6), could be due to the structure of the tertiary amine and how the substituents affect access to the lone pair of electrons. As can be seen in Figure 2.25, in the quinuclidine ring the 'alkyl groups' are part of a rigid ring system that holds them clear of the N atom lone pair thus exposing the lone pair for H-bonding interactions. In contrast, the substituents attached to the tertiary amine N atom are not 'held back' and so may hinder access to the N atom lone pair which in turn could reduce any H-bond interaction that may be

occurring (Figure 2.25). The lack of, or reduction in, H-bond interactions could result in a lower binding affinity of Takemotos catalyst for the target binding site and therefore reduce the antibacterial activity. This could also be a reason why compound **9** is less active than compound **12**. Additionally, the cLogP of Takemotos catalyst was found to be approximately 5.14, a value lower than that of compound **12** and indicating that the reduced activity observed for Takemotos catalyst in comparison to compound **12** may also be due to a reduction in lipophilicity.

Takemotos Catalyst   Compound **12**
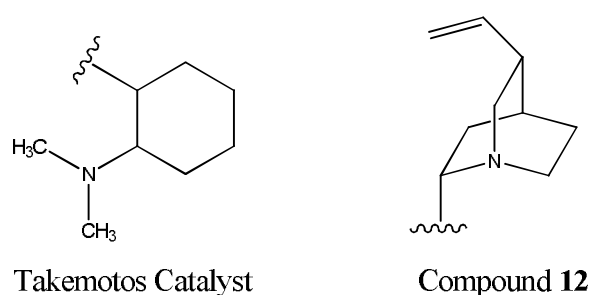
Figure 2.25: Comparison of tertiary amine structures from Takemotos catalyst and compound **12**.

Overall, none of the part two SAR study compounds were active against *P. aeruginsa*. Of the active compounds, activity was greatest against *E. coli* with only four of the compounds also exhibiting activity against *S. aureus*. In comparison to the reference drugs MIC ranges, none of the active compounds demonstrated bacteriostatic activity at lower concentrations.

The results of part two of the SAR study have been summarised in Figure 2.26. The structurally simple 1-(3,5-bis(trifluoromethyl)phenyl)-3-methylthiourea derivative exhibited little or no activity against all three bacteria. However, an increase in chain length alongside the addition of a tertiary amine (-NEt$_2$, compound **9**) did improve activity against both *E. coli* and *S. aureus* (Table 2.6). The introduction of sterically bulky groups appears to be beneficial for activity with compounds **10** and **11** exhibiting antibacterial activity (Table 2.6). The quinuclidine derivative, compound **12**, exhibited greatest activity amongst the eight SAR study compounds. Although compound **12** exhibited greater activity than that demonstrated by Takemotos catalyst, compound **12** remained less active (6- to 8-fold decrease in activity) than

the hit compound, organocatalyst (*b*) (Table 2.8), therefore suggesting that the quinoline bicycle is important for activity.
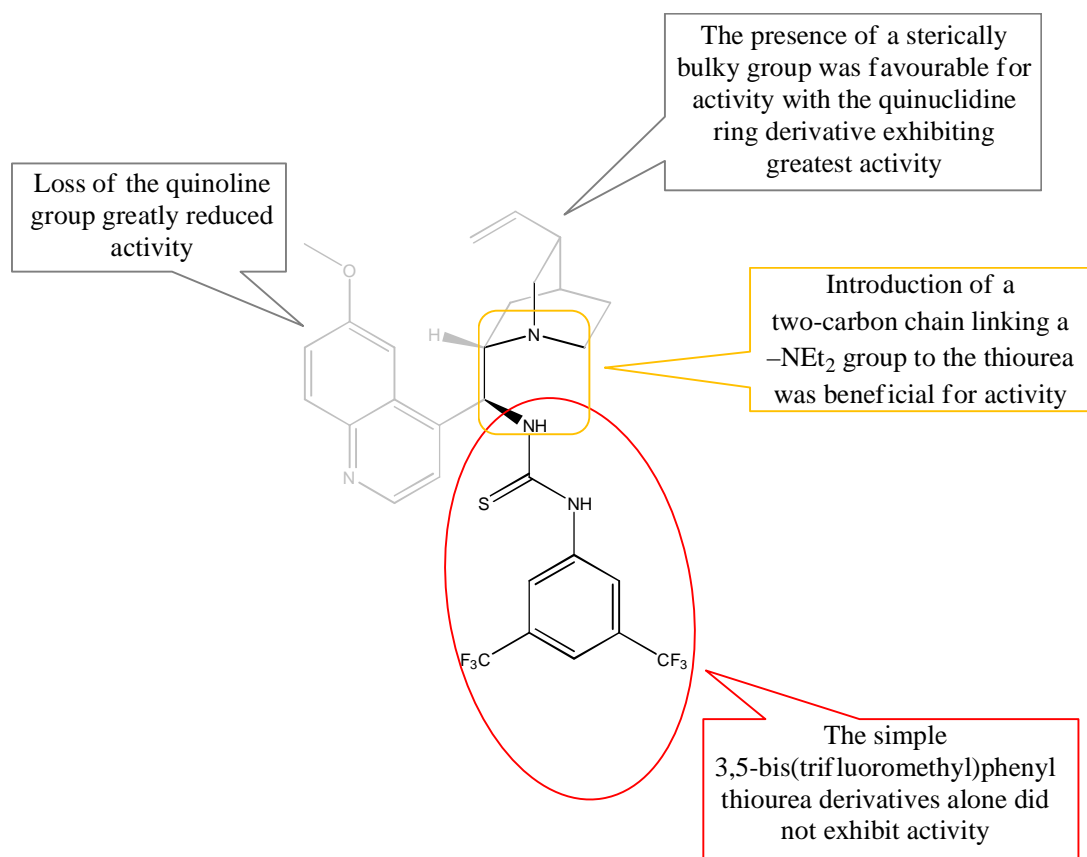
Figure 2.26: A summary of part two of the SAR study of organocatalyst (*b*).

2.2.7 *In vivo* **SAR study compound tolerance**

In an effort to further investigate the structure-activity relationship of organocatalyst (*b*) *in vivo* toxicity studies were carried out as described in section 1.2.8 using the larvae of the greater wax moth, *Galleria melonella* (*G. melonella*). Organocatalyst (*b*) and a selection of the SAR study compounds, shown in Figure 2.27, which exhibited antibacterial activity were chosen for evaluation of their toxicity. The results are presented in Table 2.9 as the survival of *G. mellonella* larvae (expressed as %) as a function of the compound dosages administered.
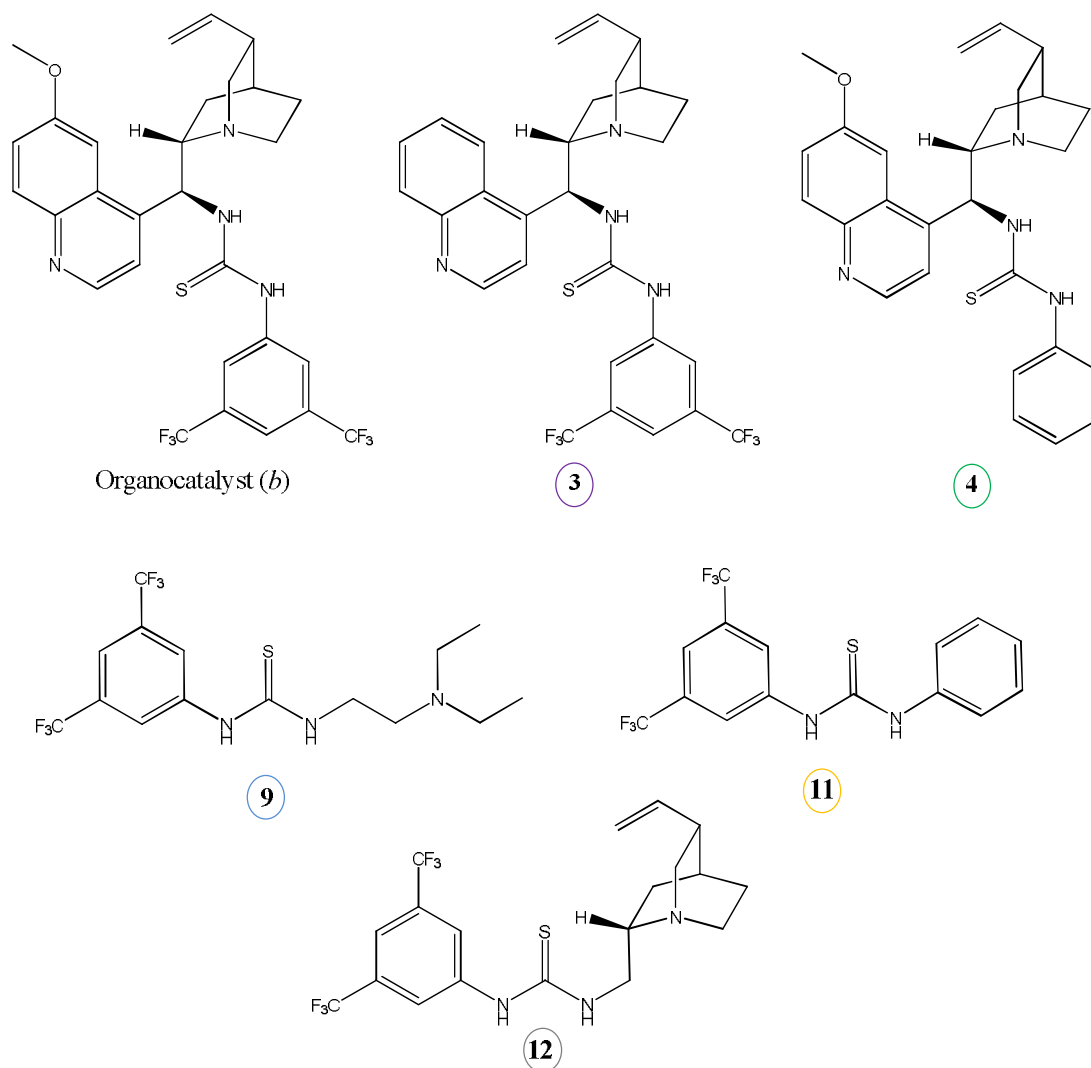
Figure 2.27: Organocatalyst (*b*) and the SAR study compounds evaluated for in vivo toxicity.

As can be seen in Table 2.9, at a concentration of 1 µg/mL a 100% survival rate was observed with each of the SAR study compounds tested after 72 hours. A 97% survival rate was observed for organocatalyst (*b*) at the same concentration as one *G. mellonella* larva died after 48 hours. However, increasing the administration dose to 10, 50 and 100 µg/mL did not appear to effect the *G. mellonella* with a 100% survival rate observed at each of these concentrations for every compound tested including organocatalyst (*b*) (Table 2.9). The *in vivo* toxicity of the hit compound organocatalyst (*b*) was also evaluated at the higher concentration of 1000 µg/mL and was found to be non-toxic at this concentration.

Table 2.9: Survival of *G. mellonella* larvae (expressed as %) post injection at 24, 48 and 72 h.

Compound	Dosage concentration (μg/mL)	*G. mellonella* survival		
		24	48	72
Organocatalyst (*b*)	1000	100	100	100
	100	100	100	100
	50	100	100	100
	10	100	100	100
	1	100	97	97
3	100	100	100	100
	50	100	100	100
	10	100	100	100
	1	100	100	100
4	100	100	100	100
	50	100	100	100
	10	100	100	100
	1	100	100	100
9	100	100	100	100
	50	100	100	100
	10	100	100	100
	1	100	100	100
11	100	100	100	100
	50	100	100	100
	10	100	100	100
	1	100	100	100
12	100	100	100	100
	50	100	100	100
	10	100	100	100
	1	100	100	100

The *G. mellonella* larvae were also monitored for their development, that is, whether or not the larvae become pupae. It was found that after seven days, at each test compound concentration, the number of the *G. mellonella* larvae that had pupated was similar to that observed for the untreated *G. mellonella* ($\geq$ 60%). These results indicate that not only were the compounds non-toxic to the larvae of the greater wax moth but they also did not appear to interfere with larval development.

Both thiourea itself and derivatives of thiourea have been shown to possess a vast array of biological activities including biocidal activity towards insects and cytotoxic activity towards mammalian cancer cell lines.[82b,94b,98] Considering the toxicity of thioureas and the positive correlation that has been observed between compound toxicity in *G. mellonella* and mice, the results of the *in vivo* toxicity evaluation of organocatalyst (*b*) and its SAR study compounds presented here are encouraging.

2.2.8 Conclusion

Herein, an investigation into the structure-activity relationship of organocatalyst (*b*) (Figure 2.28) was carried out in an attempt to uncover the structural components responsible for its antibacterial activity. The study was divided into two parts.
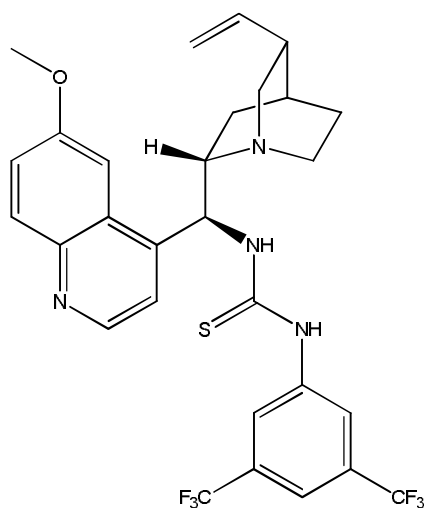
Figure 2.28: Hit compound, organocatalyst (*b*)

Initial studies involved the design and synthesis of derivatives of organocatalyst (*b*) lacking functional groups which may be important for activity. A total of five derivatives, including organocatalyst (*b*), were synthesised. Each of the derivatives, were purified by silica gel column chromatography followed by additional purification by precipitation. The organocatalyst (*b*) derivatives were isolated as white solids in reasonable yields in the range of 50-56%.

Part two of the study involved a more in depth investigation into the structure-activity relationship of organocatalyst (*b*) with the focus placed on the thiourea moiety. A series of compounds bearing the 3,5-bis(trifluoromethyl)phenyl thiourea

moiety were designed and synthesised. The nucleophilic addition of the chosen amine to 3,5-bis(trifluoromethyl)phenyl isothiocyanate generated the SAR study compounds in good to excellent yields, 75-95%, after purification by silica gel column chromatography.

All compound structures were elucidated by LC/TOF-MS, ^{1}H and ^{13}C NMR and IR spectroscopies. In some cases (compounds **8**, **9** and **12**) complex NMR spectra (CDCl$_3$) consisting of peak doubling and broadened resonance signals were obtained. It was believed that these effects were due to the formation of self-aggregates, a process known to occur with thiourea compounds, as a result of intra- and intermolecular H-bonding interactions.[96a,b] NMR experiments carried out in a protic solvent and at higher temperatures proved that this may indeed be the case for compounds **8**, **9** and **12**.

Each of the compounds synthesised were evaluated for their bacteriostatic activity against two Gram-negative bacteria, *E. coli* and *P. aeruginosa*, and the Gram-positive bacterium *S. aureus*. No compound exhibited activity against *P. aeruginosa*, a result that may be due to the intrinsic resistance mechanisms associated with this particular bacterium. In general, the SAR study compounds exhibited greatest activity against *E. coli* with a number of compounds also demonstrating activity against *S. aureus*.

A summary of the structure-activity relationships associated with organocatalyst (*b*) has been given in Figure 2.29. In part one of the SAR study, it was found that the –OMe group, although beneficial for activity, was not crucial for activity. However, the loss of –CF$_3$ groups severely reduced activity, with a 10- and 12-fold decrease in the MIC$_{50}$ range observed for compound **4** (Figure 2.23, section 2.2.6), in comparison to the hit compound.

Part two revealed that the simple 3,5-bis(trifluoromethyl)phenyl thiourea derivative bearing a methyl group was inactive suggesting that the thiourea may not be the source of activity. The addition of a two-carbon chain with a terminal tertiary amine (-NEt$_2$) to the aryl thiourea was advantageous for activity. Steric bulk appears to be favourable for activity with the phenyl and cyclohexyl thiourea derivatives

exhibiting bacteriostatic activity in MIC$_{50}$ ranges of 37.50-50.00 and 18.75-25.00 µg/mL, respectively. However, a combination of both a tertiary amine and a sterically bulky group (compound **12** and Takemotos catalyst) proved to be most effective amongst the part two SAR study compounds. Both compound **12** and Takemotos catalyst exhibited activity against *E. coli* and *S. aureus* with an increase in concentration resulting in an increase in the percentage of growth inhibition.

Loss of the –OMe group reduced potency but it may not be essential for overall activity

The presence of a stericaly bulky group was favourable for activity

A two-carbon chain linking a –NEt$_2$ group to the thiourea was beneficial for activity

The quinine-derived amine moiety alone was inactive

Structurally simple 3,5-bis(trifluoromethyl)phenyl thiourea derivatives show little or no activity

Loss of the quinoline group greatly reduced activity

Loss of the –CF$_3$ groups severely reduced activity

Figure 2.29: A summary of the SAR study of organocatalyst (*b*).

Organocatalyst (*b*) inhibited up to 90% of bacterial growth at the concentration ranges of 4.69-6.25 µg/mL (*E. coli*) and 6.25-9.38 µg/mL (*S. aureus*). These results are comparable to the results obtained here for the well-known antibacterial agent, vancomycin hydrochloride (MIC$_{90}$ in the range of 6.25-9.38 against both *E. coli* and *S. aureus*). Of the SAR study compounds synthesised within this study, compounds **3** and **12** (Figure 2.30) exhibited greatest activity and although the MICs achieved by compound **3** were comparable to those of the hit compound neither compound **3** nor compound **12** exhibited activities greater than that achieved by organocatalyst (*b*).

Figure 2.30: SAR study compounds that exhibited greatest activity.

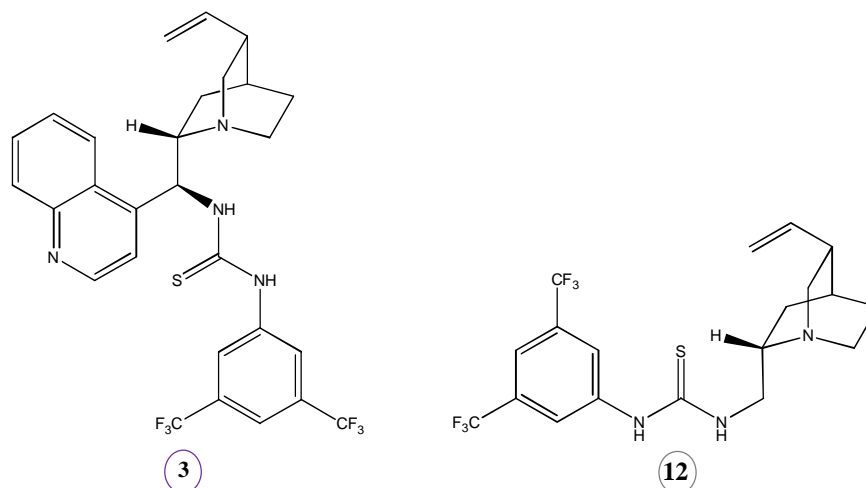In order for a compound to progress into the clinical setting, it must not only be effective but also safe to use. Organocatalyst (*b*) and a selection of the active SAR study compounds were chosen for *in vivo* toxicity studies using the larvae of the greater wax moth, *G. mellonella*. Each compound was found to be non-toxic to the *G. mellonella* at a range of concentrations (1-100 μg/mL). The hit compound was also found to be non-toxic at the higher concentration of 1000 μg/mL. Additionally, none of the compounds appeared to effect larval development as similar numbers of pupae were found for both treated and untreated larvae after one week.

To conclude, organocatalyst (*b*) was found to exhibit bacteriostatic activity against both Gram-negative and Gram-positive bacteria at concentrations comparable to that of the currently prescribed antibacterial agent, vancomycin hydrochloride. Additionally, the hit compound was both non-toxic to and did not appear to affect the development of *G. mellonella* larvae, at concentrations up to 1000 μg/mL. Although none of the compounds synthesised within this study exhibited greater activity than that of the hit compound, we have gained a valuable insight into which structural components may be beneficial for activity. Further studies into the structure-activity relationship of organocatalyst (*b*) could potentially lead to the generation of a broad spectrum, potent antibacterial agent.

2.2.9 Future work

The hit compound, organocatalyst (*b*), exhibited bacteriostatic activity against both *E. coli* and *S. aureus* at concentrations comparable to that of vancomycin hydrochloride. As mentioned in section 1.1, antibiotic resistance is a global problem and in particular infections resulting from MDR Gram-negative bacteria are on the rise. Therefore, it would be of interest to evaluate the bacteriostatic activity of organocatalyst (*b*) against resistant bacterial strains such as vancomycin-resistant *E. coli*. Furthermore, an evaluation of the bactericidal activity of organocatalyst (*b*) could also be carried out.

The study presented here disclosed some valuable information into the structure-activity relationships associated with the hit compound. However, none of the compounds described above achieved activity equivalent to or better than the hit compound thus further SAR studies are required.

As shown in section 2.2.6, the combination of the 3,5-bis(trifluoromethyl)phenyl thiourea with a sterically bulky group bearing a tertiary amine was beneficial for activity. Additionally, the loss of the quinoline moiety resulted in a significant decrease in activity. A review of the literature found that the antimalarial derivatives of quinine, chloroquine and hydroxychloroquine (Figure 2.31), have been shown to exhibit antibacterial, antifungal and antiviral activity.[99] In fact, chloroquine is used in the treatment of Q fever, a disease resulting from infection by the uncommon, Gram-negative bacterium, *Coxiella burnetii*. Considering the results of the SAR study thus far and the biological activity exhibited by the quinoline bearing antimalarial agents, chloroquine and hydroxychloroquine, an investigation into the bacteriostatic activity of 3,5-bis(trifluoromethyl)phenyl thiourea compounds bearing the quinoline moiety could be worthwhile.
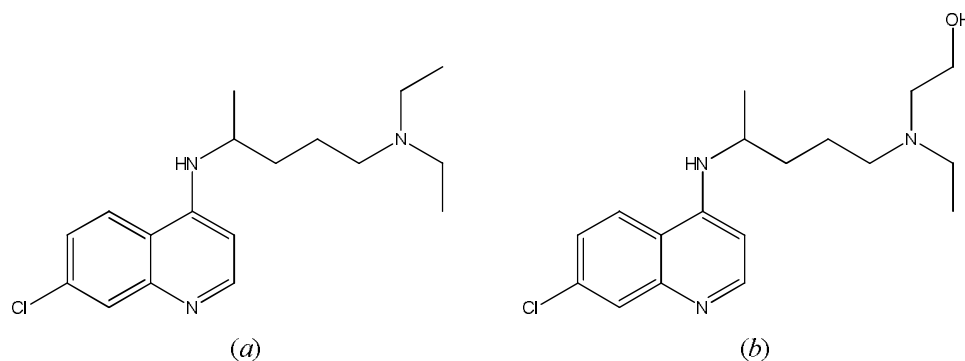
Figure 2.31: Antimalarial derivatives of quinine (*a*) chloroquine and (*b*) hydroxychloroquine.

The bacteriostatic mode of action of the hit compound, organocatalyst (*b*), is currently unknown. Identification of the bacterial target could be useful in the design of more potent SAR study compounds. In order to investigate if the hit compound is having an effect on the bacterial cell membrane an assessment of amino acid leakage from bacterial cells upon exposure to organocatalyst (*b*) could be carried out. Furthermore, an evaluation of the proteomic response exhibited by the bacteria as a result of organocatalyst (*b*) exposure could give insight into a possible mode of action.

2.3 Experimental

General procedure for the synthesis of 9-amino-(9-deoxy)-*epi*-quinine (2) and 9-amino-(9-deoxy)-*epi*-cinchonidine (5)[100]

Quinine or cinchonidine (6.14 mmol) and triphenylphosphine (2.11 g, 8.04 mmol) were dissolved in dry THF (30 mL) and the solution was cooled to 0 °C. Diisopropyl azidodicarboxylate (1.52 mL, 7.72 mmol) was added to the solution. A solution of diphenylphosphorylazide (1.63 mL, 7.56 mmol) in dry THF (13 ml) was then added dropwise at 0 °C. After addition, the mixture was allowed to warm to room temperature and was stirred for 12 hours. The solution was then heated at 50 °C for 2 hours. Triphenylphosphine (2.29 g, 8.73 mmol) was added and heating continued for a further 2 hours. The reaction mixture was allowed to cool to room temperature, water (0.70 mL) was added and the reaction mixture stirred for 3 hours. The solvent was removed under reduced pressure and the resulting residue was dissolved in DCM (30 mL) and 10% HCl (30 mL). The aqueous phase was washed with DCM (3 x 30 mL). The aqueous phase was then alkalinized with an excess of ammonium hydroxide solution and the product extracted with DCM (3 x 30 mL). The DCM solutions were dried over Na_2SO_4, filtered, and the solvent was removed under reduced pressure. The product was purified by column chromatography on silica gel and eluted with EtOAc:MeOH:NH_4OH (50:50:1).

**9-Amino-(9-deoxy)-*epi*-quinine (2)**
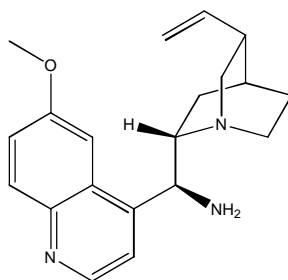
Yellow oil (yield 0.75 g, 38%); R_f: 0.37 (EtOAc:MeOH:NH_4OH, 50:50:1); $[\alpha]_D^{22}$: +90 (*c* 0.2, DCM); ^{1}H NMR (300 MHz, CDCl$_3$) δ 8.57 (d, *J* = 4.1 Hz, 1H, Ar*H*) 7.88 (d, *J* = 8.6 Hz, 1H, Ar*H*), 7.44-7.58 (m, 1H, Ar*H*), 7.30 (d, *J* = 4.1 Hz, 1H, Ar*H*), 7.21 (dd, *J* = 8.6, 3.6 Hz, 1H, Ar*H*), 5.58-5.69 (m, 1H, C*H*=CH$_2$), 4.78-4.87 (m, 2H,

CH=CH$_2$), 4.44 (d, J = 10.1 Hz, 1H, CH-NH$_2$), 3.78 (s, 3H, OCH_3), 3.00-3.14 (m, 2H, H^*), 2.89-2.98 (m, 1H, H^*), 2.57-2.67 (m, 2H, H^*), 2.32-2.46 (m, 3H, H^* and NH_2), 2.05-2.15 (m, 1H, H^*), 1.35-1.45 (m, 3H, H^*), 1.22-1.30 (m, 1H, H^*), 0.57-0.64 (m, 1H, H^*), these data match reported literature values[100]; ^{13}C NMR (75 MHz, CDCl$_3$) δ 157.5 (ArC), 147.7 (ArC), 146.9 (ArC), 144.6 (ArC), 141.7 (CH=CH$_2$), 131.6 (ArC), 128.7 (ArC), 121.2 (ArC), 119.9 (ArC), 114.2 (CH=CH$_2$), 101.9 (ArC), 61.7 (C^*), 56.2 (C^*), 55.4 (OCH$_3$), 52.8 (CH-NH$_2$), 40.8 (C^*), 39.7 (C^*), 28.1 (C^*), 27.5 (C^*), 25.9 (C^*); IR (DCM film on NaCl plate) 3367 (NH$_2$), 2940 (CH) cm^{-1}; LC/TOF-MS calcd for C$_{20}$H$_{26}$N$_3$O 324.2070, found 324.2080 (M+H$^+$).

* Quinuclidine ring.

9-Amino-(9-deoxy)-*epi*-cinchonidine (5)
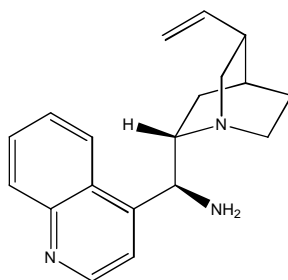
Yellow oil (yield 1.19 g, 66%); R$_f$: 0.56 (EtOAc:MeOH:NH$_4$OH, 50:50:1); [α]$_D^{22}$: +100 (*c* 0.2, DCM); ^{1}H NMR (300 MHz, CDCl$_3$) δ 8.81 (d, J = 4.4 Hz, 1H, ArH), 8.26 (br s, 1H, ArH), 8.05 (d, J = 8.3 Hz, 1H, ArH), 7.61 (app t, 1H, ArH), 7.49 (app t, 1H, ArH), 7.44 (d, J = 4.4 Hz, 1H, ArH), 5.64-5.76 (m, 1H, CH=CH$_2$), 4.84-4.93 (m, 2H, CH=CH_2), 4.61 (d, J = 9.5 Hz, 1H, CH-NH$_2$), 3.05-3.21 (m, 2H, H^*), 2.93-3.02 (m, 1H, H^*), 2.67-2.76 (m, 2H, H^*), 2.13-2.20 (m, 1H, H^*), 2.08 (br s, 2H, NH_2), 1.42-1.52 (m, 3H, H^*), 1.28-1.35 (m, 1H, H^*), 0.60-0.68 (m, 1H, H^*), these data match reported literature values[100]; ^{13}C NMR (75 MHz, CDCl$_3$) δ 150.3 (ArC), 148.7 (ArC), 148.5 (ArC), 141.8 (CH=CH$_2$), 130.4 (ArC), 129.0 (ArC), 127.8 (ArC), 126.4 (ArC), 123.3 (ArC), 119.6 (ArC), 114.3 (CH=CH$_2$), 61.9 (C^*), 56.2 (C^*), 51.6 (CH-NH$_2$), 40.9 (C^*), 39.8 (C^*), 28.0 (C^*), 27.5 (C^*), 26.0 (C^*); IR (DCM film on NaCl plate) 3368 (NH$_2$), 2940 (CH) cm^{-1}; LC/TOF-MS calcd for C$_{19}$H$_{24}$N$_3$ 294.1965, found 294.1974 (M+H$^+$).

* Quinuclidine ring.

1-((*S*)-(6-methoxyquinolin-4-yl)((1*S*,2*S*,4*S*,5*R*)-5-vinylquinuclidin-2-yl)methyl)-3-phenylthiourea (3)
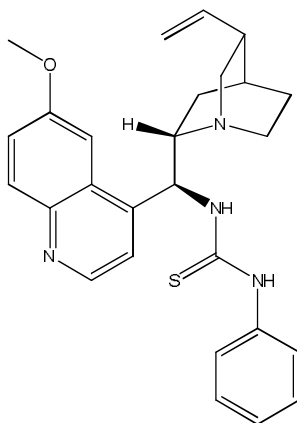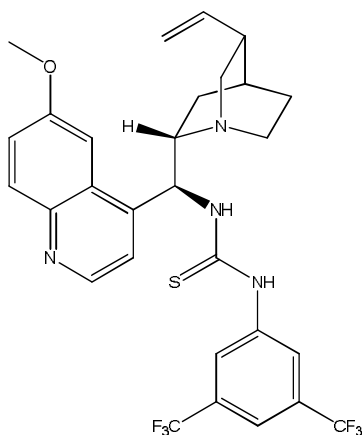

9-Amino-(9-deoxy)-*epi*-quinine (0.15 g, 0.46 mmol) was dissolved in dry DCM (5 mL) under nitrogen and cooled to 0 °C. After 10 minutes at this temperature, phenyl isothiocyanate (86 μL, 0.72 mmol) was added. The resulting solution was allowed to warm to room temperature and was stirred for 12 hours. The solvent was removed under reduced pressure and the resulting residue was purified by column chromatography on silica gel. The product was eluted with EtOAc:Et$_3$N:MeOH (90:5:5), followed by purification by precipitation from cold EtOAc with n-hexane.

White solid (yield 0.11 g, 52%); R$_f$: 0.24 (EtOAc:Et$_3$N:MeOH, 90:5:5); [α]$_D$: -220 (*c* 0.2, DCM); ^{1}H NMR (300 MHz, CDCl$_3$) δ 8.88-9.10 (br s, 1H, Ar*H*), 8.50 (d, *J* = 4.5 Hz, 1H, Ar*H*), 8.1 (br s, 1H, N*H*), 7.96 (d, *J* = 9.2 Hz, 1H, Ar*H*), 7.72-7.80 (m, 1H, Ar*H*), 7.32-7.37 (m, 3H, Ar*H*), 7.16-7.23 (m, 3H, Ar*H*), 5.89 (d, *J* = 8.3 Hz, 1H, C*H*NHC=S), 5.57-5.69 (m, 1H, C*H*=CH$_2$), 4.88-4.95 (m, 2H, CH=C*H*$_2$), 3.92 (s, 3H, OC*H*$_3$), 3.24-3.40 (m, 1H, *H**), 3.05-3.15 (m, 2H, *H**), 2.59-2.69 (m, 2H, *H**), 2.18-2.30 (m, 1H, *H**), 1.57-1.70 (m, 3H, *H**), 1.24-1.35 (m, 1H, *H**), 0.89-0.96 (m, 1H, *H**); ^{13}C NMR (75 MHz, CDCl$_3$) δ 180.5 (*C*=S), 157.8 (Ar*C*), 147.5 (Ar*C*), 144.7 (Ar*C*), 140.9 (*C*H=CH$_2$), 137.5 (Ar*C*), 131.6 (Ar*C*), 129.5 (Ar*C*), 128.2 (Ar*C*), 126.6 (Ar*C*), 125.2 (Ar*C*), 121.9 (Ar*C*), 114.8 (CH=*C*H$_2$), 102.4 (Ar*C*), 60.8 (*C**), 55.7 (O*C*H$_3$), 55.3 (*C**), 41.4 (*C**), 39.3 (*C**), 27.7 (*C**), 27.3 (*C**), 25.8 (*C**), these data

match reported literature values[101]; IR (KBr) 3418 (NH), 2937 (CH), 1242 (C=S) cm^{-1}; LC/TOF-MS calcd for $C_{27}H_{31}N_4OS$ 459.2213, found 459.2207 (M+H$^+$).

* Quinuclidine ring.

1-(3,5-bis(trifluoromethyl)phenyl)-3-((S)-(6-methoxyquinolin-4-yl)-((1S,2S,4S,5R)-5-vinylquinuclidin-2-yl)methyl)thiourea (organocatalyst (b))[102]
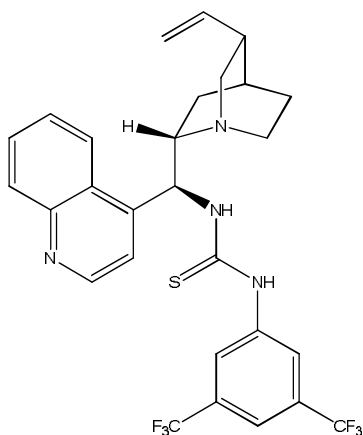

9-Amino-(9-deoxy)-*epi*-quinine (0.18 g, 0.56 mmol) was dissolved in dry DCM and cooled to 0 °C. After 10 minutes at this temperature, 3,5-bis(trifluorophenyl)methyl isothiocyanate (168 μL, 0.92 mmol) was added. The resulting solution was allowed to warm to room temperature and was stirred for 12 hours. The solvent was removed under reduced pressure and the resulting residue was purified by column chromatography on silica gel. The product was eluted with EtOAc:MeOH:Et$_3$N (90:5:5), followed by purification by precipitation from cold Et$_2$O with n-hexane.

White solid (yield 0.17 g, 50%); R$_f$: 0.37 (EtOAc:MeOH:Et$_3$N, 90:5:5); [α]$_D$: -100 (*c* 0.2, DCM); ^{1}H NMR (300 MHz, CDCl$_3$) δ 8.54 (app br s, 1H, Ar*H*), 7.96 (d, *J* = 9.0 Hz, 1H, Ar*H*), 7.81 (s, 2H, Ar*H*), 7.66 (s, 2H, Ar*H*), 7.36 (dd, *J* = 9.0, 2.8 Hz, 1H, Ar*H*), 7.13 (app br s, 1H, Ar*H*), 5.85 (app br s, 1H, C*H*NHC=S), 5.63-5.74 (m, 1H, C*H*=CH$_2$), 4.96-5.02 (m, 2H, CH=C*H*$_2$), 3.95 (s, 3H, OC*H*$_3$), 3.28-3.48 (m, 2H, *H**), 3.10-3.18 (m, 1H, *H**), 2.67-2.86 (m, 2H, *H**), 2.26-2.39 (m, 1H, *H**), 1.58-1.77 (m, 3H, *H**), 1.35-1.44 (m, 1H, *H**), 0.86-0.94 (m, 1H, *H**); ^{13}C NMR (75 MHz, CDCl$_3$) δ 180.6 (C=S), 158.1 (Ar*C*), 147.3 (Ar*C*), 144.5 (Ar*C*), 140.3 (*C*H=CH$_2$), 132.5 (q, ^2J = 33.8 Hz, *C*-CF$_3$), 131.4 (Ar*C*), 128.1 (Ar*C*), 123.6 (Ar*C*), 122.9 (q, ^1J = 270.0

Hz, CF_3), 122.2 (ArC), 118.6 (ArC), 115.3 (CH=CH$_2$), 102.1 (ArC), 60.7 (C*), 55.9 (OCH$_3$), 54.7 (C*), 41.6 (C*), 38.9 (C*), 27.3 (C*), 27.1 (C*), 25.7 (C*), these data match reported literature values[73a]; IR (KBr) 3241(NH), 2946 (CH), 1278 (C=S) cm^{-1}; LC/TOF-MS calcd for $C_{29}H_{29}F_6N_4SO$ 595.1961, found 595.1936 (M+H$^+$).

* Quinuclidine ring.

1-(3,5-Bis(trifluoromethyl)phenyl)-3-((*S*)-quinolin-4-yl((1*S*,2*S*,4*S*,5*R*)-5-vinylquinuclidin-2-yl)methyl)thiourea (4)


9-Amino-(9-deoxy)-*epi*-cinchonidine (0.20 g, 0.68 mmol) was dissolved in dry DCM and cooled to 0 °C. After 10 minutes at this temperature 3,5-bis(trifluorophenyl)methyl isothiocyanate (204 μL, 1.12 mmol) was added. The resulting solution was allowed to warm to room temperature and was stirred for 12 hours. The solvent was removed under reduced pressure and the resulting residue was purified by column chromatography on silica gel. The product was eluted with EtOAc:Et$_3$N:MeOH (90:5:5), followed by purification by precipitation from cold Et$_2$O with n-hexane..

Light yellow solid (yield 0.22 g, 56%); m.p. 148-154 °C; R$_f$: 0.42 (EtOAc:MeOH 95:5); [α]$_D$: -80 (*c* 0.2, DCM); ^{1}H NMR (300 MHz, CDCl$_3$) δ 8.38-8.54 (m, 2H, ArH), 7.97 (d, *J* = 8.9 Hz, 1H, ArH), 7.83 (s, 2H, ArH), 7.54-7.64 (m, 3H, ArH), 7.02-7.12 (m, 1H, ArH), 5.97 (br s, 1H, CHNHC=S), 5.55-5.66 (m, 1H, CH=CH$_2$), 4.87-4.94 (m, 2H, CH=CH_2), 3.26-3.40 (m, 1H, *H**), 3.08-3.22 (m, 1H, *H**), 2.96-3.04 (m, 1H, *H**), 2.58-2.74 (m, 2H, *H**), 2.18-2.30 (m, 1H, *H**), 1.50-1.74 (m, 3H,

H*), 1.23-1.31 (m, 1H, *H**), 0.82-0.96 (m, 1H, *H**); ^{13}C NMR (75 MHz, CDCl$_3$) δ 180.5 (*C*=S), 149.6 (Ar*C*), 148.0 (Ar*C*), 146.7 (Ar*C*), 140.6 (*C*H=CH$_2$), 140.0 (Ar*C*), 132.3 (q, ^2J = 34.5 Hz, *C*-CF$_3$), 129.6 (Ar*C*), 129.4 (Ar*C*), 127.0 (Ar*C*), 126.8 (Ar*C*), 123.7 (Ar*C*), 123.4 (Ar*C*), 122.8 (q, ^1J = 271.4 Hz, *C*F$_3$), 118.4 (Ar*C*), 114.7 (CH=*C*H$_2$), 60.9 (*C**), 54.7 (*C**), 41.2 (*C**), 38.9 (*C**), 27.3 (*C**), 27.0 (*C**), 25.5 (*C**); IR (KBr) 3237 (NH), 2947 (CH), 1278 (C=S) cm^{-1}, these data match reported literature values[103]; LC/TOF-MS calcd for C$_{28}$H$_{27}$F$_6$N$_4$S 565.1855, found 565.1843 (M+H$^+$).

* Quinuclidine ring.

1-(3,5-Bis(trifluoromethyl)phenyl)-3-methylthiourea (6)[104]
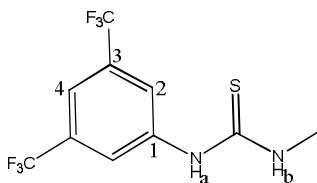
Methylamine (33% in EtOH, 188 μl, 2.0 mmol) was added to dry DCM (2 mL) under nitrogen and cooled on an ice-bath for 10 minutes. 3,5-Bis(trifluormethyl)phenyl isothiocyanate (183 μL, 1.0 mmol) was slowly added to the solution. The reaction mixture was allowed to warm to room temperature and was stirred overnight. The solvent was removed under reduced pressure and the product was purified by column chromatography on silica gel and eluted with CHCl$_3$:MeOH (90:10).

White solid (0.26 g, 87%); m.p. 118-122 $^\circ$C; R$_f$: 0.33 (CHCl$_3$:MeOH 90:10); ^{1}H NMR (300 MHz, CD$_3$OD) δ 8.16 (s, 2H, *H*2), 7.62 (s, 1H, *H*4), 3.06 (s, 3H, C*H*$_3$); ^{13}C NMR (75 MHz, CD$_3$OD) δ 183.7 (*C*=S), 143.3 (*C*1), 132.8 (q, ^2J = 33.0 Hz, *C*3), 124.8 (q, ^1J = 270.8 Hz, *C*F$_3$), 123.6 (*C*2), 117.8 (*C*4), 31.8 (*C*H$_3$); IR (KBr) 3226 (NH), 1278 (C=S) cm^{-1}; LC/TOF-MS calcd for C$_{10}$H$_9$F$_6$N$_2$S 303.0385, found 303.0386 (M+H$^+$).

**1-(3,5-Bis(trifluoromethyl)phenyl)-3-ethylthiourea (7)**
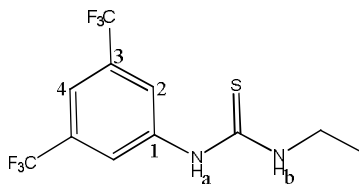
Anhydrous triethylamine (279 μL, 2.0 mmol) and ethylamine hydrochloride (82 mg, 1.0 mmol) were dissolved in dry DCM (2 mL) under nitrogen. The reaction mixture was cooled on an ice-bath for 10 minutes followed by the slow addition of 3,5-bis(trifluoromethyl)phenyl isothiocyanate (183 μL, 1 mmol). After addition, the reaction mixture was allowed to warm to room temperature and was stirred overnight. The solvent was removed under reduced pressure and the product purified by column chromatography on silica gel and eluted with $CHCl_3$:MeOH (90:10).

White solid (0.27 g, 84%); m.p. 147-150 $^{\circ}$C; R_f: 0.49 ($CHCl_3$:MeOH 90:10); ^{1}H NMR (300 MHz, CD_3OD) δ 8.16 (s, 2H, *H*2), 7.62 (s, 1H, *H*4), 3.60 (q, *J* = 7.3 Hz, 2H, C*H*$_2$), 1.23 (t, *J* = 7.3 Hz, 3H, C*H*$_3$); ^{13}C NMR (75 MHz, CD_3OD) δ 182.5 (*C*=S) 143.2 (*C*1), 132.7 (q, ^2J = 33.0 Hz, *C*3), 124.8 (q, ^1J = 270.2 Hz, *C*F$_3$), 123.8 (*C*2), 117.8 (*C*4), 40.3 (*C*H$_2$), 14.3 (*C*H$_3$); IR (KBr) 3240 (NH), 1278 (C=S) cm^{-1}; LC/TOF-MS calcd for $C_{11}H_{11}F_6N_2S$ 317.0542, found 317.0545 (M+H$^+$).

General procedure for the synthesis of 1-(3,5-bis(trifluoromethyl)phenyl)-3-thiourea derivatives 8-12

The appropriate amine (1.0 mmol) was dissolved in dry DCM (2 mL) under nitrogen. The solution was cooled on an ice-bath for 10 minutes. 3,5-Bis(trifluoromethyl)phenyl isothiocyante (183 μL, 1.0 mmol) was added slowly to the solution. The reaction mixture was allowed to warm to room temperature and was stirred overnight. The solvent was removed under reduced pressure and the product purified by column chromatography on silica gel.

**1-(3,5-Bis(trifluoromethyl)phenyl)-3-(2-(dimethylamino)ethyl)thiourea (8)**
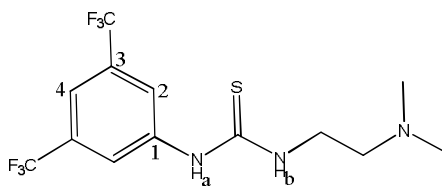
The product was eluted with $CHCl_3$:MeOH (90:10). White solid (0.27 g, 75%); m.p. 151-153 °C (154 °C)[105]; R_f: 0.26 ($CHCl_3$:MeOH 90:10); ^{1}H NMR (300 MHz, CD_3OD) δ 8.21 (s, 2H, *H*2), 7.62 (s, 1H, *H*4), 3.68-3.80 (app br s, 2H, $CH_2CH_2N(CH_3)_2$), 2.62 (t, *J* = 6.4 Hz, 2H, $CH_2CH_2N(CH_3)_2$), 2.33 (s, 6H, CH_3); ^{13}C NMR (75 MHz, CD_3OD) δ 182.9 (*C*=S), 143.3 (*C*1), 132.7 (q, [2]*J* = 33.0 Hz, *C*3), 124.8 (q, [1]*J* = 270.8 Hz, *C*F_3), 123.7 (*C*2), 117.8 (*C*4), 58.6 ($CH_2CH_2N(CH_3)_2$), 45.5 (CH_3), 43.0 ($CH_2CH_2N(CH_3)_2$); IR (KBr) 3292 (NH), 1281 (C=S) cm^{-1}; LC/TOF-MS calcd for $C_{13}H_{16}F_6N_3S$ 360.0964, found 360.0961 (M+H^{+}); Anal. (%) calcd for $C_{13}H_{16}F_6N_3S$ C, 43.45; H, 4.21; N, 11.69; found C, 43.44; H, 3.99; N, 11.60.

NMR data for compound **8** was also obtained in $CDCl_3$ at 25 °C and at 50 °C.

^{1}H NMR (300 MHz, $CDCl_3$, 25 °C) δ 13.28 (br s, 1H, N*H*a), 7.96 (br s, 2H, *H*2), 7.77 (br s, 1H, N*H*b), 7.58 (s, 1H, *H*4), 3.68 (app br s, 1H, C*H*2), 3.40 (app br s, 1H, C*H*2), 2.61 (app br s, 2H, C*H*2), 2.38 (app br s, 6H, C*H*3); ^{13}C NMR (75 MHz, $CDCl_3$) δ 183.0, 180.0, 142.1, 139.7, 131.8, 123.1, 122.7, 117.7, 61.3, 56.8, 45.0, 43.4, 42.3.

^{1}H NMR (300 MHz, $CDCl_3$, 50 °C) δ 7.93 (s, 2H, *H*2), 7.58 (s, 1H, *H*4), 3.52 (app br s, 2H, C*H*2$CH_2N(CH_3)_2$), 2.59 (app br s, 2H, CH_2C*H*2$N(CH_3)_2$), 2.32 (s, 6H, C*H*3); ^{13}C NMR (75 MHz, $CDCl_3$, 50 °C) δ 181.9 (*C*=S), 141.1 (*C*1), 132.3 (q, [2]*J* = 30.8 Hz, *C*3), 123.1 (q, [1]*J* = 271.1 Hz, *C*F_3), 122.7 (*C*2), 117.9 (*C*4), 59.7 ($CH_2CH_2N(CH_3)_2$), 44.9 (CH_3), 43.0 ($CH_2CH_2N(CH_3)_2$).

**1-(3,5-Bis(trifluoromethyl)phenyl)-3-(2-(diethylamino)ethyl)thiourea (9)**
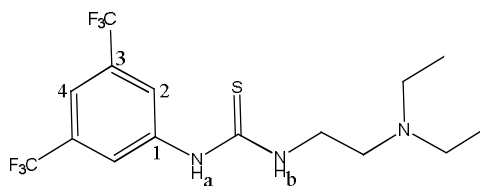
The product was eluted with $CHCl_3$:MeOH (90:10). Yellow oil (0.36 g, 92%); R_f: 0.34 ($CHCl_3$:MeOH, 90:10); ^{1}H NMR (300 MHz, CD_3OD) δ 8.19 (s, 2H, *H*2), 7.59 (s, 1H, *H*4), 3.71 (app br s, 2H, C*H*$_2$CH$_2$N(CH$_3$)$_2$), 2.72-2.82 (m, 2H, CH$_2$C*H*$_2$N(CH$_3$)$_2$), 2.67 (q, *J* = 7.1 Hz, 4H, C*H*$_2$-CH$_3$), 1.07 (t, *J* = 7.1 Hz, 6H, C*H*$_3$); ^{13}C NMR (75 MHz, CD_3OD) δ 183.0 (*C*=S), 143.1 (*C*1), 132.7 (q, ^2J = 33.0 Hz, *C*3), 124.7 (q, ^1J = 270.8 Hz, *C*F$_3$), 123.6 (*C*2), 117.9 (*C*4), 51.8 (CH$_2$*C*H$_2$N(CH$_3$)$_2$), 48.2 (*C*H$_2$-CH$_3$), 42.4 (*C*H$_2$CH$_2$N(CH$_3$)$_2$), 11.5 (*C*H$_3$); IR (DCM film on NaCl plate) 3224 (NH), 2977 (CH), 1280 (C=S) cm^{-1}; LC/TOF-MS calcd for $C_{15}H_{20}F_6N_3S$ 388.1277, found 388.1270 (M+H$^+$).

NMR data for compound **9** was also obtained in $CDCl_3$ at 25 ^{o}C and at 50 ^{o}C.

^{1}H NMR (300 MHz, $CDCl_3$, 25 ^{o}C) δ 8.05 (br s, 1H, N*H*), 7.91 (s, 2H, *H*2), 7.52 (s, 1H, *H*4), 3.73 (app br s, 1H, C*H*$_2$), 3.38 (app br s, 1H, C*H*$_2$), 2.64 (m, 6H, C*H*$_2$), 0.98 (t, *J* = 7.3 Hz, 6H, C*H*$_3$); ^{13}C NMR (75 MHz, $CDCl_3$) δ 182.8, 180.4, 141.7, 139.9, 131.5, 123.3, 123.0, 117.6, 55.6, 50.6, 47.0, 44.1, 41.3, 10.4.

^{1}H NMR (300 MHz, $CDCl_3$, 50 ^{o}C) δ 7.95 (s, 2H, *H*2), 7.53 (s, 1H, *H*4), 3.52 (app br s, 2H, C*H*$_2$CH$_2$N(CH$_3$)$_2$), 2.72 (app br s, 2H, CH$_2$C*H*$_2$N(CH$_3$)$_2$), 2.65 (q, *J* = 7.2 Hz, 4H, C*H*$_2$-CH$_3$), 1.00 (t, *J* = 7.2 Hz, 6H, C*H*$_3$); ^{13}C NMR (75 MHz, $CDCl_3$, 50 ^{o}C) δ 182.3 (*C*=S), 141.1 (*C*1), 131.8 (q, ^2J = 33.0 Hz, *C*3), 123.3 (*C*2), 123.0 (q, ^1J = 271.1 Hz, *C*F$_3$), 117.6 (*C*4), 54.5 (CH$_2$*C*H$_2$N(CH$_3$)$_2$), 47.2 (*C*H$_2$-CH$_3$), 43.2 (*C*H$_2$CH$_2$N(CH$_3$)$_2$), 10.6 (*C*H$_3$).

1-(3,5-Bis(trifluoromethyl)phenyl)-3-cyclohexylthiourea (10)
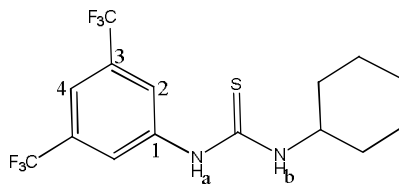
The product was eluted with $CHCl_3$ (100%). White solid (0.35 g, 95%); m.p. 152-156 °C; R_f: 0.31 ($CHCl_3$ 100%); ^{1}H NMR (300 MHz, $CDCl_3$) δ 8.42 (br s, 1H, N*H*a), 7.75 (s, 2H, *H*2), 7.68 (s, 1H, *H*4), 6.13 (br s, 1H, N*H*b), 4.19 (app br s, 1H, ipso C*H**), 2.00-2.05 (m, 2H, C*H**), 1.57-1.71 (m, 3H, C*H**), 1.31-1.44 (m, 2H, C*H**), 1.08-1.28 (m, 3H, C*H**), these data match reported literature values[106]; ^{13}C NMR (75 MHz, $CDCl_3$) δ 179.1 (*C*=S), 139.0 (*C*1), 132.9 (q, [2]*J* = 32.3 Hz, *C*3), 123.8 (*C*2), 122.8 (q, [1]*J* = 271.5 Hz, *C*F$_3$), 119.2 (m, *C*4), 54.0 (ipso *C**), 32.3 (*C**), 25.2 (*C**), 24.5 (*C**); IR (KBr) 3296 (NH), 1280 (C=S) cm^{-1}; LC/TOF-MS calcd for $C_{15}H_{17}F_6N_2S$ 371.1011, found 371.1014 (M+H$^+$).

* Cyclohexane ring.

1-(3,5-Bis(trifluoromethyl)phenyl)-3-phenylthiourea (11)
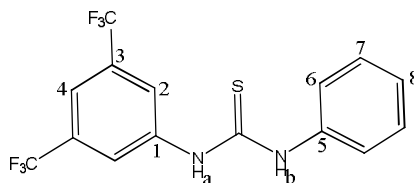
The product was eluted with $CHCl_3$ (100%). White solid (0.33 g, 92%); m.p. 128-130 °C; R_f: 0.44 ($CHCl_3$ 100%); ^{1}H NMR (300 MHz, $CDCl_3$) δ 8.89 (br s, 1H, N*H*b), 7.94 (s, 2H, *H*2), 7.88 (br s, 1H, N*H*a), 7.66 (s, 1H, *H*4), 7.44-7.49 (m, 2H, phenyl *H*), 7.30-7.38 (m, 3H, phenyl *H*); ^{13}C NMR (75 MHz, $CDCl_3$) δ 179.6 (*C*=S), 139.5 (*C*1), 135.6 (phenyl *C*), 132.0 (q, [2]*J* = 33.0 Hz, *C*3), 130.4 (phenyl *C*H), 128.2, (phenyl *C*H), 125.4 (phenyl *C*H), 124.7 (*C*2), 122.9 (q, [1]*J* = 270.0 Hz, *C*F$_3$), 119.3 (m, *C*4), these data match reported literature values[107]; IR (KBr) 1275 (C=S) cm^{-1}; LC/TOF-MS calcd for $C_{15}H_{11}F_6N_2S$ 365.0542, found 365.0545 (M+H$^+$).

1-(3,5-Bis(trifluoromethyl)phenyl)-3-(((1*S*,2*S*,4*S*,5*R*)-5-vinylquinuclidin-2-yl)methyl)thiourea (12)
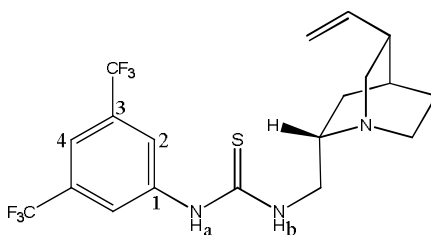
The product was eluted with CHCl$_3$:MeOH (90:10). White solid (0.41 g, 93%); m.p. 53-57 $^{\circ}$C (lit 54-59 $^{\circ}$C)[108]; R$_f$: 0.47 (CHCl$_3$:MeOH, 90:10); [α]$_D$: +120 (*c* 0.2, DCM); ^{1}H NMR (300 MHz, CD$_3$OD) δ 8.18 (s, 2H, *H*2), 7.60 (s, 1H, *H*4), 5.93 (ddd, *J* = 17.7, 10.7, 7.1 Hz, 1H, C*H*=CH$_2$), 5.04-5.11 (m, 2H, CH=C*H*$_2$), 3.76 (app br s, 1H, C*H*$_2$NHC=S), 3.55-3.63 (m, 1H, C*H*$_2$NHC=S), 3.08-3.19 (m, 1H, *H**), 2.85-2.95 (m, 4H, *H**), 2.31-2.39 (m, 1H, *H**), 1.64-1.74 (m, 4H, *H**), 1.37-1.45 (m, 1H, *H**); ^{13}C NMR (75 MHz, CD$_3$OD) δ 182.8 (*C*=S), 143.3 (*C*1), 141.2 (*C*H=CH$_2$), 132.8 (q, ^2J = 31.5 Hz, *C*3), 124.8 (q, ^1J = 270.0 Hz, *C*F$_3$), 123.7 (*C*2), 117.8 (*C*4), 115.5 (CH=*C*H$_2$), 56.3 (*C*H*), 49.8 (*C*H$_2$*), 47.8 (*C*H$_2$*), 47.1 (*C*H$_2$NHC=S), 40.9 (*C*H*), 29.0 (*C*H*), 27.3 (*C*H$_2$*), 26.3 (*C*H$_2$*); IR (KBr) 3267 (NH), 2944 (CH), 1279 (C=S) cm^{-1}; LC/TOF-MS calcd for C$_{19}$H$_{22}$F$_6$N$_3$S 438.1433, found 438.1435 (M+H$^+$).

NMR data for compound **12** was also obtained in CDCl$_3$ at 25 $^{\circ}$C and at 50 $^{\circ}$C.

^{1}H NMR (300 MHz, CDCl$_3$, 25 $^{\circ}$C) δ 7.92 (s, 2H, *H*2), 7.47 (s, 1H, *H*4), 5.67-5.78 (m, 1H, C*H*=CH$_2$), 4.94-5.00 (m, 2H, CH=C*H*$_2$), 3.44-3.64 (m, 1H, C*H*$_2$NH$_2$), 2.70-3.20 (m, 5H, C*H*$_2$NH$_2$ and *H**), 2.20-2.36 (m, 1H, *H**), 1.73 (app br s, 1H, *H**), 1.60 (app br s, 3H, *H**), 1.18-1.34 (m, 1H, *H**); ^{13}C NMR (75 MHz, CDCl$_3$) δ 182.1, 180.2, 142.1, 140.4, 138.3, 131.4, 122.8, 122.3, 117.1, 115.2, 58.5, 55.2, 47.9, 45.9, 38.6, 27.1, 25.2, 24.4.

^{1}H NMR (300 MHz, CDCl$_3$, 50 $^{\circ}$C) δ 7.91 (s, 2H, *H*2), 7.57 (s, 1H, *H*4), 5.76-5.90 (ddd, *J* = 17.2, 10.6, 6.7 Hz, 1H, C*H*=CH$_2$), 5.01-5.11 (m, 2H, CH=C*H*$_2$), 3.46-3.64 (m, 1H, C*H*$_2$NHC=S), 2.97-3.07 (m, 2H, C*H*$_2$NHC=S and *H**), 2.73-2.92 (m, 4H, *H**), 2.30-2.38 (m, 1H, *H**), 1.81 (app br s, 1H, *H**), 1.59-1.71 (m, 3H, *H**), 1.32-

1.39 (m, 1H, H^*); ^{13}C NMR (75 MHz, CDCl$_3$, 50 $^{\circ}$C) δ 182.3 (C=S), 141.0 (C1), 139.0 (CH=CH$_2$), 131.6 (q, ^2J = 33.0 Hz, C3), 123.1 (q, ^1J = 270.8 Hz, CF$_3$), 122.6, (C2), 117.7 (C4), 115.5 (CH=CH_2), 58.5 (CH^*), 48.3 (CH_2^*), 46.6 (CH_2^*), 46.3 (CH_2NHC=S), 39.2 (CH^*), 27.6 (CH^*), 25.9 (CH_2^*), 25.1 (CH_2^*).

* Quinuclidine ring.

Chapter III

A study of quinolone antibacterial agents

3.1 An Introduction to Quinolones

During the synthesis of the antimalarial agent, chloroquine, chemists at Sterling-Winthorp laboratories isolated compound **1** as a by-product (Figure 3.1). Due to the antibacterial properties exhibited by compound **1** a series of derivatives were synthesised in an attempt to find a novel antibacterial agent.[109] In 1963, one of these derivatives, nalidixic acid, was introduced into the clinical settings for the treatment of UTIs (Table 3.1).[109-110] Since the discovery of nalidixic acid numerous quinolone derivatives have been developed, many of which have made it to the clinical setting.

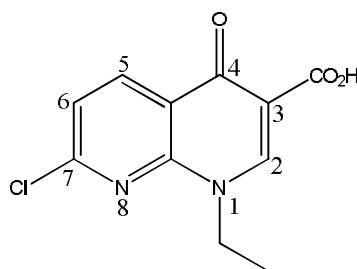**Figure 3.1**: By-product isolated during chloroquine production, compound **1**.[110]

Quinolones are classified into generations based on their spectrum of activity against bacteria (Table 3.1). The first-generation quinolones include the naphythyridone derivative, nalidixic acid, and the dioxolane bearing compounds, cinoxacin and oxolinic acid. These compounds were active against Enterobacteria with cinoxacin and oxolinic acid exhibiting increased activity in comparison to nalidixic acid.[109] The introduction of a piperazine ring at C-7, as in pipemidic acid, gave rise to activity against *P. aeruginosa*.[109] In the 1980's, the combination of the C-7 piperazine and a fluorine atom at the C-6 position resulted in the fluoroquinolone, norfloxacin (Table 3.1). In comparison to the first-generation quinolones, norfloxacin demonstrated improved anti-Gram-negative bacteria and some activity against Gram-positive bacteria.[109] Replacement of the N-1 ethyl group with a cyclopropyl group produced one of the most well-known fluoroquinolones, ciprofloxacin (Table 3.1). Ciprofloxacin exhibited enhanced activity against both Gram-negative and Gram-positive bacteria and was the first quinolone to be used in the treatment of infections other than UTIs.[109]

95

Table 3.1: Quinolone classification[109,111]
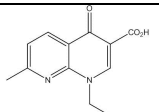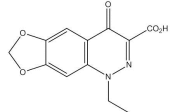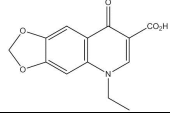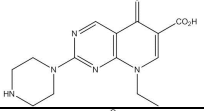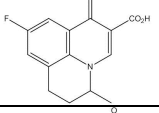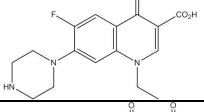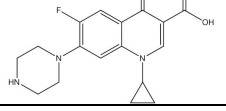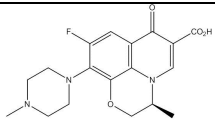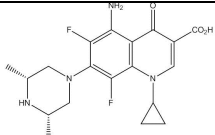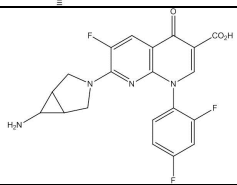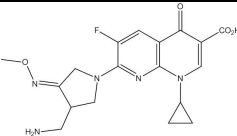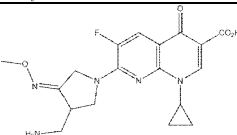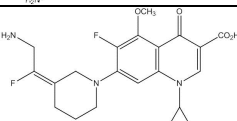
Generation	Quinolone	Structure	Activity	Clinical application
1st	Nalidixic acid		Anti-Gram-negative bacteria (*Enterobacteria* only)	UTI
	Cinoxacin			
	Oxolinic acid			
	Pipemidic acid		Introduction of anti-*P. aeruginosa* activity	
2nd	Flumequine		Anti-Gram-negative activity (less active than piperazinyl derivatives)	UTI
	Norfloxacin		Enhanced anti-Gram-negative activity including *P. aeruginosa* and limited anti-Gram-positive activity	UTI, sexually transmitted diseases, skin and soft tissue infections
	Ciprofloxacin			

Table 3.1 *continued*

3rd	Levofloxacin		Broad-spectrum activity with enhanced anti-Gram-positive activity and anti-pneomonoccal activity	Respiratory tract infections
	Sparfloxacin			
4th	Trovafloxacin[a]		Enhanced potency and expanded spectrum including anerobic bacteria	As for 1st, 2nd, and 3rd generations
	Gemifloxacin			
In Development:	Nemonoxacin (TG-873870)[112]		Enhanced anti-Gram-positive activity including MDR *S. pneumoniae* and quinolone-resistant MRSA	Skin infections and community-acquired pneumonia
	JNJ-Q2 (Avarofloxacin)[113]			

[a] Withdrawn due to adverse side effects.

In the third-generation quinolones the introduction of a C-8 moiety has led to improved activity against Gram-positive bacteria.[109,111b] The fourth-generation quinolones exhibit increased potency and a broader spectrum of activity, including anaerobic bacteria.[109,111b] Currently under development are two quinolone compounds JNJ-Q2 and nemonoxacin (Table 3.1). These compounds exhibit activity against MDR *S. pneuminiae* as well as quinolone-resistant MRSA.[111b,112-113]

The quinolones are attractive antibacterial agents not only because of their broad spectrum activity but also because of their molecular target. Quinolone antibacterials work by interfering with bacterial DNA replication.[109,114] DNA consists of two polynucleotide strands paired together through H-bonds which results in the formation of a double helix structure (Figure 3.2).[14] During DNA replication, the two strands are unwound and pulled apart, forming a replication bubble, allowing each strand to act as a template for the synthesis of two new strands (Figure 3.2).[14] DNA replication proceeds in both directions thus the replication bubble expands laterally, which can induce supercoiling ahead of the replication fork.[14]
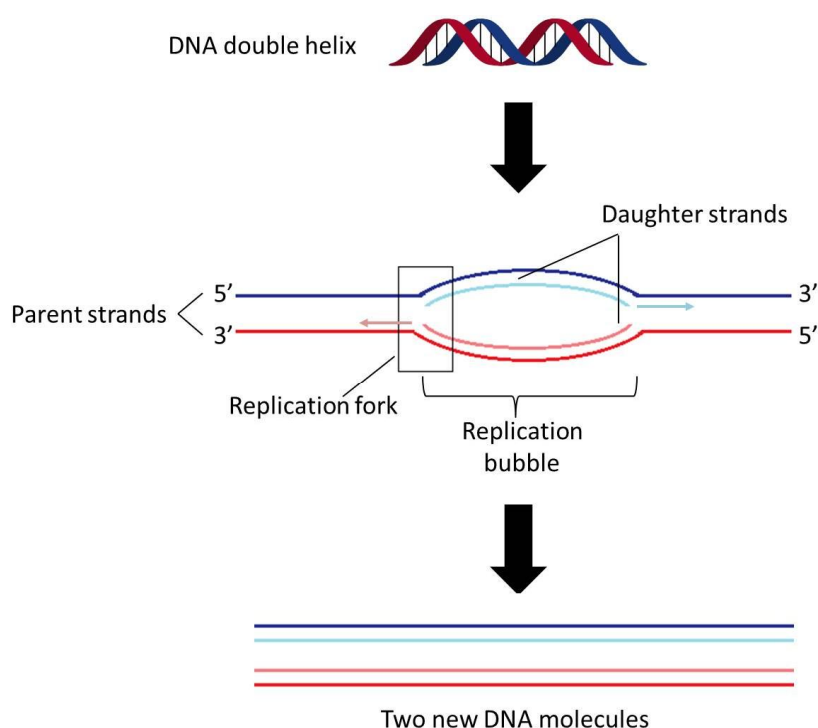
Figure 3.2: DNA replication.

In bacteria, an enzyme known as DNA gyrase (a type II topoisomerase) is responsible for relieving the strain caused by supercoiling during DNA replication.[109,115] As shown in Figure 3.3, DNA gyrase is a tetramer consisting of two GyrA units and two GyrB units. When double stranded DNA (the G-segment) binds to the DNA gyrase a conformational change occurs resulting in the dimerization of the GyrA units, **(2)** Figure 3.3. The binding of ATP (indicated by *) initiates the dimerization of the ATPase which leads to the capture of a second segment of double stranded DNA, the T-segment **(3)**. A conformational cascade occurs, leading to the cleavage of the G-segment and passage of the T-segment through the DNA gate **(4)**. The G-segment is then resealed and the T-segment released **(5)**, relieving the supercoiling. The GyrA units dimerise and ATP is hydrolysed regenerating the initial enzyme state.
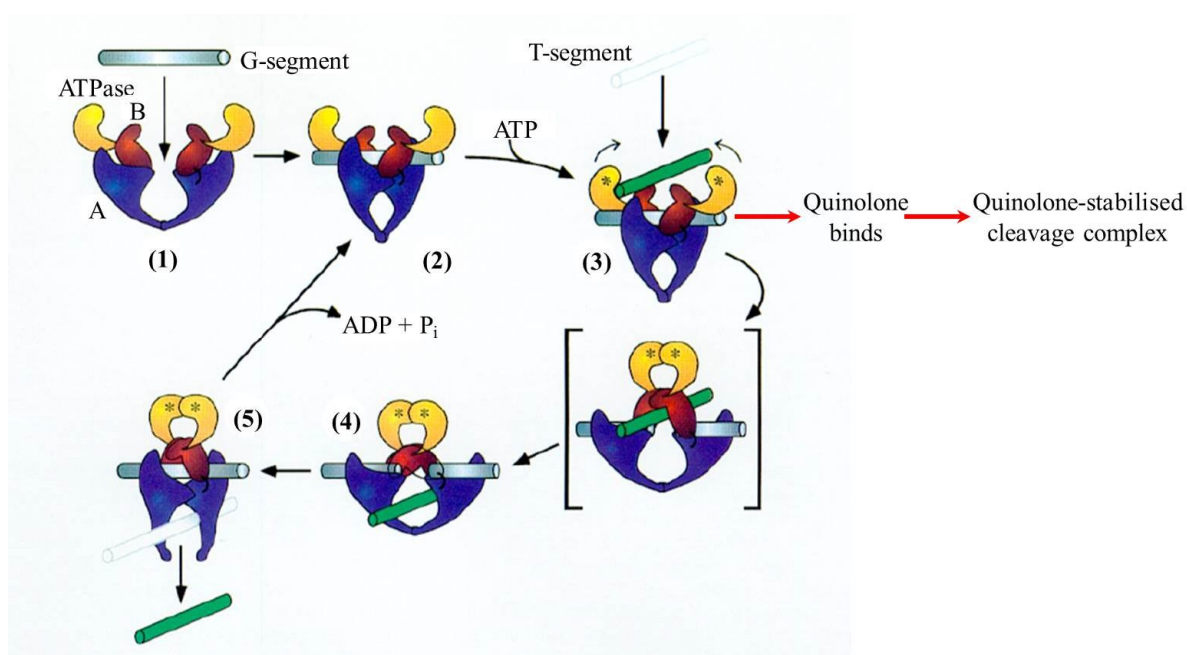
Figure 3.3: Topoisomerase II mechanism.[114-115]

Quinolones can bind to the gyrase-DNA complexes resulting in a quinolone-stabilised cleavage complex.[109,111b,114] The stabilisation of the enzyme-DNA complex blocks replication fork movement and therefore inhibits DNA synthesis.[111b,114] However, this process is reversible meaning that other events must be involved in the bactericidal activity of quinolones.[111b,114] Cell death is believed to occur as a result of

the release of DNA breaks.[111b,114] The exact molecular mechanisms involved in the release of DNA breaks are not fully understood.[111b,114]

Bacteria also have a second type II topoisomerase, known as topoisomerase IV. Like DNA gyrase, toposiomeras IV is a tetramer and is involved in the separation of linked DNA molecules.[109] Topoisomerase IV is said to be the main target in Gram-positive bacteria whereas DNA gyrase is believed to be the main target in Gram-negative bacteria.[109] A most favourable feature of the quinolone antibacterial agents is their selectivity for bacterial topoisomerase over mammalian topoisomerase. A number of quinolones, including ciprofloxacin, have demonstrated that much greater inhibitory concentrations are required to inhibit mammalian topoisomerase II reactions in comparison to those required to inhibit the bacterial enzyme reactions.[116]

3.1.1 Aim

The quinolones are broad spectrum antibacterial agents that have found use in a variety of infections including UTIs, sexually transmitted diseases, bone, skin and soft-tissue infections.[117] Fluoroquinolones are also used in the treatment of tuberculosis and some quinolone derivatives have been shown to exhibit anticancer and anti-HIV activity.[117] Modifications to the basic quinolone structure such as the introduction of the C-7 piperazine, a fluorine atom at C-6 and the N-1 cyclopropyl group have resulted in the generation of compounds with increased potency and an expanded spectrum of activity.[109] However, as can be seen from Table 3.1 (section 3.1) the C-3 carboxylic acid moiety, believed to be particularly important for the activity of the quinolones, has remained throughout the quinolone generations.

In this study we wanted to synthesise a basic quinolone molecule with an alternative C-3 moiety, a bioisostere. A bioisostere is a group that can be used in place of another group while maintaining the desired biological activity.[11] Bioisosteres are often used to investigate the structure-activity relationship of a drug or to replace substituents that are important for target interaction but responsible for toxic side effects.[11] Replacement of a functional group with a bioisostere has also been shown to improve activity. For example, replacement of the amide moiety of the dopamine

antagonist, sultopride, with a pyrrole ring resulted in increased activity and selectivity (Figure 3.4).

(a)   (b)
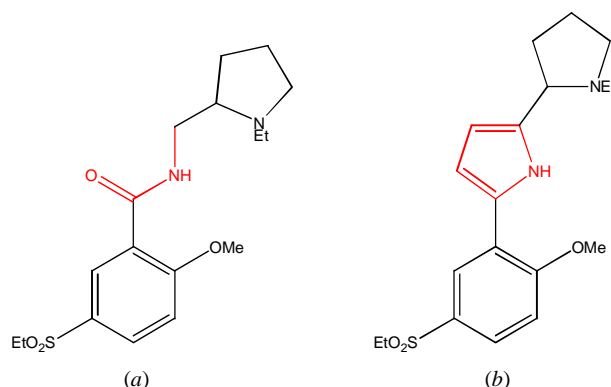
Figure 3.4: Replacement of the amide functionality of sultopride (*a*) by a non-classical isostere pyrrole to give DU 122290 (*b*), resulted in increased activity and selectivity.[11]

Tetrazoles are popular bioisosteres for carboxylic acids (Figure 3.5). Similar to a carboxylic acid, tetrazoles contain an acidic proton and are planar in structure.[11] In comparison to the carboxylate anion, tetrazoles are also 10 times more lipophilic.[11] Furthermore, many modern day drugs contain the tetrazole moiety, for example, Cefazolin (Figure 3.6), a broad spectrum first generation cephalosporin antibiotic.[118] Therefore, in an effort to improve activity the 1*H*-tetrazole was chosen as the bioisostere for the quinolone C-3 carboxylic acid.

pKa ~5   pKa ~5   pKa ~9
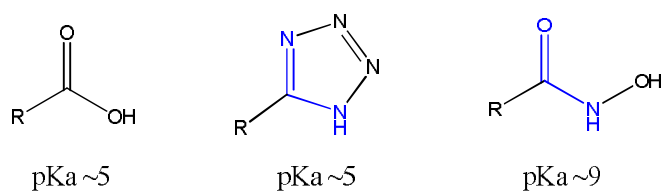
Figure 3.5: Similarities in structure and acidity of the carboxylic acid, the (1*H*)-tetrazole and the hydroxamic acid.
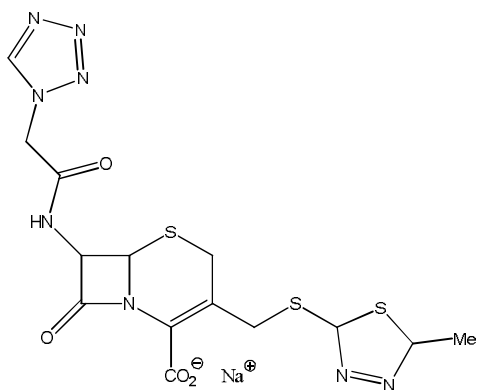
Figure 3.6: The tetrazole-containing antibiotic, Cefazolin.

In addition to the C-3 tetrazole, a second functional group was chosen to replace the carboxylic acid moiety, a hydroxamic acid. Hydroxamic acids, as well as being acidic, also possess a similar structure to that of a carboxylic acid (Figure 3.5). Furthermore, a wide spectrum of biological properties have been associated with hydroxamic acids including, anticancer, antifungal and antibacterial activity.[119]

3.2 Results and Discussion

The structure of each of the compounds synthesised in this section was elucidated using LC/TOF-MS, IR, ^{1}H and ^{13}C NMR spectoscopies. Starting materials were obtained commercially and used without further purification.

The retrosynthetic analysis for the C-3 (1*H*)-tetrazole and its carboxylic acid analogue can be seen in Scheme 3.1.
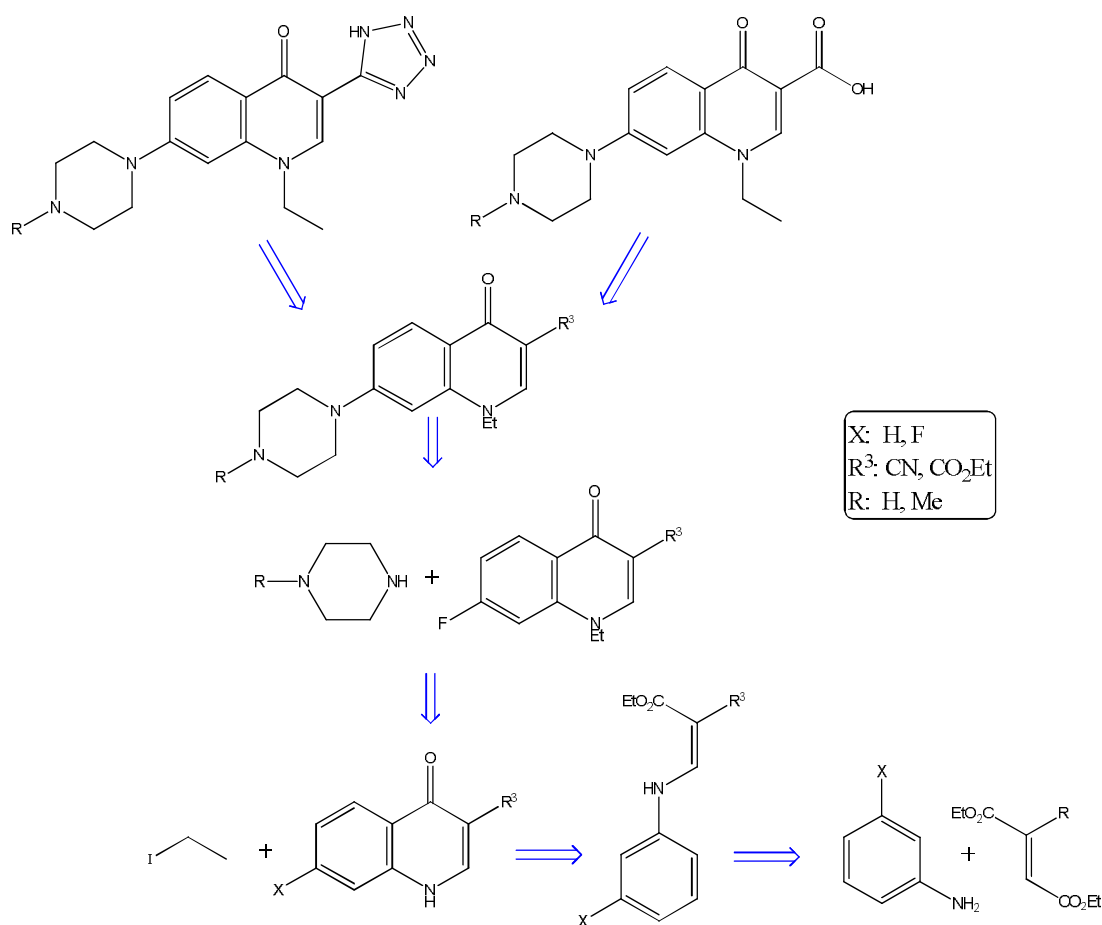
Scheme 3.1: Retrosynthetic analysis for the C-3 (1*H*)-tetrazole quinolone and its carboxylic acid analogue.

Generation of the C-3 (1*H*)-tetrazole can be carried out *via* a 1,3-dipolar cycloaddition of an azide with the quinolone C-3 nitrile precursor, whilst hydrolysis of a C-3 carboxylate quinolone will give the carboxylic acid analogue. The C-3 nitrile and carboxylate derivatives can be produced by the nucleophilic subsititution

reaction of piperazine and the fluorinated quinolone molecule. N-1 alkylation of the quinolone molecule, resulting from the electrophilic aromatic substitution of a phenylamino acrylate (or malonate in the case of the carboxylic acid derivative), can be carried out *via* the nucleophilic substitiution with ethyl iodide. The conjugate addition of aniline to a cyanoacetate, or a malonate in the case of the carboxylic acid derivative, generates the phenylamino acrylate (or malonate).

3.2.1 Synthesis of the phenylamino acrylates

The phenylamino acrylates **3.1** and **3.2** were synthesised using the procedure described by Stern *et al.*[120] with modification (Scheme 3.2). Ethyl (ethoxymethylene)cyanoacetate and aniline (3-fluoroaniline in the case of **3.2**) were allowed to reflux in EtOH for 45 minutes. On cooling, the product precipitated out of solution and the resulting solid was collected by filtration and washed with cold EtOH.
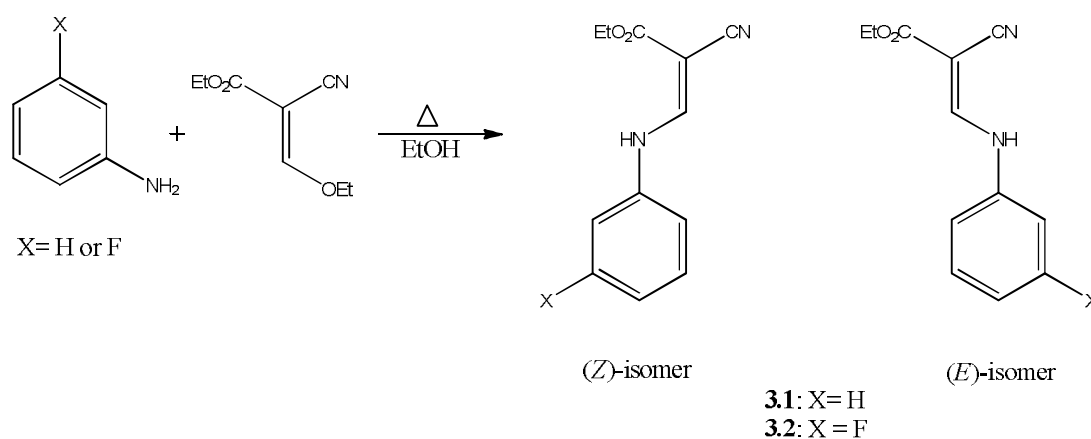
Scheme 3.2: Synthesis of phenylamino acrylates **3.1** and **3.2**.

In the NMR spectra of **3.1** and **3.2** two sets of resonance signals were observed indicating the presence of two isomers, the (*E*)- and (*Z*)-isomers. Two broad doublets at approximately 11 ppm and 9 ppm for the NHs of each isomer were observed in the ^{1}H NMR spectra of each compound, **3.1** and **3.2**, indicating successful addition of the aniline group. The loss of a set of ethoxy proton signals along with a shift in the vinyl proton signal in the ^{1}H NMR spectra from 8.00 ppm to 8.37 and 7.87 ppm in

3.1 and 8.36 and 7.90 ppm in **3.2** further confirmed formation of the phenylamino acrylates.

As mentioned in section 2.2.2, fluorine has I = ½ thus it can be detected using NMR spectroscopy. As shown in Figure 3.7, a fluorine substituent on an aromatic ring will give rise to characteristic C-F coupling constants for each of the carbon atoms in the *ipso*, *ortho*, *meta* and *para* positions. In a fluorinated aromatic ring the one-bond C-F coupling (*ipso*) is always large, approximately 245 Hz. Similarly to the C-F coupling in an aromatic ring characteristic three-bond, four-bond and five-bond H-F couplings can also be observed (Figure 3.7).
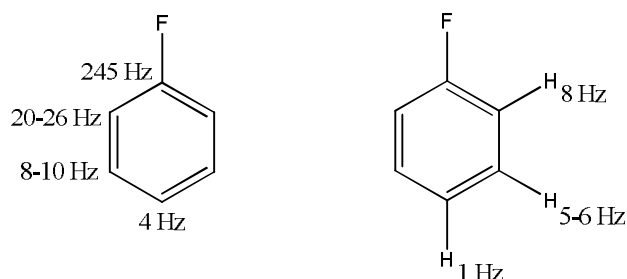
Figure 3.7: Characteristic C-F and H-F coupling constants.[91]

For **3.2**, characteristic one-bond C-F coupling constants of 245.9 and 246.5 Hz for the carbon directly attached to the fluorine atom were observed, one for each isomer. For each isomer a ^2J value of 21.8 Hz was also observed for the carbons *ortho* to the fluorine substituent and a ^4J value of 3.0 Hz for the carbon in the *para* position. The ^3J values for the carbon atoms at the *meta* position in **3.2** were also in the characteristic three-bond C-F coupling constant range of 8-10 Hz. The presence of two isomers, along with H-H and H-F coupling in the ^{1}H NMR spectrum of **3.2**, gave rise to mulitplets for the protons of the fluorinated phenyl ring. Therefore, no H-F coupling constants could be calculated.

A strong absorption band at 2211 and 2217 cm^{-1} for the ν(C≡N) was observed in the IR spectrum of **3.1** and **3.2**, respectively. Both compounds were obtained as white solids, in good yield, and were used without further purification in the synthesis of **3.5** and **3.6** (section 3.2.4).

3.2.2 Synthesis of the phenylamino malonates

As shown in Scheme 3.3, the synthesis of the phenylamino malonates **3.3** and **3.4** was carried out using the same method as that described for **3.1** and **3.2** above. Compounds **3.3** and **3.4** were obtained in good yields of 80% and 82%, respectively, and used without further purification.
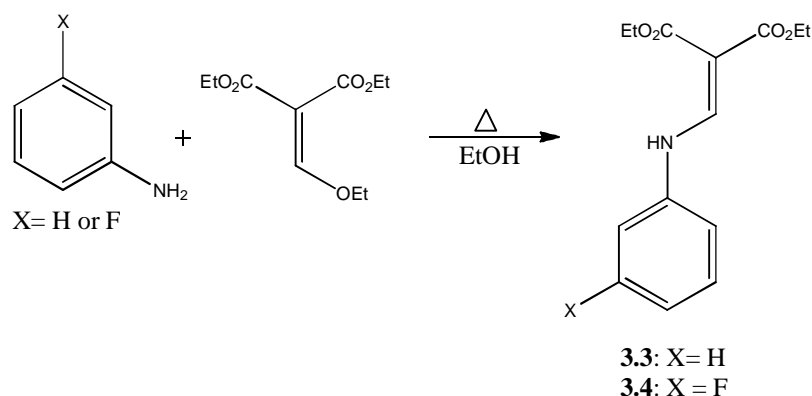
Scheme 3.3: Synthesis of phenylamino malonates **3.3** and **3.4**.

In the ^{1}H NMR spectra of both **3.3** and **3.4** a broad doublet at approximately 11 ppm was observed for the NH proton indicating formation of the products. The NH protons of each compound were found to couple to the vinyl CH proton, having a ^3J value of approximately 13 Hz, further confirming the formation of the phenylamino malonates. In the ^{13}C NMR spectra of **3.3** and **3.4** two carbon signals for each of the ester carbonyl carbons were observed. The ^{13}C signals for the carbons of the phenyl ring of **3.3** at 117.2, 124.9, 129.8 and 139.3 ppm were also observed.

For **3.4**, the presence of the fluorine substituent resulted in characteristic C-F coupling constants for each of the phenyl ring carbon atoms with the largest of these being 245.3 Hz for the one-bond coupling of the fluorine atom to the *ipso* carbon. A doublet at 103.9 and 110.0 ppm with ^2J values in the range of 21-26 Hz were assigned as the *ortho* carbon atoms with the *meta* carbon atoms observed at 140.6 and 130.8 ppm having a characteristic ^3J value of approximately 10 Hz. The ^{13}C resonance signal for the carbon *para* to the fluorine substituent was observed at 112.4 ppm with the smallest C-F coupling constant of 2.3 Hz. As was observed for **3.2**, the presence of H-H and H-F coupling resulted in multiplets being observed for

the protons of the fluorinated phenyl ring in the ^{1}H NMR spectrum, thus no H-F coupling constants could be calculated.

3.2.3 Synthesis of the quinolones
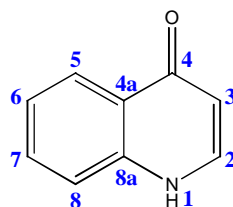
Figure 3.8: Quinolone structure with numbering system for ^{1}H and ^{13}C NMR shown.

3.2.4 The 3-carbonitrile quinolone derivatives

As shown in Scheme 3.4, the quinolone **3.5** was synthesised *via* the intramolecular electrophilic aromatic substitution reaction of **3.1.** The reaction was carried out using a procedure described by Stern *et al.*[120] Compound **3.1** was added slowly to hot diphenyl ether (240 ^{o}C). The solution was brought to reflux for four hours after which the reaction mixture was allowed to cool and petroleum ether was added. The resulting solid precipitate was collected by filtration and washed with petroleum ether to give the crude quinolone in 71% yield.
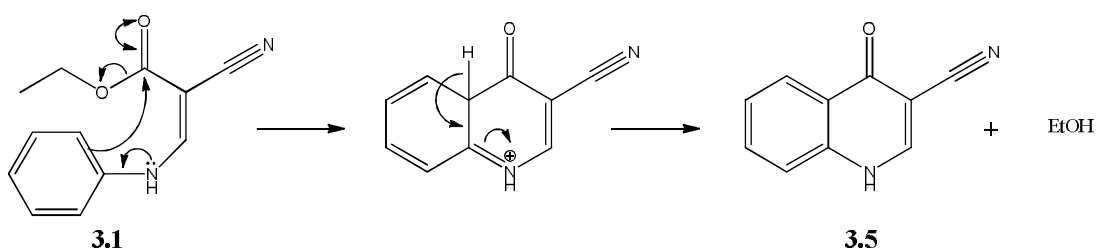
Scheme 3.4: Electrophilic aromatic substitution of **3.1**.

In the IR spectrum the ν(C≡N) absorption was observed at 2224 cm^{-1} and the ketone ν(C=O) absorption at 1628 cm^{-1}. In the ^{1}H NMR spectrum only one set of resonance signals were observed with the loss of the ethyl ester proton signals indicating formation of the quinolone product. As with the ^{1}H NMR spectrum, the ^{13}C NMR spectrum was much simpler in comparison to the quinolone precursor with only one

^{13}C signal observed for the ketone C=O at 174.4 ppm. A large downfield shift (117.3 to 125.0 ppm) of the ^{13}C signal, for the phenyl ring *ortho* carbon of **3.1**, was observed confirming the C-C bond formation of C-4a to C-4 (Figure 3.8 and Scheme 3.4).

The synthesis of the fluorine derivative, **3.6,** was carried using the same procedure as was described for **3.5** above. In the IR spectrum of **3.6** a strong absorption band at 2228 cm^{-1} was observed for ν(C≡N). As with **3.5**, loss of the –OCH$_2$CH$_3$ proton signals, in the ^{1}H NMR spectrum, indicated formation of a quinolone. However, unlike **3.5**, two sets of resonance signals were observed in both the ^{1}H and ^{13}C NMR spectra of **3.6**.

It was thought that each set of resonance signals may represent a different regioisomer (Scheme 3.5). From the ^{1}H NMR spectrum, a ratio of 1.00:0.30 was found for **3.6a**:**3.6b**, respectively. As depicted in Scheme 3.5, the production of the two regioisomers could result from nucleophilic attack at the carbonyl carbon from one of two possible carbon atoms of the phenyl ring. The atomic radius of a fluorine atom is greater than that of the hydrogen atom.[121] Therefore, the presence of the fluorine atom at C-5 may be sterically less favourable, resulting in the generation of only a small proportion of the 5-fluoro quinolone, **3.6b**.
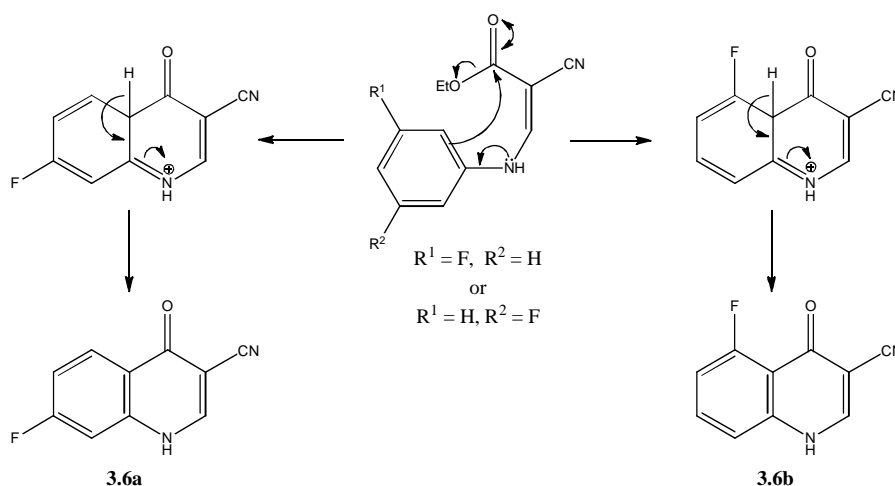
Scheme 3.5: Proposed reaction mechanism for the synthesis of regioisomers **3.6a** and **3.6b**.

In the ^{1}H NMR spectrum, two ^{1}H signals were observed at 8.75 and 8.68 ppm in the form of singlets, each having an integral of one. These were believed to be the ^{1}H signals of H-2 of each of the products. Focusing on the product of greatest abundance, a signal with an integral of one was observed at 8.18 ppm in the ^{1}H NMR spectrum. Considering its chemical shift, it is most likely the ^{1}H signal of either H-5 or H-8. However, as it was a doublet of doublets, and if this set of resonance signals were of the 7-fluoro derivative **3.6a**, then this ^{1}H signal belonged to H-5. For this doublet of doublets at 8.18 ppm, the coupling constants were 8.8 and 6.3 Hz. These *J* values are within the range of both the H-H *ortho* coupling as well as three- and four-bond H-F coupling. Using a C-H correlation NMR experiment, it was found that this ^{1}H signal corresponded to a ^{13}C signal with a C-F coupling constant of 11.3 Hz. A *J* value characteristic of a ^3J C-F coupling and therefore confirms that the ^{1}H signal at 8.18 ppm represents H-5. The observed *J* values of 8.8 and 6.3 Hz correspond to the *ortho* H-H coupling between H-5 and H-6 and the four-bond H-F coupling, respectively.

Examination of the ^{1}H NMR spectrum of the compound of least abundance reveals a doublet of doublets at 7.17 ppm. It was thought that this set of resonance signals belonged to the 5-fluoro derivative (**3.6b**), and as they are the most shielded ^{1}H signal, they most likely belonged to either H-6 or H-8. The two *J* values calculated for the doublet of doublets were found to be 11.8 and 8.1 Hz. For a typical *ortho* H-H coupling, the ^3J value falls within the range of 6.0 to 9.0 Hz, a range consistent with the *J* value of 8.1 Hz but not with the second *J* value obtained for the ^{1}H signal at 7.17 ppm. Although the coupling constant of 11.8 Hz is outside that of a typical aromatic ^3J value it is very similar to that observed for the three-bond C-F coupling of 1-fluoronaphthalene (10.7 Hz).[91] The C-H correlation NMR experiment showed that the ^{1}H signal at 7.17 ppm corresponded to a ^{13}C signal with a C-F coupling constant of 22.5 Hz (Table 3.2). This *J* value is consistent with the characteristic ^2J C-F coupling, thus confirming that the ^{1}H signal is that of H-6.

The presence of the fluorine substituent proved very useful in the characterisation of these quinolone products. As shown in Table 3.2, C-F coupling constants characteristic of fluorine coupling to *ipso*, *ortho*, *meta* and *para* carbon atoms were

observed for each set of resonance signals. Further analysis of the mixture of products using COSY and HSQC equivalent NMR experiments together with the observed C-F coupling constants confirmed the connectivity of the carbon atoms as shown in Figure 3.9.

Table 3.2: The C-F coupling constants observed for **3.6a** and **3.6b**.

Quinolone	^1J (Hz)	^2J (Hz)	^3J (Hz)	^4J (Hz)
Fluorobenzene[91]	245	20-26	8-10	4
3.6a	248.9	23.3, 24.8	12.9, 11.3	1.5
3.6b	259.9	22.5, 9.8	9.9, 4.5	4.5
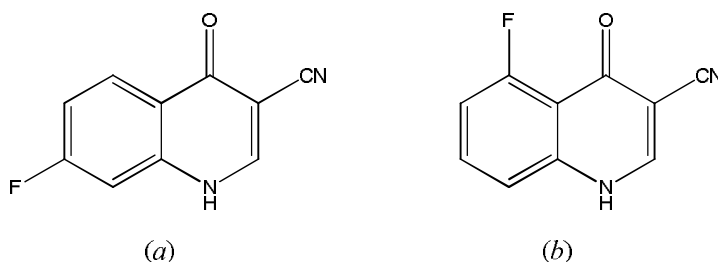
Figure 3.9: Structures of (*a*) **3.6a** (*b*) **3.6b**.

3.2.5 The 3-carboxylate quinolone derivatives

Quinolone **3.7** was synthesised as described by Lager *et al.*[122] (Scheme 3.6). The procedure was carried out in the same way as was described for quinolones **3.5** and **3.6** above, however, only a one hour reflux was required. A four hour reflux in diphenyl ether resulted in a complex mixture being returned. The resulting white solid quinolone was obtained in 72% yield and was used in the next step without further purification (section 3.2.8).
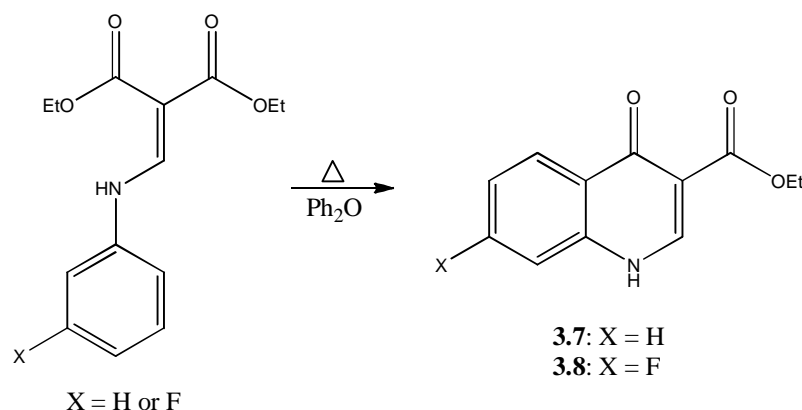
Scheme 3.6: Synthesis of **3.7** and **3.8**.

In the ^{1}H NMR spectrum of **3.7**, the loss of both the ethoxy group proton signals and the ^{1}H signal of one phenyl CH proton indicated formation of the bicycle. A large downfield shift in the ^{13}C signal for an *ortho* carbon atom of the phenyl ring in **3.3**, from 124.9 to 127.2 ppm, signified formation of the C4a-C4 bond. The presence of only one carbonyl ^{13}C signal, the ketone carbon, at 173.4 ppm further confirmed formation of **3.7**. In the IR spectrum obtained for **3.7** a strong absorption band at 1698 cm^{-1} for the ν(C=O) of the ketone was observed.

As shown in Scheme 3.6, the synthesis of **3.8** was carried out using the same procedure as was described for **3.7**. Again, loss of the ^{1}H signals for the protons of the ethyl ester, together with a loss of a phenyl proton signal in the ^{1}H NMR spectrum, indicated formation of the product. However, two sets of resonance signals were observed in the ^{1}H NMR spectrum. It was presumed that the two sets of signals were the result of a mixture of the 5-fluoro and 7-fluoro derivatives (Figure 3.10), as was observed for **3.6** above. From the ^{1}H NMR spectrum, the mixture of the isomers was found to be in a ratio of 1.00:0.08, **3.8a**:**3.8b**.

Focusing on the product of greater abundance, in the ^{1}H NMR spectrum, a doublet of doublets was observed at 8.22 ppm. The coupling constants associated with this ^{1}H signal were found to be 9.1 and 6.1 Hz. These values are consistent with *ortho* H-H and four-bond H-F coupling constants. Considering the chemical shift and observed *J* values, it was thought that this ^{1}H signal was that of the C-5 proton of the 7-fluoro quinolone derivative. A C-H correlation NMR experiment found that the ^{1}H signal

corresponded to a ^{13}C signal with a characteristic C-F ^3J value (10.5 Hz, Table 3.3), thus confirming that the ^{1}H signal at 8.22 ppm was that of H-5.
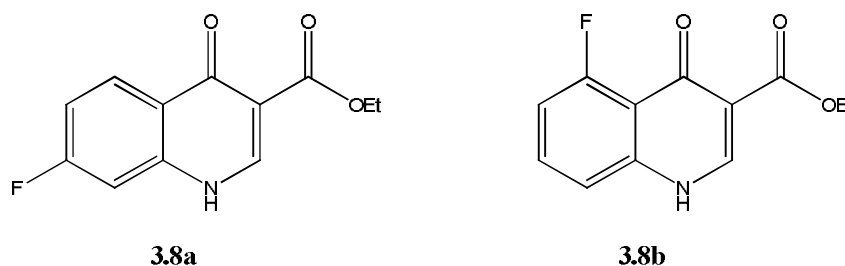
Figure 3.10: Proposed structures of the 7-fluoro- and 5-fluoro quinolone derivatives.

As shown in Table 3.3, the calculated C-F coupling constants of **3.8a** were found to be characteristic of a fluorine atom coupling to the *ipso*, *ortho*, *meta* and *para* carbon atoms of an aromatic ring. Together with the COSY and HSQC equivalent NMR experiments, these results were found to be consistent with the 7-flouro quinolone derivative, **3.8a**, as shown in Figure 3.10.

Table 3.3: The C-F coupling constants observed for **3.8a**. No ^4J value was observed for **3.8b**.

Quinolone	^1J (Hz)	^2J (Hz)	^3J (Hz)	^4J (Hz)
Fluorobenzene[91]	245	20-26	8-10	4
3.8a	248.3	24.8, 22.5	10.5, 12.8	-

Due to the generation of only a small quantity of what was thought to be the 5-fluoro derivative, **3.8b** Figure 3.10, the H-H and C-F coupling constants of **3.8b** could not be calculated. However, the structure of this second isomer will be discussed in more detail in section 3.2.8.

3.2.6 Alkylation of the quinolones

3.2.7 N-1 alkylation of the 3-carbonitrile quinolones

The alkylation of quinolone **3.5** was initially carried out using the method described by Frank and Mesaros[123] with modification. A mixture of quinolone **3.5** (Scheme

3.7) and K_2CO_3 in triethylphosphate, were brought to reflux for one hour. The reaction mixture was cooled to room temperature followed by the addition of deionised water. The resulting precipitate was collected by filtration and purified by precipitation from DCM with n-hexane to give N-alkyl quinolone **3.9** (Scheme 3.7). Although the reaction was successful, only yields of 45% were obtained and repetition of the purification step was often required resulting in further loss of material. Thus an alternative method was explored.

A review of the literature revealed a procedure whereby the quinolone can be alkylated using ethyl iodide with K_2CO_3 as base.[124] Compound **3.5** was dissolved in DMF and stirred at room temperature for two hours with ethyl iodide and K_2CO_3 followed by heating at 80 $^{\circ}$C for three hours (Scheme 3.7). Upon cooling, the reaction mixture was reduced in concentration by removal of the solvent *in vacuo* followed by the addition of water. The resulting precipitate was collected by filtration and purified by precipitation from DCM with n-hexane. It was found that the two hour stirring step was not necessary and that **3.9** could be obtained in similar yields when the reaction was carried out at 80 $^{\circ}$C for three hours with no prior stirring at room temperature (Scheme 3.7). Using this procedure, **3.9** was obtained in a yield of 72% after purification.
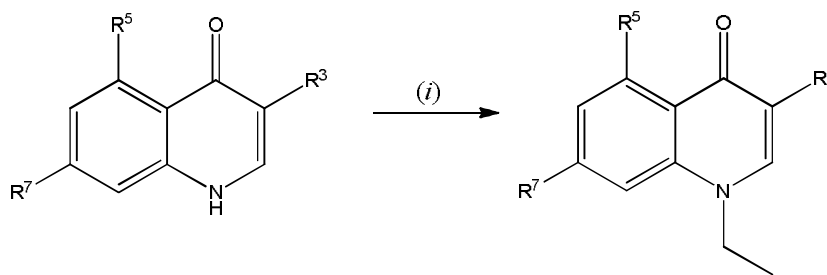
1-H-quinolone	R^3	R^5	R^7	1-Ethyl-quinolone
3.5	C≡N	H	H	**3.9**
3.6a	C≡N	H	F	**3.10a**
3.6b	C≡N	F	H	**3.10b**

Scheme 3.7: Quinolone alkylation, (*i*) K_2CO_3, EtI, DMF at 80 $^{\circ}$C for 3 h.

In the ^{1}H NMR spectrum of **3.9** the appearance of a new triplet at 4.40 ppm and quartet at 1.49 ppm representing the protons of the *N*-ethyl group indicated N-1 alkylation. The ^{3}J value for both the triplet and quartet was calculated to be 7.1 Hz, a value characteristic of vicinal H-H coupling in a saturated system. The corresponding ^{13}C signals were observed at 48.3 (*CH*$_2$) and 14.2 ppm (*CH*$_3$) in the ^{13}C NMR spectrum together with a shift in the C-2 and C-8a ^{13}C signals, further confirming formation of **3.9**.

The N-1 alkylation of **3.6** to give **3.10** was carried out as shown in Scheme 3.7. As mentioned earlier, the cyclisation of **3.2** resulted in the generation of two regiosiomers (**3.6a** and **3.6b**, section 3.2.4). Considering the small quantity of the 5-fluoro isomer (**3.6b**) that was obtained the crude mixture of isomers was used in the alkylation reaction thus producing two *N*-ethyl quinolone products, **3.10a** and **3.10b** in a yield of 72% and 15%, respectively (Scheme 3.7). The alkylated 5-fluoro and 7-fluoro quinolone derivatives were then separated by silica gel column chromatography.

The presence of two new ^{13}C signals at approximately 49.0 ppm and 14.0 ppm in the ^{13}C NMR spectrum of both **3.10a** and **3.10b** together with a shift in the C-2 ^{13}C signals indicated the addition of the ethyl group. In the ^{1}H NMR spectra of **3.10a** and **3.10b** two new signals, a triplet and quartet, were also observed. For each quinolone a ^{3}J coupling constant of 7.1 Hz was observed for both the triplet and quartet confirming that these ^{1}H signals represented the protons of the CH$_2$ and CH$_3$ components of the new ethyl group.

In addition to ^{1}H and ^{13}C NMR experiments, NOEdiff (Nuclear Overhauser Effect difference) experiments were used to assess the H-H spatial proximity within the quinolone structures in an effort to further confirm alkylation at the N-1 position as opposed to *O*-alkylation (Figure 3.11).

(*a*) R^5 = H, R^7 = F   (*b*)

or

R^5 = F, R^7 = H
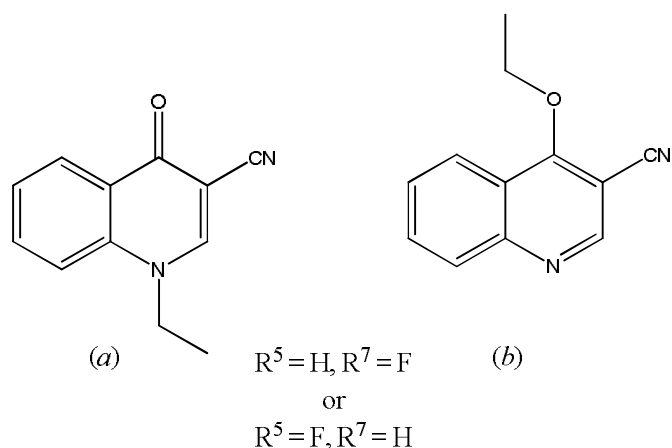
Figure 3.11: Possible *O*-alkyl and *N*-alkyl products.

NOEdiff experiments allow us to determine which two protons (or groups of protons) in a molecule are in close proximity to one another by using through-space coupling. The NOE is the change in intensity of one resonance due to the relaxation of another neighbouring saturated signal.[125] In a NOEdiff experiment a ^{1}H signal can be selectively irradiated, resulting in a build-up of NOE at a neighbouring ^{1}H resonance which can then be detected by the NMR spectrometer.[125] Thus, it can be used to determine which protons (or group of protons) are spatially close to one another by selectively irradiating a ^{1}H resonance and observing which other ^{1}H resonances are detected.[125]

The resulting spectra from the NOEdiff experiments of **3.10a** are given in Figure 3.12. The first hydrogen chosen to be irradiated was H-2. As can be seen in Figure 3.12, spectrum (*a*), irradiation of H-2 resulted in an increase in intensity of the ^{1}H resonance signals of the C*H*$_2$ and C*H*$_3$ groups presenting a positive NOE of 8% and 2%, respectively. Irradiation of the ^{1}H resonance signal of the C*H*$_2$ group was also carried out (spectrum (*b*) Figure 3.12). Both signals for H-2 and H-8 showed increased intensities resulting in a positive NOE of 15% and 13%, respectively. These results confirm alkylation at N-1 of **3.10a**.

NOEdiff experiments were also carried out for **3.10b**, the results of which were similar to that observed with **3.10a** thus confirming *N*-alkylation (Appendix B, Figure B1).
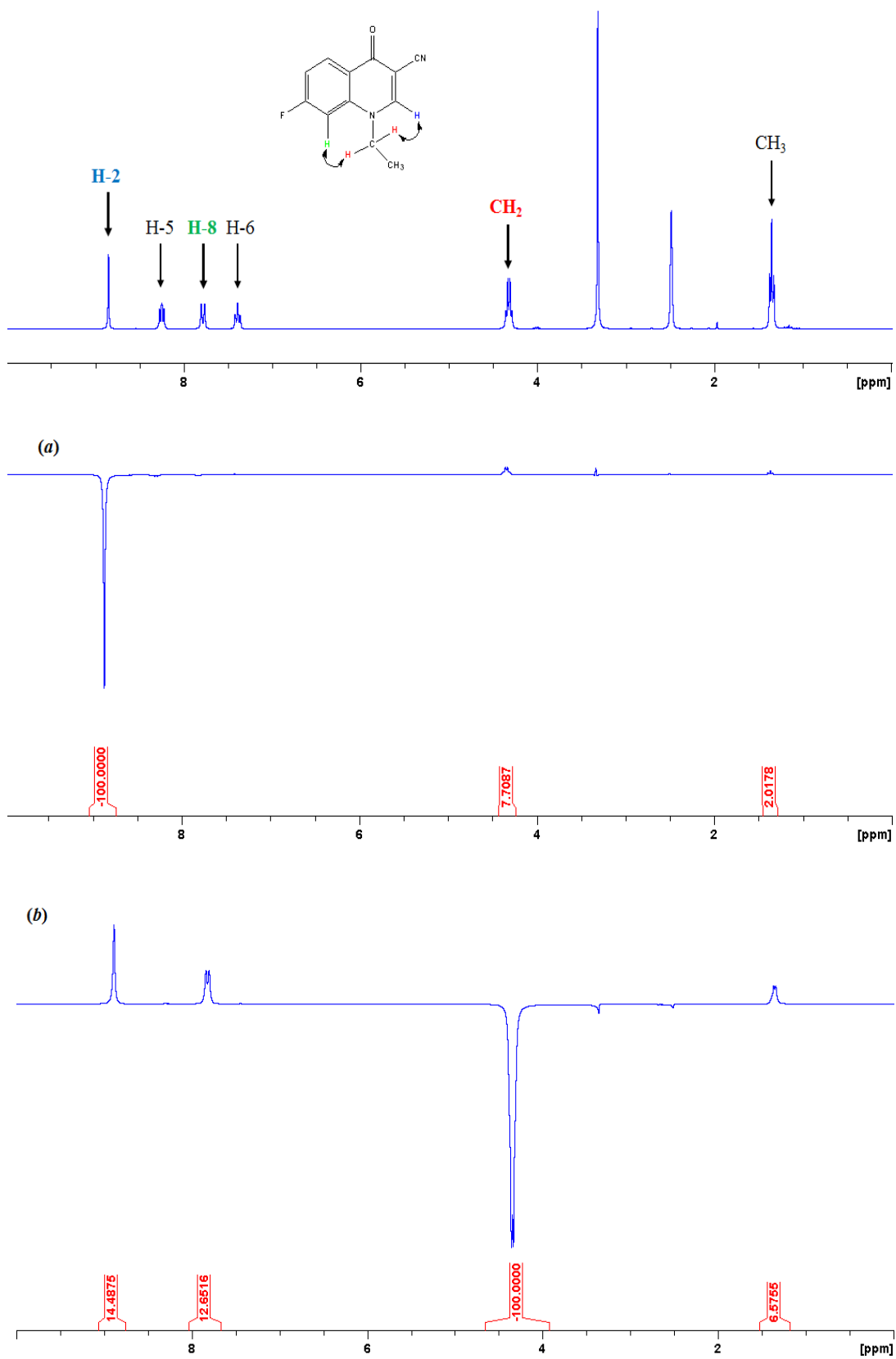
Figure 3.12: NOEdiff spectra obtained for **3.10a**.

116

3.2.8 Alkylation of the 3-carboxylate quinolones
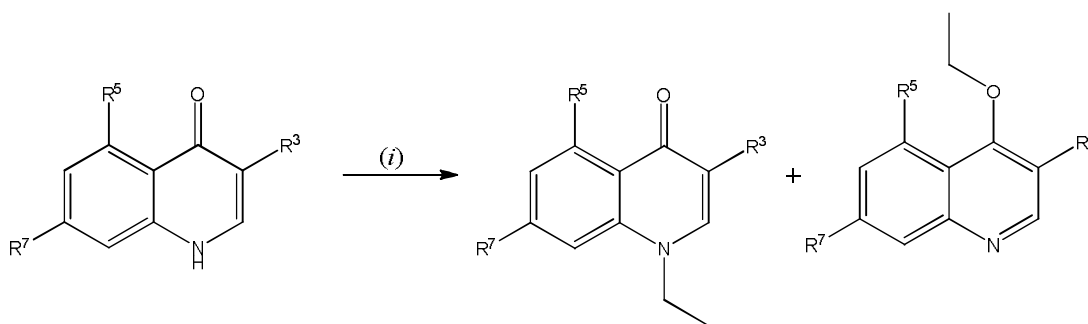
1-H-quinolone	R^3	R^5	R^7	Alkyl quinolone	Alkylation
3.7	CO_2Et	H	H	**3.11a**	N
3.7	CO_2Et	H	H	**3.11b**	O
3.8a	CO_2Et	H	F	**3.12a**	O
3.8a	CO_2Et	H	F	**3.12b**	N
3.8b	CO_2Et	F	H	**3.12c**	N

Scheme 3.8: Quinolone Alkylation, (*i*) K_2CO_3, EtI, DMF at 80 ^{o}C for 3 h.

Quinolone **3.7** was alkylated to give **3.11** using the same method as was described for **3.9** and **3.10** above (Scheme 3.8). Analysis of the crude product by ^{1}H NMR spectroscopy revealed two sets of resonance signals for what appeared to be two different alkylated quinolones. Using silica gel column chromatography the two quinolone products, **3.11a** and **3.11b**, were separated.

In the ^{1}H NMR spectrum of each product a new set of ^{1}H signals characteristic of an ethyl group were observed indicating successful alkylation. To confirm alkylation at N-1, NOEdiff experiments were carried out on both products. The resulting spectra of the NOEdiff experiments of **3.11a** are given in Figure 3.13 and 3.14.
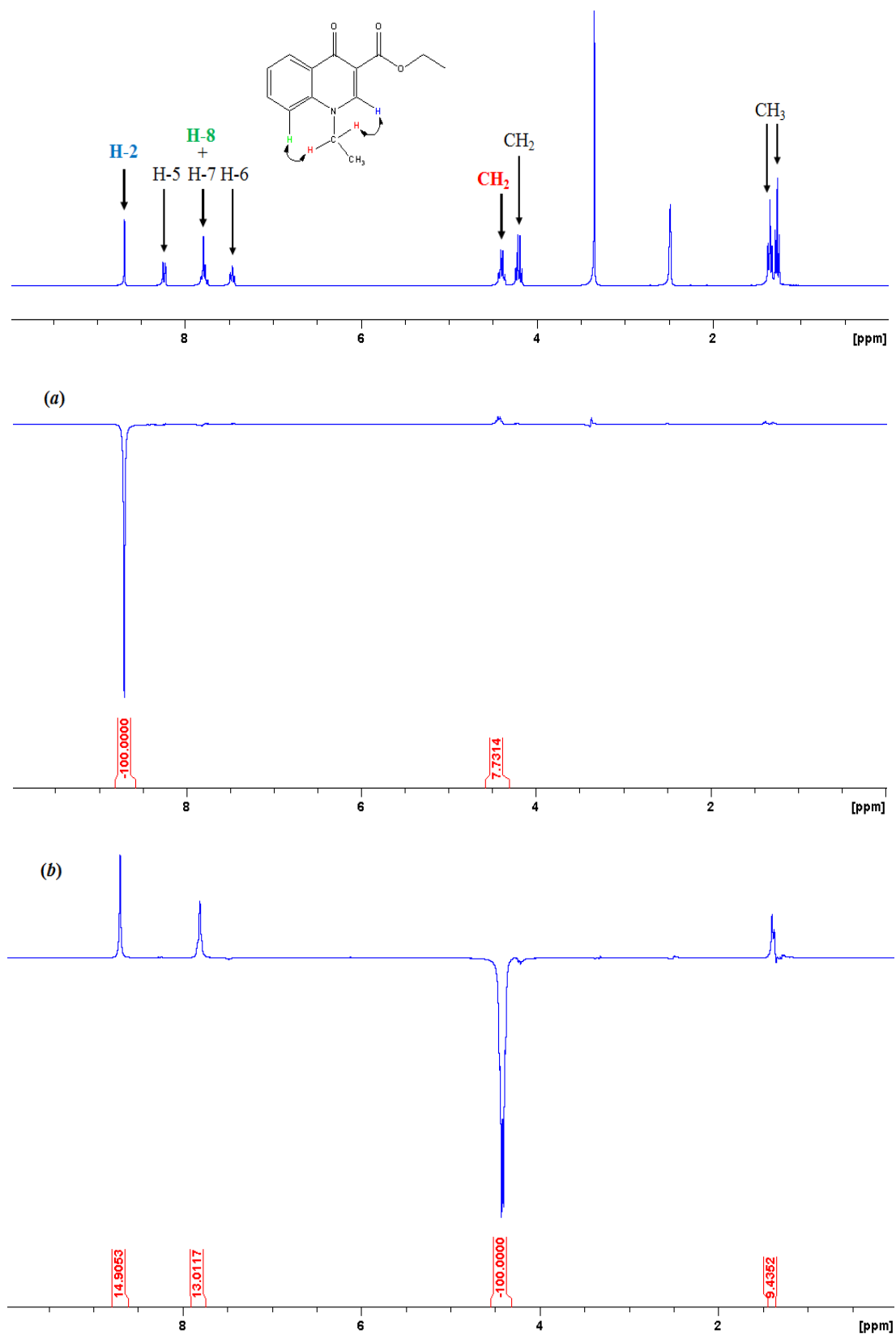
Figure 3.13: NOEdiff spectra obtained for **3.11a**.

118
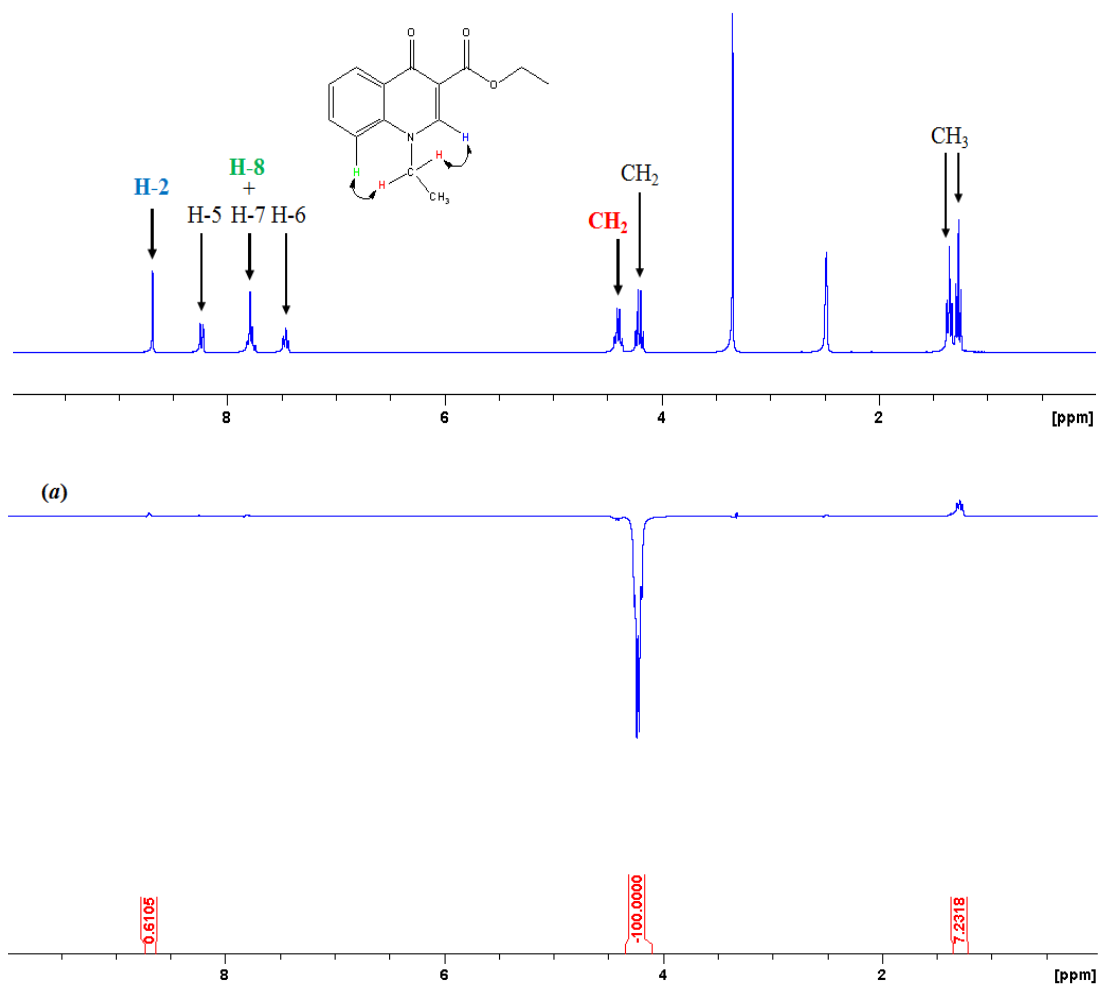
Figure 3.14: NOEdiff spectra obtained for **3.11a**.

The first hydrogen chosen for irradiation was H-2. As can be seen in Figure 3.13, spectrum (*a*), irradiation of H-2 resulted in an increase in the ^{1}H signal intensity of one of the CH_2 groups (4.41 ppm). The ^{1}H signal for the same CH_2 group was irradiated in a subsequent NOEdiff experiment the result of which was an increase in the intensity of the ^{1}H signals for H-2 and a second aromatic CH, H-8. Both signals for H-2 and H-8 presented a positive NOE of 15% and 13%, respectively (spectrum (*b*), Figure 3.13). As shown in Figure 3.13, these results indicate that the ethyl group is attached at N-1 in **3.11a**. Finally, upon irradiation of the second CH_2 group protons at 4.22 ppm, an increase in the ^{1}H signal intensity was observed for the attached CH_3 group only (spectrum (*a*), Figure 3.14). No other ^{1}H signal increased in intensity, suggesting that this CH$_2$ group belongs to the C-3 ester ethyl moiety.

119

The spectra obtained from the NOEdiff experiments of **3.11b** are given in Figure 3.15. The similarity in chemical shift of the CH_2 signals made it difficult to irradiate only one of the signals. However, looking at the resulting spectrum it can be seen that the ^{1}H signal for the attached CH$_3$ group plus the ^{1}H signal of an aromatic CH increased in intensity (Figure 3.15). Although the ^{1}H signal of H-2 also appears to have increased in intensity, this increase is less than 1% and may be a result of the slight irradiation of the ester CH$_2$ ^{1}H signal. These results suggest that the ethyl group is not attached at N-1.
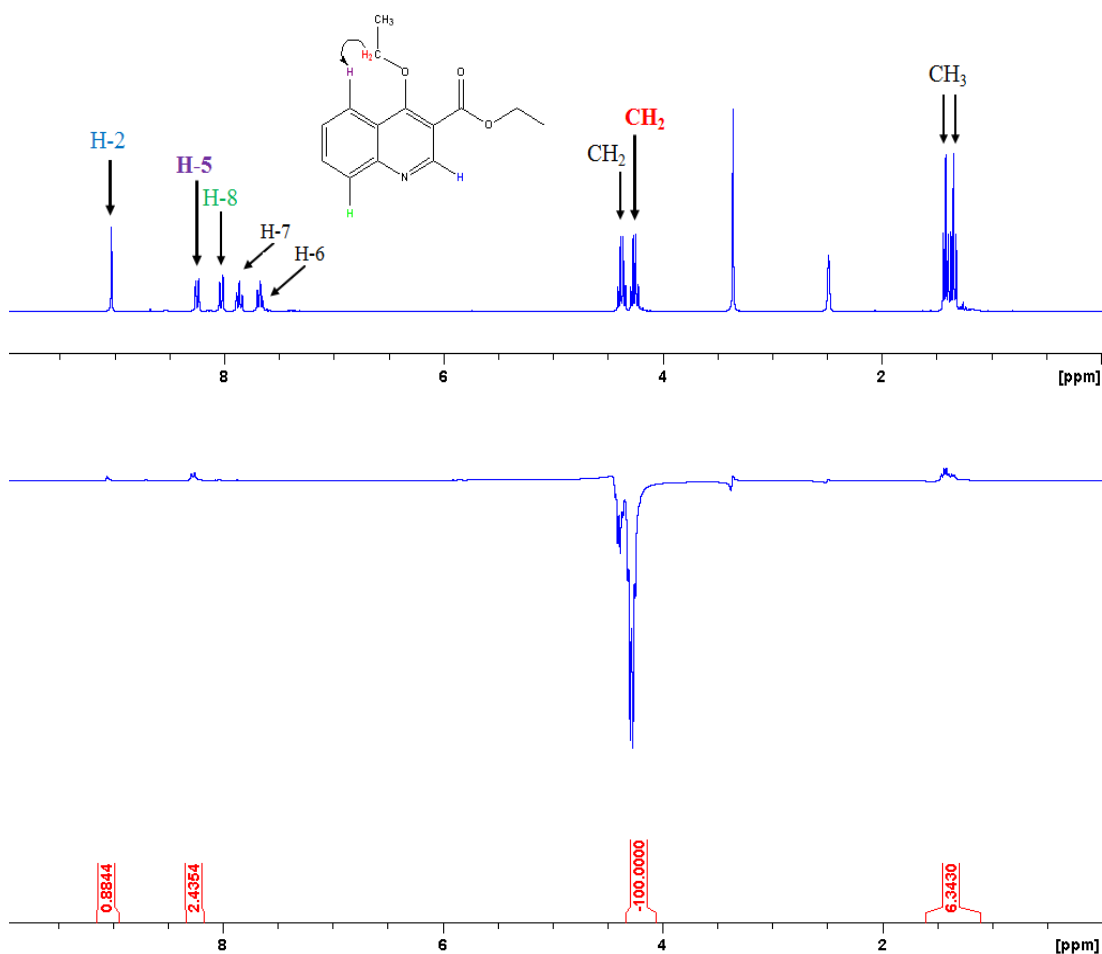
Figure 3.15: NOE spectra of **3.11b**. Both signals for CH_3 and an aromatic CH showed increased intensities presenting a positive NOE of 6% and 2%, respectively.

To ensure that this was the case, a second NOEdiff experiment was carried out wherein H-2 was irradiated. As seen in Figure 3.16, irradiation of H-2 did not

increase the intensity of any other ^{1}H signal thus H-2 is not in close proximity to the new ethyl group.
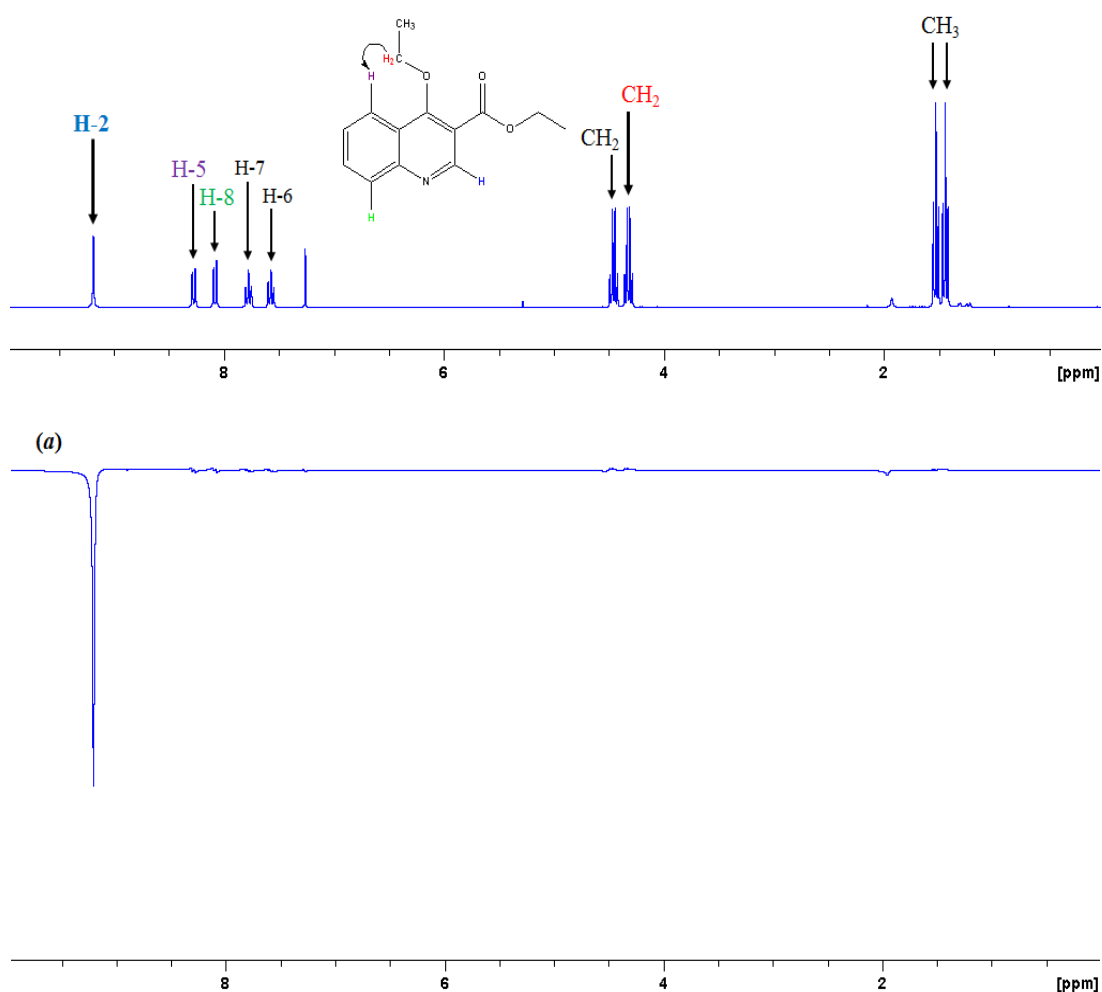
Figure 3.16: Irradiation of H-2 in **3.11b** (CDCl$_3$) did not increase the intensity of any other ^{1}H signal.

Further analysis of **3.11b** by ^{13}C NMR spectroscopy revealed two ^{13}C signals at 165.3 and 164.2 ppm. By comparison, in the ^{13}C NMR spectrum of **3.11a**, the ^{13}C signal for the ester carbonyl carbon was observed at 164.6 ppm whilst the C-4 carbonyl carbon signal was observed further downfield at 172.7 ppm. These results, together with the results from the NOEdiff experiments, suggest that alkylation also occurred at the C-4 oxygen atom thus generating **3.11b** (Figure 3.17).
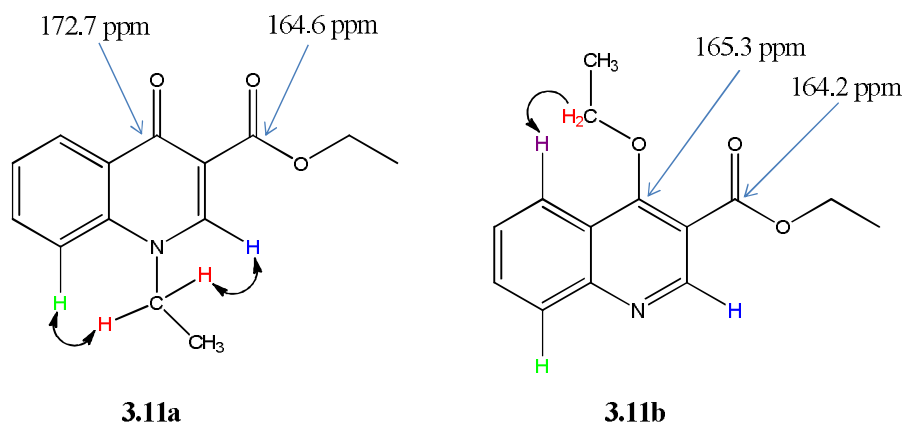
Figure 3.17: Structures of *N*-ethyl and *O*-ethyl quinolones, **3.11a** and **3.11b.**

During alkylation, the deprotonation of the quinolone NH gives rise to a negative charge on the nitrogen atom (Scheme 3.9). As shown in Scheme 3.9, quinolone **3.7** is a highly conjugated system thus electrons can delocalise around the ring from the nitrogen atom to the C-4 carbonyl oxygen atom resulting in alkylation at the C-4 oxygen.
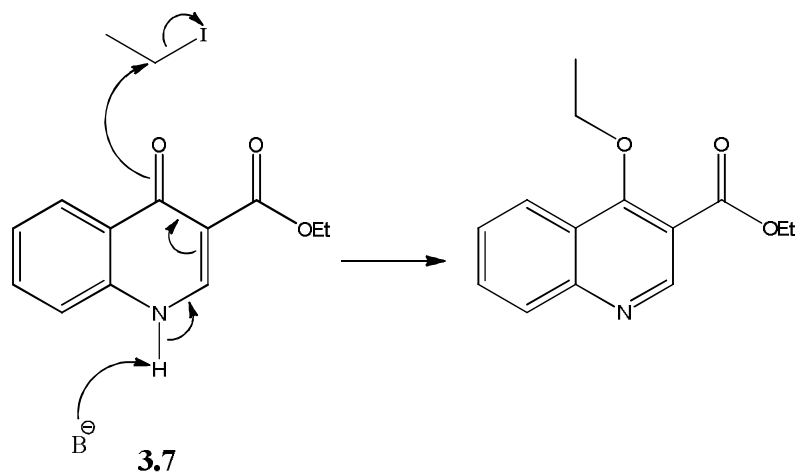
Scheme 3.9: Proposed mechanism for the synthesis of **3.11b**.

The synthesis of **3.12** was carried out using the same procedure described above in Scheme 3.8. As with **3.10**, the starting material was a mixture of two isomers and it was assumed that two *N*-ethyl quinolones would be produced. As expected, analysis by TLC revealed two spots, however, an additional third spot was also observed.

Silica gel column chromatography was carried out and each of the products were isolated.

The first product to elute was **3.12a**. Analysis by ^{1}H NMR spectroscopy revealed two sets of signals characteristic of an ethyl group, that is, one doublet and triplet for the CH_2 and CH_3 of the ester ethyl group and a second doublet and triplet for the protons of the new ethyl group. The C-F coupling constants were calculated from the ^{13}C NMR spectrum and are given in Table 3.4. As can be seen from Table 3.4 the C-F coupling constants corresponded to the characteristic ranges for [1]J, [2]J, [3]J, and [4]J C-F coupling. These values, together with the observed ^{13}C and HSQC equivalent NMR spectra, suggested that the fluorine atom was at the C-7 position in **3.12a**. Additionally, the ester C=O quaternary ^{13}C signal was observed at 164.1 ppm, together with a second quaternary ^{13}C signal at 165.1 ppm, indicating that **3.12a** may be an *O*-ethyl derivative, similar to **3.11b** above.

Table 3.4: C-F coupling constants for **3.12a**, **3.12b** and **3.12c**.

Quinolone	[1]J (Hz)	[2]J (Hz)	[3]J (Hz)	[4]J (Hz)
Fluorobenzene[91]	245	20-26	8-10	4
3.12a	250.5	24.7, 20.0	10.8, 12.0	1.13
3.12b	246.8	22.5, 27.0	11.3, 12.0	2.25
3.12c	264.8	21.8, 6.9	11.0, 3.0	4.7

To confirm *O*-alkylation, differential NOE experiments were carried out on **3.12a** the results of which are shown in Figure 3.18. As can be seen in the NOEdiff spectrum, irradiation of *H*-2 did not result in a significant increase in intensity of any other ^{1}H signal. A similar outcome was observed in the NOEdiff spectrum of **3.11b** above (Figure 3.16), thus, **3.12a** is also an *O*-alkyl derivative (Figure 3.18).
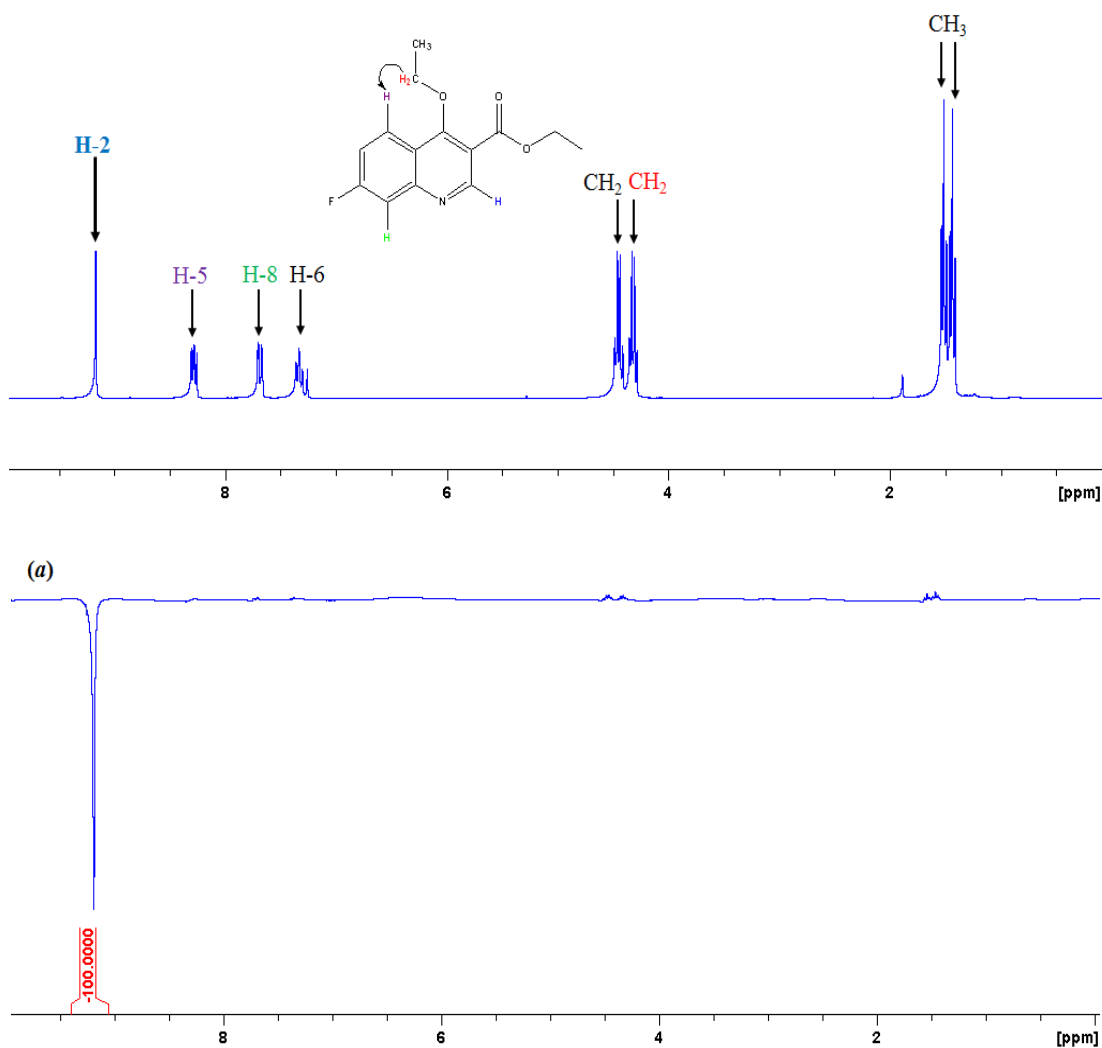
Figure 3.18: NOEdiff spectrum for irradiation of *H*-2 in **3.12a**.

The second product to be eluted was **3.12b**, in a yield of 73%. In its ^{13}C NMR spectrum, the appearance of two new peaks at approximately 14.0 and 48.0 ppm indicated addition of the ethyl group. The ^{13}C signal for the ester carbonyl carbon was observed at 164.4 ppm, with an additional quaternary ^{13}C signal at 172.1 ppm, characteristic of *C*-4. The *J* values for the coupling of the fluorine substituent to the *ipso*, *ortho*, *meta* and *para* carbon atoms were obtained from the ^{13}C NMR spectrum and are shown in Table 3.4. In addition to the C-F *J* values in Table 3.4, the ^{13}C, HSQC equivalent and COSY NMR experiments, suggested that the fluorine substituent is at C-7 of the quinolone.

The presence of an additional triplet at 4.38 ppm and quartet at 1.35 ppm in the ^{1}H NMR spectrum **3.12b** also indicated formation of the alkyl product. Assessment of

the spatial proximity of H-H using differential NOE experiments confirmed alkylation at N-1 (Appendix B, Figure B2). A melting point range of 126-130 $^{\circ}$C was also obtained for **3.12b** and found to correspond with the literature m.p. of 128-129 $^{\circ}$C.[126] Together, these results suggest that **3.12b** is ethyl 1-ethyl-7-fluoro-4-oxo-1,4-dihydroquinoline-3-carboxylate (Scheme 3.8).

As mentioned in section 3.2.5, cyclisation of **3.4** resulted in the generation of two products, **3.8a** and **3.8b**. However, the structure of only one of these products, the abundant 7-fluoro quinolone **3.8a**, could be fully characterised. Having isolated both an *N*-ethyl and *O*-ethyl 7-fluoro quinolone derivative it was believed that the third and final alkylation reaction product, **3.12c** (Scheme 3.8), was most likely the alkylated derivative of the second quinolone product obtained in the cyclisation of **3.4**.

After separation by silica gel column chromatography, **3.12c** was obtained with a yield of 3%. In the ^{1}H NMR spectrum, the presence of two triplets and two quartets in the range of 4.20-4.40 ppm and 1.35-1.55 ppm, respectively, indicated that two ethyl groups were attached to the quinolone compound. One set of signals belonging to the C-3 ethyl ester protons and the second belonging to the protons of the new ethyl group. To determine if the new ethyl group was attached to either the nitrogen atom at position one or the C-4 oxygen atom, an assessment of the H-H spatial proximity was carried out using differential NOE experiments.

The hydrogen chosen for irradiation was H-2 (spectrum (*a*), Figure 3.19). As a result, one CH_2 signal showed increased signal intensity presenting a positive NOE of 8%, thus suggesting that alkylation had occurred at N-1. The ^{1}H signal for the same CH_2 group was irradiated and resulted in an increase in intensity of three ^{1}H signals, CH_3, *H*-2 and an aromatic C*H* (spectrum (*b*), Figure 3.19). These results confirm alkylation at N-1.
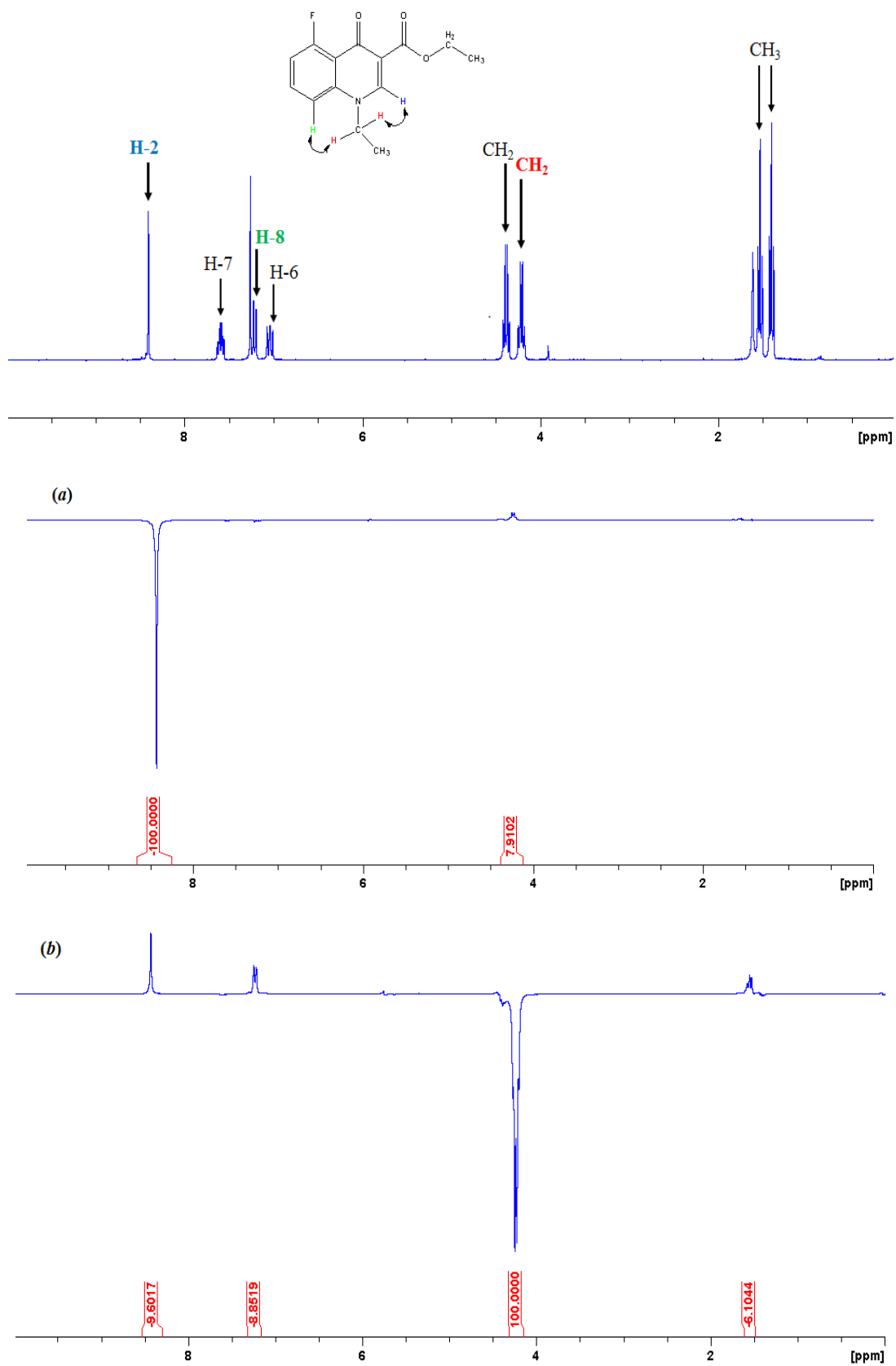
Figure 3.19: ^{1}H and NOEdiff spectra of **3.12c**.

126

In the ^{13}C NMR spectrum the ^{13}C signal for the ester carbonyl carbon was observed at 165.8 ppm with a second quaternary ^{13}C signal at 173.3 ppm for *C*-4, further confirming that *O*-alkylation had not occurred. The C-F coupling constants were obtained from the ^{13}C NMR spectrum and are given in Table 3.4. It can be seen that the calculated C-F *J* values correspond to the characteristic coupling constants for one-, two-, three- and four-bond C-F coupling. These values, in conjunction with C-H correlation and COSY NMR experiments, suggest that the fluorine substituent is at C-5 on the quinolone molecule **3.12c** (Figure 3.19). A C-F coupling constant of 2.3 Hz was also observed for *C*-4, further indicating that the fluorine substituent is at the C-5 position.

3.2.9 Hydrolysis of the quinolone carboxylates

Hydrolysis of **3.11a** was carried out using a procedure described by Sayyed *et al.*[127] The method involves ester hydrolysis under basic conditions as shown in Scheme 3.10.
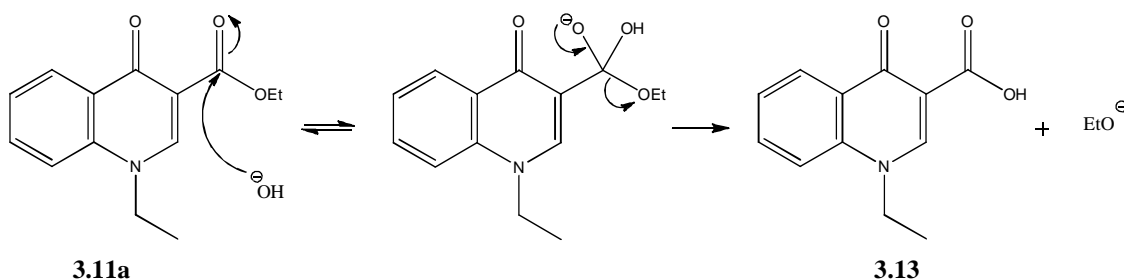
Scheme 3.10: Base-catalysed ester hydrolysis.

Compound **3.11a** was dissolved in a methnal:water solution of KOH and brought to reflux for three hours, after which, the methanol was removed under reduced pressure. Water was added to the remaining solution and acidified with HCl to give **3.13** (Scheme 3.10) as a white solid with a yield of 95%.

In the ^{1}H NMR spectrum of **3.13,** the loss of the ^{1}H signals for the ethyl protons, together with the appearance of a broad singlet at 15.27 ppm for the –OH proton, indicated formation of the carboxylic acid. A downfield shift in the carbonyl ^{13}C signal from 172.7 ppm to 177.6 ppm, due to the loss of the –CH$_2$CH$_3$, further

confirmed formation of the carboxylic acid. These NMR data were found to be in agreement with the reported literature values[127], thus confirming the structure of **3.13** (Scheme 3.10).

The procedure described for the hydrolysis of **3.11a** above was also used for the hydrolysis of the 7-fluoro derivative **3.12b**. As with **3.11a**, the loss of the ethyl group ^{1}H signals together with a downfield shift in the carbonyl ^{13}C signal (172.1 ppm to 176.9 ppm) indicated formation of the carboxylic acid. However, a new sharp singlet at 3.99 ppm was also observed in the ^{1}H NMR spectrum. In addition to this new peak, the ^{13}C NMR spectrum appeared to be less complex, in comparison to the ester precursor, as no peak splitting was observed. The lack of C-F coupling in the ^{13}C NMR spectrum suggested that the fluorine substituent had been removed from C-7. A ^{19}F NMR experiment was carried out and confirmed that this was indeed the case.
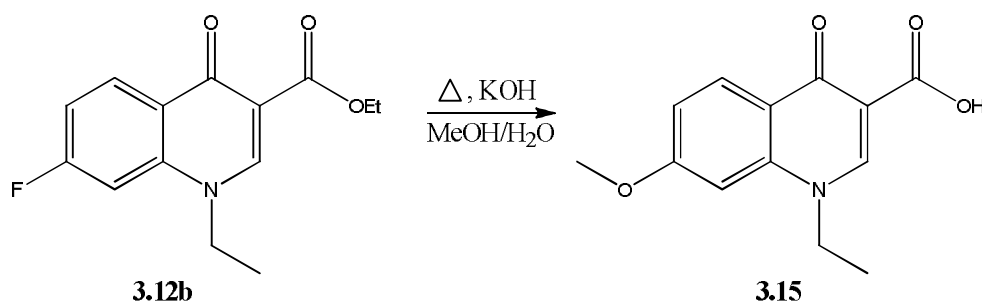
Scheme 3.11: Loss of the C-7 fluorine substituent resulted in the formation of **3.15**.

Taking these results into account, it was believed that perhaps a nucleophilic methoxide ion, generated during the hydrolysis reaction, had attacked the electrophilic C-7 thus replacing the fluorine substituent and resulting in the formation of a 7-methoxy quinolone (Scheme 3.11). These NMR data presented here are consistent with the structure of **3.15** and were found to be in agreement with reported literature data[128], thus confirming the structure of **3.15**.

Having lost the fluorine substituent during hydrolysis by the method described by Sayyed *et al.*[127] an alternative method was employed for the hydrolysis of **3.12b** (Scheme 3.12).
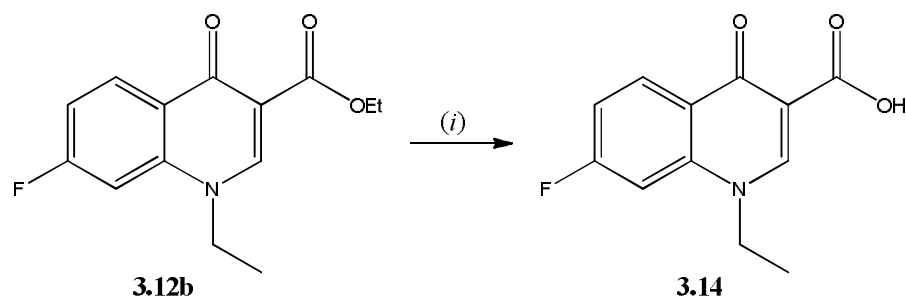
Scheme 3.12: Ester hydrolysis, (*i*) dioxane:H_2O, LiOH, at 50 ^{o}C for 30 mins.[129]

Quinolone **3.12b** was dissolved in a 1:1 dioxane:H_2O mixture followed by addition of LiOH. The reaction was allowed to stir at 50 ^{o}C for 30 minutes after which the solvent was removed under reduced pressure followed by the addition of water. The solution was acidified and the resulting white precipitate collected by filtration.

A ^{19}F NMR experiment was carried out, the result of which confirmed the presence of the fluorine substituent. In the ^{1}H NMR spectrum the loss of the triplet and quartet signals of the ester ethyl group indicated generation of the carboxylic acid. In the ^{13}C NMR spectrum, the C-5, C-6, C-7 and C-8 ^{13}C signals exhibited characteristic C-F coupling constants, further confirming the presence of the fluorine substituent. A downfield shift in the ^{13}C signal for the carbonyl carbon, from 172.1 ppm to 176.8 ppm, also indicated formation of the carboxylic acid. The m.p. range of 126-130 ^{o}C obtained for **3.14** was found to be in agreement with the literature m.p. range of 128-129 ^{o}C[126], thus confirming the formation of the carboxylic acid derivative **3.14**.

3.2.10 Synthesis of the C-7 piperazine quinolones

The C-7 piperazine quinolones were synthesised *via* a nucleophilic substitution reaction (Scheme 3.13). Quinolone **3.10a** (or **3.14**) and piperazine were dissolved in pyridine and allowed to reflux for 16 hours, after which the solvent was removed under reduced pressure.[130] The resulting residue was purified from cold EtOH to give the solid product, **3.16**, in a yield of 57% (86% for **3.17**).

R = CN, R' = H
R = CO$_2$Et, R' = H
R = CN, R' = Me
R = CO$_2$Et R' = Me

3.16: R = CN, R' = H
3.17: R = CO$_2$Et, R' = H
3.18: R = CN, R' = Me
3.19: R = CO$_2$Et = Me
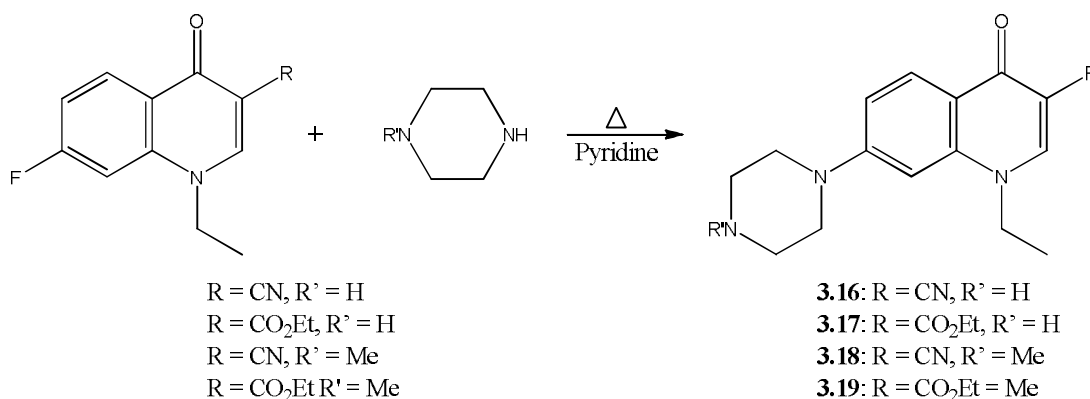
Scheme 3.13: Synthesis of 7-piperazine quinolone derivatives.

In the ^{1}H NMR spectrum of **3.16**, the appearance of two additional peaks at 3.32 and 2.85 ppm, each having an integral of four, signified formation of the C-7 piperazine quinolone. The two corresponding ^{13}C signals were found at 47.7 and 45.2 ppm in the ^{13}C NMR spectrum. Consistent with replacement of the fluorine substituent by a less electronegative nitrogen atom, a large upfield shift of the C-7 ^{13}C signal from 164.9 to 154.4 ppm was also observed. Additionally, the ^{13}C NMR spectrum was less complex in comparison to the C-7 precursor, having only singlets. No C-F coupling was observed in the ^{13}C NMR spectrum, indicating replacement of the fluorine substituent with the new piperazine group. A ^{19}F NMR experiment, having no ^{19}F signal, further confirmed the loss of the fluorine substituent.

Similar to **3.16** (Scheme 3.13), the appearance of two new peaks in the ^{1}H NMR spectrum of **3.17**, at 3.40 and 2.85 ppm for the piperazine CH_2's, were observed. In the ^{13}C NMR spectrum, the corresponding ^{13}C signals were observed at 47.7 and 45.3 ppm. In addition to the piperazine ^{13}C signals, no C-F coupling was observed, with all ^{13}C signals appearing as singlets. A large upfield shift of approximately 10 ppm, of the C-7 ^{13}C signal indicated replacement of the fluorine substituent with the piperazine group. Furthermore, no signal was observed in the ^{19}F NMR spectrum, thus confirming loss of the C-7 fluorine atom.

The synthesis of the *N*-methylpiperazine quinolones, **3.18** and **3.19**, was carried out using the same method as described for **3.16** and **3.17** above (Scheme 3.13). Similar to the piperazine derivatives, the appearance of two new signals, at approximately

3.40 and 2.60 ppm, suggested formation of the C-7 piperazine derivatives, **3.18** and **3.19** (Scheme 3.13). An additional singlet, at approximately 1.50 ppm, with an integral of three for the three equivalent protons of the piperazine N-Me was also observed in each of the quinolone's ^{1}H NMR spectra. In the ^{13}C NMR spectra of both **3.18** and **3.19**, all of the ^{13}C signals appeared as singlets and no C-F coupling was observed indicating loss of the fluorine substituent. This was confirmed by ^{19}F NMR experiments of each quinolone. The replacement of the C-7 fluorine substituent by the N-methylpiperazine group was further confirmed by an upfield shift of approximately 10 ppm for the C-7 ^{13}C signal.

3.2.11 Synthesis of tributyltin azide (TBTA)

The synthesis of TBTA was carried out using the procedure described by Gernon (Scheme 3.14).[131] A solution of sodium azide in distilled water and tributyltin chloride in diethyl ether were shaken together for 10 minutes. The organic and aqueous phases were separated followed by a second diethyl ether extraction of the aqueous layer. TBTA was obtained as a yellow oil (74%) after removal of the diethyl ether solvent.
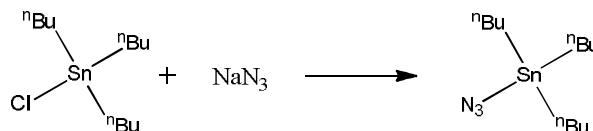
Scheme 3.14: Synthesis of TBTA.

In the ^{1}H NMR spectrum of TBTA, a triplet at 0.93 ppm was observed for the protons of the three CH_3 groups, with the ^{1}H signals of the CH_2 groups presenting as three multiplets in the region of 1.20-1.70 ppm. A ^{13}C signal for the carbons of the three equivalent CH_3 groups was observed at 13.6 ppm, with the ^{13}C signals for the carbons of the CH_2 groups being observed at 27.8, 26.9 and 15.4 ppm. A strong absorption at 2073 cm^{-1}, characteristic of the azide stretching frequency, was observed in the IR spectrum, thus confirming formation of TBTA.

3.2.12 Synthesis of quinolone (1*H*)-tetrazoles

The (1*H*)-tetrazoles were synthesised *via* a 1,3-dipolar cycloaddition reaction as shown in Scheme 3.15. In this study, the azide was employed as the 1,3-dipole whilst the dipolarophile was the quinolone C-3 nitrile. The [2+3] cycloaddition is known to occur, traditionally, by a concerted mechanism (Scheme 3.15).[132] However, it has also been suggested to occur *via* a two-step, anionic process wherein the nucleophilic azide attacks the nitrile first followed by ring closure.[132b,133]
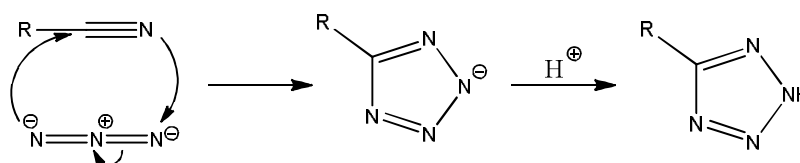
Scheme 3.15: Concerted mechanism of the 1,3-dipolar cycloaddition of a nitrile and azide.[132a]

Tetrazoles can be synthesised *via* the neat reaction of a nitrile with TBTA.[134] Thus, initial synthesis of the C-3 tetrazole quinolone **3.20** (Figure 3.21) was carried out by the neat reaction of **3.9** with TBTA under nitrogen gas. The reaction was monitored using IR spectroscopy, with the disappearance of the $\nu(C{\equiv}N)$ at ca. 2220 cm^{-1} and $\nu(N_3)$ at ca. 2070 cm^{-1} indicating completion. Reactions were carried out at 60, 140 and 175 $^{\circ}$C for one hour. However, as can be seen in the IR spectra below, the absorption bands of $\nu(C{\equiv}N)$ and $\nu(N_3)$ were still observed (Figure 3.20). The reaction was repeated with overnight heating at 175 $^{\circ}$C and again both the nitrile and N$_3$ absorption bands remained. Thus, the reaction was repeated at 200 $^{\circ}$C overnight (15 hours). The resulting IR spectrum (Appendix B, Figure B3) indicated that the reaction had gone to completion. The tributyltin moiety was cleaved, using HCl, producing **3.20** in 75% yield.
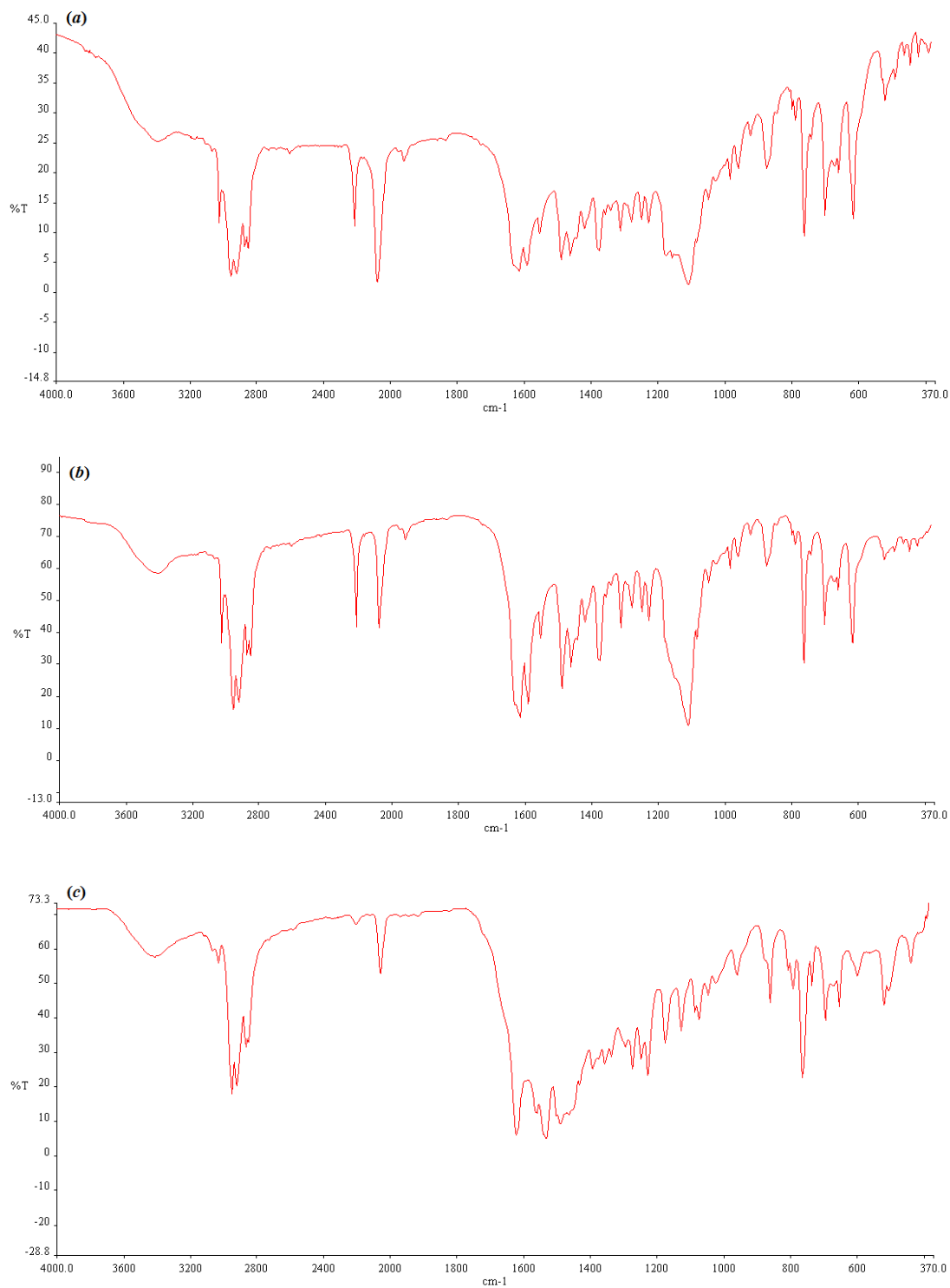
Figure 3.20: IR spectra of the reaction of TBTA with **3.9** at (*a*) 60 ^{o}C, (*b*) 140 ^{o}C and (*c*) 175 ^{o}C degrees after one hour. All samples were prepared as KBr discs.

In the ^{1}H NMR spectrum, a shift in the ^{1}H signals was observed, with the largest shift, from 8.86 ppm to 9.11 ppm, being observed for H-2, indicating formation of the tetrazole. A large downfield shift in the ^{13}C signal for C-3 (93.5 ppm to 104.5 ppm) was also observed in the ^{13}C NMR spectrum. Additionally, the ^{13}C signal of the nitrile carbon exhibited a dramatic downfield shift of approximately 30 ppm. This result is consistent with the addition of three electronegative nitrogen atoms, thus confirming formation of the C-3 tetrazole. Both 1,5- and 2,5-tetrazoles can be formed, with the CN$_4$ ^{13}C signals usually found at ca. 155.0 and 162.0 ppm, respectively.[132a,135] For **3.20**, the chemical shift of the CN$_4$ ^{13}C signal was 150.1 ppm and is, therefore, consistent with the (1H)-tetrazole product (Figure 3.21).

3.20
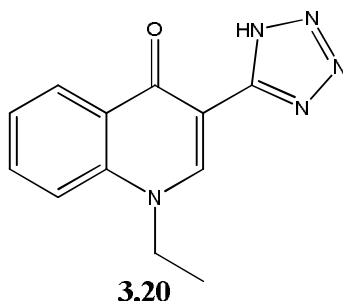
Figure 3.21: 1-Ethyl-3-(1H-tetrazol-5-yl)quinolin-4(1H)-one.

Although the synthesis of **3.20** employing TBTA as the azide source was successful, cleavage of the tributyltin group proved difficult and often had to be repeated. Therefore, an alternative synthetic method was investigated.

Tetrazoles have also been synthesised by the reaction of sodium azide with a nitrile in the presence of a Lewis acid.[136] Coordination of the Lewis acid can cause a decrease in the energy difference between the HOMO and LUMO of the reactants, therefore, resulting in a faster reaction.[136a] The synthesis of **3.20** was attempted using sodium azide and AlCl$_3$ with DMF as the reaction solvent (Scheme 3.16).[136b] However, after 24 hours only starting material was returned. Thus, an alternative method was sought.
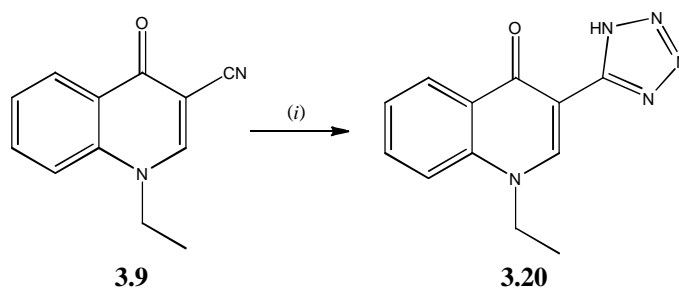
Scheme 3.16: Synthesis of 3.20. (*i*) NaN$_3$, AlCl$_3$, DMF, 24 h.

Another method of tetrazole synthesis employs ammonium azides as the 1,3-dipole. It has been suggested that the reaction occurs *via* the two-step anionic pathway, however, it has also been demonstrated that tetraalkylammonium salts are not competent dipoles whereas, ammonium azides bearing a proton, are.[132b,133] Computational studies by Himo *et al.*[132b] have demonstrated that the proton may be involved in activating the nitrile, as shown in Figure 3.22.
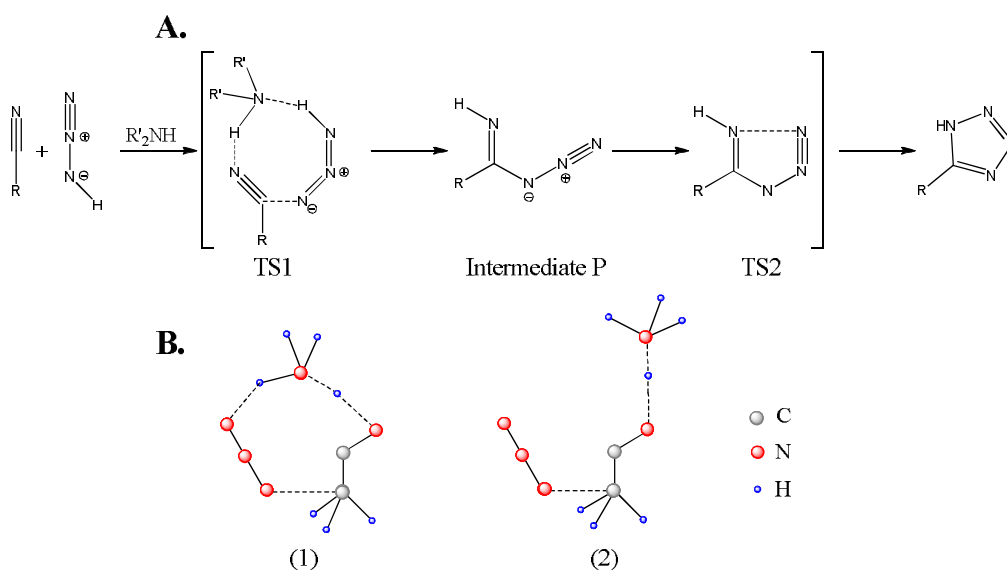
Figure 3.22: Proposed stepwise reaction by activation of the nitrile by a proton.[132b] **A.** The tetrazole reaction proceeds *via* intermediate P when a proton is available. **B.** When NH$_4^+$ is the proton source, it is believed that intermediate P can form *via* two possible pathways (1) a neutral NH$_3$ mediates the transfer of a proton from the azide to the nitrile or by (2) which involves a NH$_4^+$ and azide ion (N$_3^-$). The ammonium-mediated reaction was found to have a barrier lower than that in the concerted mechanism of the anionic [2+3] cycloaddition.

An attempt to synthesise **3.20** was also carried out using a modified procedure of that described in reference 137 (Scheme 3.17). As shown in Scheme 3.17, the reaction was carried out using various ratios of reactants with the best result obtained from the reaction of **3.9** with 11 equivalents of sodium azide and ammonium chloride (method C). After 27.5 hours, the solvent was removed and the remaining residue dissolved in water. Acidification of the solution resulted in precipitation of the product. Production of **3.20** by this method was confirmed by ^{1}H and ^{13}C NMR spectroscopies.
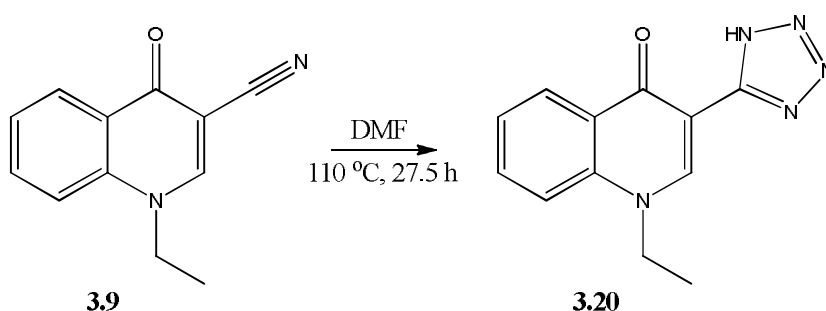
Method	**3.9**	NaN$_3$	NH$_4$Cl	LiCl	**3.20** % yield
A	1	2.2	2.2	0.7	12
B	1	5.5	5.5	1.74	63
C	1	11	11	3.48	83

Scheme 3.17: Synthesis of **3.20** using ammonium azide.[137] Table presents the equivalents of the reactants used and the resulting % yields.

Further confirmation of the structure of **3.20** was obtained by X-ray crystallography. The yellow, needle-shaped crystals of **3.20** were obtained from a DMF/water solution. The crystal structure is shown in Figure 3.23, with crystal data and structure refinement for **3.20** given in Tables B4-B6 (Appendix B).
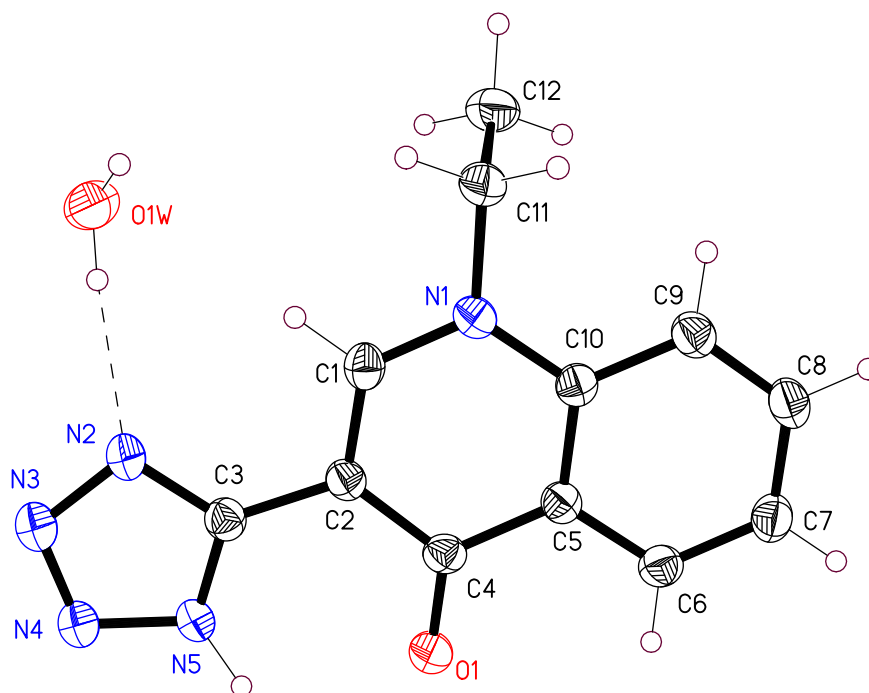
Figure 3.23: Crystal structure of **3.20**.

Molecules of **3.20** were linked into pairs by H-bonds between the C-4 C=O and tetrazole N-1 H atom and these pairs were π-stacked. The individual stacks were linked *via* H-bonds to water (Figure 3.24). Similar types of π-stacking interactions have been observed with nalidixic acid.[138] It has been suggested that these interactions play a role in the binding of the quinolone molecule to its target. Shen *et al.*[138] have proposed that once one quinolone molecule has bound to the DNA target, through H-bonds with the carbonyl oxygen atoms, a second molecule can then bind, not only through H-bonds but also through interactions with its neighbouring quinolone. Therefore, the drug is granted a strong binding affinity to the target by acquiring extra binding domains.
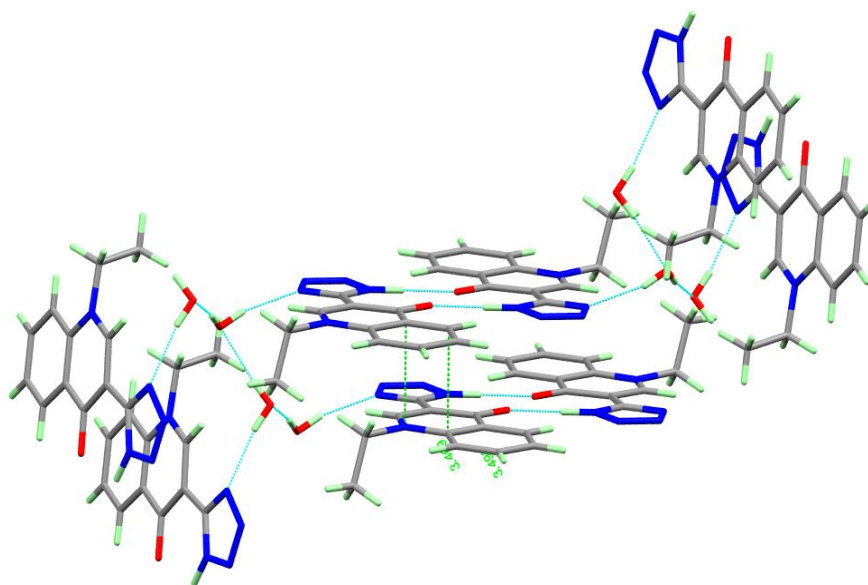
Figure 3.24: Crystal packing diagram of **3.20**.

Having successfully synthesised **3.20** the synthesis of **3.21** was attempted using the same procedure as was described for **3.20** above (Scheme 3.18). The reaction was again monitored by IR spectroscopy, with the disappearance of the $\nu(C{\equiv}N)$ at ca. 2220 cm^{-1} and $\nu(N_3)$ at ca. 2070 cm^{-1} used as an indicator for reaction completion. After 27.5 hours, a weak absorption band for $\nu(C{\equiv}N)$ was observed in the IR spectrum. A sample was taken from the reaction mixture and the acid work-up carried out. In the ^{1}H NMR spectrum of the product resulting from the mini work-up, two sets of resonance signals were observed. One set of the ^{1}H resonance signals appeared to be starting material, **3.16**. A singlet, belonging to the second set of ^{1}H resonance signals, was shifted downfield from the ^{1}H singlet for H-2 of **3.16** to ca. 9.00 ppm. A similar result was observed with the H-2 ^{1}H signal of **3.9** and **3.20**, thus suggesting formation of a possible tetrazole product. However, after a full work-up of the reaction of **3.16** in the synthesis of **3.21**, the resulting product produced a complex ^{1}H NMR spectrum. The product mixture was analysed by TLC but the crude product remained baseline with a variety of mobile phases and hence could not be purified and fully characterised.
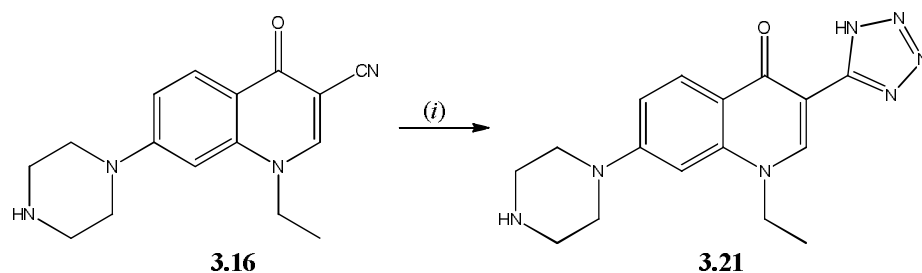
Scheme 3.18: Synthesis of the (1*H*)-tetrazole quinolone, **3.21**. (*i*) NaN$_3$, NH$_4$Cl, LiCl in DMF at 110 ^{o}C for 27.5 h.

In an effort to synthesise a 7-piperazine quinolone bearing a tetrazole at C-3 the N-methylpiperazine quinolone **3.18** (Scheme 3.19) was synthesised as described earlier in section 3.2.10. It was hoped that the presence of the methyl group in place of the hydrogen atom on the C-7 piperazine (**3.22**, Scheme 3.19) would facilitate better separation by column chromatography. Therefore, the reaction was repeated as for **3.21** above but with **3.18** instead (Scheme 3.19).
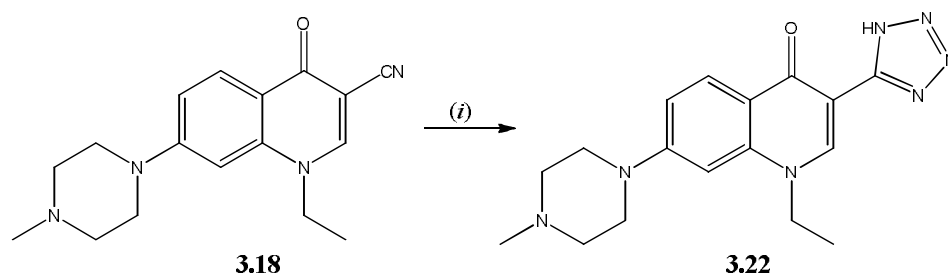
Scheme 3.19: Synthesis of the (1*H*)-tetrazole quinolone, **3.22**. (*i*) NaN$_3$, NH$_4$Cl, LiCl in DMF at 110 ^{o}C for 27.5 h.

Again, the reaction was monitored by IR spectroscopy. However, after 27.5 hours two medium absorptions for the ν(C≡N) and ν(N$_3$) were observed, therefore, the reaction was allowed to continue for a further 24 hours. Again, the IR spectrum contained both the ν(C≡N) and ν(N$_3$) absorptions. The reaction was allowed to continue and was monitored every 24 hours. Only after 14 days did the reaction appear to have gone to completion, thus the acid work-up was carried out. Upon acidification, however, no precipitate formed. The water was removed under reduced pressure and the resulting crude product analysed by ^{1}H NMR spectroscopy. In the ^{1}H NMR spectrum, a complex mixture was observed. From the TLC it appeared that

the starting nitrile, **3.18**, may be present, however, the crude mixture could not be separated.

The formation of tetrazoles is greatly influenced by the substituent on the nitrile. Electronegative substituents assist the formation of the partial positive charge on the nitrile carbon atom, which in turn, facilitates the approach of the azide ion.[132b,133,139] Therefore, it was thought that, as the quinolone molecule has a highly conjugated system, perhaps the presence of the electronegative C-7 fluorine substituent, in place of the piperazine groups, would be more favourable for reaction. Replacement of the C-7 fluorine substituent with a piperazine group could then be carried out in a subsequent reaction by the method described earlier in section 3.2.10.

In a final attempt to synthesise a 7-piperazine quinolone derivative bearing a C-3 tetrazole group the reaction was carried out using the C-7 fluoro quinolone, **3.10a**, in place of the C-7 piperazine derivative, **3.18** (Scheme 3.20). The reaction was monitored using IR spectroscopy and, as was observed with **3.21** and **3.22**, long reaction times were required before completion of the reaction appeared to have occurred. The acid work-up was carried out as for **3.20**, **3.21** and **3.22**, but again a complex mixture was observed in the ^{1}H NMR spectrum. A ^{19}F NMR experiment was also carried out. Similar to that observed with the hydrolysis of **3.12b** with KOH under reflux conditions (section 3.2.9), no ^{19}F signal was observed, suggesting that the fluorine substituent had been removed during the reaction.
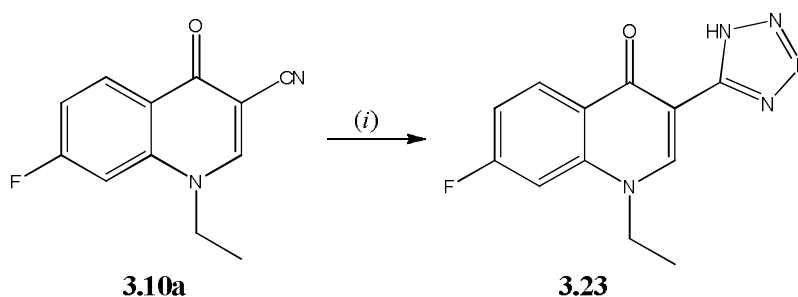
Scheme 3.20: Synthesis of the (1*H*)-tetrazole quinolone, **3.23**. (*i*) NaN$_3$, NH$_4$Cl, LiCl in DMF at 110 ^{o}C for 27.5 h.

Quinolone **3.20** was synthesised in good yield, however, when the same method was applied to **3.16**, **3.18** and **3.10a** a complex mixture resulted. As mentioned above, the

type of substituent attached to the nitrile is important in the synthesis of tetrazoles, with electronegative substituents assisting in the activation of the nitrile.[132b,133,139] Considering that the piperazine and fluorine substituents are seven bonds away from the nitrile and, in particular, that the fluorine substituent is a good electron-withdrawing group, it seems unlikely that these substituents are having a negative effect on the activation of the nitrile. Perhaps the problem lies with C-7 itself. The presence of the fluorine substituent at C-7 results in the carbon atom becoming electrophilic. Indeed, it is this property which allows for the formation of the C-7 piperazine quinolone derivatives (section 3.2.10). Therefore, perhaps the electrophilic nature of C-7 in the 7-fluoro quinolone interferes with the formation of the tetrazole due to competing SNAr with N_3^- acting as the nucleophile. The loss of the fluorine substituent, during the reaction of **3.10a** in an attempt to synthesise **3.23** (Scheme 3.20), supports this theory.

3.2.13 Esterification of levofloxacin

The C-3 ethyl ester of levofloxacin, **3.24**, was synthesised using acid catalysed esterification (Scheme 3.21). The ethyl ester product was obtained as a white solid in a yield of 87%.
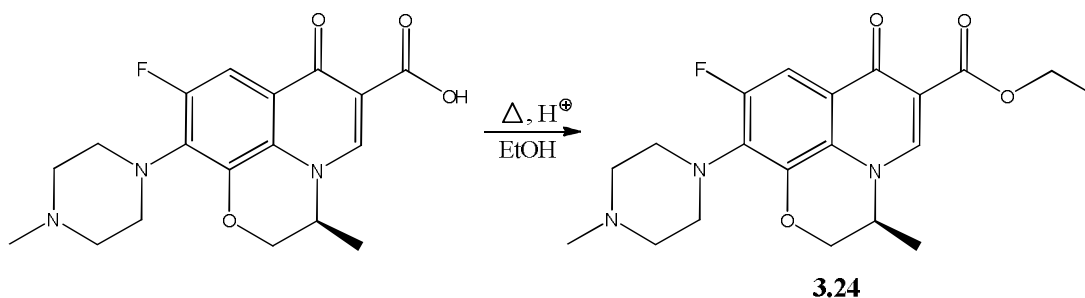
Scheme 3.21: Esterification of levofloxacin. H_2SO_4 was employed as the acid for this reaction.

In the ^{13}C NMR spectrum, two new peaks were observed at 60.8 and 14.5 ppm for the new CH$_2$ and CH$_3$ groups, respectively. Consistent with the replacement of the carboxylic acid –OH by an –OEt group, an upfield shift from 176.9 ppm to 172.8 ppm in the ^{13}C signal of the C-3 carbonyl carbon was observed. In the ^{1}H NMR spectrum a new triplet, at 1.39 ppm, having an integral of three, was observed for the

three equivalent protons of the ethyl CH$_3$ group. The expected quartet ^{1}H signal for the protons of the ethyl CH$_2$ group was found at the same chemical shift (m at 4.27-4.40 ppm) as the ^{1}H signals for the morpholine ring CH and CH$_2$ (C-12 and C-11) protons. This was confirmed by COSY and C-H correlation NMR experiments. Formation of the ethyl ester of levofloxacin was further confirmed by LC/TOF-MS, which returned a (M+H$^+$) of 390.1843 for C$_{20}$H$_{25}$FN$_3$O$_4$.

3.2.14 Synthesis of the quinolone C-3 hydroxamic acid

In an effort to synthesise a quinolone derivative with enhanced activity, the well-known quinolone, levofloxacin, was chosen as the quinolone derivative for modification with the hydroxamic acid. The synthesis of a C-3 hydroxamic acid derivative of levofloxacin, **3.25**, was first attempted using the coupling reagents HOBt and TBTU, in the presence of Et$_3$N, with DMF as the reaction solvent (Scheme 3.22).
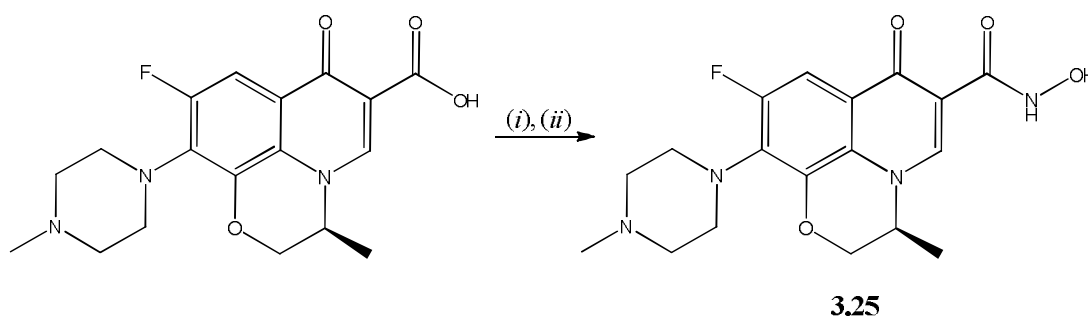
Scheme 3.22: Synthesis of levofloxacin C-3 hydroxamic acid **3.25**. Reaction carried out under nitrogen, (*i*) HOBt, TBTU, Et$_3$N, DMF, 10 min (*ii*) NH$_2$OH.HCl, Et$_3$N, DMF, 24 h, rt.

Coupling reagents are most commonly used in the synthesis of peptides.[140] TBTU is a (1*H*)-benzotriazole-based coupling reagent that is believed to exist as both the uronium and aminium salt in solution (Figure 3.25).[140-141] These uronium/aminium salts work by activating the carboxylic acid moiety which in turn facilitates the nucleophilic attack of an amine, resulting in formation of an amide bond.[141]
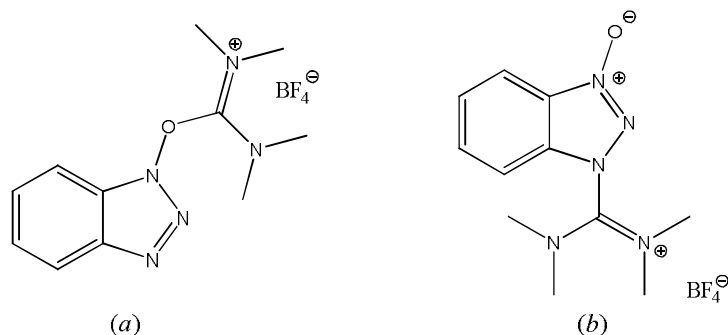
Figure 3.25: TBTU (*a*) uronium salt and (*b*) aminium salt.[140-141]

As shown in Scheme 3.23, the deprotonated carboxylic acid nucleophile attacks the electrophilic centre of TBTU. The resulting intermediate reacts with HOBt, generating the activated ester. Attack at the carbonyl carbon of the activated ester, by the amine, results in the formation of the amide bond. When carrying out the reaction, the carboxylic acid is usually stirred with base and the activating agent (TBTU) for approximately 10 minutes, to ensure formation of the activated ester, prior to the addition of the amine.
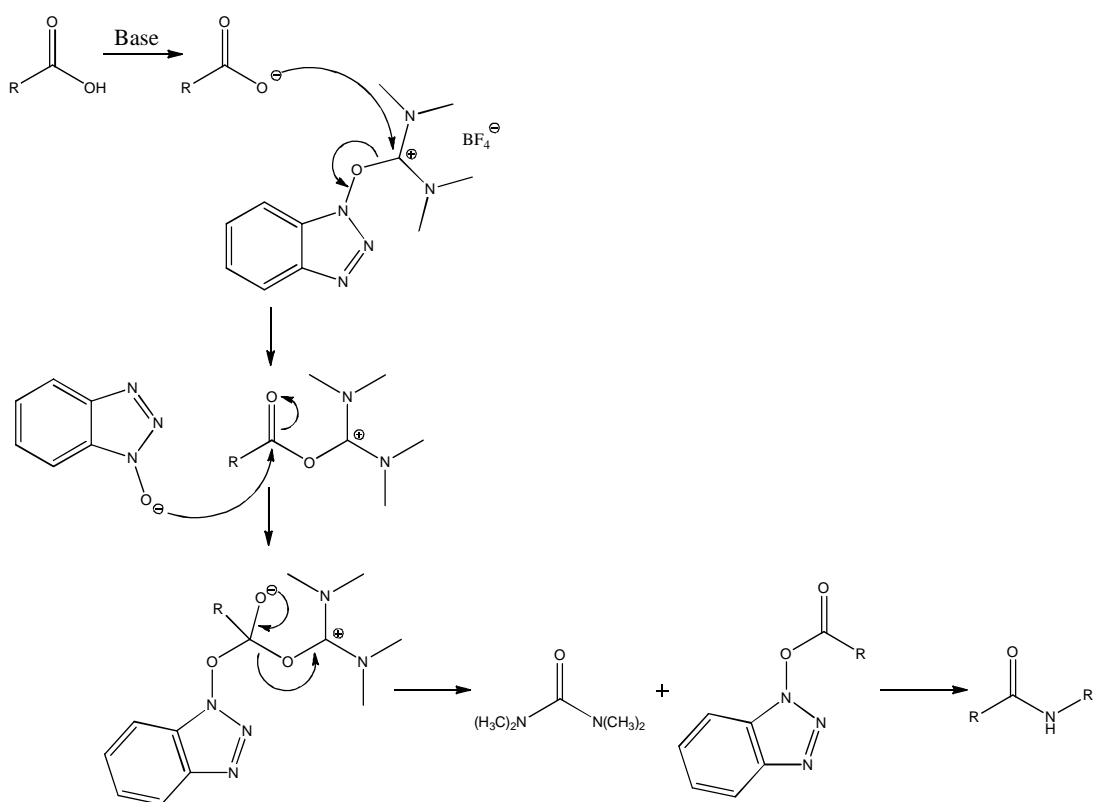
Scheme 3.23: HOBt/TBTU coupling mechanism.[141]

143

After 24 hours the solvent was removed under reduced pressure and the resulting residue analysed by ^{1}H NMR spectroscopy. In the ^{1}H NMR spectrum, only the starting material appeared to be present with no shifts in the ^{1}H signals being observed. Thus, an alternative coupling method was attempted.

COMU, shown in Figure 3.26, is a relatively new coupling reagent.[142] The presence of the oxyma leaving group in place of a benzotriazole along with the replacement of a dimethylamino group by a morpholino moiety enhances stability, solubility and reactivity of the reagent.[142-143] As mentioned earlier, the benzotriazole-type coupling reagents, such as TBTU, are believed to co-exist as the uronium and aminium salts. However, COMU exists solely as the more reactive uronium structure.[142,144] Additionally, the by-products formed by COMU are water soluble, allowing their removal by simple extraction.[143,145]
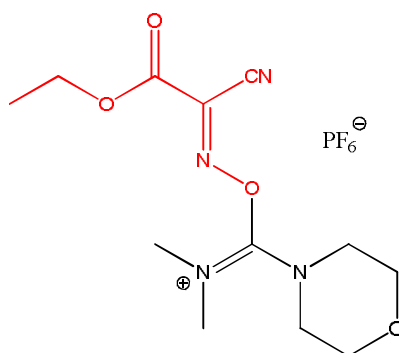
Figure 3.26: COMU coupling reagent with the oxyma moiety shown in red.

The synthesis of **3.25** was attempted using COMU coupling as described in Scheme 3.24. After 24 hours, the solvent was removed under reduced pressure and the resulting residue was analysed by ^{1}H NMR spectroscopy. As with the previous HOBt/TBTU coupling reaction, in the ^{1}H NMR spectrum, no shifts were observed for the levofloxacin ^{1}H signals, suggesting that only starting material was returned.

3.25
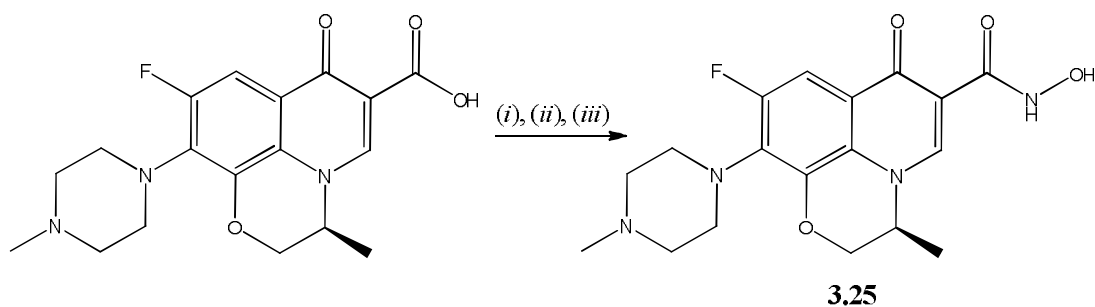
Scheme 3.24: Synthesis of **3.25** under COMU coupling conditions.[143] The reaction was carried out under nitrogen, (*i*) DIEA, 0 °C, 10 min, (*ii*) NH$_2$OH.HCl, DIEA, 10 min, (*iii*) COMU, 0 °C, 1 h followed by 24 h, rt.

After the unsuccessful attempts to synthesise **3.25**, using two different coupling reagents, a trial coupling reaction was carried out in an effort to determine if a simple amine could be coupled to the C-3 carboxylic acid of levofloxacin. As shown in Scheme 3.25, a reaction of levofloxacin with n-butylamine using standard coupling conditions of HOBt/TBTU in the presence of Et$_3$N was carried out.

3.26
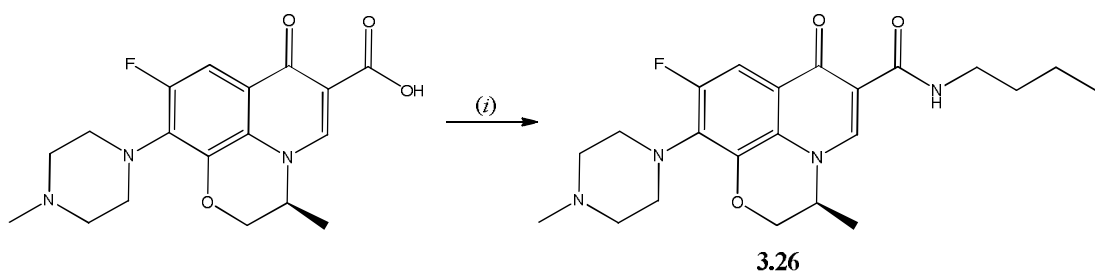
Scheme 3.25: Synthesis of **3.26**. (*i*) HOBt, TBTU, ^{n}BuNH$_2$, DMF, 24 h, rt.

In the ^{1}H NMR spectrum, the appearance of a triplet at 0.92 ppm for the protons of the n-butylamine –CH$_3$ group was observed, together with mulitplets at ca. 1.58 and 1.40 ppm for the protons of the n-butyl –CH$_2$ groups, indicating formation of **3.26**. A triplet at 9.95 ppm was also observed for the NH proton confirming generation of the amide bond. A small shift in the ^{1}H signal of H-5 was also observed. An upfield shift of the ^{13}C signal of the C-3 carbonyl carbon, from 177.0 ppm to 175.5 ppm, was observed in the ^{13}C NMR spectrum, further confirming formation of the amide derivative.

These results prove that a simple amine can be coupled to the carboxylic acid of levofloxacin. However, **3.26** was obtained in a low yield of 42% suggesting that this reaction, although successful, is not very efficient in the synthesis of a simple levofloxacin carboxamide. Therefore, an alternative synthetic approach was sought.

Reddy *et al.*[146] have demonstrated the synthesis of a variety of aliphatic and aromatic hydroxamic acid derivatives, in yields of 80-95%, using ethylchloroformate and $NH_2OH.HCl$ (Scheme 3.26). The reaction of the carboxylic acid with ethylchloroformate in the presence of base should produce the ester derivative bearing a better leaving group in comparison to the carboxylic acid –OH (Scheme 3.26). This, in turn, should facilitate attack by the hydroxylamine, resulting in formation of the hydroxamic acid derivative.
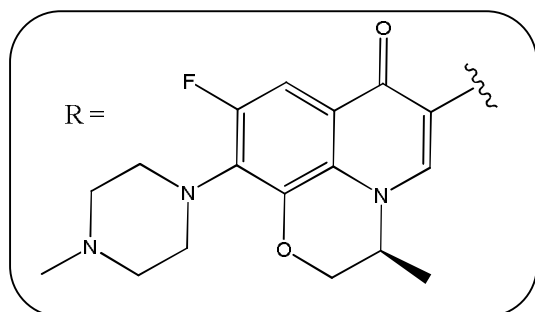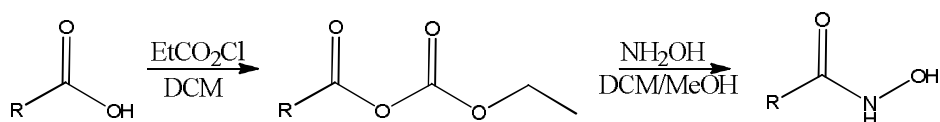
Scheme 3.26: Synthesis of **3.25**.

Hydroxylamine hydrochloride was dissolved in MeOH and added to a stirred solution of KOH in MeOH at 0 °C. After stirring for 15 minutes the solution was filtered. Levofloxacin was dissolved in DCM followed by the addition of $EtCO_2Cl$ and NMM (as base) at 0 °C. The solution was stirred for 10 minutes followed by filtration. The resulting filtrate was added to the freshly prepared hydroxylamine followed by stirring at room temperature for 30 minutes after which the solvent was removed under reduced pressure. The resulting ^1H NMR spectrum of the crude

product appeared to be a mixture of reactants, with no shifts observed in the ^{1}H signals of levofloxacin.

In a final attempt to synthesise the C-3 hydroxamic acid derivative of levofloxacin, a reaction of the C-3 ethyl ester of levofloxacin with hydroxylamine hydrochloride was carried out (Scheme 3.27).[147] Levofloxacin ethyl ester, **3.24**, was synthesised as described earlier in section 3.2.13. A methanol solution of **3.24** was added slowly to a solution of hydroxylamine and allowed to stir at room temperature for 24 hours. After 24 hours, the reaction mixture was acidified (pH 6) using concentrated HCl. The solvent was concentrated under reduced pressure and the resulting precipitate collected by filtration.
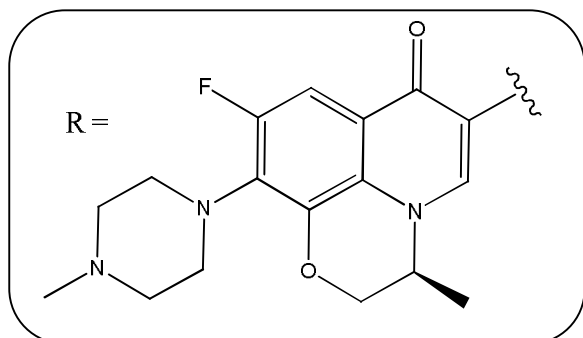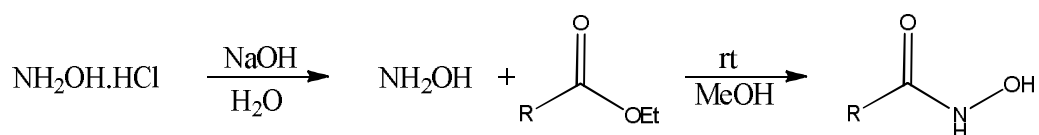
Scheme 3.27: Synthesis of **3.25**.

In the ^{1}H NMR spectrum of the resulting white solid, the disappearance of the ^{1}H signals for the ethyl group protons indicated formation of the hydroxamic acid. A downfield shift of the ^{13}C signals for *C*-2 (145.1 ppm to 146.4 ppm) and the C-3 carbonyl carbon (172.8 ppm to 176.4 ppm) was observed in the ^{13}C NMR spectrum. The strong absorption bands of the carboxylic acid and ketone v(C=O) at 1719 cm^{-1} and 1617 cm^{-1}, respectively, had shifted to 1722 cm^{-1} and 1623 cm^{-1}, further indicating formation of **3.25** (Scheme 3.27). LC/TOF-MS also confirmed formation

of the C-3 hydroxamic acid derivative of levofloxacin returning a $(M+H^+)$ of 390.1843.

3.2.15 *In vitro* antibacterial activity

Each of the compounds, the quinolones and their precursors (Appendix B, Table B1-B3), described in section 3.2, were evaluated for their antibacterial activity against *E. coli*, *P. aeruginosa* and *S. aureus* using the susceptibility assay described in section 1.2.5.

In general, the quinolone precursors, the phenylamino malonates and acrylates, were inactive against all three bacteria. The 1-H-quinolones also exhibited little or no activity against all three bacteria. Alkylation at the N-1 position of the quinolones did not improve activity, in comparison to the 1-H-quinolones, with the *N*-ethyl quinolone derivatives also exhibiting little or no activity against each of the three bacteria tested.

Neither the C-3 carboxylic acid derivative **3.13** nor the C-3 tetrazole derivative **3.20** exhibited an MIC_{50} against any of the bacteria, with the greatest bacteriostatic activity (although minimum) achieved only at the highest concentration of 100 μg/mL (Table 3.5). However, on comparing **3.13** to **3.20**, similar activity was observed for both compounds against *E. coli*, *P. aeruginosa* and *S. aureus* (Table 3.5). This result suggests that although the replacement of the carboxylic acid with the tetrazole bioisostere did not improve activity, it also does not appear to have decreased the activity of the quinolone. This result contradicts the earlier studies by Gilis *et al.*[148], wherein the presence of a tetrazole at C-3 of nalidixic acid diminished the antibacterial activity exhibited by nalidixic acid.

Table 3.5: Percentage growths of **3.13** versus **3.20** as a function of concentration of each compound.

Quinolone	Concentration (μg/mL)	*E. coli* % Growth	*P. aeruginosa* % Growth	*S. aureus* % Growth
3.13	25	88	100	100
	50	82	92	96
	100	77	74	81
3.20	25	91	95	98
	50	90	94	96
	100	88	79	91

As shown in Graph 3.1, 3.2 and 3.3, the addition of the piperazine moiety at C-7 greatly improved the bacteriostatic activity of the quinolones, not only against *P. aeruginosa*, but also against *E. coli* and *S. aureus*. In particular, **3.17** exhibited greatest activity against *P. aeruginosa* (Graph 3.2), producing an MIC_{50} in the range of 12.50-18.75 μg/mL. A similar trend in activity was also observed with the addition of the piperazine to **3.10** to give **3.16**. The addition of the *N*-methylpiperazine at C-7 of **3.14** also improved the antibacterial activity against both *P. aerugionsa* and *S. aureus* but resulted in a decrease in activity against *E. coli* (Graph 3.1, 3.2, and 3.3). For the nitrile derivative, **3.18**, the presence of the C-7 *N*-methylpiperazine moiety resulted in similar activity to that of **3.16**. Although the addition of the piperazine (and *N*-methylpiperazine) was advantageous for activity against all three bacteria, the nitrile derivatives, **3.16** and **3.18**, were less active in comparison to the carboxylic acid derivatives, **3.17** and **3.19**.
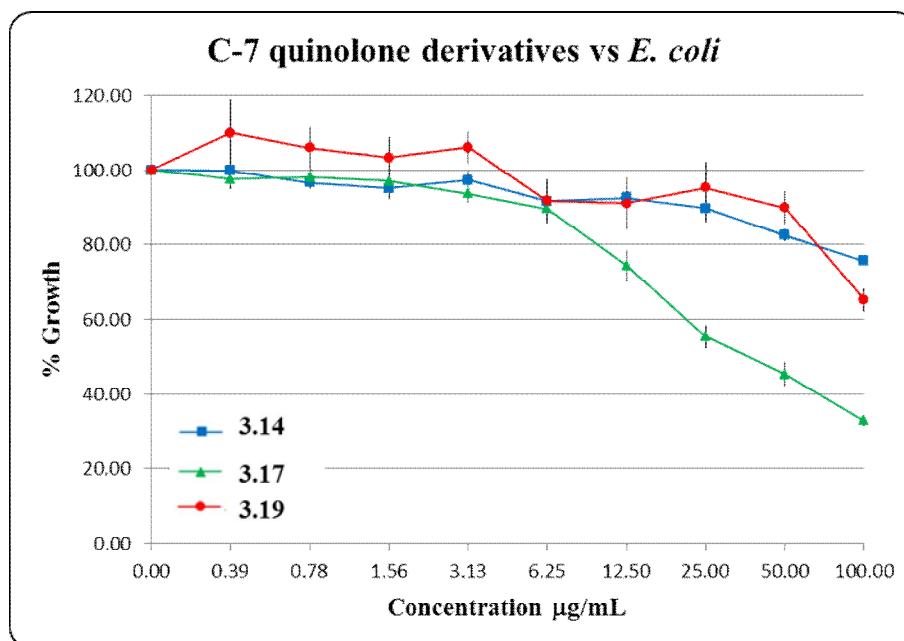
Graph 3.1: Activity profile for the C-7 quinolone derivatives versus *E. coli*.
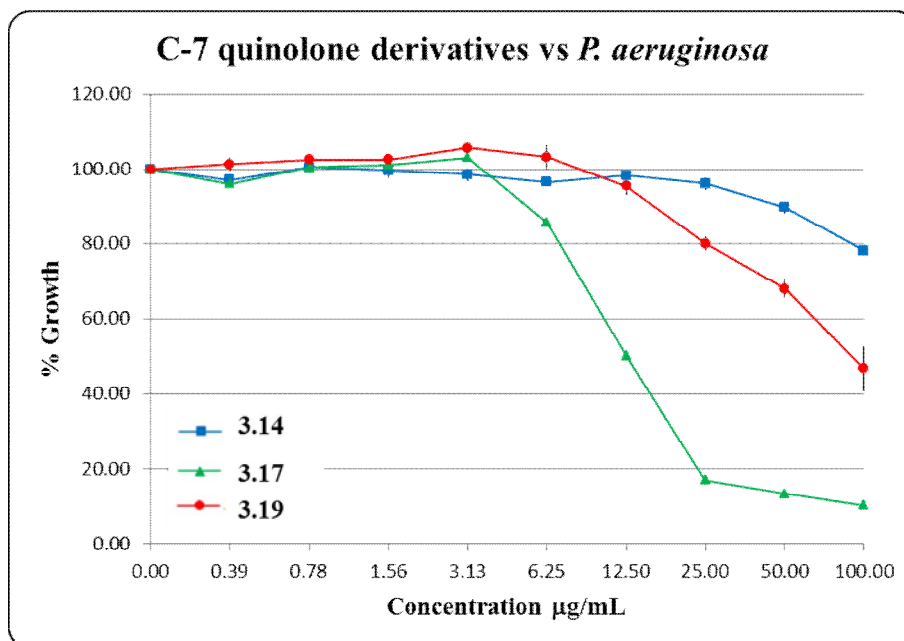
Graph 3.2: Activity profile for the C-7 quinolone derivatives versus *P. aerugionsa*.
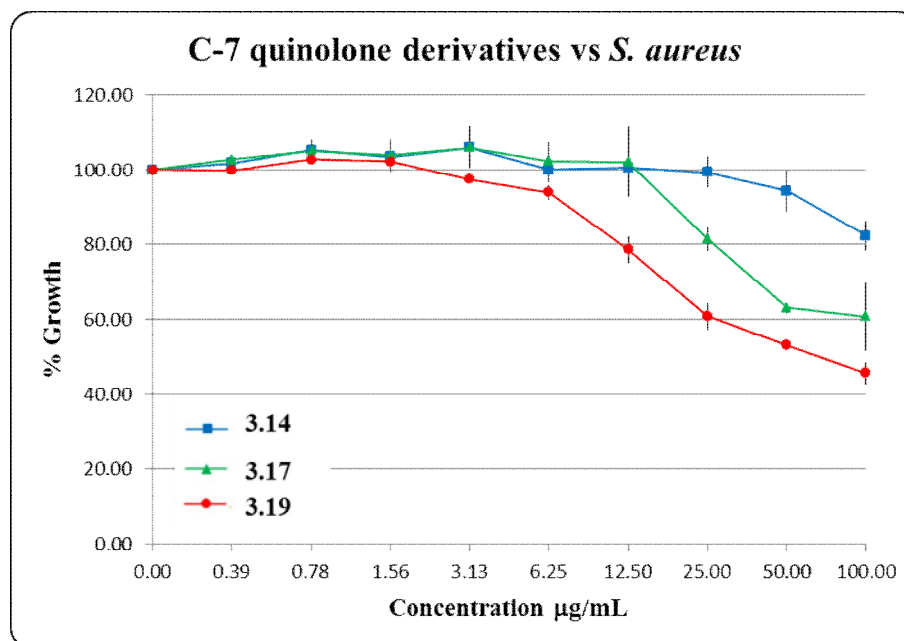
Graph 3.3: Activity profile for the C-7 quinolone derivatives versus *S. aureus*.

The bacteriostatic activity of levofloxacin versus the C-3 hydroxamic acid derivative of **3.25**, are summarised in Table 3.6. The results are expressed as the MIC_{50}, the minimum inhibitory concentration that is required to inhibit 50% of bacterial growth. As can be seen in Table 3.6, **3.25** exhibited similar activity against both the Gram-negative bacteria, *E. coli* and *P. aeurginosa*, as well as the Gram-positive bacterium, *S. aureus*. In comparison to levofloxacin, **3.25** demonstrated similar activity against *E. coli*, *S. aureus* and *P. aeruginosa* (Table 3.6). Furthermore, the bacteriostatic activity of **3.25** increased with increasing concentration, resulting in an MIC_{90} in the range of 1.17-1.56 μg/mL against *P. aeruginosa*, which is an MIC_{90} value similar to that exhibited by levofloxacin.

Table 3.6: Antibacterial activity as MIC_{50} range, values are mean of three experiments.

Compound	*E. coli*		*P. aeruginosa*		*S. aureus*	
	μM	μg/ml	μM	μg/ml	μM	μg/ml
Levofloxacin	0.54-1.08	0.2-0.39	1.62-2.16	0.59-0.78	3.24-4.33	1.17-1.56
3.25	1.56-2.08	0.59-0.78	1.04-1.56	0.39-0.59	1.56-2.08	0.59-0.78

3.2.16 Conclusion

In this study, the synthesis of a (1*H*)-tetrazole and hydroxamic acid quinolone derivatives was undertaken. For comparison, the carboxylic acid analogues were also synthesised. The structure of each synthesised compound was elucidated by means of LC/TOF-MS, ^{1}H and ^{13}C NMR and IR spectroscopies.

The synthesis of the quinolone compounds involved formation of the phenylamino acrylates or malonates, which were then cyclised, followed by alkylation at N-1. It was found that cyclisation of the phenylamino acrylates and malonates bearing a fluorine substituent resulted in the generation of two regioisomers, the 5-fluoro and 7-fluoro quinolones. Additionally, with the carboxylate derivatives, both *N*-ethyl and *O*-ethyl derivatives were generated during alkylation, the structures of which were confirmed by NOEdiff NMR experiments. The carboxylate derivatives were hydrolysed and the 7-fluoro quinolones were then used in the synthesis of the 7-piperazine derivatives. 1-Ethyl-3-(1*H*-tetrazol-5-yl)quinolin-4(1*H*)-one (**3.20**) was successfully synthesised with a yield of 83%. However, the synthesis of a 7-piperazine derivative bearing a tetrazole moiety proved difficult and could not be generated using the same method.

The X-ray crystal structure was obtained for **3.20**, and revealed that the quinolone molecules were linked into pairs by H-bonds between the C-4 C=O and tetrazole N-1 H atom and that these pairs were π-stacked.

The synthesis of the C-3 hydroxamic acid derivative was carried out by the reaction of levofloxacin with hydroxylamine hydrochloride. Initial attempts employing different coupling reagents or ethylchloroformate were unsuccessful. However, the levofloxacin C-3 hydroxamic acid derivative was successfully synthesised in the simple reaction of hydroxylamine with the ethyl ester of levofloxacin.

Each of the quinolone compounds and their precursors were evaluated for their bacteriostatic activity against two Gram-negative bacteria (*E. coli* and *P. aeruginosa*) and a Gram-positive bacterium, *S. aureus*. The phenylamino acrylates and malonates were found to be inactive against each of the bacteria tested. In general, the quinolones exhibited similar activity, although poor, against each of the bacteria. In

comparison to the carboxylate analogue, the C-3 tetrazole derivative exhibited similar activity against all three bacteria. Addition of a piperazine or N-methylpiperazine at C-7, resulted in improved activity against all three bacteria, exhibiting MIC_{50} values in the range of 25-100 µg/mL.

The hydroxamic acid derivative of levofloxacin, **3.25**, however, was the quinolone that exhibited greatest activity against each of the bacteria. Compound **3.25** demonstrated an increase in activity with increasing concentration against each of the bacteria with greatest activity observed against *P. aeruginosa* (MIC_{90} 1.17-1.56 µg/mL). Although the presence of the hydroxamic acid did not improve on the bacteriostatic activity of levofloxacin, the results obtained were similar (Table 3.6, section 3.2.15).

3.2.17 Future work

Tetrazoles have been shown to from complexes with a variety of metal ions.[149] Additionally, the coordination of metal ions to quinolone compounds have resulted in enhanced activities.[150] As mentioned earlier the bacteriostatic activity exhibited by both the C-3 tetrazole and its carboxylic acid analogue, although poor, was very similar. Taking this into account, an investigation into the complexation of metal ions with the quinolone tetrazole derivative may generate a quinolone with enhanced activity.

An initial study into the complexation of the (1*H*)-tetrazole, **3.20**, with copper(II) chloride in MeOH was carried out. The IR spectrum of the resulting green precipitate suggested that coordination had occurred. Thus, further investigations into metal complexes of a (1*H*)-tetrazole quinolone derivative could be carried out.

Additionally, considering hydroxamic acids are well known for their role as siderophores[119b], an investigation into the metal complexation of the hydroxamic acid quinolone could also be carried out. The bacteriostatic activity results obtained for **3.25** were very similar to those exhibited by the parent compound, levofloxacin. The complexation of metal ions to **3.25** may enhance its antibacterial activity.

3.3 Experimental

General procedure for the synthesis of 3.1 and 3.2

Ethyl (ethoxymethylene)cyanoacetate (50 mmol) and the appropriate aniline (50 mmol) were dissolved in EtOH (25 mL) and heated to reflux for 45 minutes. The reaction mixture was allowed to cool to room temperature. On cooling, the product precipitated out of solution and the resulting solid was collected by filtration and washed with ice-cold EtOH. In each case, the crude product was used for the next step without further purification.

Ethyl 2-cyano-3-(phenylamino)acrylate (3.1)
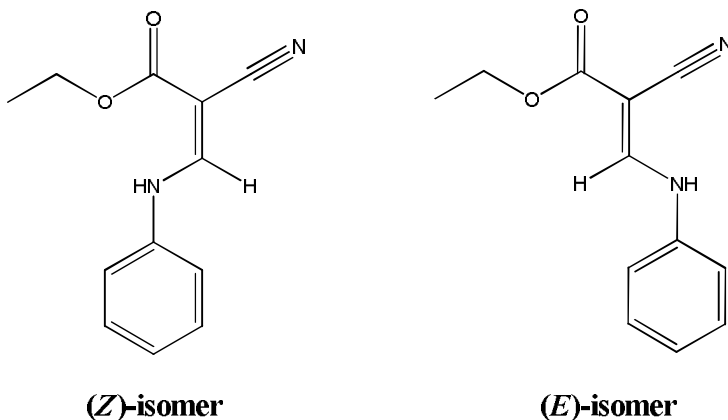
(*Z*)-isomer   (*E*)-isomer

White solid (10.42 g, 96%), 1.00:0.63 mixture of isomers; m.p. 90-94 $^\circ$C (lit 108 $^\circ$C)[151]; ^{1}H NMR (300 MHz, CDCl$_3$) δ 10.73 (d, *J* = 13.4 Hz, 1H, N*H*), 8.59 (d, *J* = 14.8, 1H, N*H*), 8.37 (d, *J* = 14.8 Hz, C=C*H*), 7.87 (d, *J* = 13.4 Hz, 1H, C=C*H*), 7.33-7.39 (m, 4H, *E* & *Z* isomers, phenyl C*H*), 7.14-7.20 (m, 4H, *E* & *Z* isomers, phenyl C*H*), 7.07 (d, *J* = 7.3 Hz, 2H, *E* & *Z* isomers, phenyl C*H*), 4.22-4.30 (m, 4H, *E* & *Z* isomers, C*H*$_2$), 1.29-1.35 (m, 6H, *E* & *Z* isomers, C*H*$_3$), these data match reported literature values[152]; ^{13}C NMR (75 MHz, CDCl$_3$) δ 167.5 (*C*=O), 164.6 (*C*=O), 151.9 (C=*C*H), 151.8 (C=*C*H), 138.6 (phenyl *C*), 138.3 (phenyl *C*), 130.0 (phenyl *C*H), 129.9 (phenyl *C*H), 125.7 (phenyl *C*H), 125.5 (phenyl *C*H), 117.9 (*C*N), 117.3 (phenyl *C*H), 117.2 (phenyl *C*H), 115.7 (*C*N), 77.2 (*C*-CN), 75.4 (*C*-CN), 61.2 (*C*H$_2$), 14.4 (*C*H$_3$), 14.3 (*C*H$_3$); IR (KBr) 3441 (NH), 2211 (CN) cm^{-1}; LC/TOF-MS

calcd for $C_{12}H_{13}N_2O_2$ 217.0972, found 217.0975 (M+H$^+$); Anal. (%) calcd for $C_{12}H_{12}N_2O_2$ C, 66.64; H, 5.60; N, 12.96; found C, 66.49; H, 5.68; N, 12.92.

Ethyl 2-cyano-3-((2-fluoro)phenylamino)acrylate (3.2)
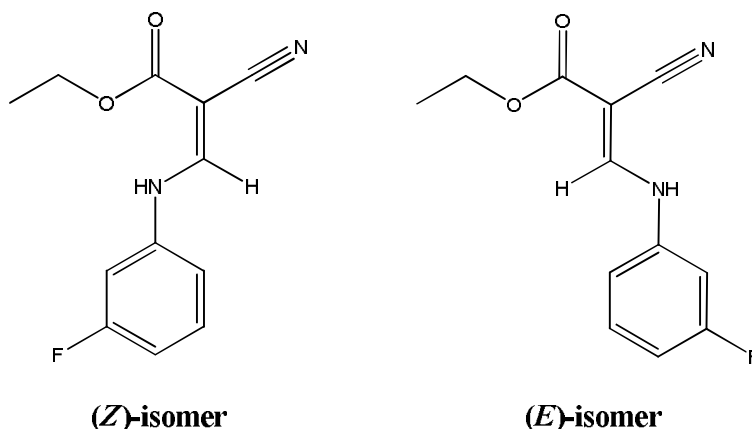
(*Z*)-isomer   (*E*)-isomer

White solid (9.17 g, 78%), 1.08:1.00 mixture of isomers; m.p. 87-90 ^{o}C; ^{1}H NMR (300 MHz, CDCl$_3$) δ 10.76 (d, J = 13.2 Hz, 1H, NH), 8.91 (d, J = 14.5 Hz, 1H, NH), 8.36 (d, J = 14.5 Hz, 1H, C=CH), 7.90 (d, J = 13.2 Hz, 1H, C=CH), 7.28-7.39 (m, 2H, *E* & *Z* isomers, phenyl CH), 6.81-7.01 (m, 6H, *E* & *Z* isomers, phenyl CH), 4.30 (app q, J = 7.1 Hz, 4H, *E* & *Z* isomers, CH_2), 1.32-1.38 (m, J = 7.1 Hz, 6H, *E* & *Z* isomers, CH_3); ^{13}C NMR (75 MHz, CDCl$_3$) δ 167.2 (C=O), 164.3 (C=O), 163.5 (d, ^1J = 246.5 Hz, CF) 163.4 (d, ^1J = 245.9 Hz, CF), 151.7 (C=CH), 151.7 (C=CH), 140.5 (d, ^3J = 10.1 Hz, phenyl C), 139.8 (d, ^3J = 10.0 Hz, phenyl C), 131.4 (d, ^3J = 9.4 Hz, phenyl CH), 131.1 (d, ^3J = 9.4 Hz, phenyl CH), 117.4 (CN), 115.5 (CN), 112.8 (d, ^4J = 3.0 Hz, phenyl CH), 112.7 (d, ^4J = 3.0 Hz, phenyl CH), 112.3 (d, ^2J = 21.8 Hz, phenyl CH), 112.0 (d, ^2J = 21.8 Hz, phenyl CH), 104.7 (app t, J = 26.3 Hz, 2 x phenyl CH), 77.4 (C-CN), 76.3 (C-CN), 61.3 (CH$_2$), 61.2 (CH$_2$), 14.2 (CH$_3$), 14.1 (CH$_3$); ^{19}F NMR (282 MHz, CDCl$_3$) δ -109.7, -109.8 (*E* & *Z* isomers, phenyl-F); IR (KBr) 3440 (NH), 2982, 2217 (CN) cm^{-1}; LC/TOF-MS calcd for $C_{12}H_{12}FN_2O_2$ 235.0877, found 235.0887 (M+H$^+$).

General procedure for the synthesis of 3.3 and 3.4

Diethyl (ethoxymethylene)malonate (25 mmol) and the appropriate aniline (25 mmol) were dissolved in EtOH (12.5 mL) and heated to reflux for 1 hour. The reaction mixture was allowed to cool to room temperature. The solvent was removed under reduced pressure and the resulting oil was cooled on ice to give the solid product. The product was collected by filtration and washed with ice-cold EtOH. In each case, the crude product was used for the next step without further purification.

Diethyl 2-((phenylamino)methylene)malonate (3.3)
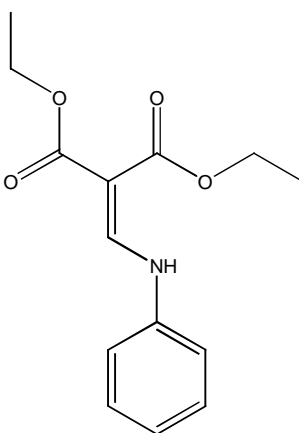
White solid (5.25 g, 80%); m.p. 34-38 °C; ^{1}H NMR (300 MHz, CDCl$_3$) δ 11.01 (d, J = 13.7 Hz, 1H, NH), 8.54 (d, J = 13.7 Hz, 1H, C=CH), 7.35-7.40 (m, 2H, phenyl CH), 7.12-7.17 (m, 3H, phenyl CH), 4.31 (q, J = 7.1 Hz, 2H, CH_2), 4.25 (q, J = 7.1 Hz, 2H, CH_2), 1.38 (t, J = 7.1 Hz, 3H, CH_3), 1.33 (t, J = 7.1 Hz, 3H, CH_3); ^{13}C NMR (75 MHz, CDCl$_3$) δ 169.1 (C=O), 165.7 (C=O), 151.9 (C=CH), 139.3 (phenyl C), 129.8 (phenyl CH), 124.9 (phenyl CH), 117.2 (phenyl CH), 93.5 (C(CO$_2$Et)$_2$), 60.4 (CH$_2$), 60.1 (CH$_2$), 14.4 (CH$_3$), 14.3 (CH$_3$), these data match reported literature values[153]; IR (KBr) 3445 (NH), 2988 (CH), 1692 (C=O) cm^{-1}; LC/TOF-MS calcd for C$_{14}$H$_{18}$NO$_4$ 264.1230, found 264.1234 (M+H$^+$).

Diethyl 2-(((3-fluorophenyl)amino)methylene)malonate (3.4)
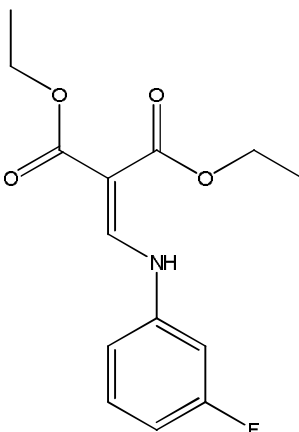
White solid (5.79 g, 82%); m.p. 33-37 °C; ^{1}H NMR (300 MHz, CDCl$_3$) δ 11.02 (d, *J* = 13.5 Hz, 1H, N*H*), 8.48 (d, *J* = 13.5 Hz, 1H, C=C*H*), 7.31-7.38 (m, 1H, phenyl C*H*), 6.83-6.94 (m, 3H, phenyl C*H*), 4.33-4.23 (m, *J* = 7.1 Hz, 4H, C*H*$_2$), 1.40 (t, *J* = 7.1 Hz, 3H, C*H*$_3$), 1.35 (t, *J* = 7.1 Hz, 3H, C*H*$_3$), these data match reported literature values[154]; ^{13}C NMR (75 MHz, CDCl$_3$) δ 168.4 (*C*=O), 165.0 (*C*=O), 163.2 (d, ^1J = 245.3 Hz, *C*F), 150.8 (C=*C*H), 140.6 (d, ^3J = 10.5 Hz, phenyl *C*), 130.8 (d, ^3J = 9.8 Hz, phenyl *C*H), 112.4 (d, ^4J = 2.3 Hz, phenyl *C*H), 110.0 (d, ^2J = 21.0 Hz, phenyl *C*H), 103.9 (d, ^2J = 25.5 Hz, phenyl *C*H), 94.2 (*C*(CO$_2$Et)$_2$), 60.1 (*C*H$_2$), 59.8 (*C*H$_2$), 14.0 (*C*H$_3$), 13.8 (*C*H$_3$); ^{19}F NMR (282 MHz, CDCl$_3$) δ -110.5 (phenyl-*F*); IR (KBr) 2985 (NH), 1689 (C=O) cm^{-1}; LC/TOF-MS calcd for C$_{14}$H$_{17}$FNO$_4$ 282.1136, found 282.1145 (M+H$^+$).

General procedure for the synthesis of 3.5 and 3.6

Diphenyl ether (26 mL) was heated to 240 °C. The appropriate malonate (13.8 mmol) was added slowly to the hot diphenyl ether and the resulting solution was allowed to reflux for 4 hours. The reaction mixture was allowed to cool and petroleum ether 60-80 (130 mL) was added. The resulting precipitate was collected by filtration and washed with excess petroleum ether 60-80. In each case, the product was used in the next step without further purification.

4-Oxo-1,4-dihydroquinoline-3-carbonitrile (3.5)
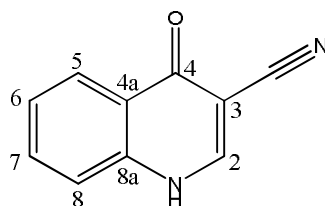
Yellow solid (1.66 g, 71%); m.p. dec; ^{1}H NMR (300 MHz, DMSO-d$_6$) δ 12.83 (br s, 1H, N*H*), 8.73 (d, *J* = 3.9 Hz, 1H, *H*2), 8.13 (dd, *J* = 8.1, 1.2 Hz, 1H, *H*5), 7.77 (app t, *J* = 8.3, 7.1, 1.2 Hz, 1H, *H*7), 7.63 (d, *J* = 8.3 Hz, 1H, *H*8), 7.46 (app t, *J* = 8.1, 7.1, 1.0 Hz, 1H, *H*6); ^{13}C NMR (75 MHz, DMSO-d$_6$) δ 174.4 (*C*=O), 146.6 (*C*2), 139.0 (*C*8a), 133.2 (*C*7), 125.5 (*C*6), 125.0 (*C*4a), 124.9 (*C*5), 119.2 (*C*8), 116.8 (*C*N), 93.5 (*C*3), these data match reported literature values[155]; IR (KBr) 3481 (NH), 2916, 2224 (CN), 1628 (C=O) cm^{-1}; LC/TOF-MS calcd for C$_{10}$H$_6$N$_2$ONa 193.0372, found 193.0378 (M+Na$^+$).

7-Fluoro-4-oxo-1,4-dihydroquinoline-3-carbonitrile (3.6a) and 5-fluoro-4-oxo-1,4-dihydroquinoline-3-carbonitrile (3.6b)
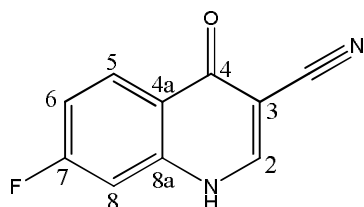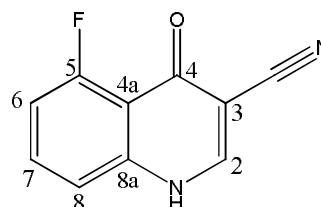
3.6a   **3.6b**

Yellow solid (1.61 g, 62%); 1.00:0.30 mixture of isomers; m.p. >300 °C; ^{1}H NMR (300 MHz, DMSO-d$_6$) δ 8.75 (s, 1H, H2), 8.68 (s, 1H, *H*2*), 8.18 (dd, *J* = 8.8, 6.3 Hz, 1H, *H*5), 7.69-7.76 (m, 1H, *H*7*), 7.30-7.43 (m, 3H, *H*6, *H*8, and *H*8*), 7.17 (dd, *J* = 11.8, 8.1 Hz, 1H, *H*6*), these data match reported literature values[156,157]; ^{13}C NMR (75 MHz, DMSO-d$_6$) δ 173.6 (*C*=O), 172.8 (d, ^3J = 2.3 Hz, *C*=O*), 164.3 (d, ^1J = 248.9, *C*F), 160.0 (d, ^1J = 259.9 Hz, *C*F*), 147.5 (*C*2), 146.5 (*C*2*), 141.3 (d, ^3J = 4.5 Hz, *C*8a*), 140.8 (d, ^3J = 12.9 Hz, *C*8a), 133.9 (d, ^3J = 9.9 Hz, *C*7*), 128.4 (d, ^3J = 11.3 Hz, *C*5), 122.1 (d, ^4J = 1.5 Hz, *C*4a), 116.5 (*C*N), 116.4 (*C*N*), 115.2 (d, ^4J = 4.5 Hz, *C*8*), 114.9 (d, ^2J = 9.8 Hz, *C*4a*), 114.1 (d, ^2J = 23.3 Hz, *C*6), 111.6 (d,

158

^2J = 22.5 Hz, $C6^*$), 104.8 (d, ^2J = 24.8 Hz, $C8$), 95.3 (C-CN*), 93.9 (C-CN); ^{19}F NMR (282 MHz, DMSO-d$_6$) δ -105.0 (C7-F), 112.2 (C7-F); IR (KBr) 2228 (CN), 1631 (C=O) cm^{-1}; LC/TOF-MS calcd for $C_{10}H_5FN_2OK$ 227.0017, found 227.0025 (M+H$^+$).

* 5-Fluoro-4-oxo-1,4-dihydroquinoline-3-carbonitrile (**3.6b**)

General procedure for the synthesis of 3.7 and 3.8

Diphenyl ether (4 mL) was heated to 240 ^{o}C. The appropriate acrylate (3.5 mmol) was added slowly to the hot diphenyl ether and the resulting solution was allowed to reflux for 1 hour. The reaction mixture was allowed to cool and petroleum ether 60-80 (20 mL) was added. The resulting precipitate was collected by filtration and washed with excess petroleum ether 60-80. In each case, the product was used in the next step without further purification.

Ethyl 4-oxo-1,4-dihydroquinoline-3-carboxylate (3.7)
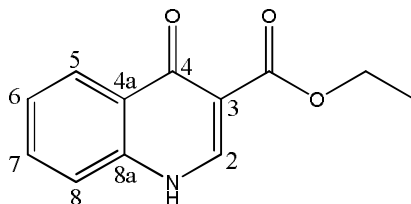
White solid (0.55 g, 72%); m.p. 252-256 ^{o}C; ^{1}H NMR (300 MHz, DMSO-d$_6$) δ 12.31 (br s, 1H, NH), 8.54 (s, 1H, H2), 8.16 (d, J = 8.1 Hz, 1H, H5), 7.70 (app t, 1H, H7), 7.61 (d, J = 7.8 Hz, 1H, H8), 7.41 (app t, 1H, H6), 4.22 (q, J = 7.1 Hz, 2H, CH_2), 1.28 (t, J = 7.1 Hz, 3H, CH_3); ^{13}C NMR (75 MHz, DMSO-d$_6$) δ 173.4 (C=O), 164.8 (C=O), 144.8 (C2), 138.9 (C8a), 132.4 (C7), 127.2 (C4a), 125.6 (C5), 124.6 (C6), 118.8 (C8), 109.8 (C3), 59.5 (CH$_2$), 14.3 (CH$_3$), these data match reported literature values[155]; IR (KBr) 3438 (NH), 2978 (CH), 1698 (C=O) cm^{-1}; LC/TOF-MS calcd for $C_{12}H_{11}NO_3Na$ 240.0631, found 240.0635 (M+Na$^+$).

Ethyl 7-fluoro-4-oxo-1,4-dihydroquinoline-3-carboxylate (3.8a) and ethyl 5-fluoro-4-oxo-1,4-dihydroquinoline-3-carboxylate (3.8b)

3.8a   **3.8b**
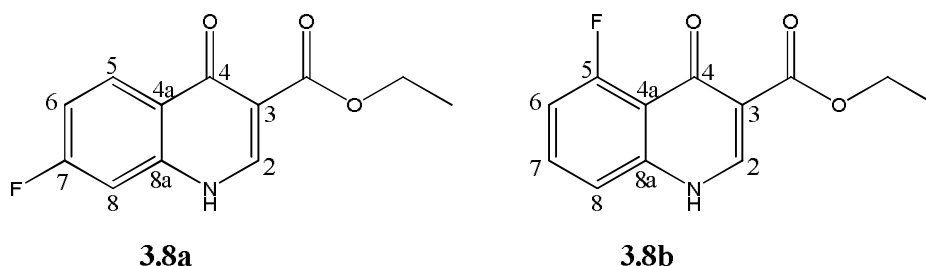
White solid (0.45 g, 55%); 1.00:0.08 mixture of isomers; m.p. dec.

The product showed improved solubility in DMSO-d_6 at 60 ^{o}C and hence the data were recorded at 60 ^{o}C.

^{1}H NMR (300 MHz, DMSO-d_6, 60 ^{o}C) δ 8.52 (s, 1H, *H*2), 8.40 (s, 1H, **H*2), 8.22 (dd, *J* = 9.1, 6.1 Hz, 1H, *H*5), 7.61-7.68 (m, 1H, *C*H*), 7.37 (dd, *J* = 9.3, 2.7 Hz, 1H, *H*8), 7.40-7.42 (m, 1H, *C*H*), 7.21-7.27 (m, 1H, *H*6), 7.03-7.10 (m, 1H, *C*H*), 4.24 (q, *J* = 7.1 Hz, 2H, C*H*$_2$), 1.30 (t, *J* = 7.1 Hz, 3H, C*H*$_3$), these data match reported literature values[126, 154]; ^{13}C NMR (75 MHz, DMSO-d_6, 60 ^{o}C) δ 172.7 (*C*=O), 164.6 (*C*=O), 164.1 (d, ^1J = 248.3, *C*F), 145.2 (*C*2), 140.6 (d, ^3J = 12.8 Hz, *C*8a), 129.0 (d, ^3J = 10.5 Hz, *C*5), 124.3 (*C*4a), 113.1 (d, ^2J = 22.5 Hz, *C*6), 110.6 (*C*3), 104.2 (d, ^2J = 24.8, *C*8), 59.6 (*C*H$_2$), 14.2 (*C*H$_3$), the peaks representing the second *isomer could not be observed in the ^{13}C NMR spectrum; ^{19}F NMR (282 MHz, DMSO-d_6, 60 ^{o}C) δ -107.6, -112.9 (C7-*F*); IR (KBr) 3435 (NH), 3114, 2981 (CH), 1695 (C=O) cm^{-1}; LC/TOF-MS calcd for $C_{12}H_{11}FNO_3$ 236.0717, found 236.0725 (M + H$^+$).

* 5-Fluoro-4-oxo-1,4-dihydroquinoline-3-carboxylate (**3.8b**)

The synthesis of 1-ethyl-4-oxo-1,4-dihydroquinoline-3-carbonitrile (3.9)
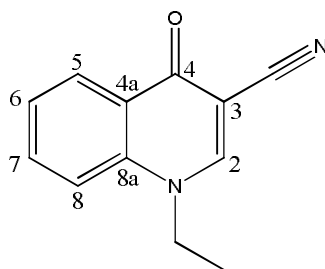
Method A:

Quinolone **3.5** (0.50 g, 2.94 mmol) and K_2CO_3 (0.41 g, 2.96 mmol) were heated to reflux in triethyl phosphate (2.65 mL) for 1 hour. The reaction mixture was allowed to cool to room temperature and was added to deionised water (14.7 mL). The resulting precipitate was collected by filtration and purified by precipitation from hot DCM with n-hexane.

Method B:

The quinolone **3.5** (0.50 g, 2.94 mmol) was dissolved in anhydrous DMF (14.5 mL) under nitrogen. Iodoethane (355 μL, 4.41 mmol) and K_2CO_3 (1.22 g, 8.82 mmol) were added to the solution and the reaction mixture was heated to 80 °C for 3 hours. The solvent was removed under reduced pressure. Distilled water was added to the remaining residue and the solid product was collected by filtration. The product was purified by precipitation from hot DCM with n-hexane.

Brown solid (method A: 0.26 g, 45%, method B: 0.42 g, 72%); m.p. 227-230 °C (226 °C)[123]; ^{1}H NMR (300 MHz, DMSO-d$_6$) δ 8.86 (s, 1H, *H*2), 8.22 (d, *J* = 7.6 Hz, 1H, *H*5), 7.82-7.89 (m, 2H, *H*7 & *H*8), 7.51-7.58 (m, 1H, *H*6), 4.40 (q, *J* = 7.1 Hz, 2H, C*H*$_2$), 1.39 (t, *J* = 7.1 Hz, 3H, C*H*$_3$); ^{13}C NMR (75 MHz, DMSO-d$_6$) δ 173.8 (*C*=O), 150.4 (*C*2), 138.6 (*C*8a), 133.6 (*C*7), 126.1 (*C*4a), 125.8 (*C*5), 125.6 (*C*6), 117.6 (*C*8), 116.5 (*C*N), 93.5 (*C*3), 48.3 (*C*H$_2$), 14.2 (*C*H$_3$); IR (KBr) 2219 (CN), 1615 (C=O) cm^{-1}; LC/TOF-MS calcd for $C_{12}H_{11}N_2O$ 199.0866, found 199.0868 (M+H$^+$).

General procedure for the synthesis of 3.10-3.12

The appropriate quinolone (2.94 mmol) was dissolved in anhydrous DMF (14.5 mL) under nitrogen. Iodoethane (355 µL, 4.41 mmol) and K_2CO_3 (1.22 g, 8.82 mmol) were added to the solution and the reaction mixture was heated to 80 °C for 3 hours. The solvent was removed under reduced pressure and the remaining residue was dissolved in $CHCl_3$ and filtered. The filtrate was reduced under vacuum and the product was purified by column chromatography on silica gel. The product was eluted with EtOAc:EtOH (90:10).

1-Ethyl-7-fluoro-4-oxo-1,4-dihydroquinoline-3-carbonitrile (3.10a)
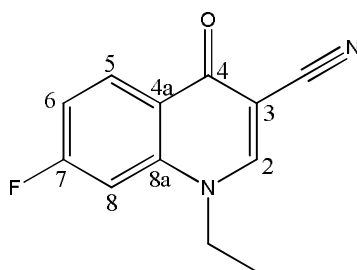
White solid (0.46 g, 72%); m.p. 230-234 °C; R_f: 0.75 (EtOAc:EtOH 90:10); ^{1}H NMR (300 MHz, DMSO-d_6) δ 8.88 (s, 1H, $H2$) 8.26 (dd, J = 8.7, 6.7 Hz, 1H, $H5$), 7.81 (d, J = 11.4 Hz, 1H, $H8$), 7.38-7.44 (m, 1H, $H6$), 4.34 (q, J = 7.1 Hz, 2H, CH_2), 1.37 (t, J = 7.1 Hz, 3H, CH_3), ^{1}H NMR assignments are supported by NOEdiff experiments; ^{13}C NMR (75 MHz, DMSO-d_6) δ 173.0 (C=O), 164.9 (d, ^1J = 248.8 Hz, CF), 151.2 ($C2$), 140.5 (d, ^3J = 12.5 Hz, $C8$a), 129.2 (d, ^3J = 10.9 Hz, $C5$), 123.0 (d, ^4J = 1.7 Hz, $C4$a), 116.1 (CN), 114.1 (d, ^2J = 23.3 Hz, $C6$), 104.2 (d, ^2J = 27.0 Hz, $C8$), 94.1 (C-CN), 48.5 (CH$_2$), 14.1 (CH$_3$); ^{19}F NMR (282 MHz, DMSO-d_6) δ -103.7 (C7-F); IR (KBr) 2226 (CN), 1642 (C=O) cm^{-1}; LC/TOF-MS calcd for $C_{12}H_{10}FN_2O$ 217.0772, found 217.0772 (M + H$^+$).

1-Ethyl-5-fluoro-4-oxo-1,4-dihydroquinoline-3-carbonitrile (3.10b)
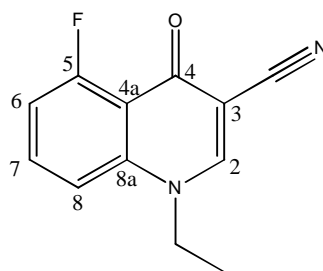
White solid (0.10 g, 15%); m.p. 210-212 $^{\circ}$C; R_f: 0.50 (EtOAc:EtOH 90:10); ^{1}H NMR (300 MHz, DMSO-d$_6$) δ 8.83 (s, 1H, *H*2), 7.79-7.86 (m, 1H, *H*7), 7.67 (d, *J* = 8.6 Hz, 1H, *H*8), 7.27 (dd, *J* = 11.6, 8.2 Hz, 1H, *H*6), 4.34 (q, *J* = 7.1 Hz, 2H, C*H$_2$*), 1.37 (t, *J* = 7.1 Hz, 3H, C*H$_3$*), ^{1}H NMR assignments are supported by NOEdiff experiments; ^{13}C NMR (75 MHz, DMSO-d$_6$) δ 172.4 (d, ^{3}J = 1.8 Hz, *C*=O) 160.7 (d, ^{1}J = 260.8 Hz, *C*F), 150.4 (*C*2), 140.7 (d, ^{4}J = 3.2 Hz, *C*8a), 134.3 (d, ^{3}J = 11.0 Hz, *C*7), 116.1 (*C*N), 115.9 (d, ^{2}J = 8.0 Hz, *C*4a), 113.6 (d, ^{3}J = 4.5 Hz, *C*8), 112.2 (d, ^{2}J = 20.7 Hz, *C*6), 95.5 (*C*3), 49.1 (*C*H$_2$), 14.0 (*C*H$_3$); ^{19}F NMR (282 MHz, DMSO-d$_6$) δ -111.2 (C5-*F*); IR (KBr) 2223 (CN), 1633 (C=O) cm^{-1}; LC/TOF-MS calcd for C$_{12}$H$_{10}$FN$_2$O 217.0772, found 217.0782 (M + H^{+}).

Ethyl 1-ethyl-4-oxo-1,4-dihydroquinoline-3-carboxylate (3.11a)
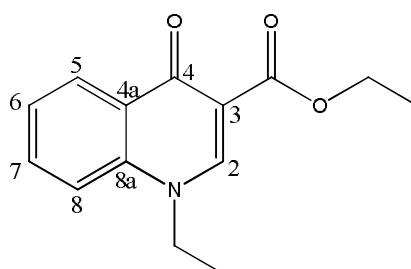
White solid (0.55 g, 76%); m.p. 61-64 $^{\circ}$C; R_f: 0.49 (EtOAc:EtOH 90:10); ^{1}H NMR (300 MHz, DMSO-d$_6$) δ 8.70 (s, 1H, *H*2), 8.24 (d, *J* = 8.0 Hz, 1H, *H*5), 7.73-7.81 (m, 2H, *H*7 and *H*8), 7.43-7.49 (m, 1H, *H*6), 4.41 (q, *J* = 7.0 Hz, 2H, C*H$_2$*), 4.22 (q, *J* = 7.1 Hz, 2H, C*H$_2$*), 1.36 (t, *J* = 7.0 Hz, 3H, C*H$_3$*), 1.28 (t, *J* = 7.1 Hz, 3H, C*H$_3$*), ^{1}H NMR assignments are supported by NOEdiff experiments; ^{13}C NMR (75 MHz, DMSO-d$_6$) δ 172.7 (*C*=O), 164.6 (*C*=O), 148.9 (*C*2), 138.5 (*C*8a), 132.6 (*C*7), 128.3 (*C*4a), 126.4 (*C*5), 124.7 (*C*6), 117.1 (*C*8), 109.9 (*C*3), 59.6 (*C*H$_2$), 47.8 (*C*H$_2$), 14.3

(2 x CH_3), these data match reported literature values[155]; IR (KBr) 2971 (CH), 1719 (C=O) cm^{-1}; LC/TOF-MS calcd for C$_{14}$H$_{16}$NO$_3$ 246.1125, found 246.1136 (M + H$^+$).

Ethyl 4-ethoxy-1,4-dihydroquinoline-3-carboxylate (3.11b)
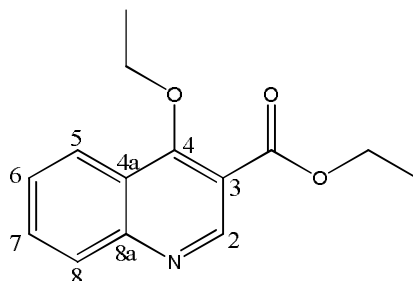
Clear oil (0.40 g, 5%); R$_f$: 0.85 (EtOAc:EtOH 90:10); ^{1}H NMR (300 MHz, CDCl$_3$) δ 9.18 (s, 1H, *H*2), 8.26 (app d, *J* = 8.3 Hz, 1H, *H*5), 8.07 (d, *J* = 8.5 Hz, 1H, H8), 7.74-7.79 (m, *J* = 8.5, 6.9, 1.5 Hz, 1H, *H*7), 7.54-7.59 (m, *J* = 8.3, 6.9, 1.3 Hz, 1H, *H*6), 4.45 (q, *J* = 7.1 Hz, 2H, C*H*$_2$), 4.32 (q, *J* = 6.8 Hz, 2H, C*H*$_2$), 1.52 (t, *J* = 6.8 Hz, 3H, C*H*$_3$), 1.44 (t, *J* = 7.1 Hz, 3H, C*H*$_3$), ^{1}H NMR assignments are supported by NOEdiff experiments; ^{13}C NMR (75 MHz, CDCl$_3$) δ 165.3 (*C*=O), 164.2 (*C*-O), 152.1 (*C*2), 151.0 (*C*8a), 131.6 (*C*7), 129.3 (*C*8), 126.8 (*C*6), 123.9 (*C*4a), 123.4 (*C*5), 114.2 (*C*3), 72.3 (*C*H$_2$), 61.5(*C*H$_2$), 15.8 (*C*H$_3$), 14.3 (*C*H$_3$); IR (neat film on NaCl plate) 2982 (CH), 1722 (C=O) cm^{-1}; LC/TOF-MS calcd for C$_{14}$H$_{16}$NO$_3$ 246.1125, found 246.1127 (M + H$^+$).

Ethyl 4-ethoxy-7-fluoroquinoline-3-carboxylate (3.12a)
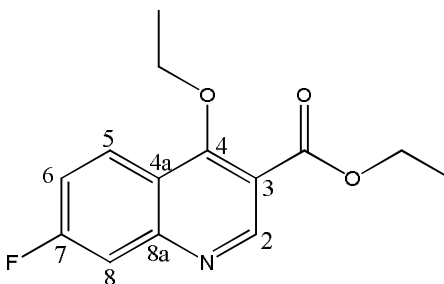
White solid (0.08 g, 10%); m.p. 31-33 ^{o}C; R$_f$: 0.88 (EtOAc:EtOH 90:10); ^{1}H NMR (300 MHz, CDCl$_3$) δ 9.16 (s, 1H, *H*2), 8.28 (dd, *J* = 9.2, 6.1 Hz, 1H, *H*5), 7.68 (dd, *J* = 9.9, 2.4 Hz, 1H, *H*8), 7.29-7.36 (m, 1H, *H*6), 4.45 (q, *J* = 7.1 Hz, 2H, C*H*$_2$), 4.32 (q, *J* = 7.0 Hz, 2H, C*H*$_2$), 1.51 (t, *J* = 7.0 Hz, 3H, C*H*$_3$), 1.43 (t, *J* = 7.1 Hz, 3H,

CH_3), ^{1}H NMR data is supported by NOEdiff experiments; ^{13}C NMR (75 MHz, CDCl$_3$) δ 165.1 (*C*=O), 164.5 (d, ^1J = 250.5 Hz, *C*F), 164.1 (*C*-O), 153.5 (*C*2), 152.3 (d, ^3J = 12.0 Hz, *C*8a), 126.0 (d, ^3J = 10.8 Hz, *C*5), 120.8 (d, ^4J = 1.13 Hz, *C*4a), 117.1 (d, ^2J = 24.7 Hz, *C*6), 113.6 (d, *J* = 2.5 Hz, *C*3), 113.2 (d, ^2J = 20.0 Hz, *C*8), 72.4 (CH_2), 61.5 (CH_2), 15.7 (CH_3), 14.3 (CH_3); ^{19}F NMR (282 MHz, CDCl$_3$) δ -106.5 (C7-*F*); IR (KBr) 2982 (CH), 1727 (C=O) cm^{-1}; LC/TOF-MS calcd for C$_{14}$H$_{15}$FNO$_3$ 264.103, found 264.1038 (M + H$^+$).

Ethyl 1-ethyl-7-fluoro-4-oxo-1,4-dihydroquinoline-3-carboxylate (3.12b)
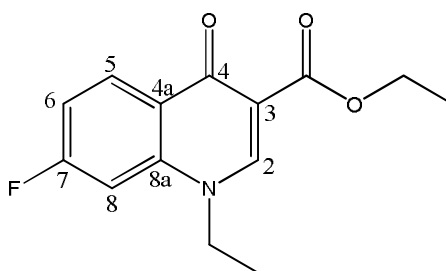
White solid (0.56 g, 73%); m.p. 126-130 $^{\circ}$C (lit 128-129 $^{\circ}$C)[126]; R$_f$: 0.55 (EtOAc:EtOH 90:10); ^{1}H NMR (300 MHz, DMSO-d$_6$) δ 8.69 (s, 1H, *H*2), 8.29 (dd, *J* = 8.9, 6.7 Hz, 1H, *H*5), 7.72 (d, *J* = 11.3, 2.2 Hz, 1H, *H*8), 7.34 (app t, *J* = 2.2 Hz, 1H, *H*6), 4.38 (q, *J* = 7.1 Hz, 2H, CH_2), 4.23 (q, *J* = 7.1 Hz, 2H, CH_2), 1.35 (t, *J* = 7.1 Hz, 3H, CH_3), 1.28 (t, *J* = 7.1 Hz, 3H, CH_3), ^{1}H NMR assignments are supported by NOEdiff experiments; ^{13}C NMR (75 MHz, DMSO-d$_6$) δ 172.1 (*C*=O), 164.6 (d, ^1J = 246.8 Hz, *C*F), 164.4 (*C*=O), 149.5 (*C*2), 140.3 (d, ^3J = 12.0 Hz, *C*8a), 129.6 (d, ^3J = 11.3 Hz, *C*5), 125.2 (d, ^4J = 2.25 Hz, *C*4a), 113.2 (d, ^2J = 22.5 Hz, *C*6), 110.5 (*C*3), 103.5 (d, ^2J = 27.0 Hz, *C*8), 59.8 (CH_2), 48.0 (CH_2), 14.3 (CH_3), 14.2 (CH_3); ^{19}F NMR (282 MHz, DMSO-d$_6$) δ -105.6 (C7-*F*); IR (KBr) 2982 (CH), 1679 (C=O) cm^{-1}; LC/TOF-MS calcd for C$_{14}$H$_{15}$FNO$_3$ 264.1030, found 264.1043 (M + H$^+$).

Ethyl 1-ethyl-5-fluoro-4-oxo-1,4-dihydroquinoline-3-carboxylate (3.12c)
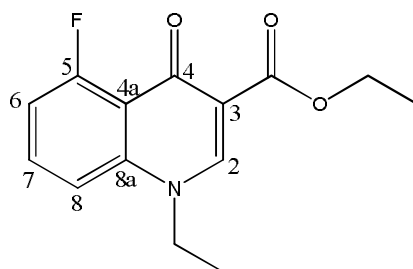
White solid (0.03 g, 3%); m.p. 108-112 $^{\circ}$C (lit 115-118 $^{\circ}$C)[126]; R$_f$: 0.38 (EtOAc:EtOH 90:10); ^{1}H NMR (300 MHz, CDCl$_3$) δ 8.39 (s, 1H, *H*2), 7.54-7.62 (m, *J* = 13.7, 8.4 Hz, 1H, *H*7), 7.20 (d, *J* = 8.4 Hz, 1H, *H*8), 7.03 (dd, *J* = 11.2, 8.4 Hz, 1H, *H*6), 4.37 (q, *J* = 7.1 Hz, 2H, C*H*$_2$), 4.21 (q, *J* = 7.2 Hz, 2H, C*H*$_2$), 1.52 (t, *J* = 7.2 Hz, 3H, C*H*$_3$), 1.39 (t, *J* = 7.1 Hz, 3H, C*H*$_3$), ^{1}H NMR assignments are supported by NOEdiff experiments; ^{13}C NMR (75 MHz, CDCl$_3$) δ 173.3 (d, ^{3}J = 2.3 Hz, *C*=O), 165.8 (*C*=O), 163.0 (d, ^{1}J = 264.8 Hz, *C*F), 148.2 (*C*2), 140.8 (d, ^{3}J = 3.0 Hz, *C*8a), 132.9 (d, ^{3}J = 11.0 Hz, *C*7), 119.1 (d, ^{2}J = 6.9 Hz, *C*4a), 112.8 (*C*3), 112.1 (d, ^{2}J = 21.8 Hz, *C*6), 111.2 (d, ^{4}J = 4.7 Hz, *C*8), 61.0 (*C*H$_2$), 49.5 (*C*H$_2$), 14.4 (*C*H$_3$), 14.2 (*C*H$_3$); ^{19}F NMR (282 MHz, CDCl$_3$) δ -109.4 (C5-*F*); IR (KBr) 2972 (CH), 1720 (C=O) cm^{-1}; LC/TOF-MS calcd for C$_{14}$H$_{15}$FNO$_3$ 264.1030, found 264.1032 (M + H^{+}).

The synthesis 1-ethyl-4-oxo-1,4-dihydroquinoline-3-carboxylic acid (3.13)
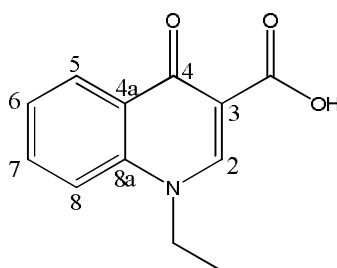
Compound 3.11a (0.25 g, 1.01 mmol) was added to 3.0 mL of a 1:1 water:methanolic KOH (20%) solution and brought to reflux for 3 hours. The MeOH was removed under reduced pressure. Distilled water (5 mL) was added to the remaining residue and the solution was acidified to pH 6 with conc. HCl. The resulting precipitate was collected by filtration and washed with distilled water.

166

White solid (0.21 g, 95%); m.p. 246-248 $^{\circ}$C; ^{1}H NMR (300 MHz, DMSO-d_6) δ 15.27 (s, 1H, O*H*), 9.08 (s, 1H, *H*2), 8.40 (d, *J* = 8.1 Hz, 1H, *H*5), 8.07 (d, *J* = 8.6 Hz, 1H, *H*8), 7.96-8.01 (m, 2H, *H*7), 7.65-7.71 (app t, 1H, *H*6), 4.62 (q, *J* = 7.1 Hz, 2H, C*H*$_2$), 1.43 (t, *J* = 7.1 Hz, 3H, C*H*$_3$); ^{13}C NMR (75 MHz, DMSO-d_6) δ 177.6 (*C*=O), 166.0 (*C*=O), 149.1 (*C*2), 139.0 (*C*8a), 134.3 (*C*7), 126.2 (*C*6), 125.9 (*C*5), 125.5 (*C*4a), 118.0 (*C*8), 107.6 (*C*3), 48.9 (*C*H$_2$), 14.5 (*C*H$_3$), these data match reported literature values[155]; IR (KBr) 1712 (C=O) cm^{-1}; LC/TOF-MS calcd for $C_{12}H_{12}NO_3$ 218.0812, found 218.0811 (M + H$^+$).

The synthesis of 1-ethyl-7-fluoro-4-oxo-1,4-dihydroquinoline-3-carboxylic acid (3.14)
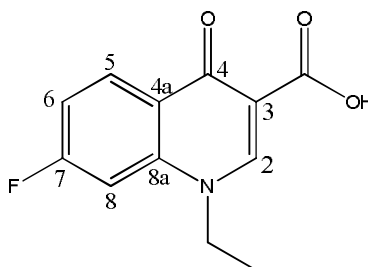
Compound **3.12b** (0.26 g, 1.00 mmol) was dissolved in a 1:1 water:dioxane (8.60 mL) solution. Lithium hydroxide (0.08 g, 3.34 mmol) was added to the solution and the reaction mixture was stirred at 50 $^{\circ}$C for 30 minutes. The solvent was removed under reduced pressure and distilled water (5 mL) was added to the resulting residue. The solution was acidified to pH 6 with 6M HCl. The resulting precipitate was collected by filtration and washed with distilled water.

White solid (0.20 g, 83%); m.p. >300 $^{\circ}$C (lit 302-304 $^{\circ}$C)[158].

The product showed improved solubility in DMSO-d_6 at 60 $^{\circ}$C and hence the data were recorded at 60 $^{\circ}$C.

^{1}H NMR (300 MHz, DMSO-d_6, 60 $^{\circ}$C) δ 14.92 (br s, 1H, O*H*), 9.01 (s, 1H, *H*2), 8.46 (dd, *J* = 9.0, 6.5 Hz, 1H, *H*5), 7.91 (dd, *J* = 11.2, 2.2 Hz, 1H, *H*8), 7.52 (app t, *J* = 2.2 Hz, 1H, *H*6), 4.56 (q, *J* = 7.1 Hz, 2H, C*H*$_2$), 1.43 (t, *J* = 7.1 Hz, 3H, C*H*$_3$); ^{13}C NMR (75 MHz, DMSO-d_6, 60 $^{\circ}$C) δ 176.8 (*C*=O), 165.3 (*C*=O), 165.1 (d, ^{1}J = 250.5

Hz, *C*F), 149.4 (*C*2), 140.7 (d, ^3J = 12.2 Hz, *C*8a), 129.0 (d, ^3J = 11.0 Hz, *C*5), 122.4 (d, ^4J = 1.4 Hz, *C*4a), 114.6 (d, ^2J = 23.6 Hz, *C*6), 108.0 (*C*3), 104.0 (d, ^2J = 27.1 Hz, *C*8), 48.8 (*C*H$_2$), 14.0 (*C*H$_3$); ^{19}F NMR (282 MHz, DMSO-d$_6$, 60 ^{o}C) δ -102.6 (C7-F); IR (KBr) 1722 (C=O) cm^{-1}; LC/TOF-MS calcd for C$_{12}$H$_{11}$FNO$_3$ 236.0717, found 236.0728 (M + H$^+$).

The synthesis of 1-ethyl-7-methoxy-4-oxo-1,4-dihydroquinoline-3-carboxylic acid (3.15)
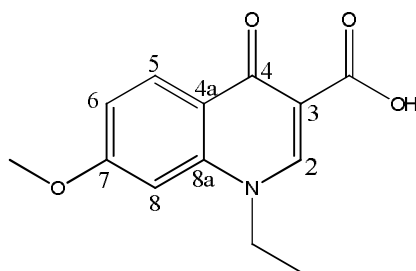
Compound **3.12b** (0.26 g, 1.01 mmol) was added to 3.0 mL of a 1:1 water:methanolic KOH (20% w/v) solution and brought to reflux for 3 hours. The MeOH was removed under reduced pressure. Distilled water (5 mL) was added to the remaining residue and the solution was acidified to pH 6 with conc. HCl. The resulting precipitate was collected by filtration and washed with distilled water.

White solid (0.22 g, 88%); m.p. 258-262 ^{o}C; ^{1}H NMR (300 MHz, DMSO-d$_6$) δ 8.98 (s, 1H, *H*2), 8.29 (d, *J* = 8.9 Hz, 1H, *H*5), 7.25-7.30 (m, 2H, *H*6 and *H*8), 4.59 (q, *J* = 7.1 Hz, 2H, C*H*$_2$), 3.99 (s, 3H, OC*H*$_3$), 1.42 (t, *J* = 7.1 Hz, 3H, C*H*$_3$), these data match reported literature values[128]; ^{13}C NMR (75 MHz, DMSO-d$_6$) δ 176.9 (*C*=O), 166.1 (*C*=O), 163.9 (*C*7), 149.0 (*C*2), 141.1 (*C*8a), 127.8 (*C*5), 119.3 (*C*4a), 115.7 (*C*6), 107.3 (*C*3), 99.9 (*C*8), 56.2 (O*C*H$_3$), 48.8 (*C*H$_2$), 14.3 (*C*H$_3$); IR (KBr) 2975 (CH), 1713 (C=O) cm^{-1}; LC/TOF-MS calcd for C$_{13}$H$_{13}$NO$_4$Na 270.0737, found 270.0744 (M + H$^+$).

General procedure for the synthesis of 7-piperazine and 7-N-methylpiperazine quinolones 3.16-3.19

Anhydrous piperazine or N-methylpiperazine (4.55 mmol) and the appropriate quinolone (0.50 mmol) were brought to reflux at 125 ^{o}C in anhydrous pyridine (1

mL) under nitrogen. After 16 hours the solvent was removed under reduced pressure and the resulting solid was recrystallised from cold EtOH. The product was collected by filtration.

1-Ethyl-4-oxo-7-(piperazin-1-yl)-1,4-dihydroquinoline-3-carbonitrile (3.16)
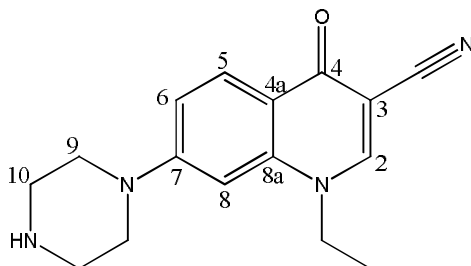
White solid (0.08 g, 57%); m.p. 226-230 °C; ^{1}H NMR (300 MHz, DMSO-d$_6$) δ 8.67 (s, 1H, *H*2), 7.99 (d, *J* = 9.6 Hz, 1H, *H*5), 7.16 (dd, *J* = 9.6, 2.2 Hz, 1H, *H*6), 6.82 (d, *J* = 2.2 Hz, 1H, *H*8), 4.32 (q, *J* = 7.7 Hz, 2H, C*H*$_2$), 3.32 (app br s, 4H, *H*9), 2.83-2.87 (m, 4H, *H*10), 1.36 (t, *J* = 7.7 Hz, 3H, C*H*$_3$); ^{13}C NMR (75 MHz, DMSO-d$_6$) δ 172.7 (*C*=O), 154.4 (*C*7), 150.0 (*C*2), 140.4 (*C*8a), 127.0 (*C*5), 117.3 (*C*4a), 116.8 (*C*N), 113.5 (*C*6), 98.3 (*C*8), 92.9 (*C*3), 47.8 (*C*H$_2$), 47.7 (*C*9), 45.2 (*C*10), 14.0 (*C*H$_3$); IR (KBr) 2215 (CN), 1620 (C=O) cm^{-1}; LC/TOF-MS calcd for C$_{16}$H$_{19}$N$_4$O 283.1553, found 283.1561 (M + H$^+$).

1-Ethyl-4-oxo-7-(piperazin-1-yl)-1,4-dihydroquinoline-3-carboxylic acid (3.17)
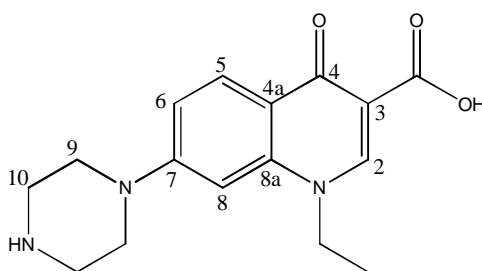
White solid (0.13 g, 86%); m.p. 236-240 °C (lit 272-275 °C)[159]; ^{1}H NMR (300 MHz, DMSO-d$_6$) δ 8.86 (s, 1H, *H*2), 8.12 (d, *J* = 9.3 Hz, 1H, *H*5), 7.31 (d, *J* = 9.3 Hz, 1H, *H*6), 6.92 (s, 1H, *H*8), 4.52 (q, *J* = 7.0 Hz, 2H, C*H*$_2$), 3.38-3.42 (m, 4H, *H*9), 2.85 (app br s, 4H, *H*10), 1.39 (t, *J* = 7.0 Hz, 3H, C*H*$_3$); ^{13}C NMR (75 MHz, DMSO-d$_6$) δ 176.3 (*C*=O), 166.6 (*C*=O), 154.8 (*C*7), 148.4 (*C*2), 141.1 (*C*8a), 127.0 (*C*5), 116.1

(*C*4a), 114.5 (*C*6), 106.7 (*C*3), 97.9 (*C*8), 48.5 (*C*H$_2$), 47.7 (*C*9), 45.3 (*C*10), 14.2 (*C*H$_3$); IR (KBr) 1620 (C=O) cm^{-1}; LC/TOF-MS calcd for C$_{16}$H$_{20}$N$_3$O$_3$ 302.1499, found 302.1510 (M + H$^+$).

1-Ethyl-7-(4-methylpiperazin-1-yl)-4-oxo-1,4-dihydroquinoline-3-carbonitrile (3.18)
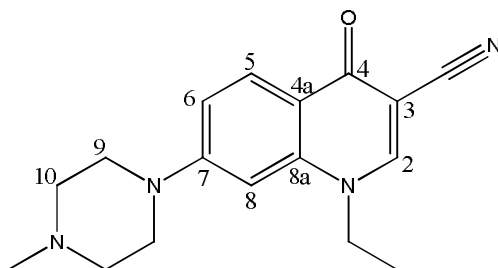
White solid (0.07 g, 47%); m.p. 222-225 °C; ^{1}H NMR (300 MHz, CDCl$_3$) δ 8.23 (d, *J* = 9.1 Hz, 1H, *H*5), 7.91 (s, 1H, *H*2), 7.01 (d, *J* = 9.1 Hz, 1H, *H*6), 6.57 (s, 1H, *H*8), 4.16 (q, *J* = 6.8 Hz, 2H, C*H*$_2$), 3.39 (app br s, 4H, *H*9), 2.57 (app br s, 4H, *H*10), 2.35 (s, 3H, N-C*H*$_3$), 1.52 (t, *J* = 6.8 Hz, 3H, C*H*$_3$); ^{13}C NMR (75 MHz, CDCl$_3$) δ 173.7 (*C*=O), 154.5 (*C*7), 147.6 (*C*2), 140.6 (*C*8a), 128.5 (*C*5), 118.6 (*C*4a), 116.1 (*C*N), 114.1 (*C*6), 98.0 (*C*8), 95.5 (*C*3), 54.6 (*C*10), 48.9 (*C*H$_2$), 47.4 (*C*9), 46.1 (N-C*H*$_3$), 14.3 (*C*H$_3$); IR (KBr) 2218 (CN), 1623 (C=O) cm^{-1}; LC/TOF-MS calcd for C$_{17}$H$_{21}$N$_4$O 297.1710, found 297.1721 (M + H$^+$).

1-Ethyl-7-(4-methylpiperazin-1-yl)-4-oxo-1,4-dihydroquinoline-3-carboxylic acid (3.19)
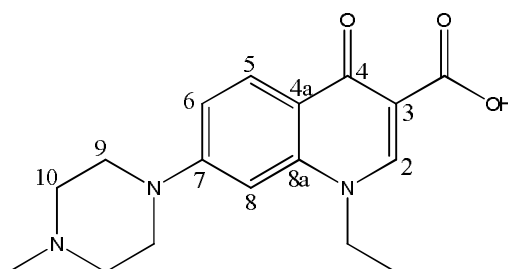
White solid (0.14 g, 87%); m.p. 207-210 °C (lit 220.5-222.5 °C)[159]; ^{1}H NMR (300 MHz, CDCl$_3$) δ 15.38 (br s, 1H, O*H*), 8.56 (s, 1H, *H*2), 8.24 (d, *J* = 9.2 Hz, 1H, *H*5), 7.09 (dd, *J* = 9.2, 2.0 Hz, 1H, *H*6), 6.63 (d, *J* = 2.0 Hz, 1H, *H*8), 4.25 (q, *J* = 7.2 Hz,

2H, CH_2), 3.44 (t, J = 5.1 Hz, 4H, H9), 2.58 (t, J = 5.1 Hz, 4H, H10), 2.35 (s, 3H, N-CH_3), 1.54 (t, J = 7.2 Hz, 3H, CH_3); ^{13}C NMR (75 MHz, CDCl$_3$) δ 177.4 (C=O), 167.7 (C=O), 154.8 (C7), 147.3 (C2), 141.3 (C8a), 128.3 (C5), 117.9 (C4a), 114.7 (C6), 108.3 (C3), 97.6 (C8), 54.6 (C10), 49.3 (CH_2), 47.4 (C9), 46.1 (N-CH$_3$), 14.4 (CH$_3$); IR (KBr) 1702 (C=O) cm^{-1}; LC/TOF-MS calcd for C$_{17}$H$_{22}$N$_3$O$_3$ 316.1656, found 316.1670 (M + H$^+$).

The synthesis of 1-ethyl-3-(1H-tetrazol-5-yl)quinolin-4(1H)-one (3.20)
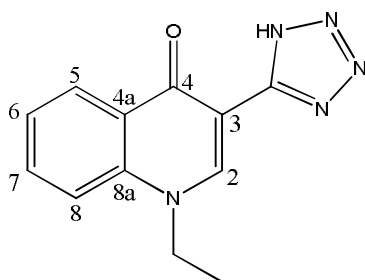
Method A:

Quinolone **3.9** (0.13 g, 0.65 mmol) and tributyltin azide (0.21 g, 0.65 mmol) were heated at 200 ^{o}C under nitrogen for 15 hours. The reaction mixture was allowed to cool to room temperature. MeOH (7.9 mL) and conc. HCl (80 μL) were added to the reaction mixture and it was brought to reflux for 2 hours. The solvent was removed under reduced pressure and n-hexane (20 mL) was added. The product was collected by filtration and washed with n-hexane (100 mL).

Method B:

Quinolone **3.9** (0.50 g, 2.50 mmol) was dissolved in anhydrous DMF (25 mL) under nitrogen. Sodium azide (1.79 g, 27.53 mmol), ammonium chloride (1.47 g, 27.50 mmol), and lithium chloride (0.38 g, 8.96 mmol) were added to the solution and the reaction mixture was heated to reflux at 110 ^{o}C for 27.5 hours. The reaction mixture was filtered and the filtrate was reduced in volume under vacuum. Distilled water was added to the resulting residue and the solution acidified with conc. HCl. The resulting precipitate was collected by filtration and washed with distilled water.

Light yellow solid (method A: 0.12 g, 75%, method B: 0.50 g, 83%); m.p. 284-288 °C; ^{1}H NMR (300 MHz, DMSO-d$_6$) δ 9.11 (s, 1H, H2), 8.40 (dd, *J* = 7.9, 1.5 Hz, 1H, *H*5), 7.94 (d, *J* = 8.4 Hz, 1H, *H*8), 7.87 (app t, *J* = 8.4, 6.8, 1.5 Hz, 1H, *H*7), 7.57 (app t, *J* = 7.9, 6.8, 1.0 Hz, 1H, *H*6), 4.55 (q, *J* = 7.1 Hz, 2H, C*H*$_2$), 1.43 (t, *J* = 7.1 Hz, 3H, C*H*$_3$); ^{13}C NMR (75 MHz, DMSO-d$_6$) δ 172.8 (*C*=O), 150.1 (*C*N$_4$), 144.9 (*C*2), 138.6 (*C*8a), 133.0 (*C*7), 126.5 (*C*4a), 126.0 (*C*5), 125.0 (*C*6), 117.4 (*C*8), 104.5 (*C*3), 48.1 (*C*H$_2$), 14.41 (*C*H$_3$); IR (KBr) 1628 (C=O) cm^{-1}; LC/TOF-MS calcd for C$_{12}$H$_{12}$N$_5$O 242.1036, found 242.1047 (M+H$^+$).

The synthesis of levofloxacin ethyl ester (3.24)
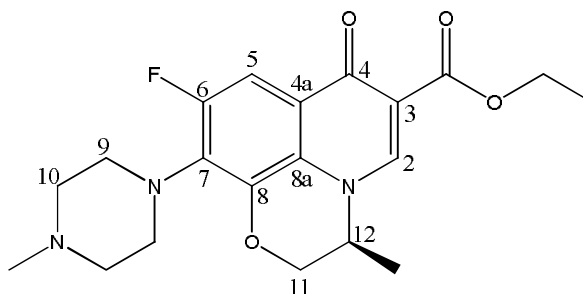
Levofloxacin (0.36 g, 1 mmol) was heated to reflux overnight in EtOH (30 mL) with conc. H$_2$SO$_4$ (3 mL). The reaction mixture was allowed to cool and the solvent volume reduced by half under vacuum. Distilled water (15 mL) was added and the solution neutralised with aqueous saturated K$_2$CO$_3$ and then washed with DCM (2 x 50 mL). The combined DCM extracts were washed with 2.5 M potassium hydroxide (2 x 25 mL). The organic phase was dried over Na$_2$SO$_4$, filtered, and the solvent removed under reduced pressure.

White solid (0.34 g, 87%); m.p. 223-225 °C; ^{1}H NMR (300 MHz, CDCl$_3$) δ 8.25 (s, 1H, *H*2), 7.61 (d, *J* = 13.4 Hz, 1H, *H*5), 4.27-4.40 (m, 5H, *H*11, *H*12 and C*H*$_2$CH$_3$), 3.26-3.39 (m, 4H, *H*9), 2.51-2.54 (m, 4H, *H*10), 2.34 (s, 3H, N-C*H*$_3$), 1.53 (d, *J* = 6.7 Hz, 3H, C*H*$_3$), 1.39 (t, *J* = 7.4 Hz, 3H, CH$_2$C*H*$_3$); ^{13}C NMR (75 MHz, CDCl$_3$) δ 172.8 (*C*=O), 165.6 (*C*=O), 155.7 (d, ^1J = 245.5 Hz, *C*F), 145.1 (*C*2), 139.6 (d, ^3J = 6.7 Hz, *C*8), 131.7 (d, ^2J = 14.4 Hz, *C*7), 123.7 (*C*8a), 123.4 (d, ^3J = 8.4 Hz, *C*4a), 109.7 (*C*3), 105.5 (d, ^2J = 23.9 Hz, *C*5), 68.1 (*C*11), 60.8 (*C*H$_2$CH$_3$), 55.7 (*C*10), 54.7 (*C*12), 50.6 (d, ^4J = 3.8 Hz, *C*9), 46.5 (N-*C*H$_3$), 18.3 (*C*H$_3$), 14.5 (CH$_2$*C*H$_3$); IR

172

(KBr) 1719 (C=O), 1617 (C=O) cm^{-1}; LC/TOF-MS calcd for $C_{20}H_{25}FN_3O_4$ 390.1824, found 390.1843 (M + H$^+$).

The synthesis of levofloxacin C-3 hydroxamic acid (3.25)
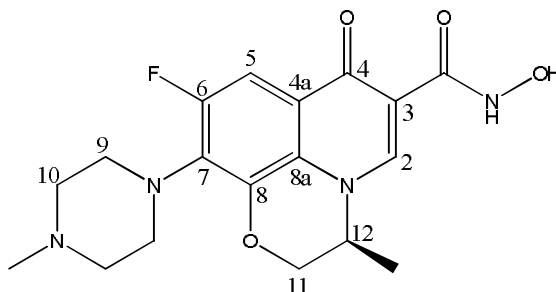
Sodium hydroxide (0.05 g, 1.12 mmol) and hydroxylamine hydrochloride (0.04 g, 0.56 mmol) were dissolved in distilled water (3 mL) and stirred at 25 $^{\circ}$C for 30 minutes. Compound **3.24** (0.20 g, 0.51 mmol) was dissolved in MeOH (2 mL) and slowly added to the hydroxylamine solution over 10 minutes. The reaction mixture was allowed to stir at 25 $^{\circ}$C for 24 hours. After 24 hours, conc. HCl was slowly added to the reaction mixture until pH 6 was reached. The solution was reduced under vacuum until a precipitate began to form and this was collected by filtration. The resulting solid was washed with a minimum of cold MeOH and allowed to dry.

White solid (0.02 g, 11%); ^{1}H NMR (300 MHz, DMSO-d$_6$) δ 15.16 (br s, 1H, O*H*), 9.00 (s, 1H, *H*2), 7.60 (d, *J* = 12.2 Hz, 1H, *H*5), 4.89-5.02 (m, 1H, *H*12), 4.57-4.67 (m, 1H, *H*11), 4.35-4.46 (m, 1H, *H*11), 3.55 (app br s, 4H, *H*9), 3.18 (app br s, 4H, *H*10), 2.73 (s, 3H, N-C*H*$_3$), 1.45 (d, *J* = 6.7 Hz, C*H*$_3$); ^{13}C NMR (75 MHz, DMSO-d$_6$) δ 176.4 (*C*=O), 166.0 (*C*=O), 155.3 (d, ^1J = 245.3 Hz, *C*F), 146.4 (*C*2), 140.5 (d, ^3J = 6.8 Hz, *C*8), 130.7 (d, ^2J = 14.3 Hz, *C*7), 124.7 (*C*8a), 120.4 (d, ^3J = 9.2 Hz, *C*4a), 106.8 (*C*3), 103.2 (d, ^2J = 23.7 Hz, *C*5), 68.2 (*C*11), 54.8 (*C*12), 53.3 (*C*10), 47.4 (*C*9), 42.8 (N-*C*H$_3$), 18.0 (*C*H$_3$); IR (KBr) 1712 (C=O), 1623 (C=O) cm^{-1}; LC/TOF-MS calcd for $C_{18}H_{22}FN_4O_4$ 377.1620, found 377.1633 (M + H$^+$).

The synthesis of levofloxacin C-3 n-butylamine (3.26)
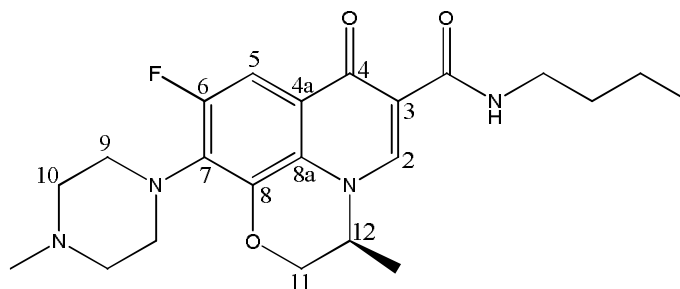
Levofloxacin (0.10 g, 0.28 mmol) was added to a solution of TBTU (0.10 g, 0.31 mmol) and HOBt (0.04 g, 0.031 mmol) in anhydrous DMF (3.0 mL), under nitrogen, and stirred at room temperature for 10 minutes. Triethylamine (0.06 mL, 0.43 mmol) was added to the solution and allowed to stir for a further 10 minutes. In a separate flask, n-butylamine (0.03 mL, mmol) and triethylamine (0.06 mL, 0.43 mmol) were stirred at room temperature in anhydrous DMF (2 mL) for 10 minutes. The n-butylamine solution was added to the levofloxacin solution and allowed to stir at room temperature for 24 hours, after which the solvent was removed under reduced pressure. The resulting residue was dissolved in DCM and washed with 1M HCl followed by sat. aq. NaHCO$_3$.The organic layer was dried over Na$_2$SO$_4$, and filtered, followed by removal of the solvent under reduced pressure.

Yellow oil (0.05 g, 42%); ^{1}H NMR (300 MHz, CDCl$_3$) δ 9.95 (t, J = 6.6 Hz, 1H, NH), 8.62 (s, 1H, H2), 7.68 (d, J = 12.2 Hz, 1H, H5), 4.28-4.43 (m, 1H, H12), 4.24 (app d, 2H, H11), 3.20-3.48 (m, 6H, H9 and N-CH_2), 2.50-2.54 (m, 4H, H10), 2.34 (s, 3H, N-CH_3), 1.53-1.64 (m, 5H, CH_3 and n-butyl CH_2) 1.35-1.48 (m, 2H, n-butyl CH_2), 0.92 (t, J = 7.2 Hz, n-butyl CH_3); ^{13}C NMR (75 MHz, CDCl$_3$) δ 175.5 (C=O), 165.0 (C=O), 155.8 (d, ^1J = 245.6 Hz, CF), 143.9 (C2), 139.6 (d, ^3J = 6.8 Hz, C8), 131.7 (d, ^2J = 14.4 Hz, C7), 124.4 (C8a), 122.6 (d, ^3J = 8.7 Hz, C4a), 111.4 (C3), 105.2 (d, ^2J = 23.9 Hz, C5), 68.3 (C11), 55.7 (C10), 54.9 (C12), 50.4 (d, ^4J = 4.5 Hz, C9), 46.3 (N-CH$_3$), 39.1 (N-CH$_2$), 31.78 (n-butyl CH$_2$), 20.4 (n-butyl CH$_2$), 18.4 (CH$_3$), 13.9 (n-butyl CH$_3$); IR (KBr) 3445 (NH), 1633 (C=O) cm^{-1}; LC/TOF-MS calcd for C$_{22}$H$_{30}$FN$_4$O$_3$ 417.2296, found 417.2305 (M + H$^+$).

The synthesis of tributyltin azide (TBTA)[131]
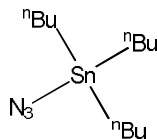
A solution of sodium azide (3.99 g, 61.4 mmol) in distilled water (31.9 mL) and tributyltin chloride (10 g, 30.7 mmol) in diethyl ether (80.9 mL) were shaken together for 10 minutes. The organic phase was separated and the aqueous phase washed with diethyl ether (50 mL). The organic washings were combined, dried over magnesium sulphate, and the solvent removed under reduced pressure.

Clear yellow oil (5.53 g, 74%); ^{1}H NMR (300 MHz, CDCl$_3$) δ 1.42-1.67 (m, 6H, CH_2), 1.32-1.40 (m, 6H, CH_2), 1.24-1.32 (m, 6H, CH_2), 0.93 (t, 9H, J = 7.3 Hz, CH_3); ^{13}C NMR (75 MHz, CDCl$_3$) δ 27.8 (CH$_2$), 26.9 (CH$_2$), 15.4 (CH$_2$), 13.6 (CH$_3$); IR (neat film on NaCl plate) 2073 (N$_3$) cm^{-1}.

Chapter IV

A study of organotin(IV) antibacterial agents

4.1 An Introduction to Tin

4.1.1 Tin metal

Tin metal has been mined and used by man since ca. 3000 B.C.[160] The chemical symbol for tin, Sn, originates from its latin name: stannum.[160] The Earth's crust contains an approximate distribution of 2 ppm of tin; considerably less than zinc (94 ppm), copper (63 ppm) or lead (12 ppm).[161] Cassiterite (tin oxide, SnO_2) is the principal tin-containing ore, and is excavated by hard rock and alluvial mining.[161,162] China and Indonesia have been the major producers of tin over the last few years.[160,163] Between the 1950s and 2011, China produced 2.7 million tonnes and Indonesia 2.6 million tonnes of tin metal.[160] Tin metal is obtained through a smelting and refining process by reducing SnO_2 in the presence of carbon monoxide (Equation 4.1) in a blast, electric or reverberatory furnace.[161] The recycling of tin metal by re-refining is on the rise; over 65,000 tonnes were produced by re-refining in 2010.[160]

$$\textbf{Equation 4.1: } SnO_2 + 2CO \longrightarrow Sn + 2CO_2$$

Tin metal has found use in a number of applications (Figure 4.1). Its major use is in soldering. The Pb/Sn alloy was 40:60, Pb:Sn, but due to the toxicity of lead, today's solders are almost purely tin (95% tin in 2012).[160] Tinplate constitutes almost 20% of tin usage.[164] The process coats a thin layer of tin (0.4 – 25 μm) over sheet steel, providing a corrosion-resistant cover that is ideal for packaging and product containers, for example, drink cans.[164]
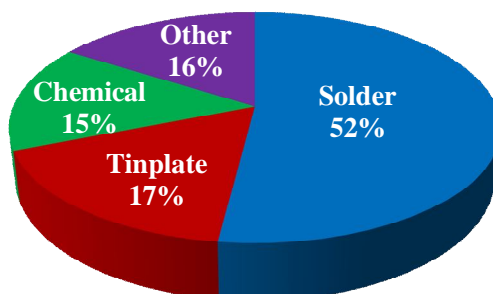
Figure 4.1: Tin applications.[165]

177

The biggest use of tin chemicals is in PVC (polyvinyl chloride) stabilisers.[160] During the fabrication of PVC, HCl is eliminated and this continuous elimination of HCl results in the formation of a brittle polyolefin by-product (Scheme 4.1).
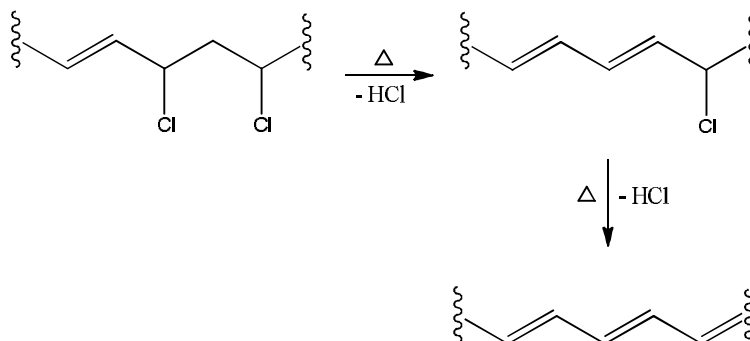
Scheme 4.1: The elimination of HCl from PVC.[166]

Organotins stabilise the PVC in two ways (Scheme 4.2):

(a) the organotin compounds react with the eliminated HCl to give organotin chlorides, which in turn do not catalyse any further elimination of HCl, and

(b) the organotin stabilisers introduce other groups, which are not easily eliminated, in place of the chlorides, thus preventing the formation of a polyolefin structure.

There are two main types of tin-based PVC stabilisers: sulfur containing stabilisers (containing sulfides and mercaptides) and sulfur-free stabilisers (containing carboxylates).[161] Tin has also found use in a variety of other areas including alloys, catalysis, gas sensors, flame retardants, biocides, antimicrobials, dental formulations, construction and the manufacture of high-quality glass by the Pilkington process.[160,161,162]
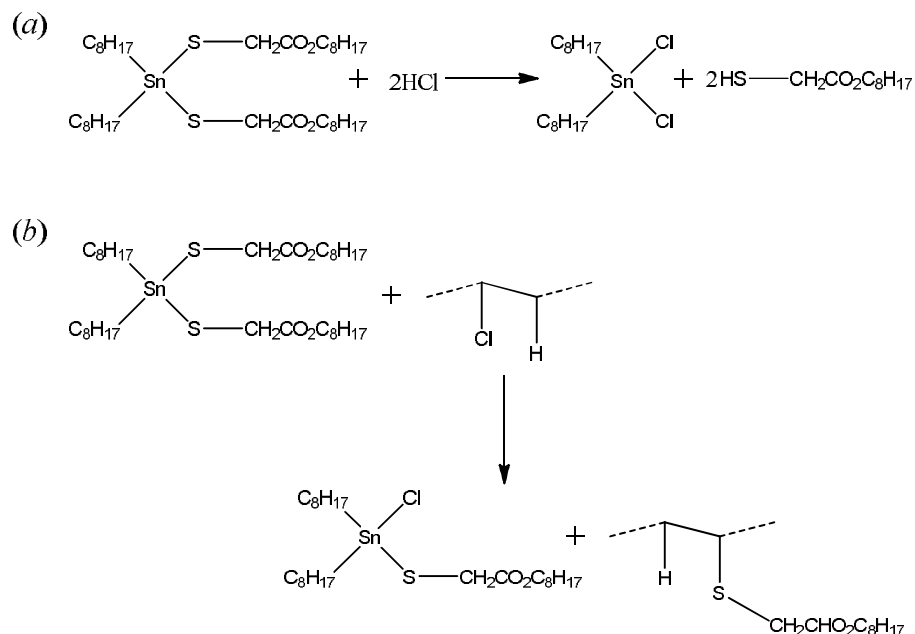
Scheme 4.2: (*a*) The reaction of a sulphur-based organotin stabiliser with HCl and (*b*) the substitution of an organotin stabiliser with PVC.[166]

4.1.2 Tin: the element and its chemistry

Tin is a group 14 (IV) *p*-block metal with the electronic configuration: [Kr] $4d^{10}$ $5s^2$ $5p^2$. Of all of the elements, tin has the largest number of isotopes; 10 stable isotopes (Table 4.1), giving it a characteristic isotopic pattern as shown in Figure 4.2. The ^{117}Sn and ^{119}Sn isotopes have spin ½ and can therefore be used in NMR spectroscopy.

Table 4.1: The isotopes of tin.

Isotope	Mass	Spin	Abundance (%)
112	111.90494	0	0.95
114	113.90296	0	0.65
115	114.90353	1/2	0.34
116	115.90211	0	14.24
117	116.90306	1/2	7.57
118	117.90339	0	24.01
119	118.90213	1/2	8.58
120	119.90213	0	32.97
122	121.90341	0	4.17
124	123.90524	0	5.98
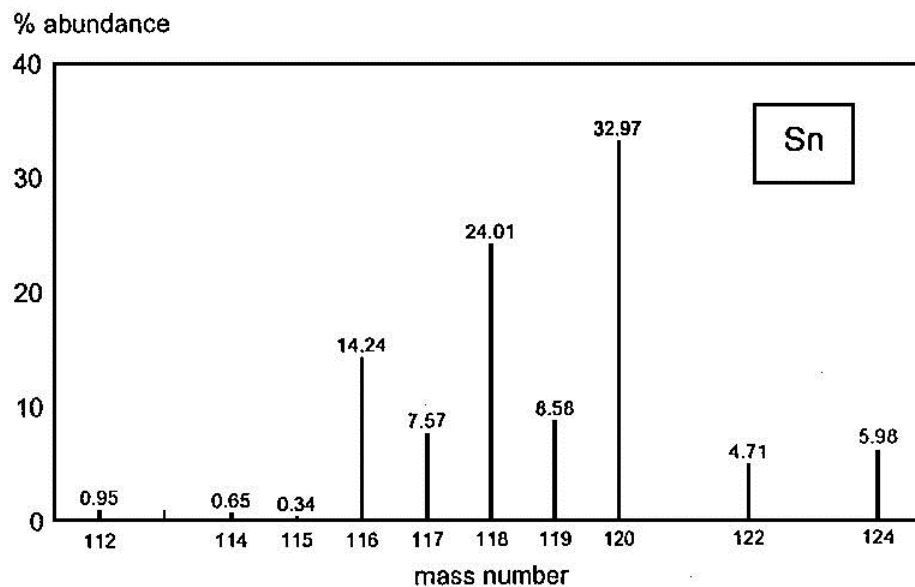
Figure 4.2: Tin isotope pattern.[167]

There are two allotropes of tin; β-tin (white tin) has a body centred tetragonal form and α-tin (grey tin) which has a diamond cubic structure.[168] Above 10 °C tin exists as β-tin, but below 10 °C, its volume increases by ca. 27% and it changes into α-tin, this is known as tin pest or tin plaque (Figure 4.3).[161,168]
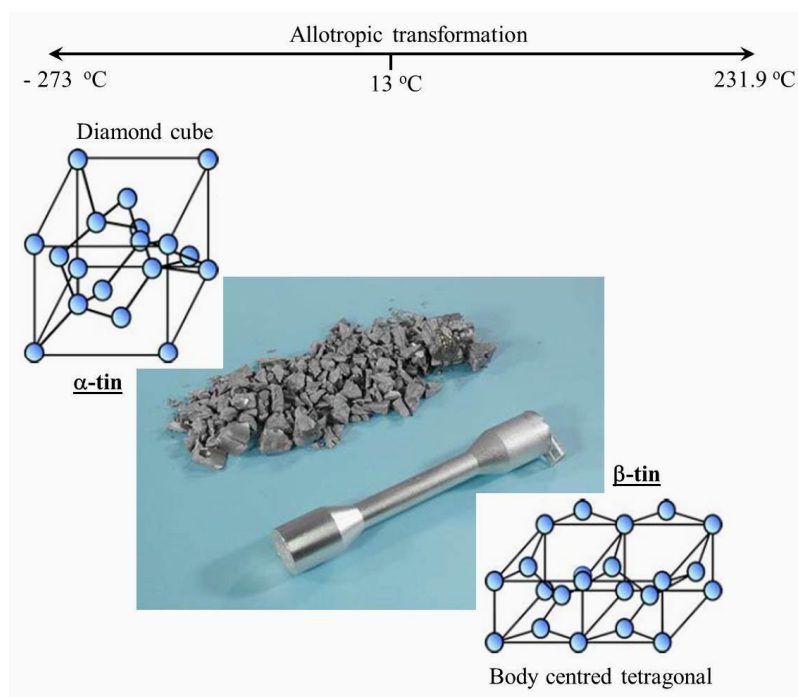
Figure 4.3: The allotropes of tin.[168]

180

Tin mainly forms compounds that have either the Sn(II) or Sn(IV) oxidation state, and examples of the types of structures that can form are shown in Figure 4.4. In the Sn(II) state compounds, it is mainly the 5p orbitals that are involved in bonding and as a result, the $5s^2$ electrons exist as a lone pair on the Sn atom.[164] This lone pair is often stereochemically active e.g. [:SnCl$_3$]$^-$ has a pyrimidal structure (Figure 4.5).[169] This non-bonding pair of electrons allows the Sn(II) compounds to act as donors with Lewis acids.[164] The simplest structure formed by Sn(II) compounds are of the type :SnX$_2$ (stannylenes, Figure 4.4 (*a*)).[164] These compounds are most stable when X is a bulky group or an electron-withdrawing group, otherwise these compounds are readily oxidised to the Sn(IV) oxidation state to give compounds such as the stannanes (*d*) with a tetrahedral type structure (Figure 4.4).[161]
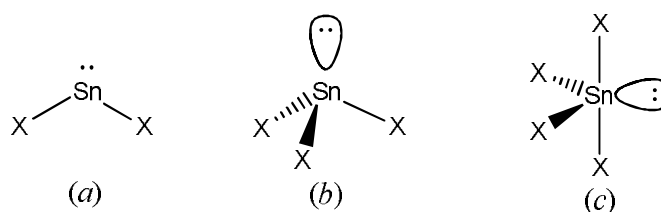
Sn(II) compound structures
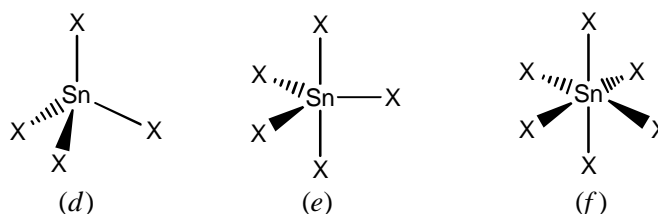
Sn(IV) compound structures

Figure 4.4: Tin compound structures.[161]

Figure 4.5: [:SnCl$_3$]$^-$

181
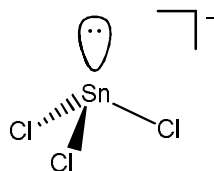
In addition to having the ability to act as donors, Sn(II) compounds can act as acceptors; likewise for Sn(IV) compounds.[164,169] The Sn(IV) compounds use the $5s^2$ $5p^2$ valence electrons for bonding.[164] The vacant 5d orbitals of the Sn(II) and Sn(IV) compounds permit the bonding of ligands, giving structures of the type *b*, *c*, *e*, and *f* (Figure 4.4.) These structures are often distorted and, depending on the type of ligand or X group, the coordination number of the Sn(II) and Sn(IV) compounds can be increased through intramolecular or intermolecular coordination to the Sn atom.[161] For example, SnF_2 (Figure 4.6), exists as a cyclic tetramer in the solid state but in the vapour phase it exists as a monomer.[161]

(*a*) (*b*)
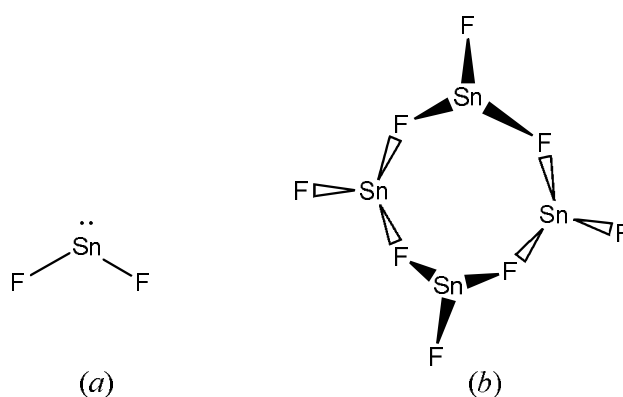
Figure 4.6: Structures of SnF_2 in (*a*) monomer, vapour phase and (*b*) cyclic tetramer, solid state.

4.1.3 The synthesis of organotin compounds

In 1849, Frankland synthesised the first organotin compound, Et_2SnI_2.[161] Löwig later demonstrated that ethyl iodide could react with a tin/sodium alloy to give the polymer diethyltin which in turn could react with air to give Et_2SnO, and with halogens to give Et_2SnX_2 (X = halogen).[170] Since then, numerous organotin compounds have been synthesised. An overview of the synthesis of the principal classes of organotin compounds is shown in Scheme 4.3.

The most commonly used reaction is of $SnCl_4$ with a Grignard reagent to produce R_4Sn, (R can be an alkyl, allyl, aryl alkenyl or alkynyl).[161,170] Unless the R group is bulky it is difficult to stop this reaction at an organotin halide stage.[161] The R_4Sn can then be used in a Kocheshkov redistribution reaction to yield the organotin halide

R_nSnCl_{4-n} (n = 1, 2 or 3).[171] Substitution of the chlorine with a nucleophile, X^-, occurs readily to give R_nSnX_{4-n}.[170] If the nucleophile is a metal hydride, R_nSnH_{4-n} is produced, which can undergo hydrostannation with an alkene or alkyne to give the corresponding stannane or vinyl stannane.[132a] The organotin hydrides can react with metallic bases such as BuLi, LDA, NaH and Grignard reagents to give the stannylmetallic compounds, R_3SnM (M = Li, Na, MgX).[161] These compounds can react with electrophiles such as organic halides.[164] In the presence of base or a palladium catalyst, the organotin hydrides can give the distannanes, R_2SnSnR_2, and the oligostananes, $(R_2Sn)_n$.[170] The organotin hydroxides are produced by hydrolysis of R_nSnX_{4-n} which can undergo spontaneous dehydration to give the organotin oxides.[161] The stannylenes (:SnX_2) can be produced *via* alkylation or arylation of $SnCl_2$, but as stated earlier, these are only stable when X is very bulky or electron-withdrawing.[161] Reaction of $SnCl_2$ with cyclopentadienyl lithium can be used to prepare stannocene (CpSn:) and reduction of $SnCl_2$ can produce the distannynes (RSnSnR).[161]
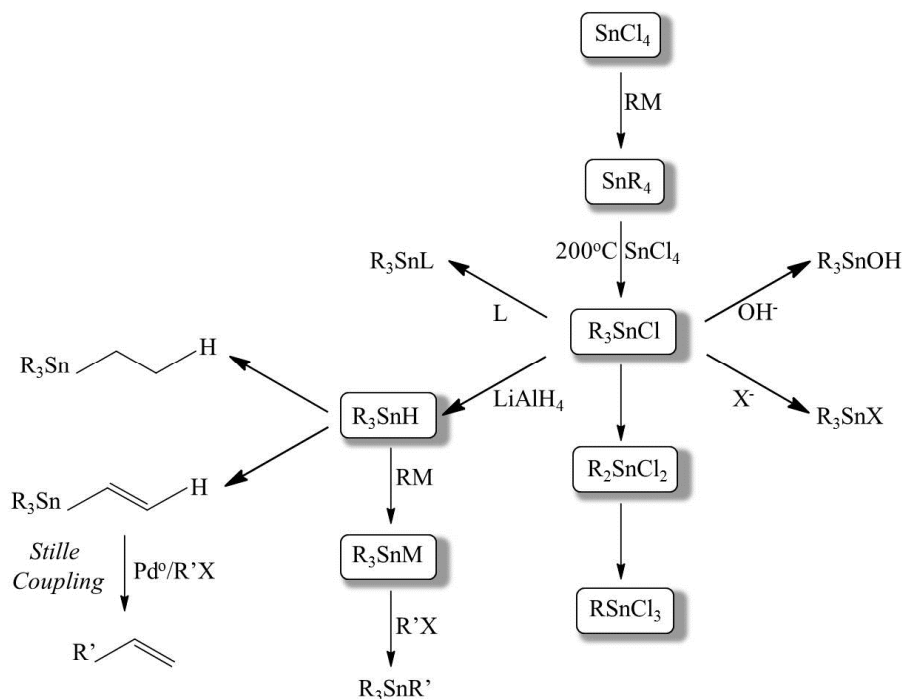
Scheme 4.3: Overview of some of the methods of preparation of organotin(IV) compounds. (Note: the reactions that occur with R_3SnCl can also occur with R_2SnCl_2 and $RSnCl_3$.)[161,170]

4.1.4 Biological activity of organotin compounds

The toxicity of organotin compounds was reported back in 1886.[172] However, studies into the toxicities of organotins only started to be carried out in the 1950s.[172,173] In 1955, Stoner *et al.*[173] carried out a number of studies of mono-, di-, tri- and tetraorganotins and their effects on rats, rabbits, guinea-pigs and fowls. Their results showed that, of all of the compounds tested, the triethyltin-containing compounds were the most toxic, with animals exhibiting muscular weakness followed by muscular tremors, convulsions, and, eventually death. In the rabbit studies, a dose of 10 mg/kg resulted in death within three hours of intravenous administration. Since then, numerous organotin toxicity studies have been carried out and as a result a general trend has emerged. The toxicity of organotins is governed mainly by the type and number of organic groups attached to the tin atom.[172] Organotins containing alkyl groups are generally more toxic than aryltin compounds.[161,172] Triorganotin compounds are considered to be the most toxic followed by the di-substituted and mono-substituted organotins, with the ethyl derivative of each exhibiting greatest toxicity.[172,174,175] The toxicity of tetraorganotins is believed to be due to their decomposition to the more toxic triorganotin derivative.[175] As the length of the carbon chain increases, a decrease in activity is seen with R_3SnX compounds; tri-*n*-octyl derivatives are essentially non-toxic to mammals.[161,176] The nature of the triorganotin substitutent is also important in determining the species to which the organotin compound is most toxic against (Table 4.2.).[161,172,171] The role of the X group, in R_3SnX, has been reported as playing a minor role in the toxicity, unless the X group itself exhibits biological activity and/or increases the solubility of the compound.[161,172] A decrease in activity has been associated with the ability of the X group to chelate to the tin atom.[172]

Table 4.2: The organic substituents of the triorganotins and the species to which they are toxic.[161,172,171]

Triorganotin R group	Species
Methyl	Insects and mammals
Ethyl	Mammals
n-Propyl	Gram negative bacteria
n-Butyl	Gram positive bacteria, fungi, fish and molluscs
Phenyl	Fungi, fish and molluscs
Cy	Mites

Due to their various biocidal activities, the organotin compounds have found use in a number of biological applications.[161,174,175,177] For example, a number of tributyl- and triphenyltin compounds have been used in antifouling paints including Bu_3SnO, Bu_3SnF, Bu_3SnCl, Ph_3SnX (X = F, Cl, OAc, OH).[176] One of the first to be used was Bu_3SnO.[176] Not only can it inhibit growth of fouling species such as algae at concentrations as low as 0.005 ppm, but it is also effective against fungi and Gram-positive bacteria.[176] The use of organotins in antifouling paints had many advantages:

(1) they are very active against a range of fouling species (Table 4.3);

(2) they did not cause corrosion of aluminium hulls;

(3) they are colourless, allowing a wide range of coloured paints to be made; and

(4) most importantly, they could be easily degraded by UV light and microogranisms into less toxic organotins and ultimately harmless tin residues (Scheme 4.4).[176,178]

However, in the 1980s it was suspected that tributyltin compounds were having adverse effects on marine species other than fouling species.[176] It has since been shown that organotins can act as endocrine disruptors resulting in imposex (imposed sexual organ) of marine species such as gastropods.[178] Studies into the half-lives of organotins found that organotins could be stable in sediments for up to 9 years and,

more worrying, is the bioaccumulation of organotins in marine species.[176] For example. the bioaccumulation levels of tributyltin in dogwhelks was found to be 1000 times greater than that found in surrounding water.[178] As a result, a number of countries started to ban the use of organotin antifouling paints and, in 1999, a global ban was introduced by the International Maritime Organisation (IMO).[176] As of January 1, 2008, the use of organotin antifouling paints on vessels is prohibited.[176]

Table 4.3: The growth inhibition concentrations (ppm) of tributyltin antifouling agents against a range of fouling species.[176]

Organotin	Barnacles	*Enteramorpha*	*Chlamydomas*	Lobsters
Bu_3SnO	0.01	0.02	0.005	0.02
Bu_3SnF	0.1	0.01	0.001	0.005
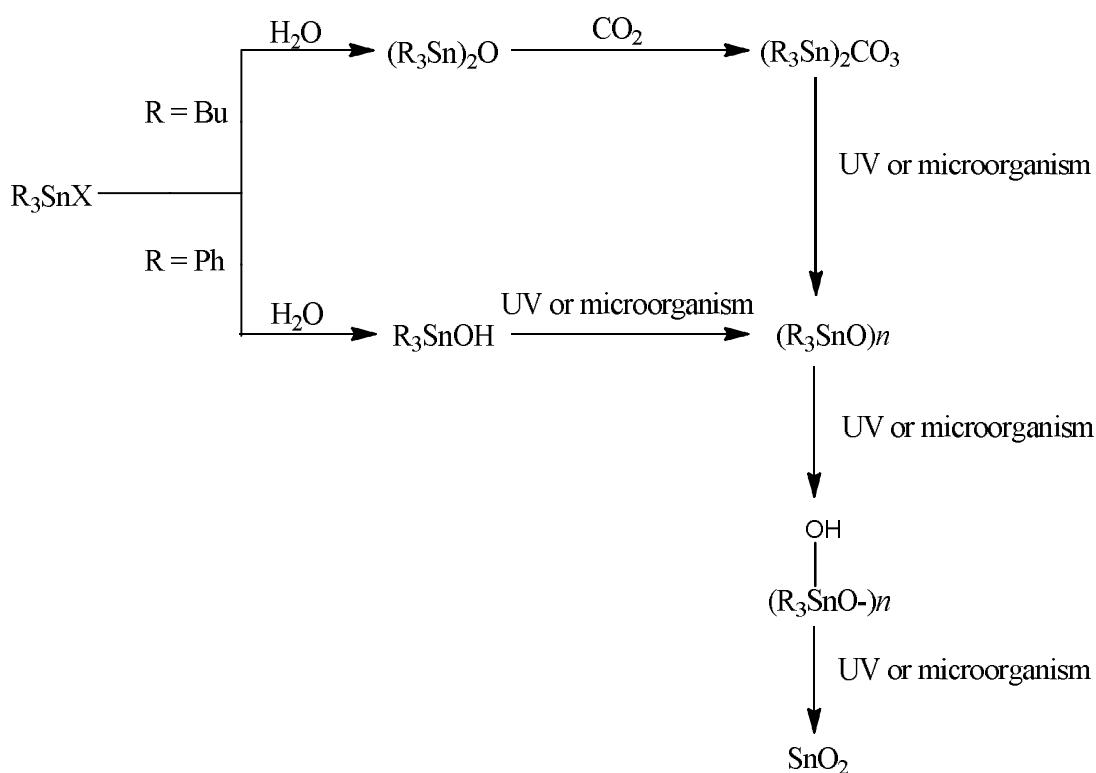
Scheme 4.4: General scheme for the environmental degradation of tributyl and triphenyltin compounds.[176]

Despite the unfortunate outcome of the use of organotin antifouling paints, there has been a great deal of research into the use of organotins in other areas in which its biocidal activity can be exploited.[175,177,179]

The anti-tumour properties of tin complexes were first observed in 1929.[177] However, it wasn't until the 1980's that organotin anticancer compounds were synthesised and these were based on cisplatin or its analogues.[180] Gielen *et al*.[180] synthesised the di-*n*-butyl analogue of carboplatin and screened it against mammary and colon cancer cell lines. The organotin analogue exhibited almost 10 times greater activity compared to that of cisplatin against these cell lines.[180] Numerous di- and triorganotin derivatives have been synthesised and tested against various cancer cell lines.[181] Over 2000 organotin compounds have been screened by the NCI (National Cancer Institute), rendering tin as the metal with the greatest number of compounds to be screened.[182] Some compounds have exhibited lower toxicity and better activity than cisplatin.[183]

It has been suggested that there are a couple of factors that may play a role in the antiproliferative activity of organotin compounds:

(1) the availability of coordination sites at the Sn atom, and

(2) the existence of stable Sn-ligand bonds and their slow hydrolytic decompostition.[184]

Crowe *et al*.[185] also demonstrated that $R_2SnCl_2.L$ (L = N containing bidentate ligand) complexes with Sn-N bond lengths < 2.39 Å are inactive whereas complexes with Sn-N bond lengths > 2.39 Å are active and suggested that predissociation of the ligand is important in activity. The mode of action of organotin anticancer agents is not fully understood, however, DNA interaction and apoptosis have been observed.[186,187] The ID_{50} (the dose required to inhibit 50% of the cell line) values of a selection of organotin compounds and the various cell lines they are active against in comparison to cisplatin are given in Table 4.4.

Table 4.4: ID_{50} values of some organotin compounds against a variety of human cell lines. Flu = flufenamic acid and HL-7 = Gly-Leu.

Cell	Cancer	Cisplatin	Organotin compound	Organotin
A549	Lung	3.3[a]	$[Bu_2(flu)SnOSn(flu)Bu_2]$[b]	0.24[181f]
A498	Renal	2.253	$Ph_3Sn(HL-7)$	0.03[181e]
IGROV	Ovarian	0.169	$Ph_3Sn(HL-7)$	0.006[181e]
M19	Melanoma	0.558	$Ph_3Sn(HL-7)$	0.016[181e]
MCF7	Mammary	0.699	$[(Bu_2Sn(O_2CCF_3)_2)_2O]_2$	0.057[181h]
WiDr	Colon	0.697	$Ph_3Sn(HL-7)$	0.008[181e]
HeLa	Cervix	1.443	$2\text{-}PhC_2N_3CO_2SnPh_3$	0.005[181c]

[a] ID_{50} value obtained from Matysiak *et al*.[188] [b] The complex also exhibited better activity than carboplatin (108.0 μg/mL) against A549.

An important area in organotin research is in antimicrobial activity.[161,175] Organotins are well known for their fungicidal properties.[161,171] Triphenyltin acetate (Brestan®) and triphenyltin hydroxide (Du-ter®) were in use (discontinued in 1993 and 2002 respectively) as fungicides for leaf spot on sugar beet and celery, rice blast, coffee leaf rust and potato blight.[171,189] Numerous organotin compounds have been synthesised for antimicrobial purposes with a variety of ligands including carboxylates,[190] amino acids and peptides,[191] Schiff bases[175,192], hydrazones,[193] triazoles,[194] sulfur containing ligands,[195] and biologically active ligands.[196] The literature shows that many of the organotins have a tendency to be more active against Gram-positive bacteria compared to Gram-negative bacteria.[191d,193a,194a,197] The general known trends of toxicity are usually followed: for example, tri- are better than diorganotins,[190b,190c] and alkyl are more active than aryl organotins.[191c] It has also been noted that the organotin complexes are more active than their ligands alone.[190d,191b] It has been suggested that this may be due to chelation theory.[198] Due to the partial sharing of positive charge by the metal with the ligand donor groups and the possible π-electron delocalisation created over the chelate ring, a reduction in the polarity of the metal ion occurs upon chelation.[198,199] This in turn increases the lipophilicity of the metal-chelate assisting its passage through cell membranes.[198,199] But the opposite affect has also been observed i.e. chelation results in a decrease in activity.[193b,195] This may be due to the metal-chelate being unable to bind to an

active site.[172] An interesting study by Eng *et al.*[200] of the inhibition of *Ceratocystis ulmi* by triaryltin chlorides indicated that it is the R_3Sn^+ cation that is responsible for toxicity. Again, the mode of action of the organotin compounds is not fully understood.[161,175] One possibility is the inhibition of oxidative phosphorylation which in turn prevents ATP (adenosine triphosphate) synthesis.[190a,190b] ATP is the energy source for cellular work.[14]

Organotin compounds are also well known for their use as insecticides and larvicides.[161,192,201] According to the US EPA (United States Environmental Protection Ageny), Torque® (bis(trineophyltin)oxide) is still in use as an acaricide.[189] Many di- and triorganotins have been shown to be active against mosquitos (*Aedes aegypti* and *Anopheles stephensi*) with the toxicity dependant on both the organotin compound and the species of mosquito.[179,201a] Organotins are biodegradable and so far there are no known reports of *An. Stephaesi* and *Ae. Aegypti* resistance to triorganotins, making them very attractive compounds.[201b] Research into organotins as anti-inflammatory, anti-hypertensive and antiviral agents has also been carried out.[174,181e,202]

4.2 1,10-Phenanthroline and its derivatives

(*a*) (*b*) (*c*)
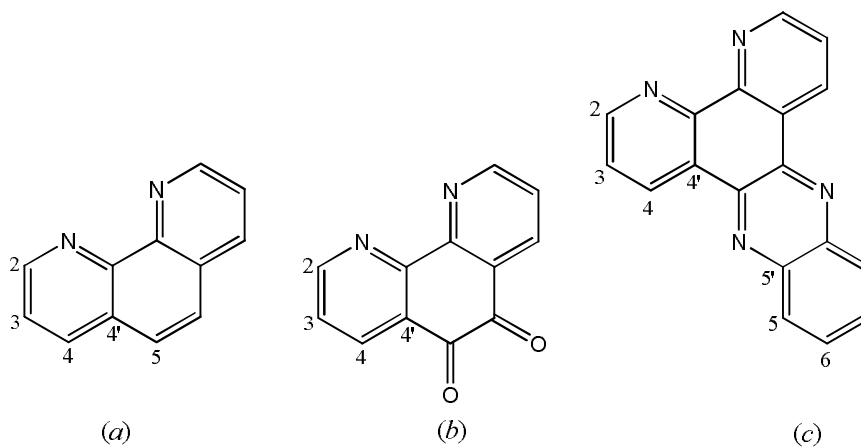
Figure 4.7: (*a*) 1,10-Phenanthroline (phen), (*b*) 1,10-phenanthroline-5,6-dione (dione) and (*c*) dipyrido[3,2-a:2',3'-c]phenazine (dppz).

4.2.1 1,10-Phenanthroline (phen)

First synthesised by Blau in 1898, 1,10-phenanthroline (phen), is a rigid, hydrophobic, electron-poor, heteroaromatic molecule consisting of two pyridine rings fused together by a central benzene ring (Figure 4.7).[203,204] A number of methods have been investigated for the synthesis of phen and its derivatives, one of the earliest methods being the Skraup reaction (Scheme 4.5).[203,204,205]
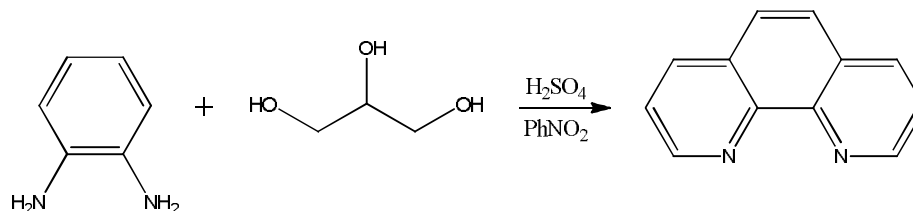
Scheme 4.5: The Skraup Reaction.

In the phen molecule, the shortest bonds (1.36 Å) are the C-N bonds, while the longest are the C-C bonds (1.49 Å) linking the pyridyl groups together.[206] Phen is a weak σ-donor but a good π-acceptor and can form complexes with a variety of metal ions.[203,207] Coordination occurs through the two N atoms in a *cis* fashion, resulting in the formation of a five-membered chelate ring that is coplanar with the rest of the phen molecule.[207] It has long been known that phen and substituted derivatives of phen can disturb a variety of biological systems in both the metal-free state and as ligands coordinated to transition metals.[208] The bioactivity of metal-free phen is believed to be due to its ability to sequester metal ions within the medium or biological system and that the resulting complexes are the active species or that the 'seized' metal ions are ions that are necessary for normal cell function and so are no longer able to carry out their role.[209,210]

Phen derivatives and their metal complexes have been used as intercalating or groove binding agents for DNA and RNA and some metal complexes of phen can efficiently cleave the DNA backbone, for example, $[Cu(phen)_2]^{2+}$.[203] Investigations into Cu, Ag, and Mn complexes of phen as anticancer and antimicrobial agents have been carried out.[71,211,212] Moreover, the addition of phen to a metal complex has been

shown to enhance the anticancer and antimicrobial activity with some complexes demonstrating values comparable to or better than that of standard drugs.[213,214,212]

4.2.2 1,10-Phenanthroline-5,6-dione (dione)

1,10-Phenanthroline-5,6-dione (dione) has been known for many years and can be synthesised by the oxidation of phen (Scheme 4.6).[215]
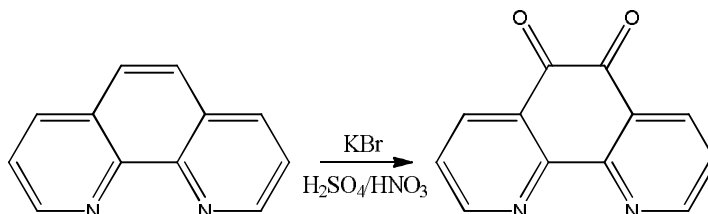
Scheme 4.6: The synthesis of 1,10-phenanthroline-5,6-dione.

Dione is a non-planar, bidentate ligand, with an *o*-quinoid functionality (Figure 4.7).[206] It has a similar structure to that of phen, the C-N bonds in dione are the shortest bonds (1.34 Å, excluding the C=O bonds, 1.21 Å in length) and the longest bonds are the OC-CO bonds (1.53 Å).[206] As with phen, dione has the ability to coordinate to metal ions through its diiminic functionality, but it can also bind to metal ions through the quinonoid functionality or through both.[206,216] Coordination through the N atoms results in a complex that can be used as a 'quinone equivalent' in reactions with compounds containing metals in low oxidation states, and coordination through O results in a complex that can act as a 'phenanthroline equivalent' in reactions with Lewis bases.[216]

Dione exhibits both anticancer and antimicrobial activity and improved activity in comparison to phen.[71,217] Dione and Co(II) complexes of dione have been shown to bind to DNA and cleave plasmid DNA.[218] Due to this biological activity, many metal complexes of dione have been investigated for their anticancer and antimicrobial activity.[219,220,221,222] The addition of dione to a metal ion has been shown to enhance biological activity.[219,71]

4.2.3 Dipyrido[3,2-a:2',3'-c]phenazine (dppz)

From dione, dipyrido[3,2-a:2',3'-c]phenazine (dppz) can be synthesised (Scheme 4.7).[215]
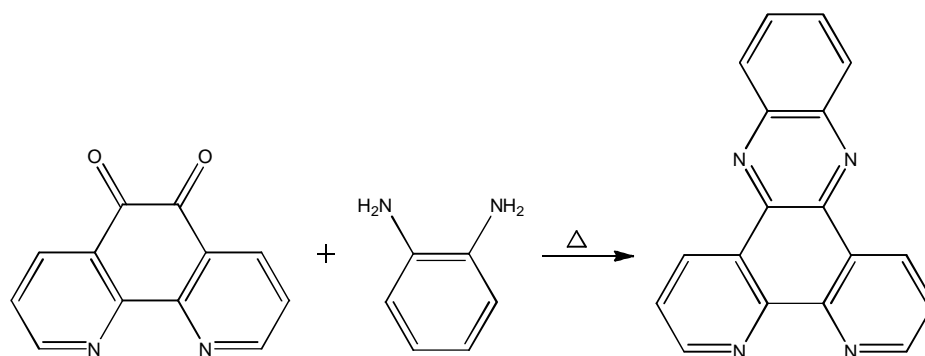
Scheme 4.7: The Synthesis of dipyrido[3,2-a:2',3'-c]phenazine (dppz).

Dppz is a planar, bidentate ligand with an extended aromatic system which facilitates its binding to DNA by intercalation (Figure 4.7).[217] This attractive property has resulted in the synthesis of various metal complexes of dppz.[223] One of the most well known complexes is the molecular 'light switch' Ru(2,2'-bipyridine)$_2$(dppz)$^{2+}$.[224] This complex displays metal-to-ligand-charge-transfer photoluminescence in hydrophobic solvents but in aqueous solution the photoluminescence is quenched by protonation of the phenazine N.[224] However, in the presence of DNA, intense photoluminescence is observed and the photoluminescence intensity and emission maximum will differ depending on the DNA substrate allowing the complex to behave as a DNA probe.[224]

Not only can dppz metal complexes bind to DNA but they have also demonstrated DNA cleavage.[218,225] It has been found that dppz itself can cleave DNA and is also cytotoxic.[217] Dppz and its metal complexes have been investigated for anticancer, antibacterial, antifungal, antiprotozoal and antiviral activity.[217,225,226,227] The Co(III) complex synthesised by Reddy *et al.*[225] displayed better antifungal and antibacterial activity than that of the well-known standards, fluconazole and streptomycin.

4.2.4 Aim

The aim of this study was to synthesise a series of diorganotin(IV) compounds ([R_2SnX_2L]) and evaluate their antibacterial activity against Gram-negative and Gram-positive bacteria. Three R groups were chosen for synthesis; Me, a structurally small and simple organic group, n-Bu a medium length alkyl chain, and a larger, aromatic phenyl group. These three R groups were chosen in the hopes that their differences in both structure and electronic features would give rise to differences in their biological activity. As mentioned earlier with the triorganotin compounds, the nature of the R group is important in determining the species to which it is most toxic against, for example, the tributyl tin compounds are known to be active against Gram-positive bacteria.[161,171]

Since a variety of tin carboxylates have been investigated in a number of biological systems and have exhibited some promising antimicrobial results, three carboxylate groups were chosen as the X group of the [$R_2SnX_2(L)$] compounds in this study.[190a,b, 190f] Firstly, the $CH_3CO_2^-$ group was chosen due to its small and simple structure. Secondly, taking into account the fact that the X group in R_3SnX compounds has been reported as playing a minor role in the toxicity unless the X group itself exhibits biological activity, two biologically active carboxylates were chosen.[161,172] These are nicotinic acid and its isomer, picolinic acid.

Nicotinic acid, better known as niacin or vitamin B_3, is an essential vitamin in humans and is produced from L-tryptophan.[14,228] As well as being a precursor to the coenzyme NAD (nicotinamide adenine dinucleotide), nicotinic acid is known for its antidyslipidemic effects and its ability to inhibit vascular inflammation and atherosclerosis progression.[228-229] Picolinic acid is also a naturally occurring metabolite of L-tryptophan.[230] It is known for its ability to facilitate the absorption of dietary zinc in rats and has been shown to act as a costimulator of macrophage tumoricidal activity *in vitro*.[231]

Finally, 1,10-phenanthroline (phen) and two of its derivatives, 1,10-phenanthroline-5,6-dione (dione) and dipyrido[3,2-a:2',3'-c]phenazine (dppz), were chosen as the ligands, L, of the [R_2SnX_2L] compounds. The phen, dione and dppz ligands are

attractive ligands to work with not only because of their differences in electronic and steric features, and their varying degrees of biological activity, but also the ease at which the dione and dppz can be synthesised from phen.[208,210,217,232]

It was envisioned that a diorganotin(IV) compound combined with a carboxylate moiety and either a phen, dione or dppz ligand could potentially produce a metal-based antibacterial compound with exceptional activity.

4.3 Results and Discussion

4.3.1 Synthesis of the ligands
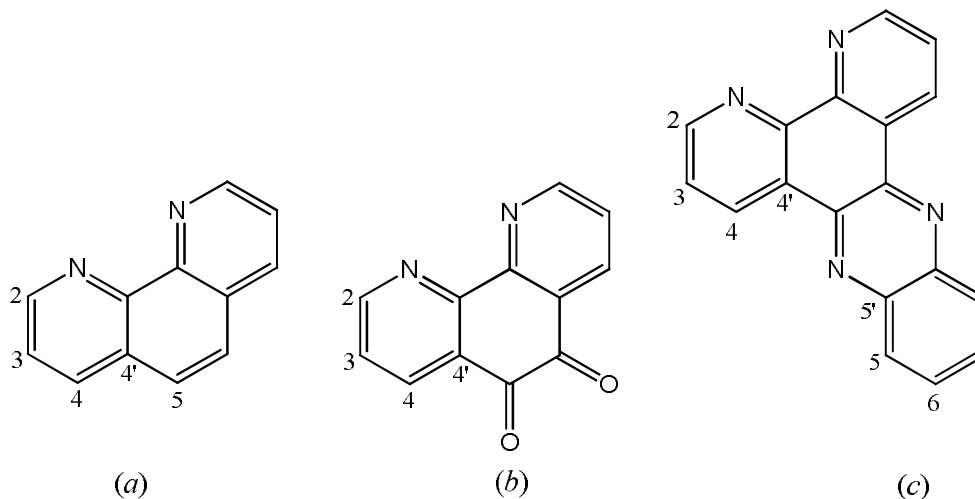
Figure 4.8: (*a*) 1,10-Phenanthroline (phen), (*b*) 1,10-phenanthroline-5,6-dione (dione) and (c) dipyrido[3,2-a:2',3'-c]phenazine (dppz). Numbering system for ^{1}H and ^{13}C NMR also shown.

1,10-Phenanthroline (phen) was obtained commercially and used without any further purification. 1,10-Phenanthroline-5,6-dione (dione) was synthesised from phen as previously described by Paw and Eisenberg[232a] resulting in a fine, yellow solid, upon purification. The dione was then reacted further with *o*-phenylenediamine in EtOH to produce dppz in good yield, 75%.[232b] A proposed mechanism for the synthesis of dppz is given in Scheme 4.8. Nucleophilic attack of the primary amine of *o*-phenylenediamine at the electrophilic carbonyl carbon of the dione, followed by the loss of water, results in formation of the new imine bond to give the dppz ligand.
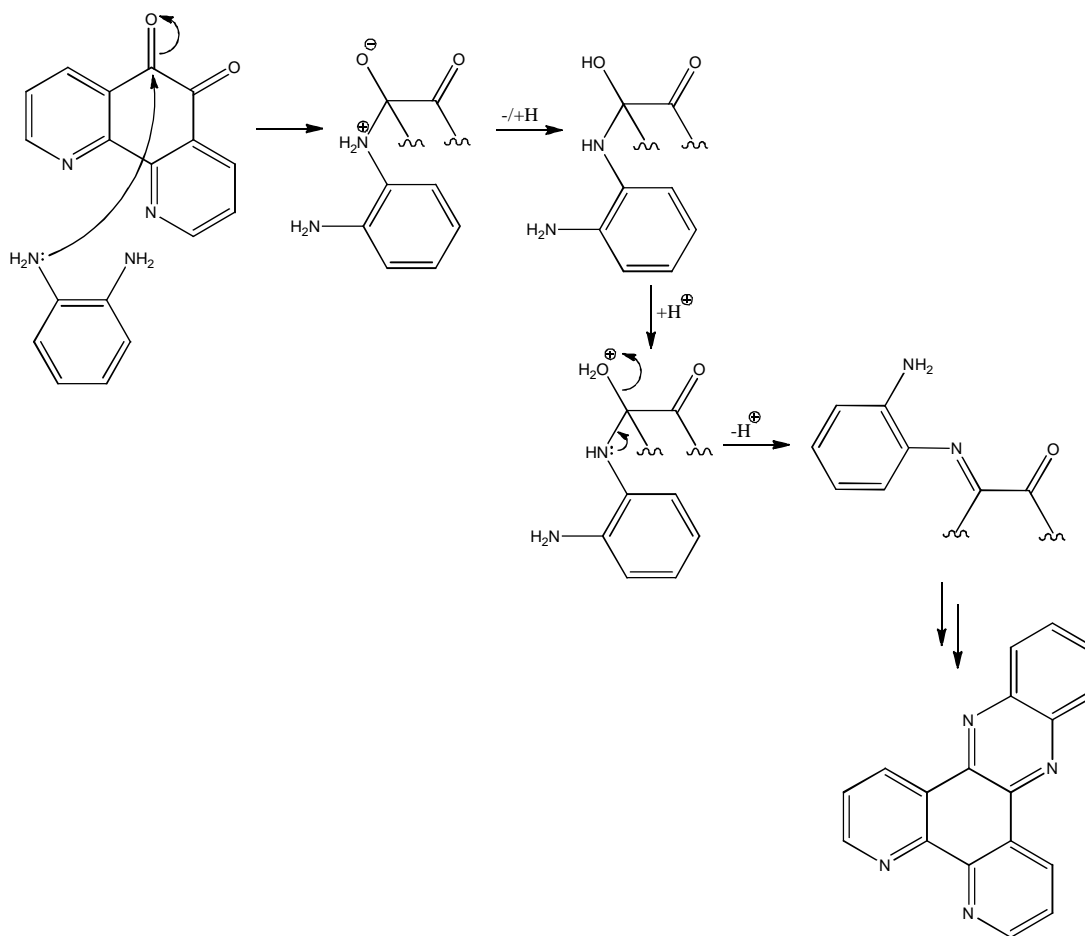
Scheme 4.8: Proposed mechanism for the synthesis of dppz. (For clarity, the full structure of the dione ligand has been excluded throughout the reaction scheme.)

The simplicity of the ^{1}H NMR spectra of each of the phen ligands is due to the plane of symmetry in the molecules (Figure 4.9). In the ^{1}H NMR spectrum of dione it can be seen that the H-5 of phen, found at 7.99 ppm, has disappeared. A new carbonyl carbon signal appears in the ^{13}C NMR spectrum of dione (at 177.7 ppm), the formation of which is confirmed further by the presence of the characteristic ν(C=O) absorption band at 1686 cm^{-1} in the IR spectrum. Formation of the dppz ligand is confirmed by the disappearance of the dione ^{13}C NMR C=O signal, along with the appearance of two new signals (8.36 and 8.04 ppm, the protons of the new aromatic ring in the dppz molecule) in the ^{1}H NMR spectrum. The protons of each of the ligands, phen, dione and dppz, expected to be affected most by complexation to tin were the H-2 protons. These signals appear as a doublet of doublets at 9.10, 8.98 and

9.49 ppm in the ^{1}H NMR spectra of the free ligands phen, dione and dppz, respectively.
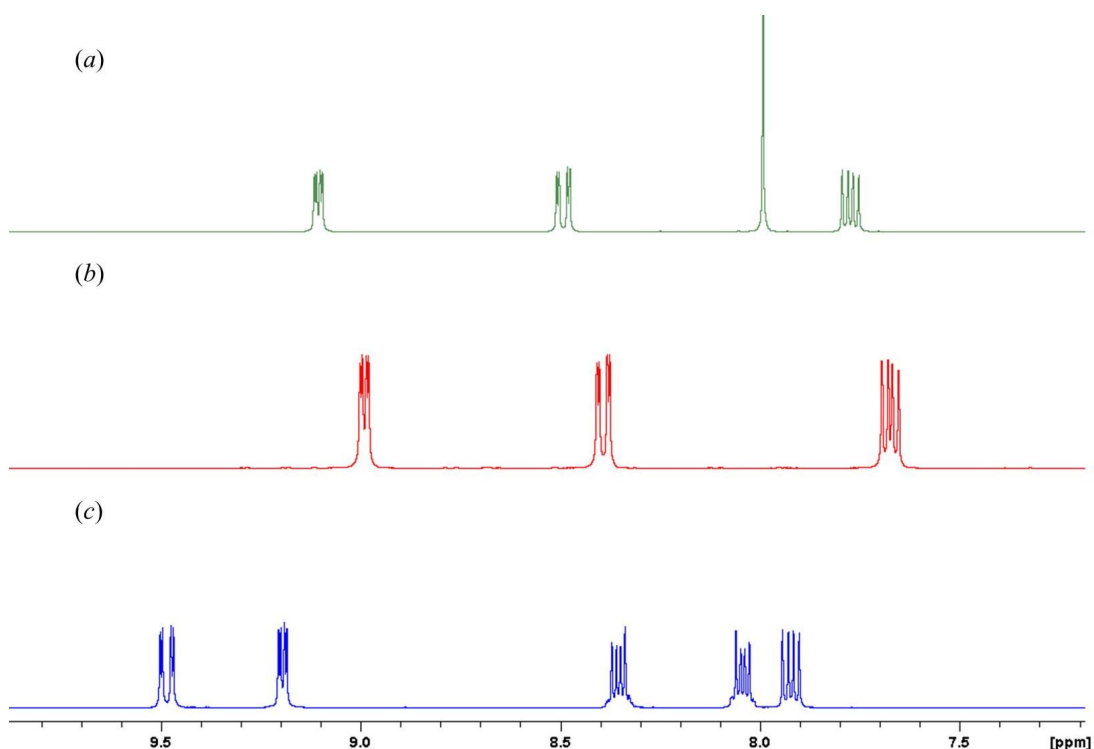
Figure 4.9: ^{1}H NMR spectra of (*a*) phen, (*b*) dione and (*c*) dppz in DMSO-d$_6$.

4.3.2 Synthesis of the diorganotin(IV) monoacetate compounds

The organotin(IV) monoacetate compounds (R$_2$Sn(O$_2$CMe)Cl, R = Me, n-Bu, or Ph) were synthesised from the corresponding diorganotin(IV) dichlorides. The diorganotin(IV) dichlorides were obtained commercially and used without any further purification. For the dimethyl- and dibutylchlorotin(IV) acetate compounds, Et$_3$N was added slowly to a solution of the appropriate dichloride and acetic acid in toluene followed by a three hour reflux (Scheme 4.9). The resulting Et$_3$N.HCl salt by-product was removed by filtration through celite to give [Me$_2$Sn(O$_2$CMe)Cl] and [n-Bu$_2$Sn(O$_2$CMe)Cl] with yields of 73% and 88%, respectively.
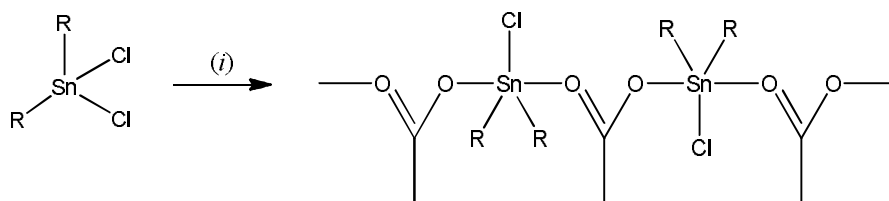
Scheme 4.9: Synthesis of diorganotin(IV) monoacetate compounds [$R_2Sn(O_2CMe)Cl$] (i) AcOH, Et_3N, Δ, 3h, toluene for R = Me and n-Bu, and AcOH, K_2CO_3, Δ, overnight, benzene for R = Ph.

The same method was used in an attempt to synthesise the diphenyltin derivative but was unsuccessful. From the ^{1}H NMR spectrum it appeared that a mixture of starting materials was being returned. This may be due to the limited solubility in toluene of diphenyltin(IV) dichloride. Diphenyltin(IV) dichloride has greater solubility in benzene thus, the reaction was repeated as in Scheme 4.9 using benzene as the reaction solvent. Again, it appeared that a mixture of starting materials was being returned, so the reaction was repeated but allowed to reflux over longer periods of time, that is, 5, 9, 12 and 24 hours. However, no difference in the ^{1}H NMR spectra was observed with increasing reaction time. After changing both the solvent and increasing the reaction times proved unsuccessful, a change in base was attempted. The reaction was allowed to reflux in benzene overnight, with K_2CO_3 instead of triethylamine, which successfully gave the white solid product, [$Ph_2Sn(O_2CMe)Cl$].

The molecular structure of each of the three compounds was elucidated by elemental analysis, ^{1}H and ^{13}C NMR and IR spectroscopies. Elemental analysis confirmed the presence of a single Cl in each molecule. The ^{1}H NMR of the [$Me_2Sn(O_2CMe)Cl$] and [$n\text{-}Bu_2Sn(O_2CMe)Cl$] showed a distinct singlet for the acetate signals at 1.93 and 1.95 ppm, respectively, corresponding to the three protons of the acetate group in each case.

A variety of di- and trimethyltin(IV) compounds have been studied in an effort to investigate if there is a correlation between the magnitude of the Sn-carbon ($|^1J|$) or Sn-hydrogen ($|^2J|$) coupling constants and the Me-Sn-Me angle (θ).[233] It was found that in both the solid and solution state, the molecular structure of methyltin(IV)

compounds could be estimated from $|^1J|$ and $|^2J|$ as they are dependent on the Me-Sn-Me angle (Equation 4.2 and 4.3).[233] The following conclusions have been drawn:[233]

- for di- and tetramethyltin(IV) compounds with a coordination number of four $|^1J| \leq 430$ Hz, pentacoordinated tri- and dimethyltin(IV) compounds have $|^1J|$ in the range 470-610 Hz and for hexacoordinated dimethyltin(IV) compounds $|^1J| \geq 630$,

- $|^2J|$ is less than 59 Hz for trimethyltin(IV) compounds with a coordination number of four and tetracoordinated dimethyltin(IV) compounds bearing electronegative substituents can have a higher $|^2J|$, for example, Me_2SnCl_2 has $|^2J| = 69$ Hz,

- pentacoordinated dimethyltin(IV) compounds have $|^2J|$ in the range of 64-79 Hz (corresponding to $\theta = 115^o$ and 130°) and

- hexacoordinated dimethyltin(IV) compounds have $\angle$Me-Sn-Me between 109.1 and 180°.

It was noted that caution should be taken when using the equations if $|^2J|$ is < 80 Hz (or $|^1J|$ < 650 Hz) and the dimethyltin(IV) compound is likely to be hexacoordinated, as *cis*-dimethyltin(IV) compounds can have θ values that are much smaller than that predicted by Equation 4.3.[233a]

$$\textbf{Equation 4.2: } |^1J| = 11.4\theta - 875$$

$$\textbf{Equation 4.3: } \theta = 0.0161|^2J|^2 - 1.32|^2J| + 133.4$$

For [Me$_2$Sn(O$_2$CMe)Cl], $^2J(^{119/117}$Sn$)$ = 92.7/82.2 Hz were found. Using Equation 4.3. $\angle$Me-Sn-Me was calculated to be 149.4^o suggesting a hexacoordinate structure in solution.

For [Ph$_2$Sn(O$_2$CMe)Cl], the ^{1}H NMR spectrum was poorly resolved due to lack of solubility which resulted in indistinct integrations. However, the ^{13}C NMR spectrum confirms the presence of the carbonyl carbon at 178.5 ppm which is shifted downfield in comparison to the acetic acid carbonyl carbon (175.9 ppm). A HSQC equivalent experiment verified that the ^{1}H NMR singlet at 2.15 ppm corresponds to the three equivalent protons of the acetate. ^1J and ^2J ($^{119/117}$Sn) could not be found for either [n-Bu$_2$Sn(O$_2$CMe)Cl] or [Ph$_2$Sn(O$_2$CMe)Cl] due to their complex NMR spectra.

A range of different coordination modes exist for the carboxylate ion, RCO$_2$$^-$ (Figure 4.10). Deacon and Phillips[234] have studied the coordination modes of a variety of acetato and trifluoroacetato metal complexes and have proposed that the coordination mode of the carboxylate ion can be defined by measuring Δv; the difference between the asymmetric and symmetric carboxylate stretching frequencies (v_{as}COO$^-$ - v_{sym}COO$^-$). The Δv values proposed by Deacon and Phillips are tentative values, as some exceptions have been observed.[234] The general conclusions obtained by Deacon and Phillips for the diagnosis of the nature of the coordination mode of the carboxylate group have been widely used (over 2000 citings[235]) and are as follows:[179,190g,234]

(i) for unidentate coordination, Δv is larger than that observed for ionic acetates ($\Delta v > 200$ cm^{-1} for acetates and $\Delta v > 260$ cm^{-1} for trifluoroacetates),

(ii) if Δv values are less than 200 cm^{-1}, then the carboxylate group coordinates in a bidentate manner,

(iii) for acetates only, a Δv value considerably less than that observed for ionic acetates (<105 cm^{-1}) is indicative of chelating or of both chelating and bridging and

(iv) for all of the complexes studied, those that have a Δv value in the range of 150-200 cm^{-1} have chelating and/or bridging acetate groups.

Figure 4.10: Possible coordination modes of a carboxylate ion, RCO_2^-; (*a*) unidentate, (*b*) chelating, (*c*) bidentate bridging, (*d*) monatomic bridging and (*e*) chelation and bridging.[234]

In the IR spectra of each of the monoacetate derivatives a strong absorption band in the range 1550-1640 cm^{-1} corresponding to ν(C=O) of the carboxyl group can be seen. The $\nu_{as}COO^-$ and $\nu_{sym}COO^-$ stretching frequencies for each of the monoacetate compounds are given in Table 4.5. For [Me$_2$Sn(O$_2$CMe)Cl], [n-Bu$_2$Sn(O$_2$CMe)Cl] and [Ph$_2$Sn(O$_2$CMe)Cl], $\Delta\nu$ = 144, 143 and 122 cm^{-1} respectively. All three compounds have a $\Delta\nu$ less than 200 cm^{-1} suggesting a bidentate coordination mode for the carboxylate group.

Table 4.5: IR stretching frequencies (cm^{-1}).

Compound	$\nu_{as}COO^-$	$\nu_{sym}COO^-$	$\Delta\nu$
Na(O$_2$CMe)[234]	1578	1414	164
[Me$_2$Sn(O$_2$CMe)Cl]	1564	1420	144
[n-Bu$_2$Sn(O$_2$CMe)Cl]	1637, 1571	1376, 1428	261, 143
[Ph$_2$Sn(O$_2$CMe)Cl]	1551	1429	122

The crystal structure for [Me$_2$Sn(O$_2$CMe)Cl] has been reported, and consists of Me$_2$SnCl units linked together by bridging acetates with the two methyl group

carbons and the chlorine atom forming a trigonal arrangement about the Sn atom.[236] The compound is described as having a distorted trigonal bipyramidal structure with distortions being attributed to a second, weak Sn-O intramolecular interaction which increases the overall Sn coordination number to six (Figure 4.11).[236] The above results are in agreement with the reported crystal structure.

C(3)-Sn-(C4)	140.9°
O(2)-Sn-O(1')	170.1°
Sn-O(2)	2.165 Å
Sn-O(1')	2.392 Å
Sn-O(1)	2.782 Å

Figure 4.11: Molecular structure of [Me$_2$Sn(O$_2$CMe)Cl] (see Allen *et al.*[236]).

Interestingly, the dibutyltin(IV) derivative appears to have a second set of ν_{as}COO$^-$ and ν_{sym}COO$^-$ stretching frequencies (1637 and 1376 cm^{-1}), where $\Delta\nu = 261$ cm^{-1}. This value is greater than $\Delta\nu$ of sodium acetate which would imply that the carboxylate may also be coordinating in a second, unidentate manner. In general, a ν_{as}COO$^-$ absorption in the range ca. 1560-1540 cm^{-1} is found for bridging organotin(IV) carboxylate compounds whereas for the unidentate structures a ν_{as}COO$^-$ absorption in the range ca. 1660-1640 has been observed.[237] In the IR spectrum of [n-Bu$_2$Sn(O$_2$CMe)Cl], the ν_{as}COO$^-$ absorption at 1637 cm^{-1} is weaker in comparison to the 1571 cm^{-1} absorption band. The two sets of ν_{as}COO$^-$ and ν_{sym}COO$^-$ stretching frequencies observed for [n-Bu$_2$Sn(O$_2$CMe)Cl] could be due to both a dimeric and a monomeric form being present in the solid state (Figure 4.12). Elemental analysis for [n-Bu$_2$Sn(O$_2$CMe)Cl] suggests the presence of one acetate molecule, one Cl atom and two n-butyl groups per tin atom, a composition that supports both the dimeric and monomeric forms in the solid state. On review of the

202

literature, there appears to be no reported crystal structure for [n-Bu$_2$Sn(O$_2$CMe)Cl] thus the exact mode of coordination is unclear.

(a)   *(b)*

Figure 4.12: Proposed structures for [n-Bu$_2$Sn(O$_2$CMe)Cl], (*a*) dimer and (*b*) monomer.

However, Honnick and Zuckerman[237] have carried out studies on [n-Bu$_2$Sn(O$_2$CMe)Cl] in an effort to determine its structure. They found that in the solid state IR spectrum a ν_{as}COO$^-$ absorption in the range 1560-1551 cm^{-1} was observed and in the solution state IR spectrum an additional ν_{as}COO$^-$ absorption at a frequency ca. 100-125 cm^{-1} higher than the solid state ν_{as}COO$^-$ absorption was observed.[237] The appearance of an additional band suggests that there is a change in structure on going from the solid to the solution state. The authors suggested a dimeric structure for [n-Bu$_2$Sn(O$_2$CMe)Cl] in which a four-membered SnO$_2$ or SnOX ring exists giving a free carboxyl group (Figure 4.13). Organotin compounds consisting of these structures are known and exhibit ν_{as}COO$^-$ absorption bands at ca. 1700 cm^{-1}.[237]

Figure 4.13: Possible dimeric equilibrium structures proposed by Honnick and Zuckerman for di-n-butyltin chloride acetate (R = n-Bu and X = Cl).[237]

4.3.3 Synthesis of the diorganotin(IV) diacetate compounds; diorganotin(IV) dipicolinate

Figure 4.14: Diorganotin(IV) dipicolinate where R = Me, n-Bu or Ph. Labelling system for ^{1}H and ^{13}C NMR also shown.

The synthesis of the [Me$_2$Sn(picolinate)$_2$] was first carried out by a method similar to that of the diorganochlorotin(IV) acetate compounds above (section 4.3.2); two equivalents of picolinic acid were stirred with two equivalents of Et$_3$N in toluene followed by the addition of Me$_2$SnCl$_2$ and a three hour reflux. The reaction mixture was allowed to cool and the resulting precipitate was collected by filtration. From the ^{1}H NMR spectrum, the reaction appeared to be successful, however, both the filter and filtrate contained the product along with the Et$_3$N.HCl by-product. In an effort to purify the product, the crude mixture was dissolved in DCM and washed with

distilled water. However, some Et$_3$N.HCl was still present in the ^{1}H NMR spectrum. The crude mixture was dissolved in DCM and n-hexane was added slowly in an attempt to purify the product by precipitation. Unfortunately, this only removed some of the Et$_3$N.HCl. Thus, on review of the literature, a different approach to the synthesis was taken which would exclude the production of Et$_3$N.HCl as a by-product.

Scheme 4.10: Synthesis of [R$_2$Sn(picolinate)$_2$]; (i) picolinic acid, Δ, 2h, toluene (method B).

[Me$_2$Sn(picolinate)$_2$] was synthesised by the procedure described by Szorcsik *et al.*[238] with some modification (Scheme 4.10). After a two hour reflux, the reaction mixture was allowed to cool and the product was collected by filtration and washed with cold MeOH. This procedure was used for the synthesis of the [n-Bu$_2$Sn(picolinate)$_2$] and [Ph$_2$Sn(picolinate)$_2$] compounds also. The compounds [Me$_2$Sn(picolinate)$_2$], [n-Bu$_2$Sn(picolinate)$_2$] and [Ph$_2$Sn(picolinate)$_2$] were obtained in good yields of 83, 80 and 77%, respectively.

In the ^{1}H NMR spectra of the diorganotin(IV) dipicolinate compounds a 1:1 acid:organic group ratio can be seen. Only small shifts in the proton signals of the picolinate groups were observed, with the largest shift observed for H-d, indicating coordination to the tin atom (Figure 4.14). However, in the ^{13}C NMR spectra a large upfield shift in C-a can be seen, indicating coordination of the pyridine ring N atom to the Sn centre. Although $^2J(^{119/117}$Sn,^{1}H) coupling constants of 76.5 and 73.5 Hz were obtained for [Me$_2$Sn(picolinate)$_2$] Equation 4.3 cannot be used to determine θ for this compound. Studies by Lockhart *et al.*[239] have found that Me$_2$Sn(chelate)$_2$ compounds (chelate = tropolonate, kojate or picolinate) do not obey these equations. It is unclear why these compounds, containing five-membered chelate rings, do not obey the equations.[239]

Due to the complex butyl region of the [n-Bu$_2$Sn(picolinate)$_2$] ^{1}H NMR spectrum, no $^2J($$^{119/117}$Sn,^{1}H) coupling constants could be obtained, but the ^2J and $^3J($^{119}Sn, ^{13}C) coupling constants (33.8 Hz and 124.5 Hz) were found. These values are in accordance with other dibutyltin(IV) compounds with ^3J larger than ^2J but without the $^1J($^{119}Sn, ^{13}C) value the coordination number about the tin atom cannot be predicted.[240] Unfortunately, no $^{119/117}$Sn coupling constants for the diphenyltin(IV) dipicolinate compound could be calculated from the ^{1}H or ^{13}C NMR spectra.

For the free picolinic acid, the νOH of the carboxylate moiety occurs at ca. 2500 cm^{-1} and disappears in the IR spectra of the dipicolinate compounds, indicating deprotonation of the COOH and coordination with the Sn(IV) molecule. In both the [Me$_2$Sn(picolinate)$_2$] and [n-Bu$_2$Sn(picolinate)$_2$] IR spectra, the presence of two ν_{as}COO$^-$ and ν_{sym}COO$^-$ stretching frequencies suggest coordination by two different modes (Table 4.6). The $\Delta\nu$ values of 326 and 323 cm^{-1} are greater than that of the picolinate sodium salt which according to Deacon and Phillips, indicate a unidentate mode of coordination.[234] The second set of ν_{as}COO$^-$ and ν_{sym}COO$^-$ stretching frequencies give $\Delta\nu$ values in the range ca. 150-200 cm^{-1}, suggesting a bridging bidentate coordination mode.

Table 4.6: IR stretching frequencies (cm^{-1}) for the diorganotin(IV) diacetate compounds.

Compound	ν_aCOO$^-$	ν_sCOO$^-$	$\Delta\nu$
Na-picolinate[238]	1607	1411	196
[Me$_2$Sn(picolinate)$_2$]	1675, 1561	1349, 1386	326, 175
[n-Bu$_2$Sn(picolinate)$_2$]	1670, 1564	1347, 1384	323, 180
[Ph$_2$Sn(picolinate)$_2$]	1678	1332	346
Na-nicotinate[241]	1615	1375	240
[Me$_2$Sn(nicotinate)$_2$]	1605	1399	206
[n-Bu$_2$Sn(nicotinate)$_2$]	1609	1409	201
[Ph$_2$Sn(nicotinate)$_2$]	1608	1411	197

The crystal structures of [Me$_2$Sn(picolinate)$_2$], [n-Bu$_2$Sn(picolinate)$_2$], and [Ph$_2$Sn(picolinate)$_2$] have been previously reported.[239,242] In each of the compounds, the two picolinic acid molecules coordinate to the Sn centre through the pyridine ring N atom and one O atom of the carboxylate moiety resulting in a five-membered chelate ring.[239,242] In [Me$_2$Sn(picolinate)$_2$] and [n-Bu$_2$Sn(picolinate)$_2$] each Sn atom is also bridged by a second O atom of one of the picolinic acids giving rise to a polymeric structure wherein the compounds are seven-coordinate with a distorted, pentagonal bipyramidal geometry (Figure 4.15).[239] [Ph$_2$Sn(picolinate)$_2$] is slightly different in structure, as it is monomeric in nature with a distorted octahedral geometry.[242] The lack of molecular aggregation in [Ph$_2$Sn(picolinate)$_2$] is believed to be due to the steric bulk of the phenyl groups.[242] The results presented above are in accordance with the reported crystal structures of the diorganotin(IV) dipicolinate compounds.

(*a*)

(*b*)
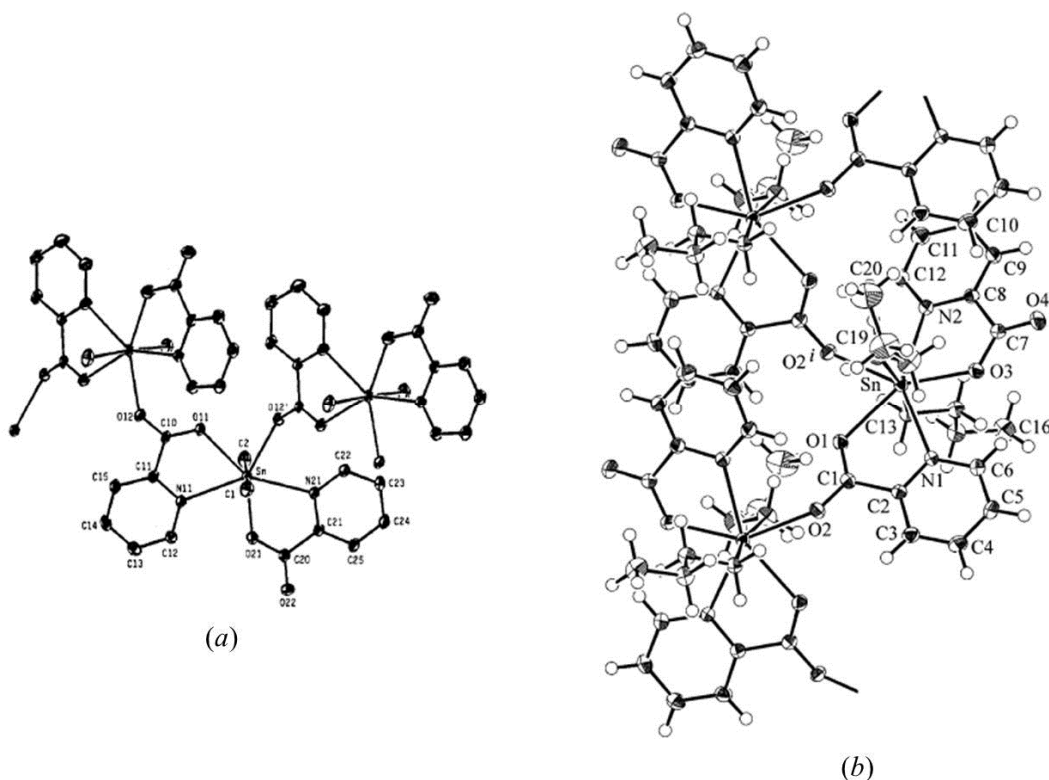
Figure 4.15: X-ray crystal structures of diorganotin(IV) dipicolinate compounds, (*a*) [Me$_2$Sn(picolinate)$_2$] and (*b*) [n-Bu$_2$Sn(picolinate)$_2$].[239,242]

207

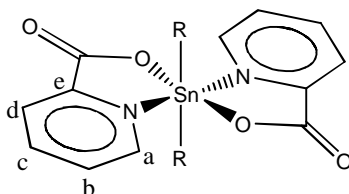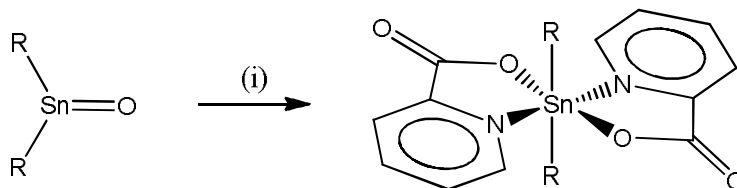### 4.3.4 Synthesis of the diorganotin(IV) diacetate compounds; diorganotin(IV) dinicotinate
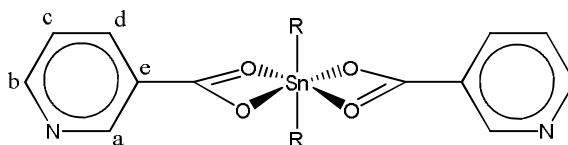
Figure 4.16: Diorganotin(IV) dinicotinate where R = Me, n-Bu or Ph. Labelling system for ^{1}H and ^{13}C NMR also shown.

The [Me$_2$Sn(nicotinate)$_2$], [n-Bu$_2$Sn(nicotinate)$_2$] and [Ph$_2$Sn(nicotinate)$_2$] derivatives were synthesised by the same method as described for the dipicolinate compounds earlier (Scheme 4.10). CHN analysis indicated formation of a 2:1 acid:metal complex and as with the dipicolinate compounds, only small shifts in the ^{1}H NMR signals were observed for the protons of the nicotinate groups. $^2J(^{119/117}$Sn,^{1}H) coupling constants for [Me$_2$Sn(nicotinate)$_2$] were not observed, however, $^3J(^{119}$Sn, ^{13}C) = 51.8 ppm for C-e (Figure 4.16) was found, indicating coordination of the carboxylate group to the Sn atom. In the ^{13}C NMR spectra, a large downfield shift has occurred with the carbonyl carbon signal for each of the dinicotinate derivatives. This is quite different to that observed for the dipicolinate compounds, in fact, unlike the dipicolinate compounds, the carbon signal for the C-H atoms adjacent to the pyridine ring N in the dinicotinate compounds do not seem to have been effected by binding to the Sn(IV) molecule. This would imply that the nicotinic acid N atom is not involved in coordination and that the carboxylate moiety is binding to the Sn(IV) molecule by a different mode of coordination to that observed for the dipicolinate compounds.

On comparing the nicotinic acid IR spectrum to the IR spectra of the dinicotinate compounds, the νOH band (ca. 2400 cm^{-1}) has disappeared, indicating deprotonation of, and binding through, the carboxylate group. Furthermore, the shift in the C=O band in the IR spectra of the three diorganotin dinicotinate compounds from 1713 cm^{-1} in nicotinic acid to 1605, 1609 and 1608 cm^{-1} was also proof of the formation of the [Me$_2$Sn(nicotinate)$_2$], [n-Bu$_2$Sn(nicotinate)$_2$] and [Ph$_2$Sn(nicotinate)$_2$] products.

Unlike the dimethyl- and di-n-butyltin(IV) dipicolinate compounds however, only one set of the $\nu_{as}COO^-$ and $\nu_{sym}COO^-$ stretching frequencies are present giving $\Delta\nu$ values of 206 and 201 cm^{-1} for [Me$_2$Sn(nicotinate)$_2$] and [n-Bu$_2$Sn(nicotinate)$_2$], respectively (Table 4.6). These $\Delta\nu$ values fall within the range of 150-200 cm^{-1} suggesting a bidentate bridging coordination mode. The diphenyltin(IV) dinicotinate compound, like [Ph$_2$Sn(picolinate)$_2$], exhibited only one $\nu_{as}COO^-$ and $\nu_{sym}COO^-$ stretching frequency with a $\Delta\nu = 197$ cm^{-1}, suggesting a bridging coordination mode for the carboxylate moiety. These results suggest that, unlike the dimethyl- and dibutyltin(IV) dipicolinates, the dinicotinate compounds do not appear to coordinate through the pyridine N atom. However, coordination does appear to be occurring through the carboxylate group most likely in a bridging behaviour.

On review of the literature there are no reported crystal structures for any of the three diorganotin(IV) dinicotinate compounds. However, Mössbauer and ^{119}Sn NMR studies have been carried out on [Me$_2$Sn(nicotinate)$_2$], [n-Bu$_2$Sn(nicotinate)$_2$] and [Ph$_2$Sn(nicotinate)$_2$] and the results point towards a distorted *trans* octahedral geometry, whereby the nicotinate groups are coordinated through the two O atoms of the carboxylate group either by a bridging or chelating mode (Figure 4.17).
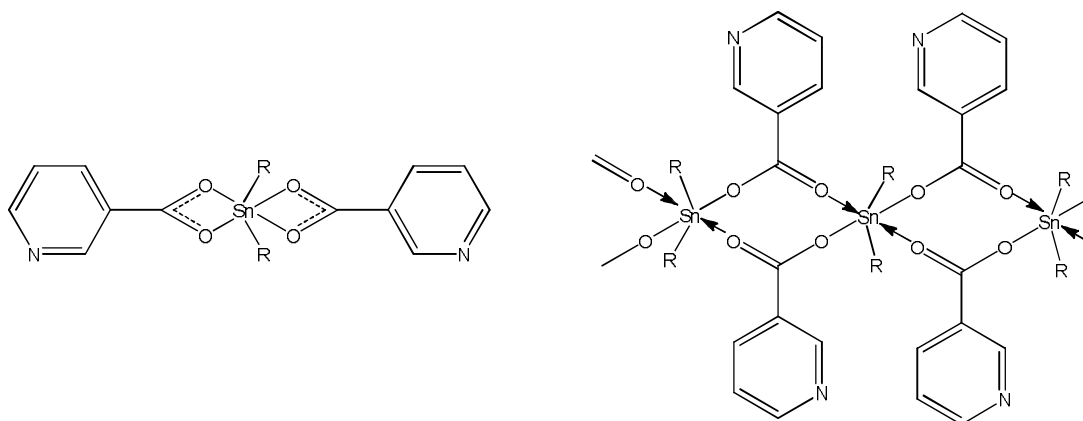
Figure 4.17: Proposed structures of diorgano(IV) dinicotinate compounds (R = Me, n-Bu or Ph).[241,243]

4.3.5 Complexation Reactions

4.3.5.1 Synthesis of [R$_2$SnCl$_2$L] complexes (R = Me, n-Bu or Ph and L = phen, dione or dppz)

Complexation reactions with the 1,10-phenanthroline ligands were first carried out with the diorganotin(IV) dichlorides, [R$_2$SnCl$_2$] (R = Me, n-Bu and Ph). The reactions involved mixing equimolar quantities of the dichlorides with the chosen ligand in EtOH at reflux temperature for three hours. After cooling the solution, the solid products precipitated out and were collected by filtration. Yields of 92, 98 and 93% were obtained for [Me$_2$SnCl$_2$(phen)], [n-Bu$_2$SnCl$_2$(phen)] and [Ph$_2$SnCl$_2$(phen)], respectively. Elemental analysis indicated that a 1:1 complex was formed between each of the the organotin(IV) compounds and the phen ligands.

In the IR spectra of [Me$_2$SnCl$_2$(phen)], [n-Bu$_2$SnCl$_2$(phen)] and [Ph$_2$SnCl$_2$(phen)] the C=N absorption of the phen ligand has shifted in frequency, from 1644 cm^{-1} to ca. 1622 cm^{-1}, indicating coordination of the phen to the organotin(IV) dichlorides. A large downfield shift in each of the proton signals of the phen ligand can also be seen in the ^{1}H NMR spectra of each of the organotin(IV) phen complexes, further confirming coordination. ^{1}H NMR data for the diorganotin(IV) dichloride complexes is given in Table 4.7.

Table 4.7: Selected ^{1}H NMR data for 1,10-phenanthroline ligands and their [R$_2$SnCl$_2$] compounds (R = Me, n-Bu or Ph) obtained in DMSO-d$_6$.

Compound	H-2[a]	H-3[a]	H-4[a]	H-5[a]	H-6[a]
phen	9.10	7.77	8.49	7.99	-
dione	8.98	7.68	8.39	-	-
dppz	9.49	7.92	9.20	8.36	8.04
[Me$_2$SnCl$_2$(phen)]	9.32	8.00	8.74	8.16	-
[Me$_2$SnCl$_2$(dione)]	9.00	7.69	8.41	-	-
[Me$_2$SnCl$_2$(dppz)]	9.42	7.91	9.20	8.29	8.01
[n-Bu$_2$SnCl$_2$(phen)]	9.44	8.16	8.90	8.27	-
[n-Bu$_2$SnCl$_2$(dione)]	-	-	-	-	-
[n-Bu$_2$SnCl$_2$(dppz)][b]	9.93	8.14	9.83	8.41	8.03
[Ph$_2$SnCl$_2$(phen)][*]	9.50	8.05	8.74	8.12	-
[Ph$_2$SnCl$_2$(phen)][#]	9.06	8.17	8.54	8.43	-
[Ph$_2$SnCl$_2$(dione)]	9.00	7.68	8.40	-	-
[Ph$_2$SnCl$_2$(dppz)]	9.44	7.95	9.26	8.28	8.00
dppz[b]	9.64	7.80	9.26	8.35	7.92

[a] Numbering system shown in Figure 4.8, [b] obtained in CDCl$_3$, [*] *trans*-isomer, [#] *cis*-isomer.

An unexpected ^{1}H NMR spectrum was obtained for [Ph$_2$SnCl$_2$(phen)], containing what appeared to be two sets of signals. A closer inspection of the ^{1}H NMR spectra using a COSY experiment indicated that there were two different [Ph$_2$SnCl$_2$(phen)] complexes present (Appendix C, Figure C1), one being more abundant than the other. These two complexes may be the *cis*- and *trans*-isomers of [Ph$_2$SnCl$_2$(phen)]. In order to investigate this possibility the ^{1}H NMR experiment was repeated but at a higher temperature (70 $^{\circ}$C) (Appendix C, Figure C2). The resulting ^{1}H NMR spectrum had only one set of signals present, supporting the above suggestion.

The X-ray crystal structures for [Me$_2$SnCl$_2$(phen)], [n-Bu$_2$SnCl$_2$(phen)] and [Ph$_2$SnCl$_2$(phen)] have been reported (Figure 4.18). In each derivative, the organo

groups sit in the axial positions with the phen ligand and two chlorine atoms occupying the equatorial positions, resulting in an octahedral geometry about the Sn(IV) centre.[244] For [Ph$_2$SnCl$_2$(phen)], having the phenyl groups *trans* to one another must be the most stable arrangement which is understandable considering the bulky nature of the phenyl groups. However, in the ^{1}H NMR spectrum there appears to be two complexes present. Tin complexes are known to alter their structure on changing from one phase to another, thus, it may be that in solution the complex can exist as two isomers, the most abundant being the more favourable *trans*-isomer.[161]
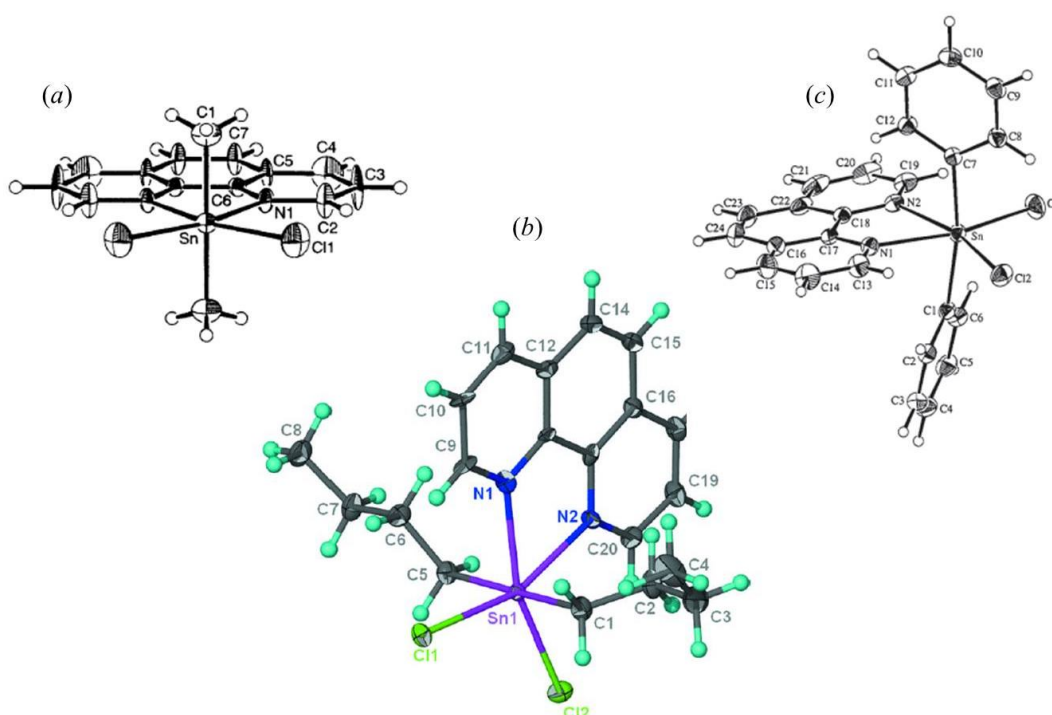
Figure 4.18: X-ray crystal structures of (*a*) [Me$_2$SnCl$_2$(phen)], (*b*) [n-Bu$_2$SnCl$_2$(phen)] and (*c*) [Ph$_2$SnCl$_2$(phen)].[244]

For the dione and dppz organotin(IV) complexes, shifts in the ^{1}H NMR signals of the ligands were also observed, although these are much smaller in nature in comparison to the organotin(IV) phen complexes (Table 4.7). This is unusual as both ligands are 1,10-phenanthroline derivatives and so chelation is expected to occur through the two nitrogen atoms which should result in shifts in the ^{1}H NMR signals similar in size to those of the phen complexes. These small shifts suggest that there is little

interaction between the ligand and the Sn(IV) centre. If the size of the ligand was an issue then it would be expected that the dppz ligand would cause problems and not the dione ligand. However, the size of the ligand cannot really be an issue, as the binding site is remote from the rest of the molecule and is consistent amongst the series.

A second explanation for the lack of interaction, with regards to the dione ligand, may be because of its dual binding ability. As mentioned earlier, dione has two potential binding sites through the diiminic and *o*-quinonoid functionalities. If binding is occurring through the *o*-quinonoid functionality then little effect on the proton NMR signals of dione would be expected. If it is binding through both functionalities then it may be forming a polymer. This may also be the reason why the NMR data for the [n-Bu$_2$SnCl$_2$(dione)] derivative was very complex.

In the IR spectrum of the free dione ligand, the stretching frequency of the C=O band occurs at 1686 cm^{-1} (Table 4.8). On examining the IR spectra of the organotin(IV) dione complexes a shift of ca. 10-30 cm^{-1} in the ν(C=O) absorption to a higher frequency (in the range 1690-1720 cm^{-1}) can be seen, indicating interaction of the ligand with the organotin(IV) dichloride. If binding was occurring through the *o*-quinonoid functionality of dione, much larger shifts (ca. 200-300 cm^{-1}) would be expected.[216] Considering that the C=O moieties are far from the coordination site of the ligand these small shifts suggest the formation of *N,N'*-coordinated complexes with the tin atom.[206,216,245]

Table 4.8: IR absorption bands for the free dione ligand and the [R$_2$SnCl$_2$(dione)] complexes (R = Me, n-Bu and Ph).

Compound	ν(C=O)	ν(C=N)/ν(C=C)	ν(C-N-C)
dione	1686	1574, 1566	738
[Me$_2$SnCl$_2$(dione)]	1700	1573	732
[n-Bu$_2$SnCl$_2$(dione)]	1718	1584	720
[Ph$_2$SnCl$_2$(dione)]	1694	1574	727

The crystal structure of [Ph$_2$SnCl$_2$(dione)]·2MeCO has been reported, and is similar to the structure reported for [Ph$_2$SnCl$_2$(phen)] with the phenyl groups in a *trans* arrangement and the dione ligand coordinated through its diiminic functionality.[244c,246] The Sn-N bond lengths, 2.394 and 2.405 Å, are only slightly longer than those of [Ph$_2$SnCl$_2$(phen)] (2.341 and 2.378 Å).[244c,246] With regards to the dione complexes synthesised here, perhaps the dione ligand does bind through the N atoms as suggested by the IR data but only associates weakly in solution giving rise to only small shifts in the ^{1}H NMR signals. Similarly, with the dppz complexes, the IR spectra of each of the complexes indicate binding through the N atoms of the ligand (Table 4.9). Absorption bands for ν(C=N) and ν(C=C) in the 1640-1400 cm^{-1} range were observed for the free dppz ligand. These bands have shifted to a lower frequency in the IR spectra of the complexes, thus, indicating coordination of the N atoms to the metal centre. However, in the ^{1}H NMR spectra of the dppz complexes, the small shifts in the proton signals of the dppz ligand suggest weak binding has occurred in solution. The elemental analysis for the dione and dppz complexes suggest formation of 1:1 complexes with the organotin(IV) dichlorides.

Table 4.9: IR absorption bands for the free dppz ligand and the [R$_2$SnCl$_2$(dppz)] complexes (R = Me, n-Bu and Ph).

Compound	ν(C=N)/ν(C=C)	ν(C-N-C)	Other absorption bands
dppz	1634, 1586	740	1490, 1415, 1362, 1338, 1074
[Me$_2$SnCl$_2$(dppz)]	1632, 1572	734	1493, 1420, 1359, 1075
[n-Bu$_2$SnCl$_2$(dppz)]	1631, 1574	736	1493, 1419, 1361, 1076
[Ph$_2$SnCl$_2$(dppz)]	1627, 1574	735	1494, 1420, 1428, 1361, 1078

4.3.5.2 Synthesis of [R$_2$Sn(O$_2$CMe)Cl(L)] complexes (R = Me, n-Bu or Ph and L = phen, dione or dppz)

An attempt to synthesise [R$_2$Sn(O$_2$CMe)Cl(phen)] was first carried out using the most soluble of the three organochlorotin(IV) acetates, [n-Bu$_2$Sn(O$_2$CMe)Cl], under the same reaction conditions as described earlier for the synthesis of [R$_2$SnCl$_2$(phen)] (section 4.3.5.1). Unexpectedly, the reaction was unsuccessful, returning only a mixture of starting materials. Hence the reaction was repeated with longer reaction

times. The reaction was allowed to reflux for a total of 24 hours and monitored by ^{1}H NMR spectroscopy, but no shift in the proton signals of the phen ligand was observed. It was thought that perhaps a different solvent was required, therefore, MeCN was chosen in an effort to increase the Lewis acidity of the Sn(IV) centre and thus help drive the reaction forward.

The first reaction was carried out at room temperature with stirring overnight, but was unsuccessful. Heating of the reaction mixture (40-50 ^{o}C) was attempted with monitoring over 24 hours but was also unsuccessful. Finally, a 24 hour reflux in MeCN was attempted but this also failed to give the [n-Bu$_2$Sn(O$_2$CMe)Cl(phen)] complex. With the steric bulk of the n-butyl groups in mind, the reaction was attempted with [Me$_2$Sn(O$_2$CMe)Cl] instead. The reaction was carried out in EtOH at reflux temperature for three hours but no product was observed in the ^{1}H NMR spectrum. The reaction was also attempted in MeCN but again the reaction failed to produce the [Me$_2$Sn(O$_2$CMe)Cl(phen)] complex.

After the unsuccessful attempts to synthesise [Me$_2$Sn(O$_2$CMe)Cl(phen)] and [n-Bu$_2$Sn(O$_2$CMe)Cl(phen)] it was unlikely that the dione and dppz complexes would form. An attempt was made to synthesise both the dione and dppz complexes of the dimethyltin and dibutyltin monoacetate derivatives. As expected, these experiments were unsuccessful. Due to the failed attempts of these reactions no attempts were made to synthesise the [Ph$_2$Sn(O$_2$CMe)Cl(L)] derivatives (L = phen, dione or dppz).

As mentioned earlier, the [Me$_2$Sn(O$_2$CMe)Cl] is polymeric in nature and can achieve a six-coordinate geometry through bridging of the carboxylate group. If the organotin(IV) monoacetate compounds have achieved the six-coordinate geometry in solution then in order for the phen ligands to bind to the Sn(IV) centre the bridging must initially be disrupted. Binding of a phen-based ligand would result in the formation of a seven-coordinate tin species as proposed in Figure 4.19. However, the phen ligands are relatively large, planar (or near planar) and rigid in nature and so may be unable to 'fit' into the geometry constraint required by the proposed seven coordination.
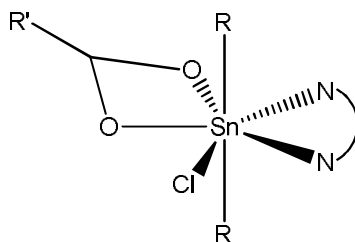
Figure 4.19: Proposed seven-coordinate organotin(IV) structure (R = Me, n-Bu, or Ph and N∩N = phen, dione or dppz).

4.3.5.3 Synthesis of [R₂Sn(picolinate)₂L] complexes (R = Me, n-Bu or Ph and L = phen, dione or dppz)

In an effort to synthesise [Me₂Sn(picolinate)₂(phen)] a 1:1 mixture of phen and [Me₂Sn(picolinate)₂] were heated to reflux in EtOH for one, three, five and eight hours. In all cases, the resulting precipitate that formed on cooling was [Me₂Sn(picolinate)₂] only, with the filtrate containing phen and a small proportion of [Me₂Sn(picolinate)₂]. With the lack of complexation in EtOH the reaction was attempted in MeCN. Again, on cooling [Me₂Sn(picolinate)₂] precipitated out of solution and the filtrate contained mostly phen. However, there was a shift in the ¹H NMR signals of the phen ligand suggesting the possible formation of a complex. In an effort to remove the excess phen the crude solid was washed with cold ethanol returning [Me₂Sn(picolinate)₂] as the solid product. A second wash of the crude solid obtained from the filtrate was then carried out with hot toluene, the resulting filter was [Me₂Sn(picolinate)₂] and the filtrate contained phen. No [Me₂Sn(picolinate)₂(phen)] was found.

The complexation reactions were also attempted with [n-Bu₂Sn(picolinate)₂] and [Ph₂Sn(picolinate)₂] in EtOH and MeCN but the same result was obtained. An attempt to synthesise the dione and dppz complexes of [Me₂Sn(picolinate)₂] was also carried out in EtOH but with no success.

It is not entirely surprising that these complexation reactions did not work. As mentioned earlier, the structures of the three organotin(IV) dipicolinates used in this study are known. Each of the compounds contain two bulky picolinate groups, each of which forms a five-membered chelate ring resulting from the coordination of the

pyridine ring N atom and a carboxylate O atom. Although coordination numbers of eight and even ten have been reported for tin complexes, the phen ligands are planar (or near planar), rigid molecules which will probably not 'fit' into the existing seven- and six-coordinate geometries of the organotin(IV) dipicolinates.[161,247] If a phen ligand is to bind to the tin atom then either the Sn-N or the Sn-O bond of the five-membered chelate rings must first be broken in order to make way for the phen ligand, as shown in Figure 4.18. It is believed that these complexes did not form because of these steric restrictions.
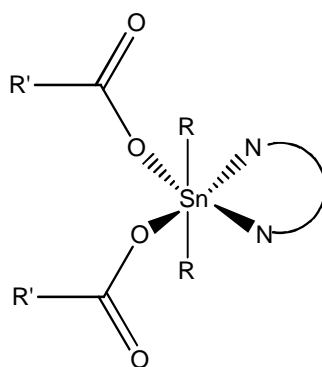
Figure 4.18: Expected structure of 1:1 complex of organotin(IV) dipicolinate and 1,10-phenathroline derivatives, where R = Me, n-Bu or Ph; N∩N = 1,10-phenathroline derivative; R'CO$_2$ = picolinate group.

4.3.5.4 Synthesis of [R$_2$Sn(nicotinate)$_2$L] complexes (R = Me, n-Bu or Ph and L = phen, dione or dppz)

The [R$_2$Sn(nicotinate)$_2$(phen)] and dppz complexes were synthesised using the same procedure as that of the [R$_2$SnCl$_2$(phen)] complexes (section 4.3.5.1). In the ^{1}H NMR spectra of both [Me$_2$Sn(nicotinate)$_2$(phen)] and [n-Bu$_2$Sn(nicotinate)$_2$(phen)] a large downfield shift was observed for the proton signals of the phen ligand (Table 4.10). As expected, H-2 has the largest shift indicating coordination through the two N atoms of the phen ligand.

Table 4.10: Selected ^{1}H NMR data for 1,10-phenanthroline ligands and their [R$_2$Sn(nicotinate)$_2$] complexes obtained in DMSO-d$_6$ (R = Me, Bu or Ph).

Compound	H-2[a]	H-3[a]	H-4[a]	H-5[a]	H-6[a]
phen	9.10	7.77	8.49	7.99	-
[Me$_2$Sn(nicotinate)$_2$(phen)]	9.46	8.00	8.73[b]	8.15	-
[n-Bu$_2$Sn(nicotinate)$_2$(phen)]	9.48	8.04	8.77	8.17	-
[Ph$_2$Sn(nicotinate)$_2$(phen)]	9.09	7.78	8.49	7.96[c]	-
dppz	9.49	7.92	9.20	8.36	8.04
[Me$_2$Sn(nicotinate)$_2$(dppz)]	9.55	7.98	9.27	8.39	8.07
[n-Bu$_2$Sn(nicotinate)$_2$(dppz)]	9.40	7.98	9.31	8.23	7.98

[a] Numbering system shown in Figure 4.8, [b] shares peak with nicotinate proton, [c] shares peak with phenyl proton.

Only the [Me$_2$Sn(nicotinate)$_2$] and [n-Bu$_2$Sn(nicotinate)$_2$] compounds could be complexed with the dppz ligand. In comparison to the [R$_2$Sn(nicotinate)$_2$(phen)] analogues, much smaller shifts in the ^{1}H NMR signals of the dppz ligand were observed. A similar trend was observed earlier for the [R$_2$SnCl$_2$L] complexes (section 4.3.5.1). It may be that in solution the dppz ligand only associates weakly with the tin atom resulting in smaller shifts in the ^{1}H NMR spectra.

Amongst the [R$_2$Sn(nicotinate)$_2$(phen)] complexes synthesised here, the smallest shifts in the ^{1}H NMR signals of the phen ligand were observed for [Ph$_2$Sn(nicotinate)$_2$(phen)]. The [Ph$_2$Sn(nicotinate)$_2$] compound consists of two phenyl groups and two nicotinate groups bound to the tin atom. These bulky groups may be making it sterically difficult for the relatively large and planar phen ligand to interact strongly with the Sn centre resulting in only small shifts in the ^{1}H NMR signals. The complexation reaction of [Ph$_2$Sn(nicotinate)$_2$] and dppz was unsuccessful. The dppz ligand is a larger molecule with an extended aromatic structure in comparison to phen making it even more difficult to 'fit in' and bind to the tin centre.

Elemental analysis for each of the complexes synthesised indicated formation of a 1:1 phen:metal or dppz:metal complex. In the IR spectra of the phen and dppz free ligands the absorption bands for ν(C=N) and ν(C=C) are found in the 1640-1400 cm^{-1} range (Table 4.11), so too are the ν_{as}(COO$^-$) and ν_{sym}(COO$^-$) stretching frequencies of the [R$_2$Sn(nicotinate)$_2$] compounds, resulting in complicated IR spectra. However, in the IR spectra of the [R$_2$Sn(nicotinate)$_2$] phen and dppz complexes the absorption bands in the 1640-1400 cm^{-1} range have broadened and shifted frequency, confirming coordintation of the ligands to the tin centres (Table 4.11).

Table 4.11: A selection of the IR absorption bands in the 1700-1400 cm^{-1} range.

Compound	IR absorption bands (cm^{-1})
phen	1643, 1617, 1586, 1561, 1504, 1495, 1422
[Me$_2$Sn(nicotinate)$_2$(phen)]	1645, 1625, 1590, 1428, 1332,
[n-Bu$_2$Sn(nicotinate)$_2$(phen)]	1648, 1625, 1599,1588, 1552, 1426
[Ph$_2$Sn(nicotinate)$_2$(phen)]	1709, 1655, 1596, 1419
dppz	1634, 1586, 1490, 1415
[Me$_2$Sn(nicotinate)$_2$(dppz)]	1605, 1592, 1554, 1486, 1415
[n-Bu$_2$Sn(nicotinate)$_2$(dppz)]	1606, 1593, 1553, 1407

The synthesis of the [R$_2$Sn(nicotinate)$_2$(dione)] complexes was attempted using the same procedure as described for the phen and dppz derivatives, but were unsuccessful. Extended reaction times (24 hours) and a change in solvent (MeCN) were also attempted but the reaction still failed to produce a [R$_2$Sn(nicotinate)$_2$(dione)] complex. If the size of the dione ligand was the issue then

a similar outcome to that of the dppz complexes would be expected where the [Me$_2$Sn(nicotinate)$_2$(dione)] and [n-Bu$_2$Sn(nicotinate)$_2$(dione)] would form but perhaps the [Ph$_2$Sn(nicotinate)$_2$(dione)] complex would not. However, none of the [R$_2$Sn(nicotinate)$_2$(dione)] complexes could be synthesised. As suggested earlier with the [R$_2$SnCl$_2$(dione)] complexes, maybe the dual binding ability of the dione ligand is causing problems. However, being the stronger site of Lewis basicity, coordination is expected to occur through the diiminic functionality of dione as is seen with the phen and dppz ligands.[206] In comparison to phen, the dione ligand is slightly non-planar.[206] Perhaps this slight deviation in planarity prohibits the dione ligand from accessing the tin centre of the R$_2$Sn(nicotinate)$_2$ compounds thus preventing formation of the [R$_2$Sn(nicotinate)$_2$(dione)] complexes.

All attempts to obtain ^{119}Sn NMR spectra of the complexes obtained during this study always resulted in broad signals being observed, no matter what solvent was chosen or the number of scans used. This is despite the fact that clean ^{1}H and ^{13}C spectra were readily obtained for the same samples.

4.3.6 Biological studies

4.3.6.1 Antibacterial activity

The antibacterial activity of the organotin(IV) complexes synthesised in this study, along with their starting materials, was investigated using the susceptibility assay described in section 1.2.5. Three bacteria were chosen for the study, two Gram-negative bacteria, *Escherichia coli* (*E. coli*) and *Pseudomonas aeruginosa (P. aeruginosa)*, and one Gram-positive bacterium *Staphylococcus aureus (S. aureus)*. The MIC$_{50}$ and MIC$_{80}$ values were taken to signify the concentration of compound that would inhibit the growth of the microorganism by 50% and 80%, respectively. The results are summarised in Tables 4.12 and 4.13. Any compound which did not exhibit an MIC$_{80}$ and/or MIC$_{50}$ for any of the three chosen bacteria has been excluded from the tables. Vancomycin hydrochloride and ciprofloxacin were chosen as the positive controls.

Of all of the organotin(IV) starting materials tested, the n-Bu$_2$SnCl$_2$ was the most active, exhibiting activity against all three bacteria. In general, the organotin(IV)

oxides were less active than the dichlorides. However, n-Bu$_2$SnO could not be tested due to its lack of solubility in the water/DMSO mixture. Acetic acid, picolinic acid and nicotinic acid were inactive against each of the bacteria tested. Amongst the phen ligands investigated, the only ligand to exhibit activity against all three bacteria was the dione. This ligand has been previously shown to be very active against several microbes, including the yeast, *Candida albicans*.[71,217] Furthermore, McCann and co-workers have shown that when a silver(I) ion is complexed with dione, an increase in activity is observed.[220]

Table 4.12: Antibacterial activity as MIC_{50} range, values are the mean of three experiments.

Compound	E. coli		P. aeruginosa		S. aureus	
	μM	μg/mL	μM	μg/mL	μM	μg/mL
Vancomycin hydrocloride	1.58-2.10	2.35-3.13	>67.31	>100.00	1.58-2.10	2.35-3.13
Ciprofloxacin	2.36-3.53	0.78-1.17	0.20-0.39	0.59-1.18	28.31-37.75	9.38-12.5
phen	> 554.91	>100.00	416.18-554.91	75.00-100.00	277.45-416.18	50.00-75.00
dione	14.88-22.34	3.13-4.69	14.88-22.34	3.13-4.69	29.76-44.63	6.25-9.38
[Me$_2$SnCl$_2$]	341.08-454.78	75.00-100.00	341.08-454.78	75.00-100.00	> 454.78	>100.00
[n-Bu$_2$SnCl$_2$]	15.44-20.56	4.69.-6.25	164.48-246.73	50.00-75.00	20.56-30.84	6.25-9.38
[Ph$_2$SnCl$_2$]	54.52-72.69	18.75-25.00	> 290.77	>100.00	> 290.77	>100.00
[Me$_2$SnO]	451.96-602.61	75.00-100.00	451.96-602.61	75.00-100.00	> 602.61	>100.00
[n-Bu$_2$Sn(O$_2$CMe)Cl]	28.58-38.11	9.38-12.50	> 304.85	>100.00	38.11-57.16	12.50-18.75
[Ph$_2$SnCl(O$_2$CMe)]	25.48-33.97	9.38-12.50	> 271.77	>100.00	16.99-25.48	6.25-9.38
[Me$_2$SnCl$_2$(phen)]	> 250.03	>100.00	125.01-187.52	50.00-75.00	> 250.03	>100.00
[n-Bu$_2$SnCl$_2$(phen)]	25.82-38.74	12.50-18.75	103.30-154.94	50.00-75.00	25.82-38.74	12.50-18.75

Table 4.12 *continued.*

Compound	*E. coli*		*P. aeruginosa*		*S. aureus*	
	μM	μg/mL	μM	μg/mL	μM	μg/mL
[Me$_2$SnCl$_2$(dione)]	43.61-58.15	18.75-25.00	21.81-29.07	9.38-12.50	29.08-43.61	12.50-18.75
[n-Bu$_2$SnCl$_2$(dione)]	18.24-24.32	9.38-12.50	145.91-194.54	75.00-100.00	48.64-72.95	25.00-37.50
[Ph$_2$SnCl$_2$(dione)]	22.57-33.85	12.50-18.75	22.57-33.85	12.50-18.75	5.64-8.47	3.13-4.69
[n-Bu$_2$SnCl$_2$(dppz)]	16.00-21.33	9.38-12.50	170.63+	100.00+	21.33-31.99	12.50-18.75
[Ph$_2$SnCl$_2$(dppz)]	*> 159.74*	*>100.00*	79.87-119.81	50.00–75.00	59.90-79.87	37.50–50.00
[n-Bu$_2$Sn(picolinate)$_2$]	39.22-52.29	18.75–25.00	*> 209.17*	*>100.00*	26.15-39.22	12.50–18.75
[Ph$_2$Sn(picolinate)$_2$]	*> 193.04*	*>100.00*	*> 193.04*	*>100.00*	96.52-144.78	50.00–75.00
[n-Bu$_2$Sn(nicotinate)$_2$]	39.22-52.29	18.75–25.00	*> 209.17*	*>100.00*	26.15-39.22	12.50–18.75
[Ph$_2$Sn(nicotinate)$_2$]	72.39-96.52	37.50–50.00	*> 193.04*	*>100.00*	*> 193.04*	*>100.00*
[n-Bu$_2$Sn(nicotinate)$_2$(phen)]	56.98-75.97	37.50–50.00	*> 151.94*	*>100.00*	75.97-113.95	50.00–75.00
[n-Bu$_2$Sn(nicotinate)$_2$(dppz)]	32.89-49.33	25.00–37.50	*> 131.55*	*>100.00*	98.66-131.55	75.00–100.00

Table 4.13: Antibacterial activity as MIC_{80} range, values are the mean of three experiments.

Compound	E. coli		P. aeruginosa		S. aureus	
	μM	μg/mL	μM	μg/mL	μM	μg/mL
Vancomycin hydrochloride	2.10-3.16	3.13-4.69	>67.31	>100.00	3.16-4.21	4.69-6.25
Ciprofloxacin	>301.99	>100.00	1.18-1.77	0.39-0.59	>301.99	>100.00
dione	29.76-44.63	6.25-9.38	22.34-29.76	4.69-6.25	44.63-59.51	9.38-12.50
[Me$_2$SnCl$_2$]	>454.78	>100.00	341.08-454.78	75.00-100.00	>454.78	>100.00
[n-Bu$_2$SnCl$_2$]	41.12-61.68	12.50-18.75	>328.99	>100.00	41.12-61.68	12.50-18.75
[Ph$_2$SnCl$_2$]	218.08-290.77	75.00-100.00	>290.77	>100.00	>290.77	>100.00
[n-Bu$_2$SnCl(O$_2$CMe)]	114.32-152.43	37.50-50.00	>304.86	>100.00	114.32-152.43	37.50-50.00
[Ph$_2$SnCl(O$_2$CMe)]	135.88-203.83	50.00-75.00	>271.77	>100.00	67.94-101.91	25.00-37.50
[n-Bu$_2$SnCl$_2$(phen)]	77.47-103.30	37.50-50.00	154.94-206.59	75.00-100.00	38.74-51.65	18.75-25.00
[Me$_2$SnCl$_2$(dione)]	>232.60	>100.00	43.61-58.15	18.75-25.00	43.61-58.15	18.75-25.00
[n-Bu$_2$SnCl$_2$(dione)]	36.48-48.64	18.75-25.00	>194.54	>100.00	145.91-194.54	75.00-100.00
[Ph$_2$SnCl$_2$(dione)]	>180.52	>100.00	33.85-45.13	18.75-25.00	16.92-22.56	9.38-12.50

Table 4.13 *continued.*

Compound	*E. coli*		*P. aeruginosa*		*S. aureus*	
	μM	μg/mL	μM	μg/mL	μM	μg/mL
[n-Bu$_2$SnCl$_2$(dppz)]	63.99-85.31	37.50-50.00	>170.63	>100.00	31.99-42.66	18.75-25.00
[n-Bu$_2$Sn(picolinate)$_2$]	156.87-209.17	75.00-100.00	>209.17	>100.00	52.29-78.44	25.00-37.50
[n-Bu$_2$Sn(nicotinate)$_2$]	104.58-156.87	50.00-75.00	>209.17	>100.00	78.44-104.58	37.50-50.00
[n-Bu$_2$Sn(nicotinate)$_2$(phen)]	113.95-151.94	75.00-100.00	>151.94	>100.00	113.95-151.94	75.00-100.00
[n-Bu$_2$Sn(nicotinate)$_2$(dppz)]	98.66-131.55	75.00-100.00	>131.55	>100.00	>131.55	>100.00

225

From Table 4.12, it can be seen that on changing from the organotin(IV) dichloride to the organochlorotin(IV) acetate, the dimethyl and dibutyl derivatives became less active. With regards to the dibutyltin derivatives, introduction of the dinicotinate and dipicolinate moieties resulted in a further loss in activity against *E. coli* but a slight increase in activity against *S. aureus*, in comparison to [n-Bu$_2$Sn(O$_2$CMe)Cl].

The opposite, however, is seen in the case of the diphenyl derivatives, with the [Ph$_2$Sn(O$_2$CMe)Cl] being more active than its dichloride precursor against both *E. coli* and *S. aureus*. However, [Ph$_2$Sn(picolinate)$_2$] and [Ph$_2$Sn(nicotinate)$_2$] are, as in the case of the dibutyltin(IV) derivatives, less active than [Ph$_2$Sn(O$_2$CMe)Cl]. [Me$_2$Sn(O$_2$CMe)Cl], [Me$_2$Sn(nicotinate)$_2$] and [Me$_2$Sn(picolinate)$_2$] did not exhibit activity against *S. aureus* or *E. coli* and, unfortunately, none of the carboxylate derivatives demonstrated any activity against *P. aeruginosa*.

Graphs 4.1-4.6 show the activity profiles for the phen, dione and dppz complexes that were active against *E. coli* and *S. aureus*. Of all of the compounds complexed with a phen, dione or dppz ligand, the dione complexes were the most active. Moreover, upon complexation of dione with the dimethyl- and diphenlytin(IV) dichlorides, an increase in activity was observed in comparison to the parent organotin(IV). For example, treatment of *S. aureus* with [Ph$_2$SnCl$_2$(dione)] resulted in a MIC$_{50}$ of 3.13-4.69 μg/mL, whereas, its precursor Ph$_2$SnCl$_2$ was inactive against *S. aureus*. This result may be attributed to chelation theory. As mentioned earlier, a reduction in the polarity of the metal can occur upon chelation, resulting in an increase in lipophillicity.[198-199] This increased lipophilicity can assist the passage of the metal complex through cell membranes, in turn, allowing it to interact with the cells internal components and therefore inhibit growth.

The opposite effect is seen with n-Bu$_2$SnCl$_2$, that is, a decrease in activity against *E. coli* and *S. aureus* is observed upon complexation with phen, dione or dppz. If we consider [n-Bu$_2$SnCl$_2$(phen)] and its activity against *S. aureus*, n-Bu$_2$SnCl$_2$ is more active, reaching a MIC$_{50}$ in the range of 6.25-9.38 μg/mL while the phen ligand alone is less active than [n-Bu$_2$SnCl$_2$(phen)]. Similar results have been reported

previously, and are believed to be due to complexation preventing the binding of the metal to the active site.[193b]
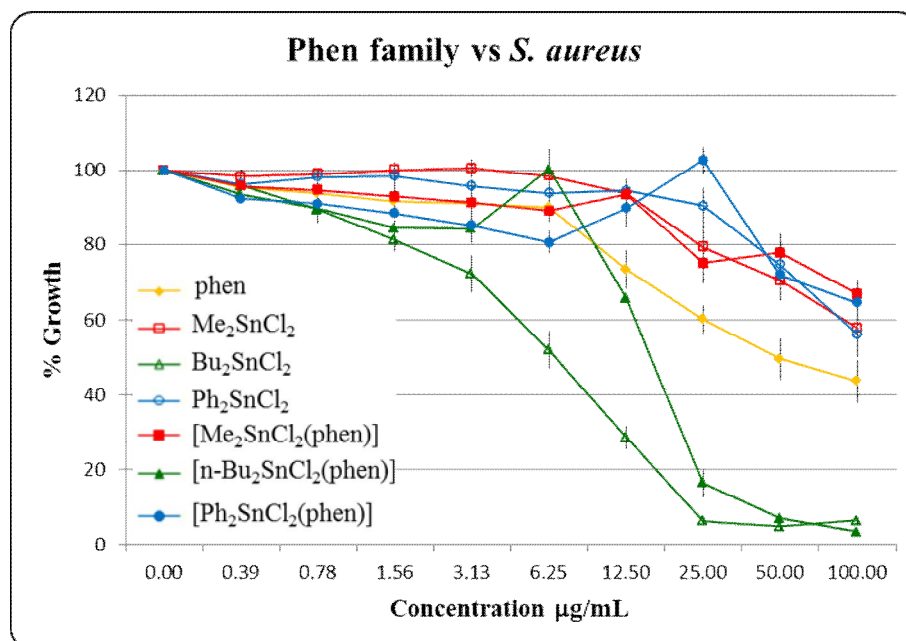
Graph 4.1: Activity profile of $[R_2SnCl_2(phen)]$ family versus *S. aureus*, where R = Me, n-Bu or Ph.
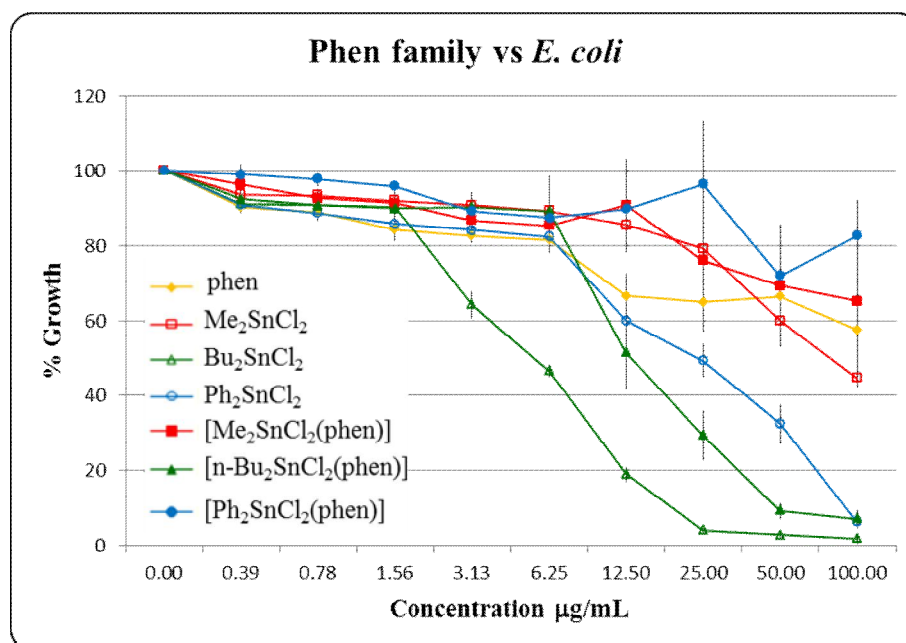
Graph 4.2: Activity profile of $[R_2SnCl_2(phen)]$ family versus *E. coli*, where R = Me, n-Bu or Ph.
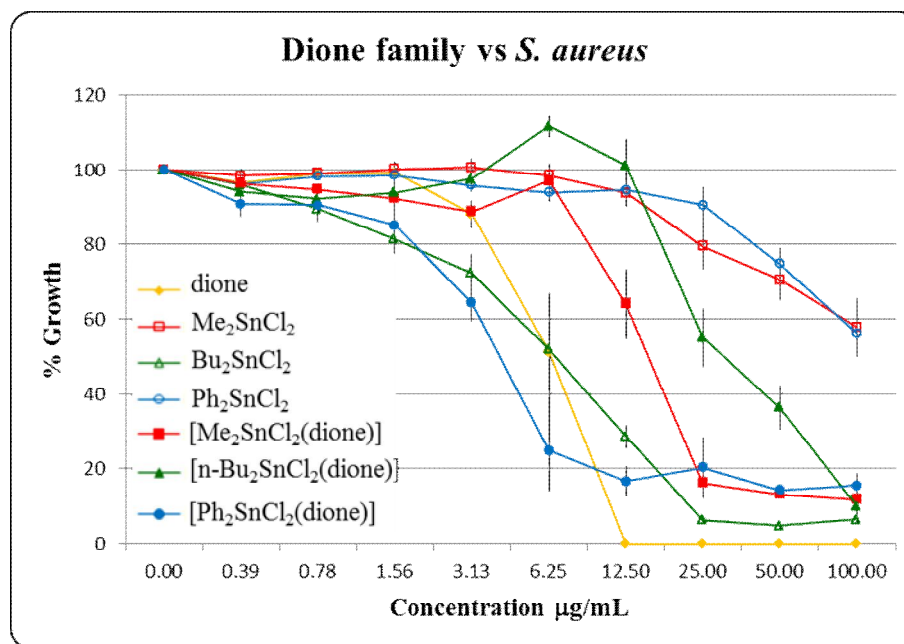
Graph 4.3: Activity profile of [R$_2$SnCl$_2$(dione)] family versus *S. aureus*, where R = Me, n-Bu or Ph.
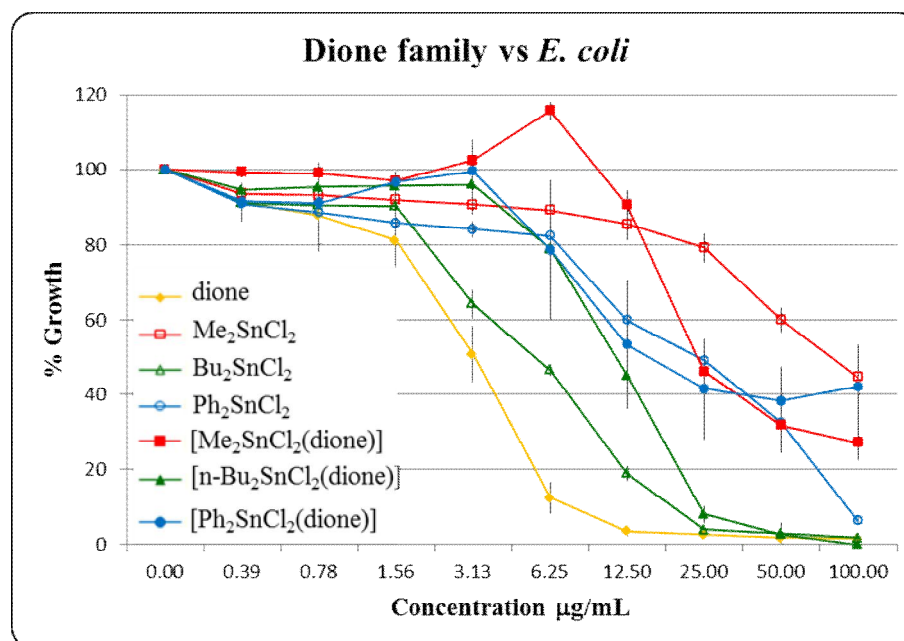
Graph 4.4: Activity profile of [R$_2$SnCl$_2$(dione)] family versus *E. coli*, where R = Me, n-Bu or Ph.

228
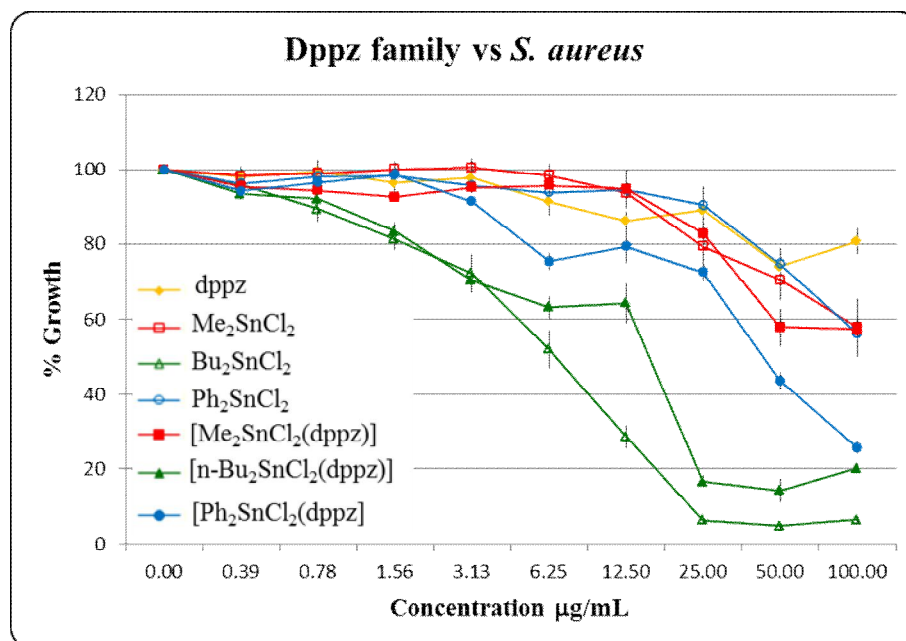
Graph 4.5: Activity profile of [R_2SnCl_2(dppz)] family versus *S. aureus*, where R = Me, n-Bu or Ph.
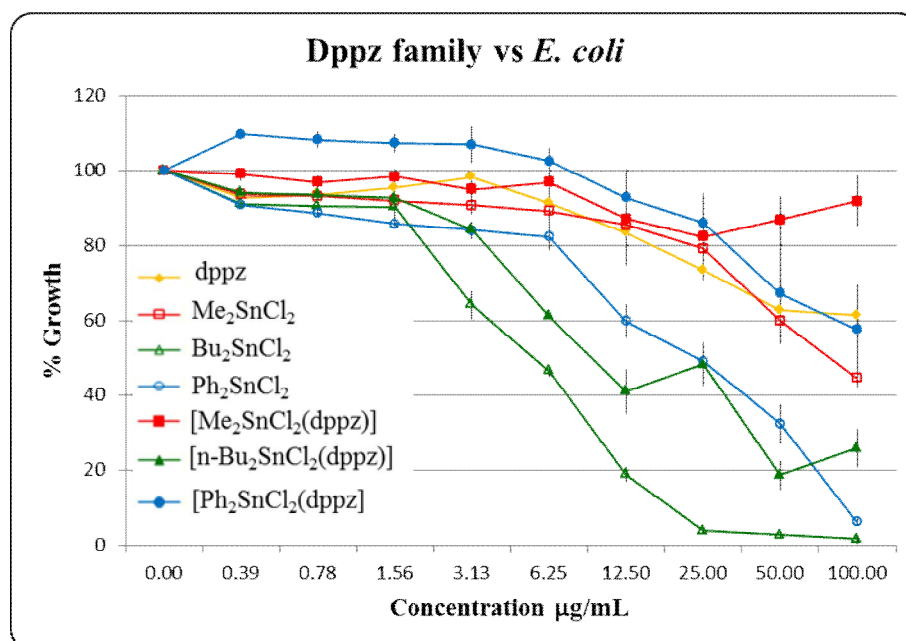
Graph 4.6: Activity profile of [R_2SnCl_2(dppz)] family versus *E. coli*, where R = Me, n-Bu or Ph.

In general, the majority of complexes synthesised exhibited little or no activity against *P. aeruginosa*. However, of the active complexes, [Me_2SnCl_2(dione)] and [Ph_2SnCl_2(dione)] exhibited good activity against *P. aeruginosa* giving an MIC_{50} range of 9.38-12.50 and 12.50-18.75 μg/mL, respectively. In both cases, the values were less than that of the parent organotin(IV) dichloride but greater than the dione ligand alone.

Of the active complexes listed in Table 4.12, [Ph_2SnCl_2(dione)] was the most active against *S. aureus*, [n-Bu_2SnCl_2(dione)] was the most active against *E. coli* and [Me_2SnCl_2(dione)] was the most active against *P. aeruginosa*. Considering these three complexes differ only by their organic group, it could be suggested that there is a degree of selectivity with regards to the bacterium and the type of organic group attached to the tin centre.

A total of twenty two compounds were synthesised and tested in this study, fifteen of these exhibited an MIC_{50}, with activity being mainly against *E. coli* and *S. aureus*. According to the literature, organotin compounds have a tendency to be more active against Gram-positive bacteria compared to Gram-negative bacteria.[191d,193a,194a,197] However, within this study, many of the active compounds exhibited similar activity against both *E. coli* and *S. aureus* and in some cases better activity was observed against *E. coli* in comparison to *S. aureus*, for example, [n-Bu_2SnCl_2(dione)]. Gram-positive and Gram-negative bacteria differ mainly in their cell wall structures, with the Gram-negative bacteria having an extra outer membrane in comparison to the Gram-positive bacteria.[14] Organotin(IV) compounds exhibiting similar activity against both *E. coli* and *S. aureus* could suggest that the extra outer membrane of the Gram-negative *E. coli* is not an obstacle for these compounds and that perhaps they are inhibiting growth by interacting with the internal components of the bacteria.

Overall, the dibutyltin(IV) derivatives were most active in comparison to the dimethyltin(IV) or diphenyltin(IV) derivatives. Introduction of a carboxylate moiety, in general, did not promote activity. Complexation with a phen, dione or dppz ligand gave mixed results, with the dione complexes exhibiting greatest activity. The

organotin(IV) compounds synthesised in this study demonstrated greatest activity against *E. coli* and *S. aureus* and were almost inactive against *P. aeruginosa*.

P. aeruginosa is well-known for its ability to grow as a biofilm, by doing so it creates a physical barrier to antibiotics.[42] Furthermore, *P. aeruginosa* produces a thick capsule which retards the entry of antibiotics.[39] It is possible that it is having the same action here, preventing entry of the organotin complexes.

Although some of the compounds tested here exhibited good activity, no compound exhibited activity greater than that of the standard, vancomycin hydrochloride. Of all of the organotin(IV) compounds synthesised and tested in this study, $[Ph_2SnCl_2(dione)]$ gave the best MIC_{50} result of 3.13-4.69 µg/mL against *S. aureus*, and thus, was chosen for further testing against *Galleria melonella*.

4.3.7 *In vivo* compound tolerance

The *in vivo* toxicity of $[Ph_2SnCl_2(dione)]$ was tested as described in section 1.2.8, using the larvae of the greater wax moth, *Galleria melonella* (*G. melonella*). The results are presented as the survival of *G. mellonella* larvae (expressed as %) as a function of the $[Ph_2SnCl_2(dione)]$ dosages administered (Table 4.14). The toxicity of dione in *G. melonella* has been tested previously by McCann *et al.*[71], the results of which have been included in Table 4.14 for comparison.

Table 4.14: Survival of *G. mellonella* larvae (expressed as %) post injection at 24, 48 and 72 h.

Compound	Dosage concentration (µg/mL)	*G. mellonella* survival		
		24	48	72
dione	100	-	-	100[71]
$[Ph_2SnCl_2(dione)]$	100	100	100	100
	50	100	100	97
	10	100	100	100
	1	100	100	100

From Table 4.14 it can be seen that, at the highest concentration of $[Ph_2SnCl_2(dione)]$ administered, there was a 100% survival rate. This result is in

agreement with that of the dione ligand alone which is also non-toxic at a concentration of 100 μg/mL, at 72 hours. The same result was also observed at the lower concentrations, with the exception of the 50 μg/mL dosage at 72 hours, where one *G. mellonella* died. The *G. mellonella* were also monitored for pupation. It was found that after seven days, 90% of the *G. mellonella* larvae had pupated. This result suggests that not only was [Ph$_2$SnCl$_2$(dione)] non-toxic at the highest concentration administered, but it also appears to have no effect on the development of the larvae, at this concentration. These results for [Ph$_2$SnCl$_2$(dione)] suggest that it may have potential as a non-toxic, antibacterial compound.

4.3.8 Conclusion

Herein, the synthesis of diorganotin(IV) dichloride complexes of the ligands, phen, dione and dppz was undertaken. Diorganochlorotin(IV) acetates and diorganotin(IV) dicarboxylates, including complexes of the biologically active groups picolinic acid and nicotinic acid, were also synthesised. Complexation reactions of these diorganotin(IV) carboxylates with the phen ligands only occurred for the [R$_2$Sn(nicotinate)$_2$] compounds. This is probably due to the difficulty in breaking the intra- and/or intermolecular interactions involved in the diorganotin(IV) carboxylate derivatives. In general, good yields were obtained for the majority of compounds, with the greatest yields obtained for the diorganotin(IV) dichloride complexes of the phen, dione and dppz ligands. The use of three different organic groups, combined with organic groups capable of unidentate and/or bidentate coordination modes, allowed for the generation of a variety of structures amongst the diorganotin(IV) compounds. All of the organotin(IV) compounds synthesised were characterised by CHN analysis, ^{1}H and ^{13}C NMR and IR spectroscopies.

Overall, the organotin(IV) compounds tested here demonstrated greatest activity against *E. coli* and *S. aureus* and were almost inactive against *P. aeruginosa.* In general, the addition of either a nicotinic acid or picolinic acid did not promote the inhibition of bacterial growth. Amongst the phen, dione and dppz ligands tested, the dione was the most active, producing MIC$_{80}$ values in the range of 6.25-9.38 μg/mL for *E. coli*, 4.69-6.25 μg/mL for *P. aeruginosa* and 9.38-12.50 μg/mL for *S. aureus.*

Of the phen, dione and dppz complexes synthesised, the [R_2SnCl_2(dione)] complexes demonstrated greatest activity. Within the [R_2SnCl_2(dione)] series, the dimethyl was the most active against *P. aeruginosa*, the di-n-butyl was most active against *E. coli*, and the diphenyl was most active against *S. aureus*, indicating a possible degree of selectivity with regards to the R group.

Although many of the organotin(IV) compounds exhibited activity, no compound exhibited activity greater than that of the standard antibacterial agent, vancomycin hydrochloride, against *E. coli* or *S. aureus*. However, [Ph_2SnCl_2(dione)] gave a *S. aureus* MIC_{50} value in the range of 3.13-4.69 μg/mL, a value close to that exhibited by vancomycin hydrochloride (2.35-3.13 μg/mL).

[Ph_2SnCl_2(dione)] was the most active organotin(IV) compound tested here and was therefore brought forward for an *in vivo* toxicity study. The results indicated that, at concentrations in the range of 1-100 μg/mL, [Ph_2SnCl_2(dione)] is non-toxic to *G. mellonella*.

4.3.9 Future Work

Having given the best result in inhibiting bacterial growth, specifically the growth of *S. aureus*, an investigation into the bactericidal activity of [Ph_2SnCl_2(dione)] would be of interest. Although the number of Methicillin-Resistant *S. aureus* (MRSA) infections in Ireland has seen a decrease from 2004 to 2013, Ireland was ranked 10th highest amongst twenty-eight European countries in 2011.[31] Furthermore, with regards to the MRSA proportions (%) of *S. aureus* infections, many European countries, such as Portugal and Italy, have been reported as having some of the highest (between 25 and 50% in 2012).[31] Therefore, an assessment of the activity of [Ph_2SnCl_2(dione)] against MRSA would also be worthwhile. In the *in vivo* toxicity assay, [Ph_2SnCl_2(dione)] was found to be non-toxic against *G. mellonella* at concentrations in the range of 1-100 μg/mL, a result similar to that of the previously reported dione ligand alone.[71] However, at higher concentrations, that is, 1000 μg/mL, dione has demonstrated a 90% mortality rate in the *G. mellonella* toxicity assay.[71] Therefore, it would be of interest to examine the toxicity of [Ph_2SnCl_2(dione)] at higher concentrations.

In this study, it was the [R_2SnCl_2(dione)] complexes that exhibited activity against all three bacteria. As mentioned earlier, an interesting trend was observed amongst the [R_2SnCl_2(dione) complexes with regards to the R group and the bacterium to which it was most active against, suggesting a possible degree of selectivity. It would be interesting to examine if this selectivity would be retained after alteration of the X group, that is, the dichloride. Additionally, it could be worth varying the R group in an effort to obtain an R group that would result in activity against all three bacteria.

The molecular target of these organotin(IV) complexes is currently unknown. Considering that dione alone has the ability to bind DNA it would be interesting to investigate the biological mode of action of these complexes. An investigation into the DNA binding capabilities of the complexes, along with an assessment of the proteomic response of the bacterium to the complexes, could give insight into a possible mode of action.

4.4 Experimental

The synthesis of 1,10-phen-5,6-dione (dione)[232a]
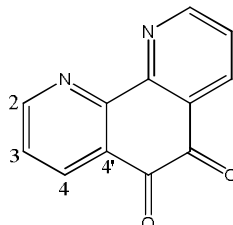
An ice-cold solution of sulphuric acid (40 mL) and nitric acid (20 mL) was added to 1,10-phenanthroline (4.0 g, 22.2 mmol) and potassium bromide (4.0 g, 33.6 mmol) on ice. The reaction mixture was heated to reflux for 3 hours and then poured into 500 mL of ice-cold water. The yellow solution was neutralised with 5M NaOH and the product extracted with CHCl$_3$ (3 x 200 mL) and dried over Na$_2$SO$_4$. The CHCl$_3$ was removed under reduced pressure and the product was purified by hot EtOH recrystallisation.

Yellow solid (4.08 g, 88%); m.p. 258-262 ^{o}C (lit 270 ^{o}C)[222]; ^{1}H NMR (300 MHz, DMSO-d$_6$) δ 8.98 (dd, *J* = 4.7, 1.7 Hz, 2H, *H*2), 8.39 (dd, *J* = 7.8, 1.7 Hz, 2H, *H*4), 7.68 (dd, *J* = 7.8, 4.7 Hz, 2H, *H*3); ^{13}C NMR (75 MHz, DMSO-d$_6$) δ 177.7 (*C*=O) 154.3 (*C*2), 152.3 (*C*=N), 135.6 (*C*4), 129.1 (*C*4'), 125.2 (*C*3); IR (KBr) 1686 (C=O), 1574 (C=N), 1567 (C=C), 1415 (C-H), 738 (C-N-C) cm^{-1}; LC/TOF-MS calcd for C$_{12}$H$_6$N$_2$O$_2$ 210.0434, found 211.0502 (M+H$^+$).

The ^{1}H NMR data for dione was also obtained in CDCl$_3$.

^{1}H NMR (300 MHz, CDCl$_3$) δ 9.10 (dd, *J* = 4.7, 1.8 Hz, 2H, *H*2), 8.49 (dd, *J* = 7.8, 1.8 Hz, 2H, *H*4), 7.57 (dd, *J* = 7.8, 4.7 Hz, 2H, *H*3), these data match reported literature values[248].

The synthesis of dipyrido[3,2-a:2',3'-c]phenazine (dppz)[232b]
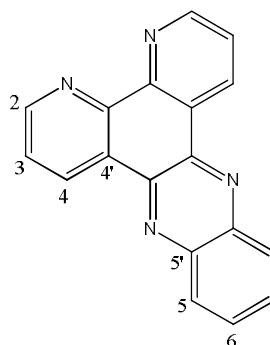
1,10-Phen-5,6-dione (0.5 g, 2.4 mmol) and *o*-phenylenediamine (0.3 g, 2.8 mmol) were heated in EtOH (198 mL) at 50 °C for 2 hours followed by an overnight reflux. The reaction mixture was allowed to cool to room temperature and the EtOH removed under reduced pressure. The resulting solid was allowed to sit for 8 hours at room temperature after which MeOH:water (10:90) was added and the product collected *via* filtration. The product was purified by hot MeOH recrystallisation.

Yellow solid (0.5 g, 75% recrystallised); m.p. 246-250 °C (lit 246-247 °C)[249]; ^{1}H NMR (300 MHz, DMSO-d$_6$) δ 9.49 (dd, J = 8.1, 1.8 Hz, 2H, *H*2), 9.20 (dd, J = 4.4, 1.8 Hz, 2H, *H*4), 8.36 (dd, J = 6.5, 3.4 Hz, 2H, *H*5), 8.04 (dd, J = 6.5, 3.4 Hz, 2H, *H*6), 7.92 (dd, J = 8.1, 4.4 Hz, 2H, *H*3), these data match reported literature values[250]; ^{13}C NMR (75 MHz, DMSO-d$_6$) δ 152.3 (*C*4), 147.8 (*C*=N), 141.7 (*C*=N), 140.7 (*C*5'), 133.0 (*C*2), 131.2 (*C*6), 129.1 (*C*5), 126.9 (*C*4'), 124.5 (*C*3); IR (KBr) 1634 (C=N), 1585 (C=C) 1490, 1415, 1362, 1338 (C-H), 1075 (C-N), 741 (C-N-C) cm^{-1}; LC/TOF-MS calcd for C$_{18}$H$_{10}$N$_4$ 282.0905, found 283.0982 (M+H$^+$).

The ^{1}H NMR data for dione was also obtained in CDCl$_3$.

^{1}H NMR (300 MHz, CDCl$_3$) δ 9.64 (dd, J = 8.1, 1.7 Hz, 2H, *H*2), 9.26 (dd, J = 4.5, 1.7 Hz, 2H, *H*4), 8.35 (dd, J = 6.5, 3.4 Hz, 2H, *H*5), 7.92 (dd, J = 6.5, 3.4 Hz, 2H, *H*6), 7.80 (dd, J = 8.1, 4.5 Hz, 2H, *H*3).

^{1}H NMR (300 MHz, DMSO-d$_6$, 80 °C) δ 9.41 (dd, J = 8.1, 1.7 Hz, 2H, *H*2), 9.13 (d, J = 4.3, 2H, *H*4), 8.27 (dd, J = 6.5, 3.4 Hz, 2H, *H*5), 7.98 (dd, J = 6.5, 3.4 2H, *H*6), 7.85 (dd, J = 8.1, 4.3 Hz, 2H, *H*3); ^{13}C NMR (75 MHz, DMSO-d$_6$) δ 152.1 (*C*4),

147.7 (*C*=N), 141.6 (*C*=N), 140.5 (*C*5'), 132.9 (*C*2), 131.0 (*C*6), 128.9 (*C*5), 126.7 (*C*4'), 124.3 (*C*3).

^{1}H NMR (300 MHz, DMSO-d$_6$, 95 $^{\circ}$C) δ 9.45 (dd, *J* = 8.1, 1.7 Hz, 2H, *H*2), 9.15 (app br s, 2H, *H*4), 8.30 (dd, *J* = 6.5, 3.5 Hz, 2H, *H*5), 7.99 (dd, *J* = 6.5, 3.5 Hz, 2H, *H*6), 7.87 (dd, *J* = 8.1, 4.4 Hz, 2H, *H*3); ^{13}C NMR (75 MHz, DMSO-d$_6$) δ 161.6 (*C*4), 151.9 (*C*=N), 141.6 (*C*=N), 140.4 (*C*5'), 132.8 (*C*2), 130.9 (*C*6), 128.8 (*C*5), 126.7 (*C*4'), 124.1 (*C*3).

General procedure for the synthesis of [R$_2$Sn(O$_2$CMe)Cl], R = Me, n-Bu
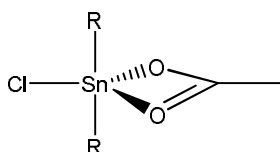
The appropriate diorganotin(IV) dichloride (4.5 mmol) and acetic acid (9.1 mmol) were dissolved in toluene (25 mL). Triethylamine (10 mmol) was added slowly and the reaction mixture heated to reflux for 3 hours under nitrogen. On cooling, a white solid precipitated, which was removed by filtration through celite. The resulting filtrate was collected and the solvent was removed under reduced pressure.

[Me$_2$Sn(O$_2$CMe)Cl]

White solid (0.80 g, 73%); m.p. >300 $^{\circ}$C; ^{1}H NMR (300 MHz, CDCl$_3$) δ 1.93 (s, 3H, O$_2$CC*H*$_3$), 0.78 (s, 3H, C*H*$_3$, $^{2}J(^{119/117}$Sn, ^{1}H) = 92.7/82.2 Hz), 0.75 (s, 3H, C*H*$_3$, $^{2}J(^{119/117}$Sn, ^{1}H) = 139.8/126.6 Hz); ^{13}C NMR (75 MHz, CDCl$_3$) δ 177.7 (*C*=O), 22.9 (O$_2$C*C*H$_3$), 8.8 (*C*H$_3$), 6.0 (*C*H$_3$); IR (KBr) 3439, 3004, 2915, 1564 (v_aCOO$^-$), 1420 (v_sCOO$^-$), 1336 (C-H), 1022 (C-O) cm^{-1}; Anal. (%) calcd for C$_4$H$_9$ClO$_2$Sn C, 19.75; H, 3.73; found C, 20.19; H, 3.55.

[n-Bu$_2$Sn(O$_2$CMe)Cl]

White waxy solid (1.30 g, 88%); m.p. 36-39 $^{\circ}$C; ^{1}H NMR (300 MHz, CDCl$_3$) δ 1.95 (s, 3H, OCOC*H*$_3$), 1.58-1.68 (m, 4H, C*H*$_2$), 1.31-1.42 (m, 8H, C*H*$_2$), 0.87-0.93 (m, 6H, C*H*$_3$); ^{13}C NMR (75 MHz, CDCl$_3$) δ 177.2 (*C*=O), 27.5 (*C*H$_2$), 27.2 (*C*H$_2$), 26.9

(CH_2), 26.7 (CH_2), 22.9 (O_2CCH_3), 13.5 (CH_3); IR (KBr) 3429, 2958, 2928, 2872 (CH), 1637, 1571 (v_aCOO⁻), 1428, 1376 (v_sCOO⁻), 1312, 1012, 737 cm^{-1}; Anal. (%) calcd for $C_{10}H_{21}ClO_2Sn \cdot 1/4(C_6H_5CH_3)$ C, 40.27; H, 6.81; found C, 39.28; H, 6.84.

The synthesis of [Ph₂Sn(O₂CMe)Cl]
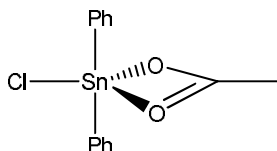
Diphenyltin(IV) dichloride (4.5 mmol) and acetic acid (10 mmol) were dissolved in benzene (25 mL). Potassium carbonate (10 mmol) was added and the reaction mixture was allowed to reflux overnight under nitrogen. The reaction mixture was allowed to cool and was filtered through celite. The filtrate was collected and the solvent removed under reduced pressure.

Cream solid (1.29 g, 79%); m.p. >300 °C;

The NMR spectra obtained for [Ph₂Sn(O₂CMe)Cl] were poorly resolved due to the lack of solubility of the compound.

^{1}H NMR (300 MHz, CDCl₃): δ 7.63-7.74 (m, phenyl C*H*), 7.35-7.50 (m, phenyl C*H*), 2.15 (s, O₂CC*H₃*); ^{13}C NMR (75 MHz, CDCl₃): δ 178.5 (*C*=O), 136.8 (phenyl C*H*), 129.9 (phenyl C*H*), 128.8 (phenyl C*H*), 20.7 (O₂C*C*H₃), (the phenyl quaternary carbon is believed to be under one of the above peaks); IR (KBr) 3044, 1551 (v_aCOO⁻), 1480, 1429 (v_sCOO⁻), 1076, 728, 696, 443 cm^{-1}; Anal. (%) calcd for $C_{14}H_{13}ClO_2Sn$ C, 45,77; H, 3.57; found C, 45.08; H, 3.24.

General procedure for the synthesis of [R$_2$Sn(nicotinate)$_2$] and [R$_2$Sn(picolinate)$_2$], R = Me, n-Bu or Ph
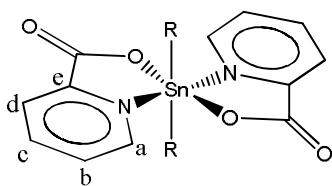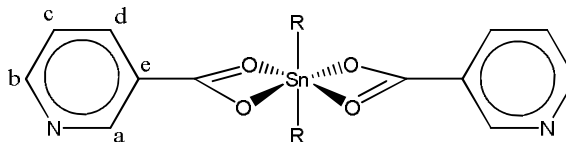
Diorganotin(IV) dipicolinate   Diorganotin(IV) dinicotinate

Method A:

The appropriate acid (2.4 mmol) and triethylamine (2.4 mmol) were stirred in toluene for 10 minutes. The appropriate diorganotin(IV) dichloride (1.2 mmol) was then added and the solution was allowed to reflux for 3 hours. The reaction mixture was allowed to cool and the solvent was removed under reduced pressure to give a white solid.

Method B:

The appropriate diorganotin(IV) oxide (1.2 mmol) and the desired acid (2.4 mmol) were brought to reflux in toluene for 2 hours. The reaction mixture was allowed to cool and the solvent was removed under reduced pressure. The resulting white solid was washed with cold MeOH and collected *via* filtration.

[Me$_2$Sn(picolinate)$_2$]

White solid (method A: 0.41 g, 86% crude, method B: 0.39 g, 83%); m.p. 259-262 $^{\circ}$C, (lit 258-261 $^{\circ}$C)[243]; ^{1}H NMR (300 MHz, CDCl$_3$) δ 8.73 (d, J = 5.0 Hz, 2H, *H*a), 8.39 (d, J = 8.0 Hz, 2H, *H*d), 8.02 (app t, J = 7.8 Hz, 2H, *H*c), 7.56-7.61 (m, 2H, *H*b), 0.59 (s, 6H, C*H*$_3$, $^2J(^{119/117}$Sn, ^{1}H) = 76.5/73.5 Hz); ^{13}C NMR (75 MHz, CDCl$_3$) δ 164.7 (*C*=O), 146.3 (*C*e), 144.6 (*C*a), 140.9 (*C*c), 128.0 (*C*b), 125.8 (*C*d), 8.5 (*C*H$_3$); IR (KBr) 3421, 3097, 2920, 1675 (v$_a$COO$^-$), 1625 (C=C), 1601 (N=C), 1561 (v$_a$COO$^-$), 1386 (v$_s$COO$^-$), 1349 (v$_s$COO$^-$), 1013, 850, 693, 635 (C=N), 547 (vSn-C) cm^{-1}; Anal. (%) calcd for C$_{14}$H$_{14}$N$_2$O$_4$Sn C, 42.79; H, 3.59; N, 7.13; found C, 42.17; H, 3.66; N, 6.99.

[n-Bu₂Sn(picolinate)₂]

White solid (method B: 0.46 g, 80%); m.p. 186-190 $^{\circ}$C; ^{1}H NMR (300 MHz, CDCl₃) δ 8.73 (d, J = 5.1 Hz, 2H, Ha), 8.40 (d, J = 8.1 Hz, 2H, Hd), 8.02 (app t, J = 8.1 Hz, 2H, Hc), 7.55-7.60 (m, 2H, Hb), 1.14-1.29 (m, 12H, CH_2), 0.73 (t, J = 7.0 Hz, 6H, CH_3); ^{13}C NMR (75 MHz, CDCl₃) δ 165.4 (C=O), 147.1 (Ce), 145.4 (Ca), 140.6 (Cc), 127.6 (Cb), 125.6 (Cd), 28.0 (CH₂), 27.3 (CH₂, ^{2}J(^{119}Sn, ^{13}C) = 33.8 Hz), 26.2 (CH₂, ^{3}J($^{119/117}$Sn, ^{13}C) = 124.5/122.3 Hz), 13.3 (CH₃); IR (KBr) 3421, 3091, 2958, 2921, 2861 (CH), 1670 (v_aCOO⁻), 1627 (C=C), 1608 (N=C), 1564 (v_aCOO⁻), 1384 (v_sCOO⁻), 1347 (v_sCOO⁻), 1012, 703, 635 (C=N), 542 (Sn-C) cm⁻¹, these data match reported literature values[251]; Anal. (%) calcd for C₂₀H₂₆N₂O₄Sn C, 50.34; H, 5.49; N, 5.87; found C, 51.51; H, 5.68; N, 5.82.

[Ph₂Sn(picolinate)₂]

White solid (method B: 0.48 g, 77%); m.p. 273-276 $^{\circ}$C (lit 274-277 $^{\circ}$C)[243]; ^{1}H NMR (300 MHz, CDCl₃) δ 8.64 (d, J = 5.0 Hz, 2H, Ha), 8.40 (d, J = 7.7 Hz, 2H, Hd), 7.91 (app t, J = 7.7 Hz, 2H, Hc), 7.42-7.49 (m, 6H, Hb & phenyl CH), 7.13-7.18 (m, 6H, phenyl CH); ^{13}C NMR (75 MHz, CDCl₃) δ 164.6 (C=O), 146.3 (Ce), 145.8 (phenyl quaternary C), 144.2 (Ca), 141.4 (Cc), 134.5 (phenyl CH), 129.2 (phenyl CH), 128.6 (phenyl CH), 128.4 (Cb), 125.9 (Cd); IR (KBr) 3433, 3068, 1678 (v_aCOO⁻), 1600 (N=C), 1467, 1332 (v_sCOO⁻), 1160, 851, 696, 643 (C=N), 534 (Sn-C) cm⁻¹; Anal. (%) calcd for C₂₄H₁₈N₂O₄Sn C, 55.74; H, 3.51; N, 5.42; found C, 55.41; H, 3.45; N, 5.31.

[Me₂Sn(nicotinate)₂]

White solid (method B: 0.36 g, 76%); m.p. dec; ^{1}H NMR (300 MHz, DMSO-d₆) δ 9.05 (s, 2H, Ha), 8.71 (d, J = 4.7 Hz, 2H, Hb), 8.24 (dt, J = 7.8, 1.9 Hz, 2H, Hd), 7.78 (dd, J = 7.8, 4.7 Hz, 2H, Hc), 0.94 (s, 6H, CH_3); ^{13}C NMR (75 MHz, DMSO-d₆) δ 170.2 (C=O), 152.4 (Cb), 150.3 (Ca), 136.9 (Cd), 128.4 (Ce, ^{3}J(^{119}Sn, ^{13}C) = 51.8 Hz), 123.5 (Cc), 11.4 (CH₃); IR (KBr) 3422, 3063, 1605 (v_aCOO⁻), 1593 (N=C), 1554 (C=C), 1441, 1417, 1399 (v_sCOO⁻), 1195, 867, 712, 435 (Sn-O) cm⁻¹; Anal.

(%) calcd for $C_{14}H_{14}O_2N_2O_4Sn$ requires C, 42.29; H, 3.59; N, 7.13; found C, 42.38; H, 3.21; N, 7.32.

[n-Bu₂Sn(nicotinate)₂]

White solid (method B: 0.41 g, 72%); m.p. 152-158 $^\circ$C; ^{1}H NMR (300 MHz, DMSO-d$_6$) δ 9.07 (s, 2H, *H*a), 8.75 (d, *J* = 4.2 Hz, *H*b), 8.26 (d, *J* = 7.8 Hz, 2H, *H*d), 7.52 (dd, *J* = 7.8, 4.2 Hz, 2H, *H*c), 1.53-1.63 (m, 8H, C*H*₂), 1.24-1.36 (m, 4H, C*H*₂), 0.81 (t, *J* = 7.3 Hz, 6H, C*H*₃); ^{13}C NMR (75 MHz, DMSO-d$_6$) δ 170.9 (*C*=O), 152.6 (*C*b), 150.3 (*C*a), 136.9 (*C*d), 127.9 (*C*e), 123.6 (*C*c), 29.8 (*C*H₂), 26.8 (*C*H₂, $^2J(^{119}Sn, {}^{13}C) = 40.5$ Hz), 25.6 (*C*H₂), 13.5 (*C*H₃); IR (KBr) 3426, 2955, 2925, 2867 (CH), 1609 (ν_aCOO$^-$), 1551, 1592 (N=C), 1434, 1409 (ν_sCOO$^-$), 1196, 863, 756, 518 (Sn-C), 431 (Sn-O) cm^{-1}, these data match reported literature values[251,241]; Anal. (%) calcd for $C_{20}H_{26}N_2O_4Sn \cdot H_2O$ C, 48.51; H, 5.70; N, 5.66; found C, 49.11; H, 5.52; N, 5.50.

[Ph₂Sn(nicotinate)₂]

White solid (method A: 0.56 g, 90% crude, method B: 0.45 g, 73%); m.p. >300 $^\circ$C; ^{1}H NMR (300 MHz, DMSO-d$_6$): δ 9.11 (s, 2H, *H*a), 8.77 (d, *J* = 4.8 Hz, 2H, *H*b), 8.31 (d, *J* = 8.4 Hz, 2H, *H*d), 7.80 (d, *J* = 8.5 Hz, 4H, phenyl C*H*), 7.52 (dd, *J* = 8.4, 4.8 Hz, 2H, *H*c), 7.23-7.37 (m, 6H, phenyl C*H*), these data match reported literature values[252]; ^{13}C NMR (75 MHz, DMSO-d$_6$) δ *169.3 (*C*=O), 153.1 (*C*b), 150.4 (*C*a), *148.6 (phenyl quaternary *C*), 137.1 (*C*d), 134.0 (phenyl *C*H), 128.7 (phenyl *C*H), 128.1 (phenyl *C*H), 127.0 (*C*e), 123.7 (*C*c); IR (KBr) 3422, 3076, 1608 (ν_aCOO$^-$), 1592 (N=C), 1541 (C=C), 1440, 1412 (ν_sCOO$^-$), 1195, 871, 695, 446 (Sn-O) cm^{-1}; Anal. (%) calcd for $C_{24}H_{18}N_2O_4Sn$ C, 55.74; H, 3.51; N, 5.42; found C, 55.91; H, 3.49; N, 5.28. *The compound is not very soluble and as a result these signals are very weak.

General procedure for the synthesis of 1,10-phenanthroline derivatives of [R$_2$SnCl$_2$] R = Me, n-Bu or Ph

The appropriate diorganotin(IV) compound (4.5 mmol) and the appropriate 1,10-phenanthroline derivative (4.5 mmol) were dissolved in EtOH (25 mL) and heated to reflux for 3 hours. On cooling a solid precipitated which was collected by filtration, was washed with EtOH and allowed to dry to yield the desired product.

(R = Me, n-Bu, Ph)
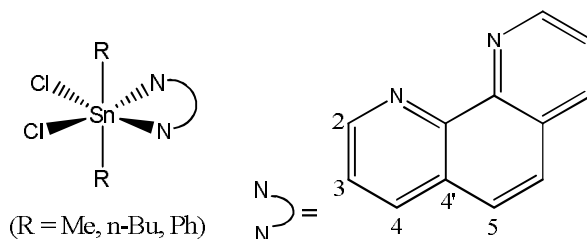
[Me$_2$SnCl$_2$(phen)]

White solid (1.68 g, 92%); m.p. dec (lit 264 $^{\circ}$C)[244a]; ^{1}H NMR (300 MHz, DMSO-d$_6$) δ 9.32 (dd, J = 4.6, 1.7 Hz, 2H, H2), 8.74 (dd, J = 8.1, 1.7 Hz, 2H, H4), 8.16 (s, 2H, H5), 8.00 (dd, J = 8.1, 4.6 Hz, 2H, H3), 0.97 (s, 6H, CH_3, ^{2}J($^{119/117}$Sn, ^{1}H) = 114.5/109.5 Hz); ^{13}C NMR (75 MHz, DMSO-d$_6$) δ 148.9 (C2), 142.4 (C=N), 138.2 (C4), 129.1 (C4'), 127.1 (C5), 124.4 (C3), 24.0 (CH$_3$); IR (KBr) 3435, 2920 (CH), 1622 (C=N), 1572, 1519, 1429, 853, 727 (C-N-C) cm^{-1}; Anal. (%) calcd for C$_{14}$H$_{14}$N$_2$Cl$_2$Sn C, 42.05; H, 3.53; N, 7.01; found C, 42.90; H, 3.75; N, 7.37.

[Me$_2$SnCl$_2$(phen)] showed improved solubility in DMSO-d$_6$ at 70 $^{\circ}$C and hence the data were recorded at 70 $^{\circ}$C.

^{1}H NMR (300 MHz, DMSO-d$_6$, 70 $^{\circ}$C) δ 9.38 (dd, J = 4.6, 1.6 Hz, 2H, H2), 8.75 (dd, J = 8.1, 1.6 Hz, 2H, H4), 8.15 (s, 2H, H5), 8.02 (dd, J = 8.1, 4.6, Hz, 2H, H3), 0.99 (s, 6H, CH_3, ^{2}J($^{119/117}$Sn, ^{1}H) = 113.1/108.0Hz); ^{13}C NMR (75 MHz, DMSO-d$_6$) δ 148.1 (C2), 141.3 (C=N), 138.1 (C4), 128.8 (C4'), 126.7 (C5), 124.1 (C3), 23.3 (CH$_3$).

[n-Bu₂SnCl₂(phen)]

White solid (2.12 g, 98%); m.p. 192-195 $^{\circ}$C (lit 198-199 $^{\circ}$C)[253]; ^{1}H NMR (300 MHz, DMSO-d₆) δ 9.44 (dd, *J* = 4.7, 1.4 Hz, 2H, *H*2), 8.90 (dd, *J* = 8.2, 1.4 Hz, 2H, *H*4), 8.27 (s, 2H, *H*5), 8.16 (dd, *J* = 8.2, 4.7 Hz, 2H, *H*3), 1.37-1.40 (m, 4H, C*H*₂), 1.19-1.31 (m, 4H, C*H*₂), 0.93-1.05 (m, 4H, C*H*₂), 0.58 (t, *J* = 7.3 Hz, 6H, C*H*₃); ^{13}C NMR (75 MHz, DMSO-d₆) δ 148.7 (*C*2), 140.7 (*C*=N), 139.6 (*C*4), 129.3 (*C*4'), 127.4 (*C*5), 125.2 (*C*3), 40.9 (C*H*₂), 27.5 (C*H*₂, $^{2}J(^{119}$Sn, ^{13}C) = 46.5 Hz), 25.2 (C*H*₂, $^{3}J(^{119/117}$Sn, ^{13}C) = 172.5/171.8 Hz), 13.3 (C*H*₃, $^{4}J(^{119}$Sn, ^{13}C) = 12.0 Hz); IR (KBr) 3434, 2956, 2919, 2852 (CH), 1622 (C=N), 1590 (C=C), 1519, 1428, 854, 729 (C-N-C) cm^{-1}; Anal. (%) calcd for C₂₀H₂₆Cl₂N₂Sn C, 49.63; H, 5.41; N, 5.79; found C, 49.40; H, 5.83; N, 5.85.

[Ph₂SnCl₂(phen)]

White solid (2.19 g, 93%); m.p. dec (lit 235 $^{\circ}$C with dec)[254]; ^{1}H NMR (300 MHz, DMSO-d₆) δ *9.50 (app s, 2H, *H*2), #9.06 (d, *J* = 8.3 Hz, 2H, *H*2), *8.74 (app s, 2H, *H*4), #8.54 (d, *J* = 4.7 Hz, 2H, *H*4), #8.43 (br s, 2H, *H*5), #8.25 (d, *J* = 8.3 Hz, 2H, phenyl C*H*), #8.16-8.18 (m, 2H, *H*3), *8.12 (br s, 2H, *H*5), *8.05 (app br s, 2H, *H*3), #7.92 (d, *J* = 7.1 Hz, 2H, phenyl C*H*), *7.72 (d, *J* = 7.1 Hz, 4H, phenyl C*H*), #7.42-7.55 (m, 6H, phenyl C*H*), *7.08-7.24 (m, 6H, phenyl C*H*); IR (KBr) 3433, 3049, 1622 (C=N), 1572 (C=C), 1519, 1429, 1103, 854, 727 (C-N-C) cm^{-1}; Anal. (%) calcd for C₂₄H₁₈Cl₂N₂Sn·H₂O C, 53.18; H, 3.72; N,5.17; found C, 53.44; H, 3.75; N, 5.22.

*Trans-isomer and #*Cis*-isomer (*Trans/Cis* ratio = 1.0:0.2)

[Ph₂SnCl₂(phen)] data were recorded at 70 $^{\circ}$C in order to investigate the presence of isomers.

^{1}H NMR (300 MHz, DMSO-d₆, 70 $^{\circ}$C) δ 9.50 (app br s, 2H, *H*2), 8.73 (app br s, 2H, *H*4), 8.00-8.14 (m, 4H, *H*3 & *H*5), 7.75 (app br s, 4H, phenyl C*H*), 7.17 (app br s, 6H, phenyl C*H*); ^{13}C NMR (75 MHz, DMSO-d₆, 70 $^{\circ}$C) δ 154.8 (phenyl quaternary *C*), 148.5 (*C*2), 141.3 (*C*=N), 138.3 (*C*4), 133.5 (phenyl *C*H), 128.9 (*C*4'), 127.4 (phenyl *C*H), 127.0 (phenyl *C*H), 126.9 (*C*5), 124.2 (*C*3).

(R = Me, n-Bu, Ph)
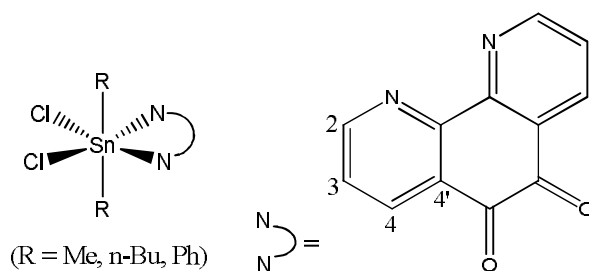
[Me$_2$SnCl$_2$(dione)]

Yellow solid (1.88 g, 97%); m.p. dec; ^{1}H NMR (300 MHz, DMSO-d$_6$) δ 9.00 (dd, J = 4.7, 1.8 Hz, 2H, H2), 8.41 (dd, J = 7.8, 1.8 Hz, 2H, H4), 7.69 (dd, J = 7.8, 4.7 Hz, 2H, H3), 1.03 (s, 6H, CH_3, $^2J(^{119/117}$Sn, ^{1}H) = 113.7/108.9 Hz); ^{13}C NMR (75 MHz, DMSO-d$_6$) δ 177.6 (C=O), 154.2 (C2), 152.0 (C=N), 135.8 (C4), 129.1 (C4'), 125.3 (C3), 22.9 (CH_3, $^1J(^{119/117}$Sn, ^{13}C) = 1014.0/968.3 Hz); IR (KBr) 3442, 3071, 1701 (C=O), 1573 (C=N), 1474, 1429, 1302, 732 (C-N-C) cm^{-1}; Anal. (%) calcd for C$_{14}$H$_{12}$Cl$_2$N$_2$O$_2$Sn·EtOH C, 40.38; H, 3.81; N, 5.89; found C, 41.24; H, 3.01; N, 6.79.

[n-Bu$_2$SnCl$_2$(dione)] (See section 4.3.5.1)

Yellow solid (2.31 g, 99%); m.p. dec; IR (KBr) 3421, 3076, 2955, 2920, 2862 (CH), 1620 (C=O), 1584 (C=N), 1436, 1376, 1069, 1042, 720 cm^{-1}; Anal. (%) calcd for C$_{20}$H$_{24}$Cl$_2$N$_2$O$_2$Sn·H$_2$O C, 45.15; H, 4.93; N, 5.27; found C, 45.07; H, 4.69; N, 5.46.

[Ph$_2$SnCl$_2$(dione)]

Yellow solid (2.42 g, 97%); m.p. dec; ^{1}H NMR (300 MHz, DMSO-d$_6$) δ 9.00 (dd, J = 4.7, 1.6 Hz, 2H, H2), 8.40 (dd, J = 7.8, 1.6 Hz, 2H, H4), 7.90 (d, J = 7.0 Hz, 4H, phenyl CH), 7.68 (dd, J = 7.8, 4.7 Hz, 2H, H3), 7.25-7.37 (m, 6H, phenyl CH); ^{13}C NMR (75 MHz, DMSO-d$_6$) δ 177.3 (C=O), 155.1 (phenyl quaternary C), 153.9 (C2), 151.6 (C=N), 136.0 (C4), 134.5 (phenyl CH, $^2J(^{119}$Sn, ^{13}C) = 69.8 Hz), 129.3 (C4'), 127.8 (phenyl CH), 127.3 (phenyl CH), 125.3 (C3), these data match reported literature values[246]; IR (KBr) 3444, 3058, 1694 (C=O), 1576 (C=N), 1477, 1430, 727 (C-N-C), 700 cm^{-1}; Anal. (%) calcd for C$_{24}$H$_{16}$Cl$_2$N$_2$O$_2$Sn C, 52.03; H, 2.91; N, 5.06; found C, 52.29; H, 3.34; N, 5.19.
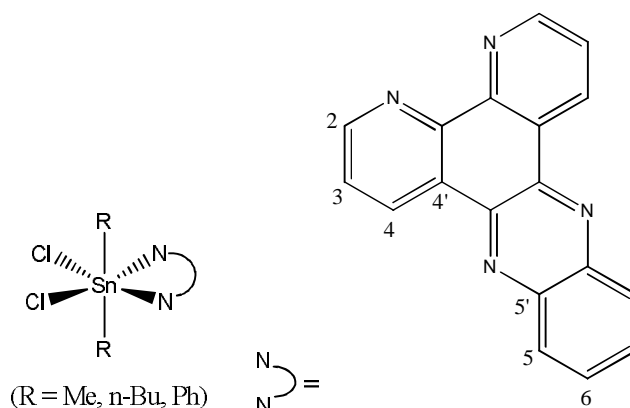
[Me₂SnCl₂(dppz)]

Yellow solid (2.13 g, 94%); m.p. 269-272 °C; ^{1}H NMR (300 MHz, DMSO-d$_6$) δ 9.42 (dd, J = 8.1, 1.6 Hz, 2H, H2), 9.20 (dd, J = 4.4, 1.6 Hz, 2H, H4), 8.29 (dd, J = 6.5, 3.4 Hz, 2H, H5), 8.01 (dd, J = 6.5, 3.4 Hz, 2H, H6), 7.91 (dd, J = 8.1, 4.4 Hz, 2H, H3), 1.03 (s, 6H, CH_3); IR (KBr) 3434, 3066, 1632 (C=N), 1572 (C=C), 1494, 1420, 1359, 1075, 772, 734 (C-N-C) cm^{-1}; Anal. (%) calcd for C$_{20}$H$_{16}$Cl$_2$N$_4$Sn C, 47.85; H, 3.21; N, 11.16; found C, 47.27; H, 3.04; N, 10.74.

[Me₂SnCl₂(dppz)] showed improved solubility in DMSO-d$_6$ at 80 °C and hence the data were recorded at 80 °C.

^{1}H NMR (300 MHz, DMSO-d$_6$, 80 °C) δ 9.46 (d, J = 8.0 Hz, 2H, H2), 9.21 (app br s, 2H, H4), 8.30 (dd, J = 6.5, 3.5 Hz, 2H, H5), 7.99 (dd, J = 6.5, 3.5 Hz, 2H, H6), 7.91 (dd, J = 8.0, 4.4 Hz, 2H, H3), 1.08 (s, 6H, CH_3, ^2J($^{119/117}$Sn, ^{1}H) = 108.3/103.8 Hz); ^{13}C NMR (75 MHz, DMSO-d$_6$) δ 152.3 (C4), 147.8 (C=N), 142.3 (C=N), 141.0 (C5'), 133.8 (C2), 131.6 (C6), 129.6 (C5), 127.6 (C4'), 125.0 (C3), 21.4 (CH$_3$).

[n-Bu₂SnCl₂(dppz)]

Pink solid (2.54 g, 96%); m.p. 197-202 °C; ^{1}H NMR (300 MHz, CDCl$_3$) δ 9.93 (dd, J = 8.2, 1.5 Hz, 2H, H2), 9.83 (dd, J = 4.9, 1.5 Hz, 2H, H4), 8.41 (dd, J = 6.6, 3.4 Hz, 2H, H5), 8.14 (dd, J = 8.2, 4.9 Hz, 2H, H3), 8.03 (dd, J = 6.6, 3.4 Hz, 2H, H6), 1.62-1.68 (m, 4H, CH_2), 1.36-1.51 (m, 4H, CH_2), 1.03-1.10 (m, 4H, CH_2), 0.62 (t, J = 6.9 Hz, 6H, CH_3); ^{13}C NMR (75 MHz, CDCl$_3$) δ 150.5 (C4), 142.9 (C=N), 142.7 (C=N), 139.3 (C5'), 136.9 (C2), 132.1 (C6), 129.7 (C5), 129.3 (C4'), 126.3 (C3), 41.9

(CH_2), 28.2 (CH_2), 25.9 (CH_2), 13.4 (CH_3); IR (KBr) 3431, 2954, 2916, 2858 (CH), 1630 (C=N), 1493, 1076 (C-N), 736 (C-N-C) cm^{-1}; Anal. (%) calcd for $C_{26}H_{28}Cl_2N_4Sn$ C, 53.28; H, 4.81; N, 9.56; found C, 52.89; H, 5.22; N, 9.47.

[Ph₂SnCl₂(dppz)]

Light yellow solid (2.76 g, 98%); m.p. 272-282 $^{\circ}$C; ^{1}H NMR (300 MHz, DMSO-d_6) δ 9.44 (dd, J = 8.1, 1.7 Hz, 2H, $H2$), 9.26 (app br s, 2H, $H4$), 8.28 (dd, J = 6.5, 3.4 Hz, 2H, $H5$), 8.00 (dd, J = 6.5, 3.4 Hz, 2H, $H6$), 7.95 (dd, J = 8.1, 4.6 Hz, 2H, $H3$), 7.23-7.89 (d, J = 6.7 Hz, 4H, phenyl CH), 7.37 (m, 6H, phenyl CH); ^{13}C NMR (75 MHz, DMSO-d_6) δ *155.1 (phenyl quaternary C), 151.9 ($C4$), *146.9 (C=N), 141.6 (C=N), 140.4 ($C5'$), 134.5 (phenyl CH), 133.5 ($C2$), 131.3 ($C6$), 129.1 ($C5$), 127.7 (phenyl CH), 127.3 (phenyl CH), 127.1 ($C4'$), 124.8 ($C3$); IR (KBr) 3443, 3067, 1627 (C=N), 1574 (C=C), 1494, 1420, 1361, 1078, 735, (C-N-C) cm^{-1}; Anal. (%) calcd for $C_{30}H_{20}Cl_2N_4Sn$ C, 57.55; H, 3.22; N, 8.95; found C, 57.09; H, 3.23; N, 9.22. *The compound is not very soluble and as a result these signals are very weak.

General procedure for the synthesis of 1,10-phenanthroline derivatives of [R₂Sn(nicotinate)₂] R = Me, Bu or Ph

The appropriate diorganotin(IV) compound (4.5 mmol) and the appropriate 1,10-phenanthroline derivative (4.5 mmol) were dissolved in EtOH (25 mL) and heated to reflux for 3 hours. In the case of the [R₂Sn(nicotinate)₂] compounds where R = Me and Bu, the reaction mixture was allowed to cool and solvent was removed under reduced pressure to give the desired product. With [Ph₂Sn(nicotinate)₂(phen)], after cooling, the reaction mixture was filtered to removed unreacted starting materials and the filtrate reduced under pressure. The remaining solid was then washed with cold EtOH to remove any remaining 1,10-phenanthroline & the filtrate reduced under pressure to give the product.

(R = Me, n-Bu, Ph; OR' = nicotinic acid)

246
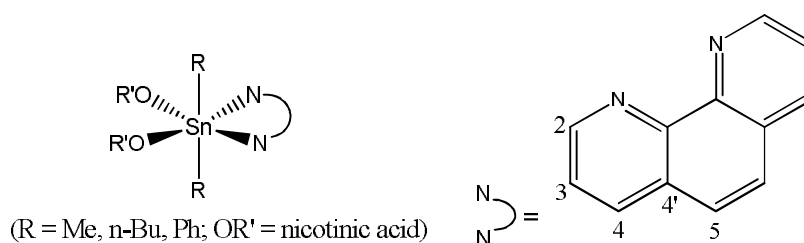
[Me₂Sn(nicotinate)₂(phen)]

Pink solid (1.99 g, 77%); m.p. 212-220 $^{\circ}$C; ^{1}H NMR (300 MHz, DMSO-d$_{6}$) δ 9.46 (d, *J* = 4.7 Hz, 2H, *H*2), 9.15 (br s, 2H, *H*a), 8.71-8.76 (m, 4H, *H*4 & *H*b), 8.30 (d, *J* = 7.7 Hz, 2H, *H*d), 8.15 (s, 2H, *H*5), 8.00 (dd, *J* = 8.5, 4.7 Hz, 2H, *H*3), 7.50 (dd, *J* = 7.7, 4.4 Hz, 2H, *H*c), 0.92 (s, 6H, C*H*₃); ^{13}C NMR (75 MHz, DMSO-d$_{6}$) δ 170.3 (*C*=O), 152.1 (*C*b), 150.5 (*C*a), 149.5 (*C*2), 142.0 (C=N), 138.4 (*C*4), 136.9 (*C*d), 129.1 (*C*e), 129.0 (*C*4'), 127.0 (*C*5), 124.5 (*C*3), 123.4 (*C*c), 14.5 (C*H*₃); IR (KBr) 3431, 3055, 1645, 1590, 1428, 1332, 1027, 846, 756 cm^{-1}; Anal. (%) calcd for C₂₆H₂₂N₄O₄Sn C, 54.48: H, 3.87: N, 9.77; found C, 54.62; H, 3.85; N, 9.66.

[n-Bu₂Sn(nicotinate)₂(phen)]

Pink solid (2.75 g, 93%); m.p. 121-127 $^{\circ}$C; ^{1}H NMR (300 MHz, DMSO-d$_{6}$) δ 9.48 (d, *J* = 4.3 Hz, 2H, *H*2), 9.17 (br s, 2H, *H*a), 8.77 (d, *J* = 7.5 Hz, 2H, *H*4), 8.71 (d, *J* = 4.8 Hz, 2H, *H*b), 8.32 (d, *J* = 7.7 Hz, 2H, *H*d), 8.17 (s, 2H, *H*5), 8.02-8.06 (m, 2H, *H*3), 7.48 (dd, *J* = 7.7, 4.8 Hz, 2H, *H*c), 1.50-1.56 (m, 4H, C*H*₂), 1.29 (br s, 4H, C*H*₂), 0.98-1.05 (m, 4H, C*H*₂), 0.52 (t, *J* = 8.7 Hz, 6H, C*H*₃); ^{13}C NMR (75 MHz, DMSO-d$_{6}$): δ 170.3 (*C*=O), 152.0 (*C*b), 150.5 (*C*a), 149.8 (*C*2), 142.3 (*C*=N), 138.5 (*C*4), 136.9 (*C*d), 129.3 (*C*4'), 129.0 (*C*e), 127.1 (*C*5), 124.6 (*C*3), 123.4 (*C*c), 31.9 (C*H*₂), 26.9 (C*H*₂), 25.4 (C*H*₂), 13.3 (C*H*₂); IR (KBr) 3429, 3047, 2948, 2925, 2865, 1648, 1599, 1588, 1552, 1426, 1332, 1143, 848, 424 cm^{-1}; Anal. (%) calcd for C₃₂H₃₆N₄O₄Sn·2H₂O C, 55.43; H, 5.52; N, 8.08; found C, 55.08; H, 5.04; N, 7.85.

[Ph₂Sn(nicotinate)₂(phen)]

Peach solid (0.35 g, 10%); m.p. dec; ^{1}H NMR (300 MHz, DMSO-d$_{6}$) δ 9.09 (app br s, 2H, H2), 9.03 (br s, 2H, *H*a), 8.71 (app br s, 2H, *H*b), 8.49 (app br s, 2H, *H*4), 8.24 (app br s, 2H, *H*d), 7.96 (app br s, 3H, *H*5 & phenyl C*H*), 7.82 (d, *J* = 6.1 Hz, 2H, phenyl C*H*), 7.78 (app br s, 2H, *H*3), 7.48-7.52 (m, 2H, *H*c), 7.37-7.45 (m, 6H, phenyl C*H*), 7.12 (app br s, 1H, phenyl C*H*); ^{13}C NMR (75 MHz DMSO-d$_{6}$) δ 167.2 (*C*=O) 153.1 (*C*b), 150.5 (*C*a), 150.2 (*C*2), 145.5 (phenyl quaternary *C*), 143.4 (*C*=N), 137.5 (*C*d), 136.8 (*C*4), 136.5 (phenyl *C*H), 129.3 (phenyl *C*H), 128.8 (*C*4'),

128.7 (phenyl *C*H), 128.3, (*C*e), 127.1 (*C*5), 124.2 (*C*c), 123.9 (*C*3); IR (KBr) 3432, 3070, 1709, 1655, 1596, 1419, 1324, 1302, 1033, 748 cm^{-1}; Anal. (%) calcd for $C_{36}H_{26}N_4O_4Sn \cdot H_2O$ C, 60.44; H, 3.95; N, 7.83; found C, 60.44; H, 3.74; N, 8.17.

(R = Me, n-Bu, Ph; OR' = nicotinic acid)
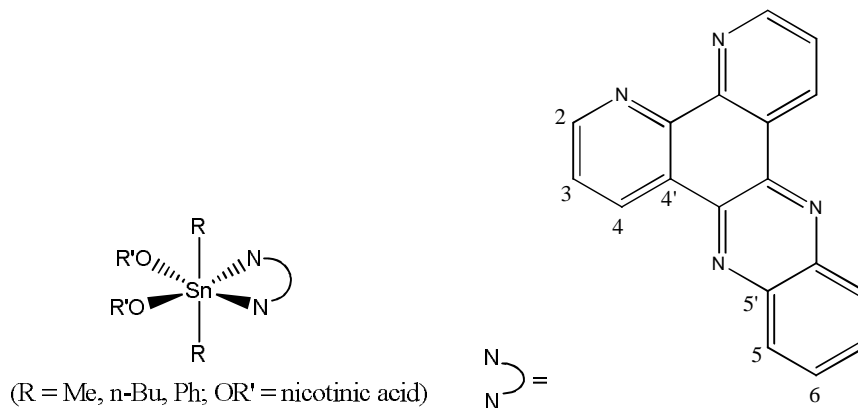
[Me₂Sn(nicotinate)₂(dppz)]

Yellow solid (2.97 g, 98%); m.p. dec; ^{1}H NMR (300 MHz, DMSO-d$_6$) δ 9.55 (d, *J* = 7.9 Hz, 2H, *H*2), 9.27 (d, *J* = 4.7 Hz, 2H, *H*4), 9.07 (d, *J* = 1.5 Hz, 2H, *H*a), 8.74 (dd, *J* = 4.9, 1.9 Hz, 2H, *H*b), 8.39 (dd, *J* = 6.6, 3.5 Hz, 2H, *H*5), 8.26 (app dt, *J* = 7.8, 1.9 Hz, 2H, *H*d), 8.07 (dd, *J* = 6.6, 3.5 Hz, 2H, *H*6), 7.98 (dd, *J* = 7.9, 4.7 Hz, 2H, *H*3), 7.50 (dd, *J* = 7.8, 4.9 Hz, 2H, *H*c), 0.95 (s, 6H, C*H*3); IR (KBr) 3427, 1605, 1592, 1554, 1486, 1415, 1400, 1362, 1336, 1073, 741 cm^{-1}; Anal. (%) calcd for $C_{32}H_{24}N_6O_4Sn$ C, 56.92; H, 3.58; N, 12.45; found C, 56.49; H, 3.57; N, 12.53.

[Me₂Sn(nicotinate)₂(dppz)] showed improved solubility in DMSO-d$_6$ at 80 °C and hence the data were recorded at 80 °C.

^{1}H NMR (300 MHz, DMSO-d$_6$, 80 °C) δ 9.47 (d, *J* = 7.9 Hz, 2H, *H*2), 9.22 (app br s, 2H, *H*4), 9.07 (br s, 2H, *H*a), 8.70 (dd, *J* = 4.8, 1.5 Hz, 2H, *H*b), 8.29 (dd, *J* = 6.5, 3.4 Hz, 2H, *H*5), 8.25 (d, *J* = 7.8 Hz, 2H, *H*d), 7.99 (dd, *J* = 6.5, 3.4 Hz, 2H, *H*6), 7.90 (dd, *J* = 7.9, 4.3 Hz, 2H, *H*3), 7.46 (dd, *J* = 7.8, 4.8 Hz, 2H, *H*c), 1.02 (s, 6H, C*H*3, $^2J(^{119/117}$Sn, ^{1}H) = 101.7/97.5 Hz); ^{13}C NMR (75 MHz, DMSO-d$_6$) δ 168.6 (*C*=O), 151.8 (*C*b), 151.5 (*C*4), 149.9 (*C*a), 147.0 (*C*=N), 141.3 (C=N), 140.1 (*C*5'), 136.2 (*C*d), 132.7 (*C*2), 130.6 (*C*6), 128.6 (*C*5), 128.2 (*C*e), 126.5 (*C*4'), 123.9 (*C*3), 122.8 (*C*c), 11.8 (*C*H3).

[n-Bu₂Sn(nicotinate)₂(dppz)]

Yellow solid (3.07 g, 90%); m.p. dec; ^{1}H NMR (300 MHz, DMSO-d$_6$) δ 9.40 (d, J = 7.8 Hz, 2H, H2), 9.31 (app br s, 2H, H4), 9.11 (br s, 2H, Ha), 8.73 (d, J = 5.0 Hz, 2H, Hb), 8.28 (d, J = 7.8 Hz, 2H Hd), 8.23 (dd, J = 6.5, 3.4 Hz, 2H, H5), 7.92-8.02 (m, 4H, H6 & H3), 7.51 (dd, J = 7.8, 5.0 Hz, 2H, Hc), 1.44-1.62 (m, 8H, CH_2), 1.17-1.24 (m, 4H, CH_2), 0.72 (t, J = 7.2 Hz, 6H, CH_3); IR (KBr) 3425, 2955, 2924, 2868 , 1606, 1593, 1553, 1407, 1361, 1337, 1074, 740 cm^{-1}; Anal. (%) calcd for C$_{38}$H$_{36}$N$_6$O$_4$Sn C, 60.10; H, 4.78; N, 11.07; found C, 60.91; H, 4.90; N, 10.40.

[n-Bu₂Sn(nicotinate)₂(dppz)] showed improved solubility in DMSO-d$_6$ at 95 °C and hence the data were recorded at 95 °C.

^{1}H NMR (300 MHz, DMSO-d$_6$, 95 °C) δ 9.38 (dd, J = 7.9, 1.7 Hz, 2H, H2), 9.14 (d, J = 3.9 Hz, 2H, H4), 9.03 (br s, 2H, Ha), 8.68 (dd, J = 4.9, 1.7 Hz, 2H, Hb), 8.19-8.24 (m, 4H, Hd & H5), 7.94 (dd, J = 6.6, 3.4 Hz, 2H, H6), 7.84 (dd, J = 7.9, 3.9 Hz, 2H, H3), 7.46 (dd, J = 8.0, 4.9 Hz, 2H, Hc), 1.61-1.71 (m, 4H, CH_2), 1.42-1.56 (m, 4H, CH_2), 1.23-1.36 (m, 4H, CH_2), 0.80 (t, J = 7.3 Hz, 6H, CH_3); ^{13}C NMR (75 MHz, DMSO-d$_6$) δ 168.4 (C=O), 152.2 (Cb), 151.9 (C4), 150.0 (Ca), 147.3 (C=N), 141.6 (C=N), 140.3 (C5'), 136.5 (Cd), 132.9 (C2), 130.8 (C6), 128.8 (C5), 128.3 (Ce), 126.7 (C4'), 124.2 (C3), 123.2 (Cc), 26.4 (CH_2), 25.6 (CH_2), 12.9 (CH_3).

Bibliography

1. http://www.nobelprize.org/nobel_prizes/medicine/laureates/1945/fleming-lecture.pdf, Fleming, A., Penicillin. Date accessed **28/09/13**.

2. Deurenberg, R. H.; Stobberingh, E. E., The evolution of *Staphylococcus aureus*. *Infect., Genet. Evol.* **2008,** *8*, 747-763.

3. Woodford, N.; Livermore, D. M., Infections caused by Gram-positive bacteria: a review of the global challenge. *J. Infect.* **2009,** *59 Suppl 1*, S4-16.

4. ECDC Summary: Point Prevalence survey of healthcare-associated infections and antimicrobial use in European hospitals 2011-2012; **2013**.

5. Suetens, C.; Hopkins, S.; Kolman, J.; Högberg, L. D., European Centre for Disease Prevention and Control. Point prevalence survey of healthcare-associated infections and antimicrobial use in European acute care hospitals 2011-2012; ECDC: Stockholm, **2013**.

6. (a) ECDC Annual Epidemiological Report 2012. Reporting on 2010 surveillance data and 2011 epidemic intelligence data.; **2012**; (b) EARS-Net Report for Quater 1 2013; **2013**.

7. CDC Antibiotic Resistance Threats in the United States, 2013; **2013**.

8. (a) Livermore, D. M.; Blaser, M.; Carrs, O.; Cassell, G.; Fishman, N.; Guidos, R.; Levy, S.; Powers, J.; Norrby, R.; Tillotson, G.; Davies, R.; Projan, S.; Dawson, M.; Monnet, D.; Keogh-Brown, M.; Hand, K.; Garner, S.; Findlay, D.; Morel, C.; Wise, R.; Bax, R.; Burke, F.; Chopra, I.; Czaplewski, L.; Finch, R.; Livermore, D.; Piddock, L. J. V.; White, T., Discovery research: the scientific challenge of finding new antibiotics. *J. Antimicrob. Chemother.* **2011,** *66*, 1941-1944; (b) Chopra, I., The 2012 Garrod Lecture: Discovery of antibacterial drugs in the 21st century. *J. Antimicrob. Chemother.* **2013,** *68*, 496-505.

9. ECDC/EMEA Joint Technical Report. The bacterial challenge: time to react. A call to narrow the gap between multidrug-resistant bacteria in the EU and the development of new antibacterial agents.; **2009**.

10. Payne, D. J.; Gwynn, M. N.; Holmes, D. J.; Pompliano, D. L., Drugs for bad bugs: confronting the challenges of antibacterial discovery. *Nat. Rev. Drug Discovery* **2007,** *6*, 29-40.

11. Patrick, G. L., *An Introduction to Medicinal Chemsity*. 3rd ed.; Oxford University Press Inc.: New York, **2005**.

12. McPhillie, M. J.; Trowbridge, R.; Mariner, K. R.; O'Neill, A. J.; Johnson, A. P.; Chopra, I.; Fishwick, C. W. G., Structure-Based Ligand Design of Novel Bacterial RNA Polymerase Inhibitors. *ACS Med. Chem. Lett.* **2011,** *2*, 729-734.

13. Jarvest, R., Pleuromutilins: antibiotic optimisation for human therapy. *Spec. Publ. - R. Soc. Chem.* **2011,** *320*, 106-116.

14. Campbell., N. A.; Reece, J. B., *Biology*. 6th Ed.; Benjamin cummings.: San Fransicisco, **2002**.

15. Nikaido, H., Prevention of drug access to bacterial targets: permeability barriers and active efflux. *Science* **1994,** *264*, 382-388.

16. Galdiero, S.; Falanga, A.; Cantisani, M.; Tarallo, R.; Della Pepa, M. E.; D'Oriano, V.; Galdiero, M., Microbe-host interactions: structure and role of Gram-negative bacterial porins. *Curr. Protein Pept. Sci.* **2012,** *13*, 843-854.

17. Nikaido, H.; Vaara, M., Molecular basis of bacterial outer membrane permeability. *Microbiol. Rev.* **1985,** *49*, 1-32.

18. Nikaido, H., The role of outer membrane and efflux pumps in the resistance of Gram-negative bacteria. Can we improve drug access? *Drug Resist. Updates* **1998,** *1*, 93-98.

19. Lowy, F. D., *Staphylococcus aureus* infections. *N. Engl. J. Med.* **1998,** *339*, 520-532.

20. (a) Foster, T. J., Immune evasion by *staphylococci*. *Nat. Rev. Microbiol.* **2005,** *3*, 948-958; (b) Foster Timothy, J., Colonization and infection of the human host by *staphylococci*: adhesion, survival and immune evasion. *Vet. Dermatol.* **2009,** *20*, 456-470.

21. Garcia-Lara, J.; Masalha, M.; Foster, S. J., *Staphylococcus aureus*: The search for novel targets. *Drug Discovery Today* **2005,** *10*, 643-651.

22. http://phil.cdc.gov/phil/home.asp, Centers for Disease Protection and Control., Public Health Library. Date accessed **12/09/13**.

23. Dinges, M. M.; Orwin, P. M.; Schlievert, P. M., Exotoxins of *Staphylococcus aureus*. *Clin. Microbiol. Rev.* **2000,** *13*, 16-34.

24. Kong, K.-F.; Vuong, C.; Otto, M., *Staphylococcus* quorum sensing in biofilm formation and infection. *Int. J. Med. Microbiol.* **2006,** *296*, 133-139.

25. Lowery, C. A.; Salzameda, N. T.; Sawada, D.; Kaufmann, G. F.; Janda, K. D., Medicinal Chemistry as a Conduit for the Modulation of Quorum Sensing. *J. Med. Chem.* **2010,** *53*, 7467-7489.

26. Costerton, J. W.; Stewart, P. S.; Greenberg, E. P., Bacterial biofilms: a common cause of persistent infections. *Science* **1999,** *284*, 1318-1322.

27. Spoering, A. L.; Lewis, K., Biofilms and planktonic cells of *Pseudomonas aeruginosa* have similar resistance to killing by antimicrobials. *J. Bacteriol.* **2001,** *183*, 6746-6751.

28. Van Houdt, R.; Michiels, C. W., Role of bacterial cell surface structures in *Escherichia coli* biofilm formation. *Res. Microbiol.* **2005,** *156*, 626-633.

29. Hiramatsu, K.; Cui, L.; Kuroda, M.; Ito, T., The emergence and evolution of methicillin-resistant *Staphylococcus aureus*. *Trends Microbiol.* **2001,** *9*, 486-493.

30. Berger-Bachi, B.; Rohrer, S., Factors influencing methicillin resistance in staphylococci. *Arch. Microbiol.* **2002,** *178*, 165-171.

31. Health Protection Surveillance Centre. Trends in *Staphylococcus aureus*/MRSA bacteraemia in Ireland, 2004 to the end of Q1 2013 (data correct as of 11th June 2013); **2013**.

32. Hiramatsu, K., Vancomycin-resistant *Staphylococcus aureus*: a new model of antibiotic resistance. *Lancet Infect. Dis.* **2001,** *1*, 147-155.

33. (a)http://www.hpa.org.uk/Topics/InfectiousDiseases/InfectionsAZ/PseudomonasAeruginosa/GeneralInformation/, Public Health England., *Pseudomonas aeruginosa*. Date accessed **17/11/13**; (b) Lyczak, J. B.; Cannon, C. L.; Pier, G. B., Establishment of *Pseudomonas aeruginosa*

infection: Lessons from a versatile opportunist. *Microbes Infect.* **2000,** *2,* 1051-1060.

34. Pier, G. B., *Pseudomonas aeruginosa* lipopolysaccharide: a major virulence factor, initiator of inflammation and target for effective immunity. *Int. J. Med. Microbiol.* **2007,** *297,* 277-295.

35. Wolf, P.; Elsasser-Beile, U., *Pseudomonas* exotoxin A: from virulence factor to anti-cancer agent. *Int. J. Med. Microbiol.* **2009,** *299,* 161-76.

36. Meyer, A. L., Prospects and challenges of developing new agents for tough Gram-negatives. *Curr. Opin. Pharmacol.* **2005,** *5,* 490-494.

37. Hahn, H. P., The type-4 pilus is the major virulence-associated adhesin of *Pseudomonas aeruginosa* - a review. *Gene* **1997,** *192,* 99-108.

38. Gerlach Roman, G.; Hensel, M., Protein secretion systems and adhesins: the molecular armory of Gram-negative pathogens. *Int. J. Med. Microbiol.* **2007,** *297,* 401-415.

39. Govan, J. R.; Deretic, V., Microbial pathogenesis in cystic fibrosis: mucoid *Pseudomonas aeruginosa* and *Burkholderia cepacia. Microbiol. Rev.* **1996,** *60,* 539-574.

40. Lau, G. W.; Hassett, D. J.; Britigan, B. E., Modulation of lung epithelial functions by *Pseudomonas aeruginosa. Trends Microbiol.* **2005,** *13,* 389-397.

41. Price-Whelan, A.; Dietrich, L. E. P.; Newman, D. K., Pyocyanin alters redox homeostasis and carbon flux through central metabolic pathways in *Pseudomonas aeruginosa* PA14. *J. Bacteriol.* **2007,** *189,* 6372-6381.

42. Hoiby, N.; Johansen, H. K.; Moser, C.; Song, Z.; Ciofu, O.; Kharazmi, A., *Pseudomonas aeruginosa* and the *in vitro* and *in vivo* biofilm mode of growth. *Microbes Infect.* **2001,** *3,* 23-35.

43. Rumbaugh, K. P.; Griswold, J. A.; Hamood, A. N., The role of quorum sensing in the *in vivo* virulence of *Pseudomonas aeruginosa. Microbes Infect.* **2000,** *2,* 1721-1731.

44. George, A. M., Multidrug resistance in enteric and other Gram-negative bacteria. *FEMS Microbiol. Lett.* **1996,** *139,* 1-10.

45. Webber, M. A.; Piddock, L. J. V., The importance of efflux pumps in bacterial antibiotic resistance. *J. Antimicrob. Chemother.* **2003,** *51,* 9-11.

46. Hamzehpour, M. M.; Pechere, J. C.; Plesiat, P.; Koehler, T., OprK and OprM define two genetically distinct multidrug efflux systems in *Pseudomonas aeruginosa. Antimicrob. Agents Chemother.* **1995,** *39,* 2392-2396.

47. Pages, J. M.; Amaral, L., Mechanisms of drug efflux and strategies to combat them: Challenging the efflux pump of Gram-negative bacteria. *Biochim. Biophys. Acta, Proteins Proteomics* **2009,** *1794,* 826-833.

48. Li, X. Z.; Nikaido, H., Efflux-mediated drug resistance in bacteria. *Drugs* **2004,** *64,* 159-204.

49. Health Protection Sureveillance Centre. Infectious Intestinal disease: Public Health and Clinical guidelines. 17. Verotoxigenic *Esherichia coli* (VTEC) and Haemolytic Uraemic Syndrome (HUS).; **2012**.

50. Le Bouguénec, C.; Garcia, M. I., Role of adhesion in pathogenicity of human uropathogenic and diarrhoeogenic *Escherichia coli. Bulletin de l'Institut Pasteur* **1996,** *64,* 201-236.

51. (a) CDC *E. coli (Escherichia coli)* General Information.; **2012**; (b) Spears, K. J.; Roe, A. J.; Gally, D. L., A comparison of enteropathogenic and enterohaemorrhagic *Escherichia coli* pathogenesis. *FEMS Microbiol. Lett.* **2006,** *255*, 187-202.

52. Coia, J. E., Clinical, microbiological and epidemiological aspects of *Escherichia coli* O157 infection. *FEMS Immunol. Med. Microbiol.* **1998,** *20*, 1-9.

53. Horwitz, M. A.; Silverstein, S. C., Influence of the *Escherichia coli* capsule on complement fixation and on phagocytosis and killing by human phagocytes. *J. Clin. Invest.* **1980,** *65*, 82-94.

54. Caprioli, A.; Falbo, V.; Ruggeri, F. M.; Baldassarri, L.; Bisicchia, R.; Ippolito, G.; Romoli, E.; Donelli, G., Cytotoxic necrotizing factor production by hemolytic strains of *Escherichia coli* causing extraintestinal infections. *J. Clin. Microbiol.* **1987,** *25*, 146-149.

55. Yi, C.-r.; Goldberg, M. B., Putting enterohemorrhagic *E. coli* on a pedestal. *Cell Host Microbe* **2009,** *5*, 215-217.

56. Donnenberg, M. S.; Kaper, J. B.; Finlay, B. B., Interactions between enteropathogenic *Escherichia coli* and host epithelial cells. *Trends Microbiol* **1997,** *5*, 109-114.

57. Frankel, G.; Phillips, A. D.; Rosenshine, I.; Dougan, G.; Kaper, J. B.; Knutton, S., Enteropathogenic and enterohemorrhagic *Escherichia coli*: more subversive elements. *Mol. Microbiol.* **1998,** *30*, 911-921.

58. Campellone, K. G., Cytoskeleton-modulating effectors of enteropathogenic and enterohaemorrhagic *Escherichia coli*: Tir, EspFU and actin pedestal assembly. *FEBS J.* **2010,** *277*, 2390-2402.

59. Hayward, R. D.; Leong, J. M.; Koronakis, V.; Campellone, K. G., Exploiting pathogenic *Escherichia coli* to model transmembrane receptor signalling. *Nat. Rev. Microbiol.* **2006,** *4*, 358-370.

60. Sperandio, V.; Li, C. C.; Kaper, J. B., Quorum-sensing *Escherichia coli* regulator A: A regulator of the LysR family involved in the regulation of the locus of enterocyte effacement pathogenicity island in enterohemorrhagic *E. coli*. *Infect. Immun.* **2002,** *70*, 3085-3093.

61. Sperandio, V.; Mellies, J. L.; Nguyen, W.; Shin, S.; Kaper, J. B., Quorum sensing controls expression of the type III secretion gene transcription and protein secretion in enterohemorrhagic and enteropathogenic *Escherichia coli*. *Proc. Natl. Acad. Sci. U. S. A.* **1999,** *96*, 15196-15201.

62. Niu, C.; Robbins, C. M.; Pittman, K. J.; Osborn, J. L.; Stubblefield, B. A.; Simmons, R. B.; Gilbert, E. S., LuxS influences *Escherichia coli* biofilm formation through autoinducer-2-dependent and autoinducer-2-independent modalities. *FEMS Microbiol. Ecol.* **2013,** *83*, 778-791.

63. Ponnusamy, P.; Natarajan, V.; Sevanan, M., *In vitro* biofilm formation by uropathogenic *Escherichia coli* and their antimicrobial susceptibility pattern. *Asian Pac. J. Trop. Med.* **2012,** *5*, 210-213.

64. Pitout, J. D. D.; Laupland, K. B., Extended-spectrum β-lactamase-producing Enterobacteriaceae: an emerging public-health concern. *Lancet Infect. Dis.* **2008,** *8*, 159-166.

65. Nordmann, P.; Naas, T.; Poirel P., Global Spread of Carbapenemase producing Enterobacteriaceae. *Emerg. Infect. Dis.* **2011**, 1791-1798.

66. Janeway, C. A.; Travers, P.; Walport, M.; Shlomchik, M. J., *Immunobiology: the immune system in health and disease*. 6th ed.; Garland Science Publishing.; New York, **2005**.

67. (a) Kavanagh, K.; Reeves, E. P., Exploiting the potential of insects for *in vivo* pathogenicity testing of microbial pathogens. *FEMS Microbiol. Rev.* **2004,** *28*, 101-112; (b) Hoffmann, J. A., Innate immunity of insects. *Curr. Opin. Immunol.* **1995,** *7*, 4-10; (c) Kimbrell, D. A.; Beutler, B., The evolution and genetics of innate immunity. *Nat. Rev. Genet.* **2001,** *2*, 256-267.

68. (a) Hamamoto, H.; Kurokawa, K.; Kaito, C.; Kamura, K.; Razanajatovo, I. M.; Kusuhara, H.; Santa, T.; Sekimizu, K., Quantitative evaluation of the therapeutic effects of antibiotics using silkworms infected with human pathogenic microorganisms. *Antimicrob. Agents Chemother.* **2004,** *48*, 774-779; (b) Jander, G.; Rahme, L. G.; Ausubel, F. M., Positive correlation between virulence of *Pseudomonas aeruginosa* mutants in mice and insects. *J. Bacteriol.* **2000,** *182*, 3843-3845; (c) Cotter, G.; Doyle, S.; Kavanagh, K., Development of an insect model for the *in vivo* pathogenicity testing of yeasts. *FEMS Immunol. Med. Microbiol.* **2000,** *27*, 163-169; (d) Brennan, M.; Thomas, D. Y.; Whiteway, M.; Kavanagh, K., Correlation between virulence of *Candida albicans* mutants in mice and *Galleria mellonella* larvae. *FEMS Immunol. Med. Microbiol.* **2002,** *34*, 153-157; (e) Peleg, A. Y.; Monga, D.; Pillai, S.; Mylonakis, E.; Moellering, R. C. Jr.; Eliopoulos, G. M., Reduced susceptibility to vancomycin influences pathogenicity in *Staphylococcus aureus* infection. *J. Infect. Dis.* **2009,** *199*, 532-536; (f) Hamamoto, H.; Tonoike, A.; Narushima, K.; Horie, R.; Sekimizu, K., Silkworm as a model animal to evaluate drug candidate toxicity and metabolism. *Comp. Biochem. Physiol., Part C Toxicol. Pharmacol.* **2009,** *149C*, 334-339; (g) Lionakis, M. S.; Kontoyiannis, D. P., Fruit flies as a minihost model for studying drug activity and virulence in *Aspergillus. Med. Mycol.* **2005,** *43*, S111-S114.

69. http://ukmoths.org.uk/show.php?bf=1425, Kimber, I., UKmoths. Your guide to the moths of the UK and Ireland. Date accessed **26/09/13**.

70. (a) Desbois, A. P.; Coote, P. J., Wax moth larva (*Galleria mellonella*): an *in vivo* model for assessing the efficacy of antistaphylococcal agents. *J. Antimicrob. Chemother.* **2011,** *66*, 1785-1790; (b) Rowan, R.; Moran, C.; McCann, M.; Kavanagh, K., Use of *Galleria mellonella* larvae to evaluate the *in vivo* antifungal activity of [Ag$_2$(mal)(phen)$_3$]. *BioMetals* **2009,** *22*, 461-467; (c) Kellett, A.; O'Connor, M.; McCann, M.; Howe, O.; Casey, A.; McCarron, P.; Kavanagh, K.; McNamara, M.; Kennedy, S.; May, D. D.; Skell, P. S.; O'Shea, D.; Devereux, M., Water-soluble bis(1,10-phenanthroline) octanedioate Cu^{2+} and Mn^{2+} complexes with unprecedented nano and picomolar *in vitro* cytotoxicity: promising leads for chemotherapeutic drug development. *MedChemComm* **2011,** *2*, 579-584.

71. McCann, M.; Santos, A. L. S.; da Silva, B. A.; Romanos, M. T. V.; Pyrrho, A. S.; Devereux, M.; Kavanagh, K.; Fichtner, I.; Kellett, A., *In vitro* and *in vivo* studies into the biological activities of 1,10-phenanthroline, 1,10-

phenanthroline-5,6-dione and its copper(II) and silver(I) complexes. *Toxicol. Res.* **2012,** *1*, 47-54.

72. Mowlds, P.; Kavanagh, K., Effect of pre-incubation temperature on susceptibility of *Galleria mellonella* larvae to infection by *Candida albicans*. *Mycopathologia* **2008,** *165*, 5-12.

73. (a) Gavin, D. P.; Stephens, J. C., Organocatalytic enantioselective Michael addition of β-diketones to β-nitrostyrene: the first Michael addition of dipivaloylmethane to an activated olefin. *ARKIVOC* **2011**, 407-421; (b) Murphy, J. J.; Quintard, A.; McArdle, P.; Alexakis, A.; Stephens, J. C., Asymmetric Organocatalytic 1,6-Conjugate Addition of Aldehydes to Dienic Sulfones. *Angew. Chem., Int. Ed.* **2011,** *50*, 5095-5098.

74. Gavin, D. P. Design, synthesis and evaluation of organocatalysts in 1,4-conjugate additions to nitroolefins and alkylidene malonates. Ph.D. NUI Maynooth, Maynooth, **2012**.

75. (a) MacMillan, D. W. C., The advent and development of organocatalysis. *Nature* **2008,** *455*, 304-308; (b) Okino, T.; Hoashi, Y.; Takemoto, Y., Enantioselective Michael Reaction of Malonates to Nitroolefins Catalyzed by Bifunctional Organocatalysts. *J. Am. Chem. Soc.* **2003,** *125*, 12672-12673.

76. Okino, T.; Hoashi, Y.; Furukawa, T.; Xu, X.; Takemoto, Y., Enantio- and Diastereoselective Michael Reaction of 1,3-Dicarbonyl Compounds to Nitroolefins Catalyzed by a Bifunctional Thiourea. *J. Am. Chem. Soc.* **2005,** *127*, 119-125.

77. McCooey, S. H.; Connon, S. J., Urea- and thiourea-substituted cinchona alkaloid derivatives as highly efficient bifunctional organocatalysts for the asymmetric addition of malonate to nitroalkenes: inversion of configuration at C9 dramatically improves catalyst performance. *Angew. Chem., Int. Ed.* **2005,** *44*, 6367-6370.

78. Vakulya, B.; Varga, S.; Csampai, A.; Soos, T., Highly enantioselective conjugate addition of nitromethane to chalcones using bifunctional cinchona organocatalysts. *Org. Lett.* **2005,** *7*, 1967-1969.

79. (a) Fan, W.; Kong, S.; Cai, Y.; Wu, G.; Miao, Z., Diastereo- and enantioselective nitro-Mannich reaction of α-substituted nitroacetates to N-phosphoryl imines catalyzed by cinchona alkaloid thiourea organocatalysts. *Org. Biomol. Chem.* **2013,** *11*, 3223-3229; (b) Zhang, F. G.; Zhu, X. Y.; Li, S.; Nie, J.; Ma, J. A., Highly enantioselective organocatalytic Strecker reaction of cyclic N-acyl trifluoromethylketimines: synthesis of anti-HIV drug DPC 083. *Chem. Commun.* **2012,** *48*, 11552-11554.

80. Hamza, A.; Schubert, G.; Soos, T.; Papai, I., Theoretical Studies on the Bifunctionality of Chiral Thiourea-Based Organocatalysts: Competing Routes to C-C Bond Formation. *J. Am. Chem. Soc.* **2006,** *128*, 13151-13160.

81. Manna, D.; Roy, G.; Mugesh, G., Antithyroid Drugs and Their Analogues: Synthesis, Structure, and Mechanism of Action. *Acc. Chem. Res.* **2013**, *46*, 2706-2715.

82. (a) Schroeder, D. C., Thioureas. *Chem. Rev.* **1955,** *55*, 181-228; (b) Mitchell, S. C.; Steventon, G. B., Thiourea and its biological interactions. *Sulfur Rep.* **1994,** *16*, 117-137.

83. Abbas, S. Y.; El-Sharief, M. A. M. S.; Basyouni, W. M.; Fakhr, I. M. I.; El-Gammal, E. W., Thiourea derivatives incorporating a hippuric acid moiety: Synthesis and evaluation of antibacterial and antifungal activities. *Eur. J. Med. Chem.* **2013,** *64*, 111-120.

84. Kalotka-Kreglewska, M., Antimalarial medications from native remedy. *Cent. Eur. J. Immunol.* **2011,** *36*, 100-103.

85. Kharal Saleem, A.; Hussain, Q.; Ali, S.; Fakhuruddin, Quinine is bactericidal. *J. Pak. Med. Assoc.* **2009,** *59*, 208-212.

86. Wolf, R.; Baroni, A.; Greco, R.; Donnarumma, G.; Ruocco, E.; Tufano, M. A.; Ruocco, V., Quinine sulfate and bacterial invasion. *Ann. Clin. Microbiol. Antimicrob.* **2002,** 1:5.

87. Purser, S.; Moore, P. R.; Swallow, S.; Gouverneur, V., Fluorine in medicinal chemistry. *Chem. Soc. Rev.* **2008,** *37*, 320-330.

88. Lipinski, C. A.; Lombardo, F.; Dominy, B. W.; Feeney, P. J., Experimental and computational approaches to estimate solubility and permeability in drug discovery and development settings. *Adv. Drug Delivery Rev.* **1997,** *23*, 3-25.

89. Arnott, J. A.; Planey, S. L., The influence of lipophilicity in drug discovery and design. *Expert Opin. Drug Discovery* **2012,** *7*, 863-875.

90. Oliva, C. G.; Silva, A. M. S.; Resende, D. I. S. P.; Paz, F. A. A.; Cavaleiro, J. A. S., Highly Enantioselective 1,4-Michael Additions of Nucleophiles to Unsaturated Aryl Ketones with Organocatalysis by Bifunctional Cinchona Alkaloids. *Eur. J. Org. Chem.* **2010**, 3449-3458.

91. Dolbier, W. R., Jr., A Guide to Fluorine NMR for Organic Chemists. John Wiley & Sons, Inc.: Hoboken, New Jersey, **2009**.

92. Gorka, A. P.; Sherlach, K. S.; de Dios, A. C.; Roepe, P. D., Relative to quinine and quinidine, their 9-epimers exhibit decreased cytostatic activity and altered heme binding but similar cytocidal activity versus *Plasmodium falciparum. Antimicrob. Agents Chemother.* **2013,** *57*, 365-374.

93. Mannschreck, A.; Kiesswetter, R., Unequal activities of enantiomers via biological receptors: Examples of chiral drug, pesticide, and fragrance molecules. *J. Chem. Educ.* **2007,** *84*, 2012-2018.

94. (a) Stefanska, J.; Szulczyk, D.; Koziol, A. E.; Miroslaw, B.; Kedzierska, E.; Fidecka, S.; Busonera, B.; Sanna, G.; Giliberti, G.; La Colla, P.; Struga, M., Disubstituted thiourea derivatives and their activity on CNS: Synthesis and biological evaluation. *Eur. J. Med. Chem.* **2012,** *55*, 205-213; (b) Saeed, S.; Rashid, N.; Jones, P. G.; Ali, M.; Hussain, R., Synthesis, characterization and biological evaluation of some thiourea derivatives bearing benzothiazole moiety as potential antimicrobial and anticancer agents. *Eur. J. Med. Chem.* **2010,** *45*, 1323-1331; (c) Khan, S. A.; Singh, N.; Saleem, K., Synthesis, characterization and *in vitro* antibacterial activity of thiourea and urea derivatives of steroids. *Eur. J. Med. Chem.* **2008,** *43*, 2272-2277.

95. Andres, J. M.; Manzano, R.; Pedrosa, R., Novel bifunctional chiral urea and thiourea derivatives as organocatalysts: enantioselective nitro-Michael reaction of malonates and diketones. *Chem. Eur. J.* **2008,** *14*, 5116-5119.

96. (a) Tarkanyi, G.; Kiraly, P.; Soos, T.; Varga, S., Active Conformation in Amine-Thiourea Bifunctional Organocatalysis Preformed by Catalyst Aggregation. *Chem. Eur. J.* **2012,** *18*, 1918-1922; (b) Tarkanyi, G.; Kiraly,

P.; Varga, S.; Vakulya, B.; Soos, T., Edge-to-face CH/π aromatic interaction and molecular self-recognition in epi-cinchona-based bifunctional thiourea organocatalysis. *Chem. Eur. J.* **2008,** *14*, 6078-6086; (c) Jang, H. B.; Rho, H. S.; Oh, J. S.; Nam, E. H.; Park, S. E.; Bae, H. Y.; Song, C. E., DOSY NMR for monitoring self aggregation of bifunctional organocatalysts: increasing enantioselectivity with decreasing catalyst concentration. *Org. Biomol. Chem.* **2010,** *8*, 3918-3922.

97.   (a) Rho, H. S.; Oh, S. H.; Lee, J. W.; Lee, J. Y.; Chin, J.; Song, C. E., Bifunctional organocatalyst for methanolytic desymmetrization of cyclic anhydrides: increasing enantioselectivity by catalyst dilution. *Chem. Commun.* **2008**, 1208-1210; (b) Berkessel, A.; Cleemann, F.; Mukherjee, S.; Mueller, T. N.; Lex, J., Highly efficient dynamic kinetic resolution of azlactones by urea-based bifunctional organocatalysts. *Angew. Chem., Int. Ed.* **2005,** *44*, 807-811.

98.   Yao, J.; He, Z.; Chen, J.; Sun, W.; Fang, H.; Xu, W., Design, synthesis and biological activities of sorafenib derivatives as antitumor agents. *Bioorg. Med. Chem. Lett.* **2012,** *22*, 6549-6553.

99.   Rolain, J. M.; Colson, P.; Raoult, D., Recycling of chloroquine and its hydroxyl analogue to face bacterial, fungal and viral infections in the 21st century. *Int. J. Antimicrob. Agents* **2007,** *30*, 297-308.

100.   Oliva, C. G.; Silva, A. M. S.; Resende, D. I. S. P.; Paz, F. A. A.; Cavaleiro, J. A. S., Highly Enantioselective 1,4-Michael Additions of Nucleophiles to Unsaturated Aryl Ketones with Organocatalysis by Bifunctional Cinchona Alkaloids. *European Journal of Organic Chemistry* **2010,** *2010*, 3449-3458.

101.   Li, X.; Deng, H.; Zhang, B.; Li, J.; Zhang, L.; Luo, S.; Cheng, J. P., Physical Organic Study of Structure-Activity-Enantioselectivity Relationships in Asymmetric Bifunctional Thiourea Catalysis: Hints for the Design of New Organocatalysts. *Chem. Eur. J.* **2010,** *16*, 450-455.

102.   McCooey, S. H.; Connon, S. J., Urea- and thiourea-substituted cinchona alkaloid derivatives as highly efficient bifunctional organocatalysts for the asymmetric addition of malonate to nitroalkenes: inversion of configuration at C9 dramatically improves catalyst performance. *Angew. Chem., Int. Ed.* **2005,** *44*, 6367-6370.

103.   Liu, T. Y.; Long, J.; Li, B. J.; Jiang, L.; Li, R.; Wu, Y.; Ding, L. S.; Chen, Y. C., Enantioselective construction of quaternary carbon centre catalyzed by bifunctional organocatalyst. *Org. Biomol. Chem.* **2006,** *4*, 2097-2099.

104.   This compound has been reported in the literature, however, to our knowledge, it appears to be spectroscopically uncharacterised.

105.   Varga, S.; Jakab, G.; Drahos, L.; Holczbauer, T.; Czugler, M.; Soos, T., Double diastereocontrol in bifunctional thiourea organocatalysis: Iterative Michael-Michael-Henry sequence regulated by the configuration of chiral catalysts. *Org. Lett.* **2011,** *13*, 5416-5419.

106.   Natarajan, A.; Guo, Y.; Arthanari, H.; Wagner, G.; Halperin, J. A.; Chorev, M., Synthetic Studies toward Aryl(4-aryl-4H-[1,2,4]triazol-3-yl)amine from 1,3-Diarylthiourea as Urea Mimetics. *J. Org. Chem.* **2005,** *70*, 6362-6368.

107. Li, X.; Deng, H.; Luo, S.; Cheng, J. P., Organocatalytic three-component reactions of pyruvate, aldehyde and aniline by hydrogen-bonding catalysts. *Eur. J. Org. Chem.* **2008**, 4350-4356.

108. Berkessel, A.; Mukherjee, S.; Mueller, T. N.; Cleemann, F.; Roland, K.; Brandenburg, M.; Neudoerfl, J. M.; Lex, J., Structural optimization of thiourea-based bifunctional organocatalysts for the highly enantioselective dynamic kinetic resolution of azlactones. *Org. Biomol. Chem.* **2006,** *4*, 4319-4330.

109. Antriole, v. T., *The Quinolones*. 3rd ed.; Academic Press.; San Diego, California, **2000**.

110. Radl, S., From chloroquine to antineoplastic drugs? The story of antibacterial quinolones. *Arch. Pharm.* **1996,** *329*, 115-119.

111. (a) Ball, P., Quinolone generations: natural history or natural selection? *J. Antimicrob. Chemother.* **2000,** *46*, 17-24; (b) Cheng, G.; Hao, H.; Dai, M.; Liu, Z.; Yuan, Z., Antibacterial action of quinolones: from target to network. *Eur. J. Med. Chem.* **2013,** *66*, 555-562; (c) King, D. E.; Malone, R.; Lilley, S. H., New classification and update on the quinolone antibiotics. *Am. Fam. Physician.* **2000,** *61*, 2741-278.

112. http://www.taigenbiotech.com.tw/news.html#21, TaiGen Biotechnology., TaiGen Biotechnology Announces Submission of New Drug Application for Nemonoxacin in Taiwan and China. Date accessed **31/10/13**.

113. http://www.furiex.com/pipeline/discoverydevelopment-pipeline/fluoroquinolone/, Furiex Pharmaceuticals., Avarofloxacin. Date accessed **31/10/13**.

114. Drlica, K.; Malik, M., Fluoroquinolones: action and resistance. *Curr. Top. Med. Chem.* **2003,** *3*, 249-282.

115. Berger, J. M.; Gamblin, S. J.; Harrison, S. C.; Wang, J. C., Structure and mechanism of DNA topoisomerase II. *Nature* **1996,** *380*, 225-232.

116. Takei, M.; Fukuda, H.; Yasue, T.; Hosaka, M.; Oomori, Y., Inhibitory activities of gatifloxacin (AM-1155), a newly developed fluoroquinolone, against bacterial and mammalian type II topoisomerases. *Antimicrob. Agents Chemother.* **1998,** *42*, 2678-2681.

117. Malik, S.; Choudhary, A.; Kumar, S.; Avasthi, G., Quinolones: a therapeutic review. *J. Pharm. Res.* **2010,** *3*, 1519-1523.

118. Ostrovskii, V. A.; Trifonov, R. E.; Popova, E. A., Medicinal chemistry of tetrazoles. *Russ. Chem. Bull.* **2012,** *61*, 768-780.

119. (a) Pal, D.; Saha, S., Hydroxamic acid - a novel molecule for anticancer therapy. *J. Adv. Pharm. Technol. Res.* **2012,** *3*, 92-99; (b) Bertrand, S.; Helesbeux, J. J.; Larcher, G.; Duval, O., Hydroxamate, a Key Pharmacophore Exhibiting a Wide Range of Biological Activities. *Mini-Rev. Med. Chem.* **2013,** *13*, 1311-1326.

120. Stern, E.; Muccioli, G. G.; Millet, R.; Goossens, J. F.; Farce, A.; Chavatte, P.; Poupaert, J. H.; Lambert, D. M.; Depreux, P.; Henichart, J. P., Novel 4-Oxo-1,4-dihydroquinoline-3-carboxamide Derivatives as New CB2 Cannabinoid Receptors Agonists: Synthesis, Pharmacological Properties and Molecular Modeling. *J. Med. Chem.* **2006,** *49*, 70-79.

121. http://www.rsc.org/periodic-table/trends, Royal Society of Chemistry., Periodic Table. Date accessed **03/11/13**.

122. Lager, E.; Andersson, P.; Nilsson, J.; Pettersson, I.; Oestergaard Nielsen, E.; Nielsen, M.; Sterner, O.; Liljefors, T., 4-Quinolone Derivatives: High-Affinity Ligands at the Benzodiazepine Site of Brain GABAA Receptors. Synthesis, Pharmacology, and Pharmacophore Modeling. *J. Med. Chem.* **2006,** *49*, 2526-2533.

123. Frank, J.; Meszaros, Z., Quinoline derivatives. **1975**, Patent 1398066.

124. Hadjeri, M.; Mariotte, A. M.; Boumendjel, A., Alkylation of 2-phenyl-4-quinolones: synthetic and structural studies. *Chem. Pharm. Bull.* **2001,** *49*, 1352-1355.

125. (a) Kemp, W., *Organic Spectroscopy*. The Macmillan Press Ltd.: **1979**; (b) Bruker, *AVANCE User's Guide*.

126. Podanyi, B.; Kereszturi, G.; Vasvaridebreczy, L.; Hermecz, I.; Toth, G., An NMR study of halogenated 1,4-dihydro-1-ethyl-4-oxoquinoline-3-carboxylates. *Magn. Reson. Chem.* **1996,** *34*, 972-978.

127. Sayyed, I. A.; Panse, D. G.; Bhawal, B. M.; Deshmukh, A. R. A. S., An efficient synthesis of N-alkyl-1,4-dihydro-4-oxo-3-quinolinecarboxylic acids via ethyl 2-(2,2,2-trichloroethylidene)-3-oxo-3-(2-chlorophenyl)propionate. *Synth. Commun.* **2000,** *30*, 2533-2540.

128. Tamura, Y.; Fujita, M.; Chen, L. C.; Ueno, K.; Kita, Y., N-Alkylation of ethyl 1,4-dihydro-4-oxopyridine-3-carboxylates *via* their thallium(I) salts. *Chem. Pharm. Bull.* **1981,** *29*, 739-743.

129. Shipe, W. D.; Lindsley, C.; Hallett, D. Preparation of quinolone M1 receptor positive allosteric modulators. Int. Pat. Appl. PCT/US2006/046332, **2007**.

130. Rueping, M.; Stoeckel, M.; Sugiono, E.; Theissmann, T., Asymmetric metal-free synthesis of fluoroquinolones by organocatalytic hydrogenation. *Tetrahedron* **2010,** *66*, 6565-6568.

131. Gernon, T. Synthesis and Characterisation of Upper and Lower Rim Derived Calixarenes: Towards the Development of a New Supramolecular Assembley. Ph.D. Institute of Technology Tallaght, Dublin, **2007**.

132. (a) Clayden, J.; Greeves, N.; Wothers, P., *Organic Chemistry*. 1st ed.; Oxford University Press.: New York, **2008**; (b) Himo, F.; Demko, Z. P.; Noodleman, L.; Sharpless, K. B., Mechanisms of Tetrazole Formation by Addition of Azide to Nitriles. *J. Am. Chem. Soc.* **2002,** *124*, 12210-12216.

133. Finnegan, W. G.; Henry, R. A.; Lofquist, R., An improved synthesis of 5-substituted tetrazoles. *J. Am. Chem. Soc.* **1958,** *80*, 3908-3911.

134. Hill, M.; Mahon, M. F.; McGinley, J.; Molloy, K. C., New supramolecular architectures based on polyfunctional organotin tetrazoles: synthesis and characterization of phenylene-bridged bis(organotin tetrazoles). *J. Chem. Soc., Dalton Trans.* **1996**, 835-845.

135. Bethel, P. A.; Hill, M. S.; Mahon, M. F.; Molloy, K. C., Reactions of organotin tetrazoles: synthesis of functionalized polytetrazoles. *J. Chem. Soc., Perkin Trans. 1* **1999**, 3507-3514.

136. (a) Gothelf, K. V.; Jorgensen, K. A., Asymmetric 1,3-Dipolar Cycloaddition Reactions. *Chem. Rev.* **1998,** *98*, 863-909; (b) Nakayama, K.; Ishida, Y.; Ohtsuka, M.; Kawato, H.; Yoshida, K.-i.; Yokomizo, Y.; Ohta, T.; Hoshino,

K.; Otani, T.; Kurosaka, Y.; Yoshida, K.; Ishida, H.; Lee, V. J.; Renau, T. E.; Watkins, W. J., MexAB-OprM specific efflux pump inhibitors in *Pseudomonas aeruginosa*. Part 2: Achieving activity *in vivo* through the use of alternative scaffolds. *Bioorg. Med. Chem. Lett.* **2003**, *13*, 4205-4208.

137. Stephens, J. C. Studies in the Higher Azole Series: (i) First Generation of Pentazole HN$_5$ (Pentazolic Acid) and N$_5$ from a New Dearylation of N-*p*-methoxyphenylazoles. (ii) First Reversible Protonation of a 1-Arylpentazole. (iii) Sequential Cycloaddition-Rearrrangement-Ring Expansion Cascades with 1,2,3-Triazolium-1-aminide 1,3-Dipoles. New Ring Systems. Ph.D. NUI Galway, Galway, **2004**.

138. Shen, L. L.; Mitscher, L. A.; Sharma, P. N.; O'Donnell, T. J.; Chu, D. W. T.; Cooper, C. S.; Rosen, T.; Pernet, A. G., Mechanism of inhibition of DNA gyrase by quinolone antibacterials: a cooperative drug-DNA binding model. *Biochemistry* **1989,** *28*, 3886-3894.

139. Carpenter, W. R., Formation of tetrazoles by the condensation of organic azides with nitriles. *J. Org. Chem.* **1962,** *27*, 2085-2088.

140. Joullie, M. M.; Lassen, K. M., Evolution of amide bond formation. *ARKIVOC* **2010**, 189-250.

141. Valeur, E.; Bradley, M., Amide bond formation: beyond the myth of coupling reagents. *Chem. Soc. Rev.* **2009**, *38*, 606-631.

142. El-Faham, A.; Funosas, R. S.; Prohens, R.; Albericio, F., COMU: A Safer and More Effective Replacement for Benzotriazole-Based Uronium Coupling Reagents. *Chem. Eur. J.* **2009,** *15*, 9404-9416.

143. El-Faham, A.; Albericio, F., COMU: A third generation of uronium-type coupling reagents. *J. Pept. Sci.* **2010,** *16*, 6-9.

144. Carpino, L. A.; Imazumi, H.; El-Faham, A.; Ferrer, F. J.; Zhang, C.; Lee, Y.; Foxman, B. M.; Henklein, P.; Hanay, C.; Mugge, C.; Wenschuh, H.; Klose, J.; Beyermann, M.; Bienert, M., The uronium/guanidinium peptide coupling reagents: finally the true uronium salts. *Angew. Chem., Int. Ed.* **2002,** *41*, 441-445.

145. Junkers, M., COMU—Safer and More Efficient Peptide Coupling Reagent. *Aldrich Chemfiles* **2010,** *10*.

146. Reddy, A. S.; Kumar, M. S.; Reddy, G. R., A convenient method for the preparation of hydroxamic acids. *Tetrahedron Lett.* **2000,** *41*, 6285-6288.

147. Zubair, M. Synthesis and Characterisation of Novel Quinolin-2(1H)-one derived Ligands and their Metal Complexes as Potential Anti-microbial Agents and Superoxide Dismutase (SOD) mimics. Institute of Technology Tallaght, Dublin, **2010**.

148. Gilis, P. M.; Haemers, A.; Bollaert, W., 1H-Tetrazol-5-yl derivatives of chemotherapeutic agents of the nalidixic acid type. *Eur. J. Med. Chem. Chim. Ther.* **1980,** *15*, 499-502.

149. Popova, E. A.; Trifonov, R. E.; Ostrovskii, V. A., Advances in the synthesis of tetrazoles coordinated to metal ions. *ARKIVOC* **2012**, 45-65.

150. Uivarosi, V., Metal complexes of quinolone antibiotics and their applications: an update. *Molecules* **2013**, *18*, 11153-11197.

151. Shivalkar, R. L.; Sunthankar, S. V., Reaction of lithium aluminum hydride with arylaminomethylenemalonate esters and related compounds. *J. Am. Chem. Soc.* **1960,** *82*, 718-721.

152. Knippel, E.; Knippel, M.; Michalik, M.; Kelling, H.; Kristen, H., On the geometric isomers of ethyl 2-nitro-3-ethoxyacrylate, ethyl 2-nitro-3-phenylaminoacrylate, and ethyl 2-cyano-3-phenylaminoacrylate. *Tetrahedron* **1977,** *33*, 231-234.

153. Banerji, B.; Conejo-Garcia, A.; McNeill, L. A.; McDonough, M. A.; Buck, M. R. G.; Hewitson, K. S.; Oldham, N. J.; Schofield, C. J., The inhibition of factor inhibiting hypoxia-inducible factor (FIH) by β-oxocarboxylic acids. *Chem. Commun.* **2005**, 5438-5440.

154. Yungjin Phatmaceutical Co. Ltd. Quinolone derivatives as caspase 3 inhibitor. Preparation process for the same and pharmaceutical composition comprising the same. Int. Pat. Appl. PCT/KR2008/000202, **2008**.

155. Zalibera, L.; Milata, V.; Ilavsky, D., 1H and 13C NMR spectra of 3-substituted 4-quinolones. *Magn. Reson. Chem.* **1998,** *36*, 681-684.

156. Boschelli, D. H.; Wu, B.; Ye, F.; Durutlic, H.; Golas, J. M.; Lucas, J.; Boschelli, F., Facile preparation of new 4-phenylamino-3-quinoline carbonitrile Src kinase inhibitors via 7-fluoro intermediates: Identification of potent 7-amino analogs. *Bioorg. Med. Chem.* **2008,** *16*, 405-412.

157. Hennequin, L. F. A.; Gibson, K. H.; Foote, K. M. Preparation of benzofuranyl substituted 3-cyanoquinolines for the treatment of solid tumors. Int. Pat. Appl. PCT/GB02/05493, **2003**.

158. Van Es, T.; Staskun, B., 1-Alkyl-1,4-dihydro-4-imino-3-quinoline carboxylates. Part 2. Hydrolysis and rearrangement products. *S. Afr. J. Chem.* **1998,** *51*, 121-126.

159. Minami, S. Piperazine Derivatives. US. Pat. Appl. 545549, **1977**.

160. ITRI Tin for Tomorrow. Contributing to Global Sustainable Development.; **2013**.

161. Davies, A. G.; Geilen, M.; Parnell, K. H.; Tiekink, E. R. T. *Tin Chemistry. Fundamentals, Frontiers, and Applications.* John Wiley & Sons, Ltd.: United Kingdom, **2008**.

162. Housecroft, C. E.; Sharpe, A. G., *Inorganic Chemistry*. 3rd ed.; Pearson Education Ltd.: **2008**.

163. ITRI The leading tin companies in 2010; **2011**.

164. King, R. B., *Encyclopedia of Inorganic Chemistry*. 2nd ed.; Wiley: **2005**.

165. http://www.lme.com/metals/non-ferrous/tin/production-and-consumption/, London Metal Exchange., Tin. Production and Consumption. Date accessed **13/06/13**.

166. Arkis, E.; Balkoese, D., Thermal stabilization of polyvinyl chloride by organotin compounds. *Polym. Degrad. Stab.* **2005,** *88*, 46-51.

167. *Inorganic Experiments*. VCH Verlagsgesellschaft mbH: D-69451 Weinheim, **1994**.

168. Plumbridge, W. J., Tin pest issues in lead-free electronic solders. *J. Mater. Sci. Mater. Electron.* **2007,** *18*, 307-318.

169. Atkins, P.; Overtone, T.; Rourke, J., *Inorganic Chemistry*. 3rd ed.; Oxford University Press: **1999**.

170. Davies, A. G., *Organotin Chemistry*. 2nd ed.; Wiley-VCH: Weinheim, Germany, **2003**.

171. Smith, A.; Davies, A. G., Tin. *Comprehensive Organometallic Chemistry. The Synthesis, Reactions and Structures of Organometallic Compounds.* **1982,** *2*.

172. Song, X.; Zapata, A.; Eng, G., Organotins and quantitative-structure activity/property relationships. *J. Organomet. Chem.* **2006,** *691*, 1756-1760.

173. Stoner, H. B.; Barnes, J. M.; Duff, J. I., Studies on the toxicity of alkyl tin compounds. *Br. J. Pharmacol. Chemother.* **1955,** *10*, 16-25.

174. Nath, M., Toxicity and the cardiovascular activity of organotin compounds: a review. *Appl. Organomet. Chem.* **2008,** *22*, 598-612.

175. Basu Baul, T. S., Antimicrobial activity of organotin(IV) compounds: a review. *Appl. Organomet. Chem.* **2008,** *22*, 195-204.

176. Omae, I., Organotin antifouling paints and their alternatives. *Appl. Organomet. Chem.* **2003,** *17*, 81-105.

177. Hadjikakou, S. K.; Hadjiliadis, N., Antiproliferative and anti-tumor activity of organotin compounds. *Coord. Chem. Rev.* **2009,** *253*, 235-249.

178. Hoch, M., Organotin compounds in the environment - an overview. *Appl. Geochem.* **2001,** *16*, 719-743.

179. Eng, G.; Song, X.; Zapata, A.; de Dios, A. C.; Casabianca, L.; Pike, R. D., Synthesis, structural and larvicidal studies of some triorganotin 2-(*p*-chlorophenyl)-3-methylbutyrates. *J. Organomet. Chem.* **2007,** *692*, 1398-1404.

180. Gielen, M., Organotin compounds and their therapeutic potential: a report from the organometallic chemistry department of the Free University of Brussels. *Appl. Organomet. Chem.* **2002,** *16*, 481-494.

181. (a) Pruchnik, F. P.; Banbula, M.; Ciunik, Z.; Chojnacki, H.; Latocha, M.; Skop, B.; Wilczok, T.; Opolski, A.; Wietrzyk, J.; Nasulewicz, A., Structure, properties and cytostatic activity of triorganotin (aminoaryl)carboxylates. *Eur. J. Inorg. Chem.* **2002**, 3214-3221; (b) Khan, M. I.; Baloch, M. K.; Ashfaq, M.; Stoter, G., *In vivo* toxicological effects and spectral studies of new triorganotin(IV)-N-maleoyltranexamates. *J. Organomet. Chem.* **2006,** *691*, 2554-2562; (c) Tian, L.; Sun, Y.; Li, H.; Zheng, X.; Cheng, Y.; Liu, X.; Qian, B., Synthesis, characterization and biological activity of triorganotin 2-phenyl-1,2,3-triazole-4-carboxylates. *J. Inorg. Biochem.* **2005,** *99*, 1646-1652; (d) Zhang, Z.-W.; Jiang, T.; Ren, S.-M.; Zhang, Y.-X.; Yu, J.-S., Synthesis, crystal structure and *in vitro* antitumor activity of Di-n-butyltin p-[N,N-bis(2-chloroethyl)amino]benzoates. *Chin. J. Chem.* **2005,** *23*, 1655-1658; (e) Nath, M.; Pokharia, S.; Song, X.; Eng, G.; Gielen, M.; Kemmer, M.; Biesemans, M.; Willem, R.; de Vos, D., New organotin(IV) derivatives of dipeptides as models for metal-protein interactions: *in vitro* anti-tumour activity. *Appl. Organomet. Chem.* **2003,** *17*, 305-314; (f) Kovala-Demertzi, D.; Dokorou, V. N.; Jasinski, J. P.; Opolski, A.; Wiecek, J.; Zervou, M.; Demertzis, M. A., Organotin flufenamates: synthesis, characterization and antiproliferative activity of organotin flufenamates. *J. Organomet. Chem.* **2005,** *690*, 1800-1806; (g) Xanthopoulou, M. N.; Hadjikakou, S. K.; Hadjiliadis, N.; Schuermann, M.; Jurkschat, K.; Binolis, J.; Karkabounas, S.;

Charalabopoulos, K., Synthesis of a novel triphenyltin(IV) derivative of 2-mercaptonicotinic acid with potent cytotoxicity *in vitro*. *Bioinorg. Chem. Appl.* **2003,** *1*, 227-231; (h) Kemmer, M.; Dalil, H.; Biesemans, M.; Martins, J. C.; Mahieu, B.; Horn, E.; De Vos, D.; Tiekink, E. R. T.; Willem, R.; Gielen, M., Dibutyltin perfluoroalkanecarboxylates: synthesis, NMR characterization and *in vitro* antitumor activity. *J. Organomet. Chem.* **2000,** *608*, 63-70.

182. Caruso, F.; Giomini, M.; Giuliani, A. M.; Rivarola, E., Synthesis, spectroscopic (Moessbauer, IR and NMR) and X-ray structural studies of diorganotin complexes of 2,2'-bipyrimidine and further NMR studies of diorganotin-pyrazine and -2,2'-azopyridine complexes. *J. Organomet. Chem.* **1996,** *506*, 67-76.

183. Li, Q.; Guedes Da Silva, M. F. C.; Pombeiro, A. J. L., Diorganotin(IV) derivatives of substituted benzohydroxamic acids with high antitumor activity. *Chem. Eur. J.* **2004,** *10*, 1456-1462.

184. Saxena, A. K.; Huber, F., Organotin compounds and cancer chemotherapy. *Coord. Chem. Rev.* **1989,** *95*, 109-123.

185. Crowe, A. J.; Smith, P. J.; Cardin, C. J.; Parge, H. E.; Smith, F. E., Possible predissociation of diorganotin dihalide complexes: relationship between antitumor activity and structure. *Cancer Lett.* **1984,** *24*, 45-8.

186. Pellerito, C.; Nagy, L.; Pellerito, L.; Szorcsik, A., Biological activity studies on organotin(IV)$^{n+}$ complexes and parent compounds. *J. Organomet. Chem.* **2006,** *691*, 1733-1747.

187. Tabassum, S.; Pettinari, C., Chemical and biotechnological developments in organotin cancer chemotherapy. *J. Organomet. Chem.* **2006,** *691*, 1761-1766.

188. Matysiak, J.; Opolski, A., Synthesis and antiproliferative activity of N-substituted 2-amino-5-(2,4-dihydroxyphenyl)-1,3,4-thiadiazoles. *Bioorg. Med. Chem.* **2006,** *14*, 4483-4489.

189. http://iaspub.epa.gov/apex/pesticides/f?p=PPLS:8:3908148030001::NO::P8_PUID:501800, Environmetnal Protection Agency. Date accessed **03/07/13**.

190. (a) Nok, A. J.; Shuaibu, M. N.; Bonire, J. J.; Dabo, A.; Wushishi, Z.; Ado, S., Triphenyltin salicylate-antimicrobial effect and resistance - the pyrophosphatase connection. *J. Enzyme Inhib.* **2000,** *15*, 411-420; (b) Sadiq ur, R.; Ali, S.; Mazhar, M.; Badshah, A.; Parvez, M., Synthesis, spectroscopic characterization, and biological activity studies of organotin(IV) derivatives of (*E*)-3-(3-fluorophenyl)-2-phenyl-2-propenoic acid. Crystal and molecular structure of $Et_2Sn[OCOC(C_6H_5)=CH(_3-FC_6H_4)]$. *Heteroat. Chem.* **2006,** *17*, 420-432; (c) Rehman, W.; Baloch, M. K.; Badshah, A., Comparative study of structure-activity relationship of di and triorganotin (IV) complexes of monomethyl glutarate. *J. Braz. Chem. Soc.* **2005,** *16*, 827-834; (d) Cai, S. L.; Chen, Y.; Sun, W. X.; Li, H.; Chen, Y.; Yuan, S.S., 2-, 3-, and 4-(1-Oxo-1H-2,3-dihydroisoindol-2-yl)benzoic acids and their corresponding organotin carboxylates: Synthesis, characterization, fluorescent, and biological activities. *Bioorg. Med. Chem. Lett.* **2010,** *20*, 5649-5652; (e) Kang, W.; Wu, X.; Huang, J., Synthesis, crystal structure and biological activities of four novel tetranuclear di-organotin(IV) carboxylates. *Journal of Organometallic Chemistry* **2009,** *694*, 2402-2408; (f) Muhammad,

N.; Zia ur, R.; Ali, S.; Meetsma, A.; Shaheen, F., Organotin(IV) 4-methoxyphenylethanoates: Synthesis, spectroscopic characterization, X-ray structures and *in vitro* anticancer activity against human prostate cell lines (PC-3). *Inorg. Chim. Acta* **2009,** *362*, 2842-2848; (g) Tariq, M.; Muhammad, N.; Sirajuddin, M.; Ali, S.; Shah, N. A.; Khalid, N.; Tahir, M. N.; Khan, M. R., Synthesis, spectroscopic characterization, X-ray structures, biological screenings, DNA interaction study and catalytic activity of organotin(IV) 3-(4-fluorophenyl)-2-methylacrylic acid derivatives. *J. Organomet. Chem.* **2013,** *723*, 79-89.

191.   (a) Nath, M.; Pokharia, S.; Yadav, R., Organotin(IV) complexes of amino acids and peptides. *Coord. Chem. Rev.* **2001,** *215*, 99-149; (b) Chaudhary, A.; Agarwal, M.; Singh, R. V., Organotin(IV) and organolead(IV) complexes as biocides and fertility regulators: synthetic, spectroscopic and biological studies. *Appl. Organomet. Chem.* **2006,** *20*, 295-303; (c) Nath, M.; Yadav, R.; Eng, G.; Nguyen, T. T.; Kumar, A., Characteristic spectral studies, and antimicrobial and anti-inflammatory activities of diorganotin(IV) derivatives of dipeptides. *J. Organomet. Chem.* **1999,** *577*, 1-8; (d) Nath, M.; Pokharia, S.; Eng, G.; Song, X.; Kumar, A., New triorganotin(IV) derivatives of dipeptides as anti-inflammatory-antimicrobial agents. *Eur. J. Med. Chem.* **2005,** *40*, 289-298.

192.   Jain, M.; Maanju, S.; Singh, R. V., Synthesis, structural studies and some biological aspects, including nematicidal and insecticidal properties, of organotin(IV) complexes formed with biologically active sulfonamide imine ligand. *Appl. Organomet. Chem.* **2004,** *18*, 471-479.

193.   (a) Carcelli, M.; Pelizzi, C.; Pelizzi, G.; Mazza, P.; Zani, F., The different behavior of the di-2-pyridyl ketone 2-thenoylhydrazone in two organotin compounds. Synthesis, X-ray structure and biological activity. *J. Organomet. Chem.* **1995,** *488*, 55-61; (b) Ianelli, S.; Mazza, P.; Orcesi, M.; Pelizzi, C.; Pelizzi, G.; Zani, F., Synthesis, structure, and biological activity of organotin compounds with di-2-pyridylketone and phenyl(2-pyridyl) ketone 2-aminobenzoylhydrazones. *J. Inorg. Biochem.* **1995,** *60*, 89-108.

194.   (a) Girasolo, M. A.; Di Salvo, C.; Schillaci, D.; Barone, G.; Silvestri, A.; Ruisi, G., Synthesis, characterization, and *in vitro* antimicrobial activity of organotin(IV) complexes with triazolo-pyrimidine ligands containing exocyclic oxygen atoms. *J. Organomet. Chem.* **2005,** *690*, 4773-4783; (b) Girasolo, M. A.; Schillaci, D.; Di Salvo, C.; Barone, G.; Silvestri, A.; Ruisi, G., Synthesis, spectroscopic characterization and *in vitro* antimicrobial activity of diorganotin(IV) dichloride adducts with [1,2,4]triazolo-[1,5-a]pyrimidine and 5,7-dimethyl-[1,2,4]triazolo-[1,5-a]pyrimidine. *J. Organomet. Chem.* **2006,** *691*, 693-701.

195.   Chauhan, H. P. S.; Shaik, N. M., Synthetic, spectral, thermal and antimicrobial studies on some mixed 1,3-dithia-2-stannacyclopentane derivatives with dialkyldithiocarbamates. *J. Inorg. Biochem.* **2005,** *99*, 538-545.

196.   Nath, M.; Jairath, R.; Eng, G.; Song, X.; Kumar, A., Triorganotin(IV) derivatives of umbelliferone (7-hydroxycoumarin) and their adducts with

1,10-phenanthroline: synthesis, structural and biological studies. *J. Organomet. Chem.* **2005,** *690*, 134-144.

197. Gleeson, B.; Claffey, J.; Ertler, D.; Hogan, M.; Mueller-Bunz, H.; Paradisi, F.; Wallis, D.; Tacke, M., Novel organotin antibacterial and anticancer drugs. *Polyhedron* **2008,** *27*, 3619-3624.

198. Joshi, A.; Verma, S.; Gaur, R. B.; Sharma, R. R., Di-n-butyltin(IV) complexes derived from heterocyclic β-diketones and N-phthaloyl amino acids: Preparation, biological evaluation, structural elucidation based upon spectral [IR, NMR (^{1}H, ^{13}C, ^{19}F and ^{119}Sn)] studies. *Bioinorg. Chem. Appl.* **2005,** *3*, 201-215.

199. Srivastava, R. S., Pseudotetrahedral cobalt(II), nickel(II) and copper(II) complexes of N1-(o-chlorophenyl)-2-(2',4'-dihydroxyphenyl)-2-benzylazomethine - their fungicidal and herbicidal activity. *Inorg. Chim. Acta* **1981,** *56*, L65-L67.

200. Eng, G.; Zhang, Y. Z.; Whalen, D.; Ramsammy, R.; Khoo, L. E.; DeRosa, M., Structure-activity relationships of effect of aryltin compounds on *Ceratocystis ulmi*. *Appl. Organomet. Chem.* **1994,** *8*, 445-449.

201. (a) Duong, Q.; Song, X.; Mitrojorgji, E.; Gordon, S.; Eng, G., Larvicidal and structural studies of some triphenyl- and tricyclohexyltin para-substituted benzoates. *J. Organomet. Chem.* **2006,** *691*, 1775-1779; (b) Eng, G.; Song, X.; Duong, Q.; Strickman, D.; Glass, J.; May, L., Synthesis, structure characterization and insecticidal activity of some triorganotin dithiocarbamates. *Appl. Organomet. Chem.* **2003,** *17*, 218-225.

202. Carraher, C. E., Jr.; Sabir, T. S.; Roner, M. R.; Shahi, K.; Bleicher, R. E.; Roehr, J. L.; Bassett, K. D., Synthesis of Organotin Polyamine Ethers Containing Acyclovir and their Preliminary Anticancer and Antiviral Activity. *J. Inorg. Organomet. Polym. Mater.* **2006,** *16*, 249-257.

203. Bencini, A.; Lippolis, V., 1,10-Phenanthroline: A versatile building block for the construction of ligands for various purposes. *Coord. Chem. Rev.* **2010,** *254*, 2096-2180.

204. Smith, G. F.; Getz, C. A., The improved synthesis of o-phenanthroline. *Chem. Rev.* **1935,** *16*, 113-120.

205. Case, F. H., Substituted 1,10-phenanthrolines. I. The synthesis of certain mono- and polymethyl-1,10-phenanthrolines. *J. Am. Chem. Soc.* **1948,** *70*, 3994-3996.

206. Calderazzo, F.; Marchetti, F.; Pampaloni, G.; Passarelli, V., Coordination properties of 1,10-phenanthroline-5,6-dione towards group 4 and 5 metals in low and high oxidation states. *J. Chem. Soc., Dalton Trans.* **1999**, 4389-4396.

207. Brandt, W. W.; Dwyer, F. P.; Gyarfas, E. C., Chelate complexes of 1,10-phenanthroline and related compounds. *Chem. Rev.* **1954,** *54*, 959-1017.

208. Butler, H. M.; Hurse, A.; Thursky, E.; Shulman, A., Bactericidal action of selected phenanthroline chelates and related compounds. *Aust. J. Exp. Biol. Med. Sci.* **1969,** *47*, 541-52.

209. Dwyer, F. P.; Reid, I. K.; Shulman, A.; Laycock, G. M.; Dixon, S., The biological actions of 1,10-phenanthroline and 2,2'-bipyridine hydrochlorides, quaternary salts and metal chelates and related compounds. Bacteriostatic

action on selected Gram-positive, Gram-negative and acid-fast bacteria. *Aust. J. Exp. Biol. Med. Sci.* **1969,** *47*, 203-208.

210. Macleod, R. A., The toxicity of *o*-phenanthroline for lactic acid bacteria. *J. Biol. Chem.* **1952,** *197*, 751-61.

211. Devereux, M.; O'Shea, D.; Kellett, A.; McCann, M.; Walsh, M.; Egan, D.; Deegan, C.; Kedziora, K.; Rosair, G.; Mueller-Bunz, H., Synthesis, X-ray crystal structures and biomimetic and anticancer activities of novel copper(II) benzoate complexes incorporating 2-(4'-thiazolyl)benzimidazole (thiabendazole), 2-(2-pyridyl)benzimidazole and 1,10-phenanthroline as chelating nitrogen donor ligands. *J. Inorg. Biochem.* **2007,** *101*, 881-892.

212. Creaven, B. S.; Egan, D. A.; Karcz, D.; Kavanagh, K.; McCann, M.; Mahon, M.; Noble, A.; Thati, B.; Walsh, M., Synthesis, characterization and antimicrobial activity of copper(II) and manganese(II) complex of coumarin-6,7-dioxyacetic acid (cdoaH$_2$) and 4-methylcoumarin-6,7-dioxyacetic acid (4-MecdoaH$_2$): X-ray crystal structures of [Cu(cdoa)(phen)$_2$]·8.8H$_2$O and [Cu(4-Mecdoa)(phen)$_2$]·13H$_2$O (phen = 1,10-phenanthroline). *J. Inorg. Biochem.* **2007,** *101*, 1108-1119.

213. Devereux, M.; O'Shea, D.; O'Connor, M.; Grehan, H.; Connor, G.; McCann, M.; Rosair, G.; Lyng, F.; Kellett, A.; Walsh, M.; Egan, D.; Thati, B., Synthesis, catalase, superoxide dismutase and antitumor activities of copper(II) carboxylate complexes incorporating benzimidazole, 1,10-phenanthroline and bipyridine ligands: X-ray crystal structures of [Cu(BZA)$_2$(bipy)(H$_2$O)], [Cu(SalH)$_2$(BZDH)$_2$] and [Cu(CH$_3$COO)$_2$(5,6-DMBZDH)$_2$] (SalH$_2$ = salicylic acid; BZAH = benzoic acid; BZDH = benzimidazole and 5,6-DMBZDH = 5,6-dimethylbenzimidazole). *Polyhedron* **2007,** *26*, 4073-4084.

214. Devereux, M.; McCann, M.; Leon, V.; Kelly, R.; O Shea, D.; McKee, V., Synthesis and *in vitro* anti-microbial activity of manganese (II) complexes of 2,2-dimethylpentanedioic and 3,3-dimethylpentanedioic acid: X-ray crystal structure of [Mn(3dmepda)(phen)$_2$]·7.5H$_2$O (3dmepdaH$_2$ = 3,3-dimethyl pentanedioic acid and phen = 1,10-phenanthroline). *Polyhedron* **2003,** *22*, 3187-3194.

215. Dickenson, J. E.; Summers, L. E., Derivatives of 1,10-phenanthroline-5,6-quinone. *Aust. J. Chem.* **1970**, 1023-1027.

216. Calderazzo, F.; Pampaloni, G.; Passarelli, V., 1,10-Phenanthroline-5,6-dione as a building block for the synthesis of homo- and heterometallic complexes. *Inorg. Chim. Acta* **2002,** *330*, 136-142.

217. Roy, S.; Hagen, K. D.; Maheswari, P. U.; Lutz, M.; Spek, A. L.; Reedijk, J.; van Wezel, G. P., Phenanthroline derivatives with improved selectivity as DNA-targeting anticancer or antimicrobial drugs. *ChemMedChem* **2008,** *3*, 1427-1434.

218. Ghosh, S.; Barve, A. C.; Kumbhar, A. A.; Kumbhar, A. S.; Puranik, V. G.; Datar, P. A.; Sonawane, U. B.; Joshi, R. R., Synthesis, characterization, X-ray structure and DNA photocleavage by *cis*-dichloro bis(diimine) Co(III) complexes. *J. Inorg. Biochem.* **2006,** *100*, 331-343.

219. Deegan, C.; Coyle, B.; McCann, M.; Devereux, M.; Egan, D. A., *In vitro* anti-tumour effect of 1,10-phenanthroline-5,6-dione (phendione),

[Cu(phendione)$_3$](ClO$_4$)$_2$·4H$_2$O and [Ag(phendione)$_2$]ClO$_4$ using human epithelial cell lines. *Chem. Biol. Interact.* **2006,** *164*, 115-125.

220. McCann, M.; Coyle, B.; McKay, S.; McCormack, P.; Kavanagh, K.; Devereux, M.; McKee, V.; Kinsella, P.; O'Connor, R.; Clynes, M., Synthesis and X-ray crystal structure of [Ag(phendio)$_2$]ClO$_4$ (phendio = 1,10-phenanthroline-5,6-dione) and its effects on fungal and mammalian cells. *BioMetals* **2004,** *17*, 635-645.

221. Eshwika, A.; Coyle, B.; Devereux, M.; McCann, M.; Kavanagh, K., Metal complexes of 1,10-phenanthroline-5,6-dione alter the susceptibility of the yeast *Candida albicans* to amphotericin B and miconazole. *BioMetals* **2004,** *17*, 415-422.

222. Rupesh, K. R.; Deepalatha, S.; Krishnaveni, M.; Venkatesan, R.; Jayachandran, S., Synthesis, characterization and *in vitro* biological activity studies of Cu-M (M = Cu^{2+}, Co^{2+}, Ni^{2+}, Mn^{2+}, Zn^{2+}) bimetallic complexes. *Eur. J. Med. Chem.* **2006,** *41*, 1494-1503.

223. Metcalfe, C.; Adams, H.; Haq, I.; Thomas, J. A., A ruthenium dipyridophenazine complex that binds preferentially to GC sequences. *Chem. Commun.* **2003**, 1152-1153.

224. Friedman, A. E.; Chambron, J. C.; Sauvage, J. P.; Turro, N. J.; Barton, J. K., A molecular light switch for DNA: Ru(bpy)$_2$(dppz)$^{2+}$. *J. Am. Chem. Soc.* **1990,** *112*, 4960-4962.

225. Reddy, K. L.; Kumar, K. A.; Satyanarayana, S., Synthesis, DNA Binding, and DNA Photocleavage of the Cobalt(III) Complexes [Co(bpy)$_2$MDPPZ]$^{3+}$, [Co(dmb)$_2$MDPPZ]$^{3+}$, and [Co(phen)$_2$MDPPZ]$^{3+}$ and their Antimicrobial Activity. *Synth. React. Inorg., Met.Org., Nano-Met. Chem.* **2011,** *41*, 182-192.

226. Benitez, J.; Guggeri, L.; Tomaz, I.; Pessoa, J. C.; Moreno, V.; Lorenzo, J.; Aviles, F. X.; Garat, B.; Gambino, D., A novel vanadyl complex with a polypyridyl DNA intercalator as ligand: A potential anti-protozoa and anti-tumor agent. *J. Inorg. Biochem.* **2009,** *103*, 1386-1394.

227. Menon, E. L.; Perera, R.; Navarro, M.; Kuhn, R. J.; Morrison, H., Phototoxicity against Tumor Cells and Sindbis Virus by an Octahedral Rhodium Bisbipyridyl Complex and Evidence for the Genome as a Target in Viral Photoinactivation. *Inorg. Chem.* **2004,** *43*, 5373-5381.

228. Wan, P.; Moat, S.; Anstey, A., Pellagra: a review with emphasis on photosensitivity. *Br. J. Dermatol.* **2011,** *164*, 1188-1200.

229. Lukasova, M.; Hanson, J.; Tunaru, S.; Offermanns, S., Nicotinic acid (niacin): new lipid-independent mechanisms of action and therapeutic potentials. *Trends Pharmacol. Sci.* **2011,** *32*, 700-707.

230. Grant, R. S.; Coggan, S. E.; Smythe, G. A., The physiological action of picolinic acid in the human brain. *Int. J. Tryptophan Res.* **2009,** *2*, 71-79.

231. (a) Evans, G. W.; Johnson, E. C., Effect of iron, vitamin B-6 and picolinic acid on zinc absorption in the rat. *J. Nutr.* **1981,** *111*, 68-75; (b) Varesio, L.; Clayton, M.; Blasi, E.; Ruffman, R.; Radzioch, D., Picolinic acid, a catabolite of tryptophan, as the second signal in the activation of IFN-γ-primed macrophages. *J. Immunol.* **1990,** *145*, 4265-4271.

232. (a) Paw, W.; Eisenberg, R., Synthesis, Characterization, and Spectroscopy of Dipyridocatecholate Complexes of Platinum. *Inorg. Chem.* **1997,** *36*, 2287-2293; (b) Greguric, A.; Greguric, I. D.; Hambley, T. W.; Aldrich-Wright, J. R.; Collins, J. G., Minor groove intercalation of Δ-[Ru(Me$_2$phen)$_2$dppz]$^{2+}$ to the hexanucleotide d(GTCGAC)$_2$. *J. Chem. Soc., Dalton Trans.* **2002**, 849-855.

233. (a) Lockhart, T. P.; Manders, W. F., Structure determination by NMR spectroscopy. Dependence of $|^2J(^{119}Sn,^1H)|$ on the Me-Sn-Me angle in methyltin(IV) compounds. *Inorg. Chem.* **1986,** *25*, 892-895; (b) Lockhart, T. P.; Manders, W. F.; Zuckerman, J. J., Structural investigations by solid-state carbon-13 NMR. Dependence of $|^1J(^{119}Sn,^{13}C)|$ on the methyl-tin-methyl angle in methyltin(IV)s. *J. Am. Chem. Soc.* **1985,** *107*, 4546-4547.

234. Deacon, G. B.; Phillips, R. J., Relationships between the carbon-oxygen stretching frequencies of carboxylato complexes and the type of carboxylate coordination. *Coord. Chem. Rev.* **1980,** *33*, 227-250.

235. A Scifinder Scholar search for reference 234 on the 15th of August 2013 gave 2213 citings.

236. Allen, D. W.; Nowell, I. W.; Brooks, J. S.; Clarkson, R. W., Moessbauer and single crystal X-ray studies of polymeric dimethylchlorotin acetate. *J. Organomet. Chem.* **1981,** *219*, 29-34.

237. Honnick, W. D.; Zuckerman, J. J., Diorganotin halide carboxylates, thiocarboxylates and halide haloacetates. *J. Organomet. Chem.* **1979,** *178*, 133-155.

238. Szorcsik, A.; Nagy, L.; Sletten, J.; Szalontai, G.; Kamu, E.; Fiore, T.; Pellerito, L.; Kalman, E., Preparation and structural studies on dibutyltin(IV) complexes with pyridine mono- and dicarboxylic acids. *J. Organomet. Chem.* **2004,** *689*, 1145-1154.

239. Lockhart, T. P.; Davidson, F., Methyltin(IV) structure determination by NMR X-ray and NMR structural analyses of three Me$_2$Sn(chelate)$_2$ compounds bearing five-membered chelate rings. *Organometallics* **1987,** *6*, 2471-2478.

240. Mitchell, T. N., Carbon-13 NMR investigations on organotin compounds. *J. Organomet. Chem.* **1973,** *59*, 189-197.

241. Boparoy, G. K. S. a. N. S., Preparation and ^{119m}Sn Mossbauer studies of organotin(IV) derivatives of nicotinic acid and nicotinic acid *N*-oxide. *J. Organomet. Chem.* **1991,** *420*, 23-34.

242. Dakternieks, D.; Duthie, A.; Smyth, D. R.; Stapleton, C. P. D.; Tiekink, E. R. T., Steric Control over Molecular Structure and Supramolecular Association Exerted by Tin- and Ligand-Bound Groups in Diorganotin Carboxylates. *Organometallics* **2003,** *22*, 4599-4603.

243. Alan. J. Crowe, R. H., Peter J. Smith, Synthesis and spectroscopic studies of mono- and di-organotin(IV) derivatives of pyridinecarboxylic acids. *J. Org. Chem.* **1981,** *204*, 47-53.

244. (a) Buntine, M. A.; Hall, V. J.; Kosovel, F. J.; Tiekink, E. R. T., Influence of Crystal Packing on Molecular Geometry: A Crystallographic and Theoretical Investigation of Selected Diorganotin Systems. *J. Phys. Chem. A* **1998,** *102*, 2472-2482; (b) Ng, S. W., Monoclinic modification of di-n-butyl-

dichlorido(1,10-phenanthroline-kappaN,N')tin(IV). *Acta Crystallogr. Sect. E Struct. Rep.* **2010,** *66*, m1669; (c) Cox, M. J.; Tiekink, E. R. T., Crystal structure of 1,10-phenanthrolinedichlorodiphenyltin, $C_{24}H_{138}Cl_2N_2Sn$. *Z. Kristallogr.* **1994,** *209*, 190-191.

245. Goss, C. A.; Abruna, H. D., Spectral, electrochemical and electrocatalytic properties of 1,10-phenanthroline-5,6-dione complexes of transition metals. *Inorg. Chem.* **1985,** *24*, 4263-4267.

246. De Alencastro, R. B.; Bomfim, J. A. S.; Filgueiras, C. A. L.; Howie, R. A.; Wardell, J. L., Evaluation of PM3 calculations applied to organotin compounds: crystal structure of $[Ph_2SnCl_2(1,10$-phenanthroline-5,6-dione)] $\cdot 2Me_2CO$. *Appl. Organomet. Chem.* **2005,** *19*, 479-487.

247. Bennett, W. E.; Broberg, D. E.; Baenziger, N. C., Crystal structure of stannic phthalocyanine, an eight-coordinated tin complex. *Inorg. Chem.* **1973,** *12*, 930-936.

248. Ocakoglu, K.; Zafer, C.; Cetinkaya, B.; Icli, S., Synthesis, characterization, electrochemical and spectroscopic studies of two new heteroleptic Ru(II) polypyridyl complexes. *Dyes Pigm.* **2007,** *75*, 385-394.

249. Krishnakumar, B.; Swaminathan, M., A recyclable and highly effective sulfated TiO2-P25 for the synthesis of quinoxaline and dipyridophenazine derivatives at room temperature. *J. Organomet. Chem.* **2010,** *695*, 2572-2577.

250. Navarro, M.; Hernandez, C.; Colmenares, I.; Hernandez, P.; Fernandez, M.; Sierraalta, A.; Marchan, E., Synthesis and characterization of $[Au(dppz)_2]Cl_3$. DNA interaction studies and biological activity against Leishmania (L) mexicana. *J. Inorg. Biochem.* **2007,** *101*, 111-116.

251. Szorcsik, A.; Nagy, L.; Sletten, J.; Szalontai, G.; Kamu, E.; Fiore, T.; Pellerito, L.; Kálmán, E., Preparation and structural studies on dibutyltin(IV) complexes with pyridine mono- and dicarboxylic acids. *J. Organomet. Chem.* **2004,** *689*, 1145-1154.

252. Corona-Bustamante, A.; Viveros-Paredes, J. M.; Flores-Parra, A.; Peraza-Campos, A. L.; Martinez-Martinez, F. J.; Sumaya-Martinez, M. T.; Ramos-Organillo, A., Antioxidant activity of butyl- and phenylstannoxanes derived from 2-, 3- and 4-pyridinecarboxylic acids. *Molecules* **2010,** *15*, 5445-5459.

253. Howard, W. F., Jr.; Crecely, R. W.; Nelson, W. H., Octahedral dialkyltin complexes: a multinuclear NMR spectral solution structural study. *Inorg. Chem.* **1985,** *24*, 2204-2208.

254. Alleston, D. L.; Davies, A. G., 383. The preparation of some organotin(IV) compounds. *J. Chem. Soc.* **1962**, 2050-2054.

Publications and presentations

Peer reviewed publications

Dolan N.; McGinley J.; Stephens J. C.; Kavanagh K.; Hurley D.; Maher N. J., Synthesis, characterisation and antimicrobial studies of organotin(IV) complexes with 1,10-phenanthroline derivatives. *Inorg. Chim. Acta* **2014**, *409*, 276–284.

Poster Presentations

The Synthesis of a Series of Quinolone Derivatives and their evaluation against *P. aeruginosa*, *S. aureus* and *E. coli*. International Conference on Antimicrobial Research, Valladolid, Spain, November 2010.

The synthesis of quinine-based, quinolone and organotin compounds and their evaluation against gram-positive and gram-negative bacteria.Centre for Synthesis and Chemical Biology, Dublin, Ireland, December 2010.

The synthesis of organotin compounds and their evaluation against Gram-positive bacteria. Irish Institute of Metal Based Drugs Symposium (IIMBD), N.U.I Maynooth, September 2011.
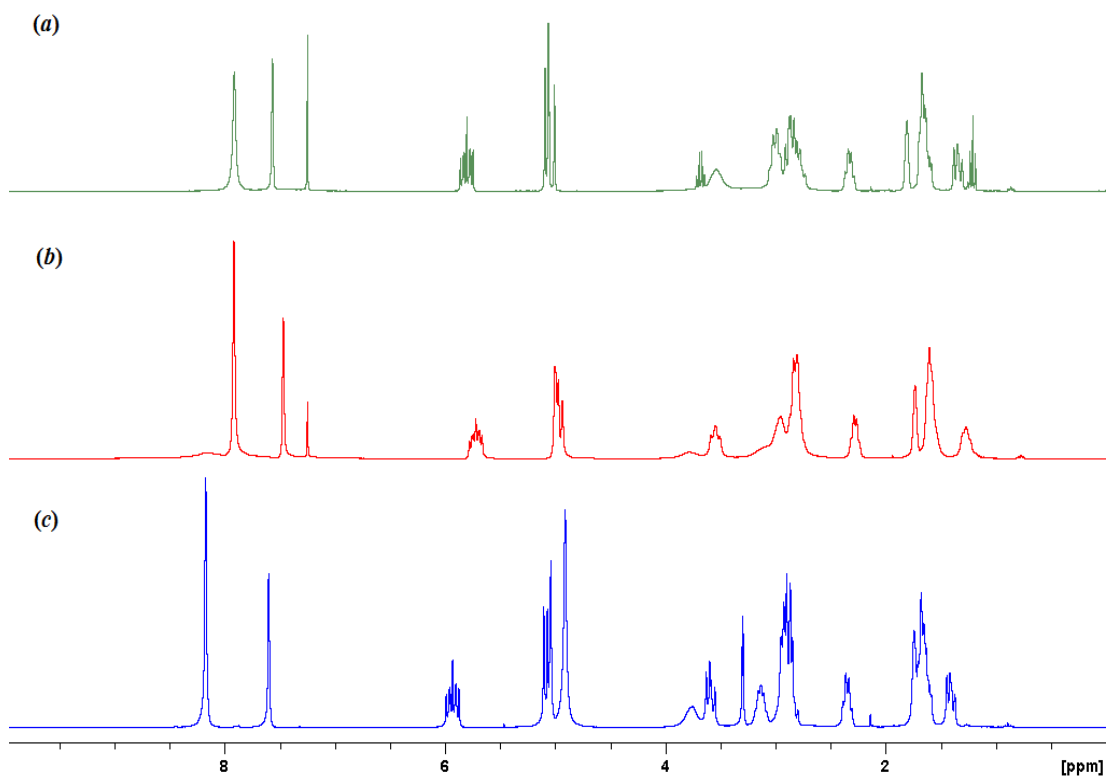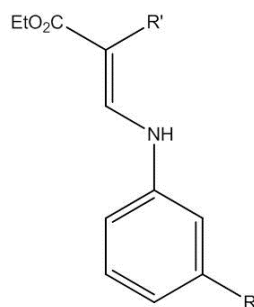
Appendix

Appendix A

(*a*)

(*b*)

(*c*)

Figure A1: ^{1}H NMR spectra for compound **12** in (*a*) CDCl$_3$ at 50 ^{o}C, (*b*) CDCl$_3$ at 25 ^{o}C and (*c*) CD$_3$OD at 25 ^{o}C. Solvent residual ^{1}H signals were also observed in each spectrum.

Appendix B

Table B1: Phenylamino acrylates and malonates tested for bacteriostatic activity.

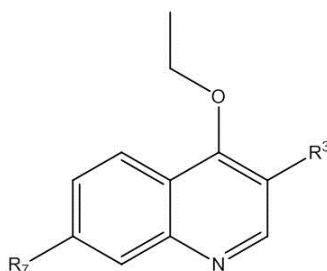| Quinolone	R	R'
3.1[a]	H	CN
3.2[a]	F	CN
3.3	H	CO_2Et
3.4	F	CO_2Et

[a] Tested as mixture of E/Z isomers

Table B2: Quinolone compounds tested for bacteriostatic activity.
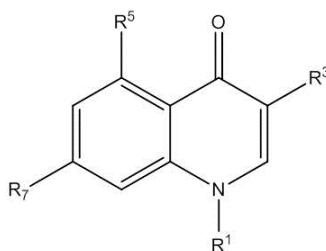
Quinolone	R^1	R^3	R^5	R^7
3.5	H	CN	H	H
[a]3.6a	H	CN	H	F
[a]3.6b	H	CN	F	H
3.7	H	CO_2Et	H	H
[b]3.8a	H	CO_2Et	H	F
[b]3.8b	H	CO_2Et	F	H
3.9	Et	CN	H	H

Table B2 *continued*

Quinolone	R^1	R^3	R^5	R^7
3.10a	Et	CN	H	F
3.10b	Et	CN	F	H
3.11a	Et	CO$_2$Et	H	H
3.12b	Et	CO$_2$Et	H	F
3.12c	Et	CO$_2$Et	F	H
3.13	Et	CO$_2$H	H	H
3.14	Et	CO$_2$H	H	F
3.15	Et	CO$_2$H	H	OMe
3.16	Et	CN	H	Piperazine
3.17	Et	CO$_2$H	H	Piperazine
3.18	Et	CN	H	*N*-Methylpiperazin
3.19	Et	CO$_2$H	H	*N*-Methylpiperazin
3.20	Et	CN$_4$	H	H

[a] Tested as mixture of 3.6a and 3.6b, [b] tested as mixture of 3.8a and 3.8b.

Table B3: *O*-Alkyl quinolone compounds tested for bacteriostatic activity.

Quinolone	R^1	R^3	R^5	R^7
3.11b	-	CO$_2$Et	H	H
3.12a	-	CO$_2$Et	H	F
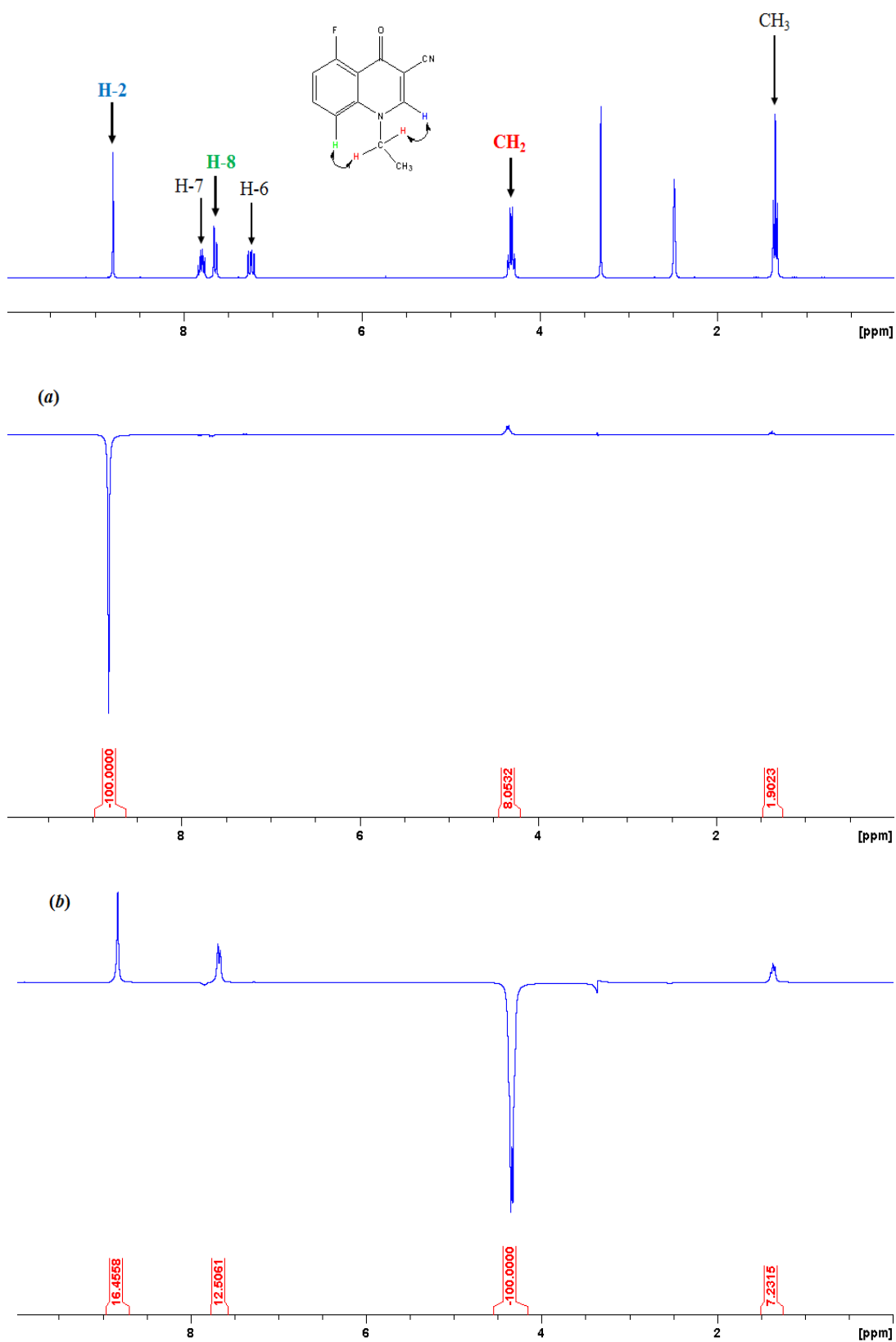
Figure B1: [1]H and NOE spectra of **3.10b**.
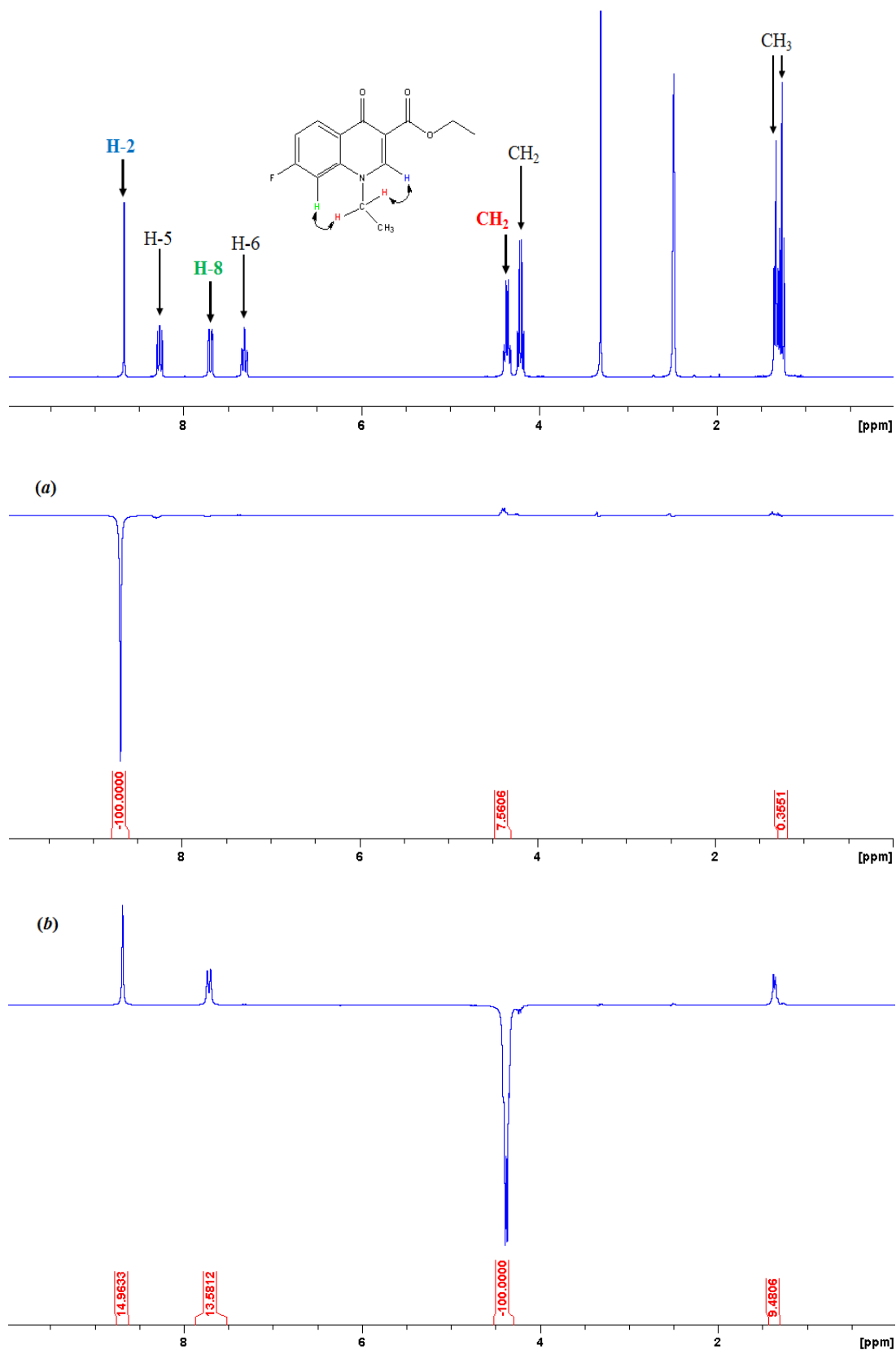
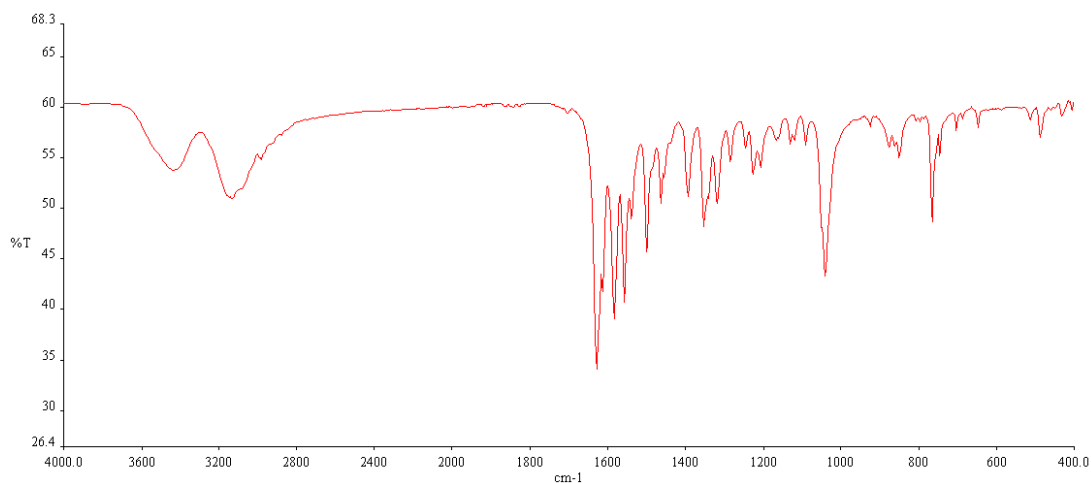**Figure B2:** [1]H and NOEdiff spectra for **3.12b**.

Figure B3: IR spectrum of **3.20**.

Table B4: Crystal structure and refinement of 1-ethyl-3-(1*H*-tetrazol-5-yl)quinolin-4(1H)-one, **3.20**.

Empirical formula	C12 H13 N5 O2
Formula weight	259.27
Temperature	150(2) K
Wavelength	0.71073 Å
Crystal system	Monoclinic
Space group	P2(1)/n
Unit cell dimensions	a = 14.993(3) Å $\quad$ α= 90°
	b = 4.3819(10) Å $\quad$ β= 92.197(4)°
	c = 17.908(4) Å $\quad$ γ = 90°
Volume	1175.7(5) Å^3
Z	4
Density (calculated)	1.465 Mg/m^3
Absorption coefficient	0.105 mm^{-1}
F(000)	544
Crystal size	0.37 x 0.07 x 0.04 mm^3
Crystal description	yellow needle
Theta range for data collection	1.74 to 26.43°
Index ranges	-18<=h<=18, -5<=k<=5, -22<=l<=22
Reflections collected	9737
Independent reflections	2428 [R(int) = 0.0644]

Table B4 *continued*

Completeness to theta = 26.43°	100.0%
Absorption correction	Semi-empirical from equivalents
Max. and min. transmission	0.9958 and 0.9621
Refinement method	Full-matrix least-squares on F^2
Data / restraints / parameters	2428 / 3 / 181
Goodness-of-fit on F^2	1.009
Final R indices [I>2sigma(I)]	R1 = 0.0478, wR2 = 0.1017
R indices (all data)	R1 = 0.0911, wR2 = 0.1196
Largest diff. peak and hole	0.166 and -0.206 e.Å^{-3}

Table B5: Atomic coordinates (x 10^4) and equivalent isotropic displacement parameters (Å^2x 10^3) for **3.20**. U(eq) is defined as one third of the trace of the orthogonalized U^{ij} tensor.

	X	Y	Z	U(eq)
N(1)	7234(1)	7632(4)	10324(1)	24(1)
C(1)	7919(1)	6967(5)	10799(1)	24(1)
C(2)	8594(1)	4988(5)	10644(1)	22(1)
C(3)	9288(1)	4391(5)	11218(1)	24(1)
N(2)	9335(1)	5638(5)	11893(1)	29(1)
N(3)	10080(1)	4435(5)	12245(1)	33(1)
N(4)	10476(1)	2555(5)	11808(1)	31(1)
N(5)	9981(1)	2511(4)	11160(1)	25(1)
C(4)	8604(1)	3514(5)	9926(1)	23(1)
O(1)	9213(1)	1709(4)	9758(1)	32(1)
C(5)	7857(1)	4239(5)	9412(1)	22(1)
(C6)	7794(2)	2902(5)	8699(1)	27(1)
C(7)	7079(1)	3493(5)	8216(1)	29(1)
C(8)	6411(2)	5468(5)	8430(1)	29(1)
C(9)	6450(1)	6839(5)	9122(1)	27(1)
C(10)	7175(1)	6249(5)	9623(1)	22(1)
C(11)	6523(1)	9644(5)	10593(1)	29(1)
C(12)	5753(2)	7877(6)	10899(1)	37(1)
O(1W)	7968(1)	8009(4)	12778(1)	38(1)

Table B6: Bond lengths [Å] and angles [°] for **3.20**.

|			
N(1)-C(1)	1.339(3)	N(4)-N(5)	1.353(2)
N(1)-C(10)	1.395(3)	C(4)-O(1)	1.253(2)
N(1)-C(11)	1.478(3)	C(4)-C(5)	1.458(3)
C(1)-C(2)	1.370(3)	C(5)-C(6)	1.405(3)
C(2)-C(4)	1.438(3)	C(5)-C(10)	1.411(3)
C(2)-C(3)	1.457(3)	C(6)-C(7)	1.377(3)
C(3)-N(2)	1.327(3)	C(7)-C(8)	1.388(3)
C(3)-N(5)	1.333(3)	C(8)-C(9)	1.375(3)
N(2)-N(3)	1.367(2)	C(9)-C(10)	1.406(3)
N(3)-N(4)	1.296(3)	C(11)-C(12)	1.510(3)
C(1)-N(1)-C(10)	119.86(18)	O(1)-C(4)-C(2)	122.04(19)
C(1)-N(1)-C(11)	117.90(18)	O(1)-C(4)-C(5)	122.38(19)
C(10)-N(1)-C(11)	122.06(17)	C(2)-C(4)-C(5)	115.57(19)
N(1)-C(1)-C(2)	124.3(2)	C(6)-C(5)-C(10)	118.60(19)
C(1)-C(2)-C(4)	119.91(19)	C(6)-C(5)-C(4)	120.40(19)
C(1)-C(2)-C(3)	118.93(19)	C(10)-C(5)-C(4)	120.99(19)
C(4)-C(2)-C(3)	121.16(19)	C(7)-C(6)-C(5)	121.1(2)
N(2)-C(3)-N(5)	108.06(18)	C(6)-C(7)-C(8)	119.7(2)
N(2)-C(3)-C(2)	125.5(2)	C(9)-C(8)-C(7)	121.0(2)
N(5)-C(3)-C(2)	126.44(19)	C(8)-C(9)-C(10)	119.9(2)
C(3)-N(2)-N(3)	105.99(18)	N(1)-C(10)-C(9)	121.04(19)
N(4)-N(3)-N(2)	110.62(17)	N(1)-C(10)-C(5)	119.33(19)
N(3)-N(4)-N(5)	106.13(17)	C(9)-C(10)-C(5)	119.6(2)
C(3)-N(5)-N(4)	109.19(18)	N(1)-C(11)-C(12)	112.55(19)

Appendix C

$[Ph_2SnCl_2(phen)]^*$ $\qquad$ $[Ph_2SnCl_2(phen)]^\#$
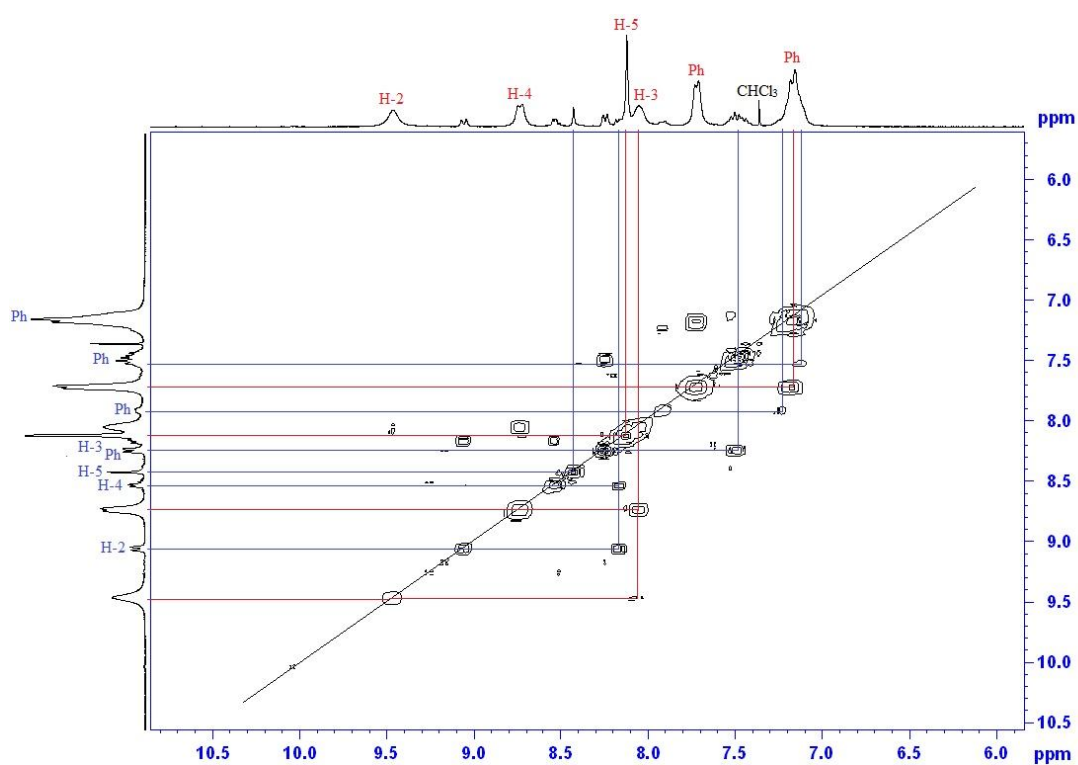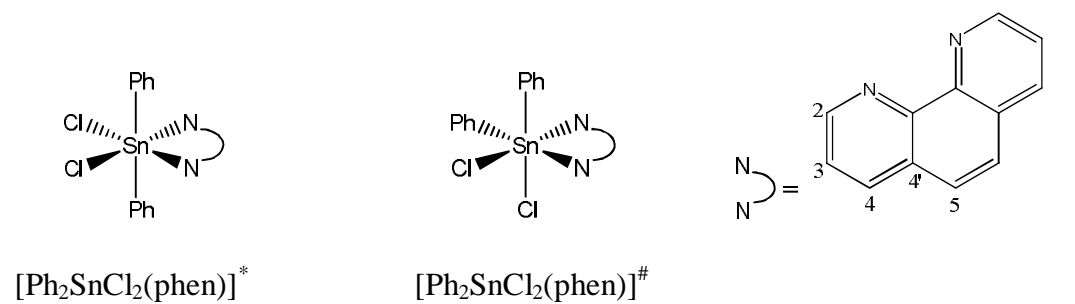
Figure C1: COSY NMR spectrum of $[Ph_2SnCl_2(phen)]$. *$[Ph_2SnCl_2(phen)]$ in red (*trans*-isomer) and #$[Ph_2SnCl_2(phen)]$ in blue (*cis*-isomer).
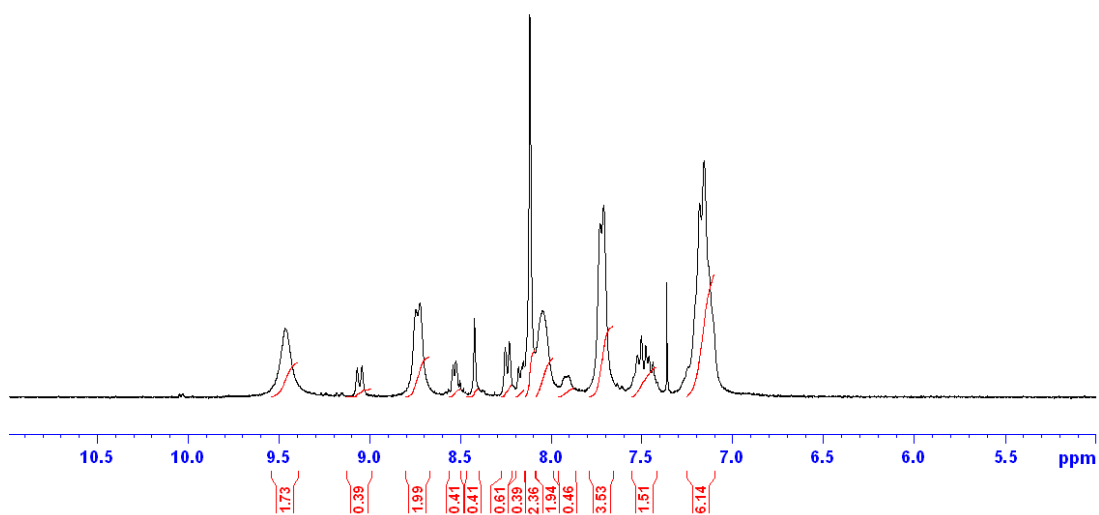
Figure C2: ^{1}H NMR of [Ph$_2$SnCl$_2$(phen)] at 25 ^{o}C (DMSO-d$_6$).
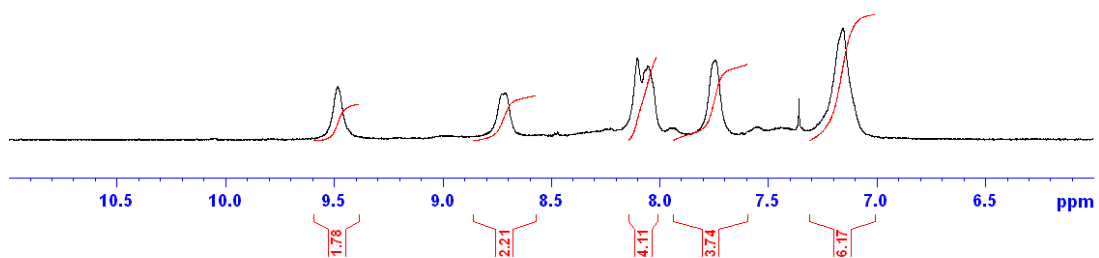
Figure C3: ^{1}H NMR of [Ph$_2$SnCl$_2$(phen)] at 70 ^{o}C (DMSO-d$_6$).